

# A plethora of new, magnetic chemically peculiar stars from LAMOST DR4

S. Hümmelich<sup>1,2</sup>, E. Paunzen<sup>3</sup>, and K. Bernhard<sup>1,2</sup>

<sup>1</sup> Bundesdeutsche Arbeitsgemeinschaft für Veränderliche Sterne e.V. (BAV), D-12169 Berlin, Germany, e-mail: ernham@rz-online.de

<sup>2</sup> American Association of Variable Star Observers (AAVSO), 49 Bay State Rd, Cambridge, MA 02138, USA

<sup>3</sup> Department of Theoretical Physics and Astrophysics, Masaryk University, Kotlářská 2, 611 37 Brno, Czech Republic

## ABSTRACT

*Context.* Magnetic chemically peculiar (mCP) stars are important to astrophysics because their complex atmospheres lend themselves perfectly to the investigation of the interplay between such diverse phenomena as atomic diffusion, magnetic fields, and stellar rotation. The most up-to-date catalogue of these objects was published a decade ago. Since then, no large scale spectroscopic surveys targeting this group of objects have been carried out. An increased sample size of mCP stars, however, is important for statistical studies.

*Aims.* The present work is aimed at identifying new mCP stars using spectra collected by the Large Sky Area Multi-Object Fiber Spectroscopic Telescope (LAMOST).

*Methods.* Suitable candidates were selected by searching LAMOST DR4 spectra for the presence of the characteristic 5200 Å flux depression. Spectral classification was carried out with a modified version of the MKCLASS code and the accuracy of the classifications was estimated by comparison with results from manual classification and the literature. Using parallax data and photometry from Gaia DR2, we investigated the space distribution of our sample stars and their properties in the colour-magnitude diagram.

*Results.* Our final sample consists of 1002 mCP stars, most of which are new discoveries (only 59 common entries with the Catalogue of Ap, HgMn and Am stars). Traditional mCP star peculiarities have been identified in all but 36 stars, highlighting the efficiency of the code's peculiarity identification capabilities. The derived temperature and peculiarity types are in agreement with manually derived classifications and the literature. Our sample stars are between 100 Myr and 1 Gyr old, with the majority having masses between  $2 M_{\odot}$  and  $3 M_{\odot}$ . Our results could be considered as strong evidence for an inhomogeneous age distribution among low-mass ( $M < 3 M_{\odot}$ ) mCP stars; however, we caution that our sample has not been selected on the basis of an unbiased, direct detection of a magnetic field. We identified several astrophysically interesting objects: the mCP stars LAMOST J122746.05+113635.3 and LAMOST J150331.87+093125.4 have distances and kinematical properties in agreement with halo stars; LAMOST J034306.74+495240.7 is an eclipsing binary system ( $P_{\text{orb}} = 5.1435 \pm 0.0012$  d) hosting an mCP star component; and LAMOST J050146.85+383500.8 was found to be an SB2 system likely comprising of an mCP star and a supergiant component.

*Conclusions.* With our work, we significantly increase the sample size of known Galactic mCP stars, paving the way for future in-depth statistical studies.

**Key words.** stars: chemically peculiar – stars: abundances – stars: binaries: eclipsing

## 1. Introduction

The chemically peculiar (CP) stars of the upper main sequence (spectral types early B to early F) are traditionally characterised by the presence of certain absorption lines of abnormal strength or weakness that indicate peculiar surface abundances (Preston 1974). For most groups of CP stars, current theories ascribe the observed chemical peculiarities to the interplay between radiative levitation and gravitational settling (atomic diffusion) (Michaud 1970; Richer et al. 2000): whereas most elements sink under the force of gravity, those with numerous absorption lines near the local flux maximum are radiatively accelerated towards the surface. Because CP stars are generally slow rotators and boast calm radiative atmospheres, atomic diffusion processes are able to significantly influence the chemical composition of the outer stellar layers.

Following Preston (1974), CP stars are traditionally divided into the following four main groups: CP1 stars (the metallic-line or Am/Fm stars), CP2 stars (the magnetic Bp/Ap stars), CP3 stars (the Mercury-Manganese or HgMn stars), and CP4 stars (the He-weak stars). Although the chemical composition

within a group may vary considerably, each group is characterised by a distinct set of peculiarities. The CP1 stars show underabundances of Ca and Sc and overabundances of the iron-peak and heavier elements. CP2 stars exhibit excesses of elements such as Si, Sr, Eu, or the rare-earth elements. The CP3 stars are characterised by enhanced lines of Hg and Mn and other heavy elements, whereas the main characteristic of the CP4 stars is anomalously weak He lines. Further classes of CP stars have been described, such as the He strong stars – early B stars with anomalously strong He lines –, the  $\lambda$  Bootis stars (Murphy & Paunzen 2017), which boast unusually low surface abundances of iron-peak elements, or the barium stars, which are characterised by enhancements of the *s*-process elements Ba, Sr, Y, and C (Bidelman & Keenan 1951). Generally, with regard to the strength of chemical peculiarities, a continuous transition from normal to peculiar stars is observed (Loden & Sundman 1987).

Most of the CP2 and He-peculiar stars possess stable and globally organised magnetic fields with strengths of up to several tens of kG (Babcock 1947; Aurière et al. 2007), the origin of which is still a matter of some controversy (Moss 2004).

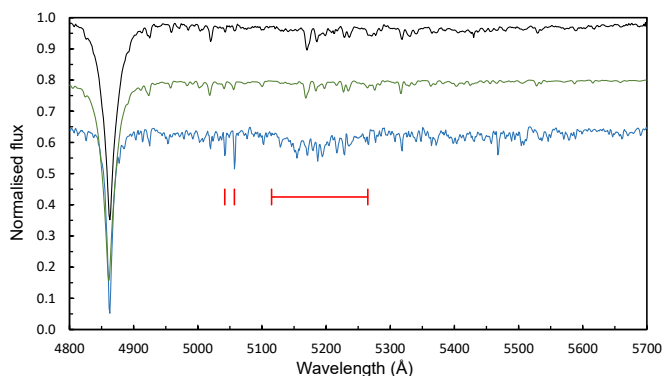


**Fig. 1.** 4800 Å to 5700 Å region of (from top to bottom) the non-CP A0 V star LAMOST J194655.00+402559.5 (HD 225785), a synthetic spectrum with  $T_{\text{eff}} = 9750$  K,  $\log g = 4.0$ ,  $[M/H] = 0.0$  and a microturbulent velocity of  $2 \text{ km s}^{-1}$ , and the newly-identified Si-strong mCP star LAMOST J025951.09+540337.5 (#78; TYC 3701-157-1). The position of the characteristic 5200 Å depression and the Si II lines at 5041 Å and 5055/56 Å are indicated. LAMOST spectra have been taken from DR4.

However, a body of evidence has been built up that strongly favours the fossil field theory, which states that the magnetic field is a relic of the ‘frozen-in’ interstellar magnetic field (e.g. Braithwaite & Spruit 2004). These stars are often referred to as magnetic chemically peculiar (mCP) stars in the literature – a convention which we will adhere to throughout this paper. The magnetic field affects the diffusion processes in such a way that mCP stars show a non-uniform distribution of chemical elements (chemical spots or belts) on their surfaces, which can be studied in detail via the technique of Doppler imaging (Kochukhov 2017). As the magnetic axis is oblique to the rotation axis (oblique rotator model; Stibbs 1950), mCP stars show strictly periodic light, spectral, and magnetic variations with the rotation period. The photometric variability arises because flux is redistributed in the abundance patches (e.g. Wolff & Wolff 1971; Molnar 1973; Krtićka et al. 2013).

The mCP stars show vastly differing abundance patterns. Some of the most peculiar objects belong to this group, such as the extreme lanthanide star HD 51418 (Jones et al. 1974) or Przybylski’s star HD 101065 (Przybylski 1966), which is widely regarded as the most peculiar star known. Excesses of several orders of magnitude are commonly observed in these objects. Morgan (1933) already recognised a relationship between a CP2 star’s temperature and the predominant spectral peculiarities and showed that the CP2 stars can thus be sorted into subgroups. Since then, many authors have proposed corresponding classification schemes with varying levels of detail (cf. the discussions in Wolff 1983 and Gray & Corbally 2009). It is generally useful to at least differentiate between the ‘cool’ CP2 stars mostly characterised by Sr, Cr and Eu peculiarities and the ‘hot’ CP2 stars that generally show Si overabundances, although considerable overlap exists.

The mCP stars are important to astrophysics in several respects. Their complex atmospheres lend themselves perfectly to the investigation of such diverse phenomena as atomic diffusion, magnetic fields, stellar rotation and their interplay. They furthermore provide important testing grounds for the evaluation of model atmospheres (Krtićka et al. 2009) and, through their characteristic light variability, allow the derivation of rotational periods with great accuracy and comparatively little effort.

The most up-to-date collection of CP stars – the most recent version of the General Catalogue of CP Stars – was published a

decade ago (Renson & Manfroid 2009). It contains about 3500 mCP stars or candidates ( $\sim 2000$  confirmed mCP stars and  $\sim 1500$  candidate mCP stars). Since then, several studies have identified new mCP stars on a minor scale (e.g. Hümmerich et al. 2018; Scholz et al. 2019; Sikora et al. 2019) but no large scale spectroscopic surveys have been conducted during the past recent decades that aim specifically at the identification of new mCP stars ‘en masse’.

The works of Hou et al. (2015) and Qin et al. (2019) warrant special mention as they exploited spectra collected by the Large Sky Area Multi-Object Fiber Spectroscopic Telescope (LAMOST) of the Chinese Academy of Science. Hou et al. (2015) presented a list of 3537 candidate CP1 stars from LAMOST Data Release (DR) 1. Building on this work, Smalley et al. (2017) investigated pulsational properties versus metallicity in this subgroup of CP stars. Qin et al. (2019) searched for CP1 stars in the low-resolution spectra of LAMOST DR5 and compiled a catalogue of 9372 CP1 stars. They identified CP2 stars as a contaminant and searched for corresponding candidates in their sample of CP1 candidates, identifying 1131 candidate CP2 stars in this process.

Here we present our efforts aimed at identifying new mCP stars using spectra from the publicly available LAMOST DR4, which have led to the discovery of 1002 mCP stars. With this work, we significantly increase the sample size of known Galactic mCP stars, paving the way for future in-depth statistical studies. Spectroscopic data and target selection process are discussed in Section 2. Spectral classification workflow and results are detailed in Section 3 and discussed, together with other interesting information on our sample of stars, in Section 4. We conclude our findings in Section 5.

## 2. Spectroscopic data and target selection

This section contains a description of the employed spectral archive and the MKCLASS code and details the process of target selection.

### 2.1. The Large Sky Area Multi-Object Fiber Spectroscopic Telescope (LAMOST)

The LAMOST telescope (Zhao et al. 2012; Cui et al. 2012), also called the Guo Shou Jing<sup>1</sup> Telescope, is a reflecting Schmidt telescope located at the Xinglong Observatory in Beijing, China. It boasts an effective aperture of 3.6–4.9 m and a field of view of  $5^\circ$ . Thanks to its unique design, LAMOST is able to take 4000 spectra in a single exposure with spectral resolution  $R \sim 1800$ , limiting magnitude  $r \sim 19$  mag and wavelength coverage from 3700 to 9000 Å. LAMOST is therefore particularly suited to survey large portions of the sky and is dedicated to a spectral survey of the entire available northern sky. LAMOST data products are released to the public in consecutive data releases and can be accessed via the LAMOST spectral archive.<sup>2</sup> With about 10 million stellar spectra contained in DR6, the LAMOST archive constitutes a real treasure trove for researchers.

### 2.2. The MKCLASS code

MKCLASS is a computer program written to classify stellar spectra on the Morgan-Keenan-Kellman (MKK) system

<sup>1</sup> Guo Shou Jing (1231–1316) was a Chinese astronomer, hydraulic engineer, mathematician, and politician of the Yuan Dynasty.

<sup>2</sup> <http://www.lamost.org>

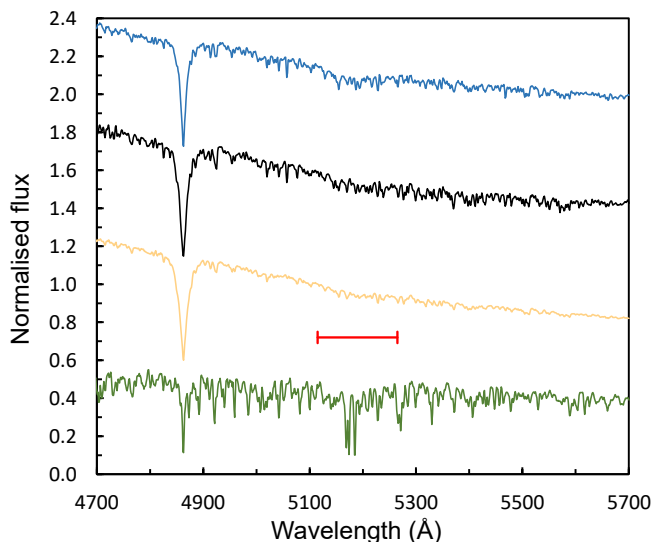


**Fig. 2.** 4700 Å to 5700 Å region of (from top to bottom) the LAMOST DR4 spectra of the mCP stars LAMOST J034458.31+464848.7 (#139; TYC 3313-1279-1), LAMOST J040642.34+454640.8 (#180; HD 25706), LAMOST J072118.92+223422.7 (#792; TYC 1909-1687-1), and the late-type ‘impostor’ LAMOST J001159.88+435908.5 (GSC 02794-00977). The position of the characteristic 5200 Å depression is indicated.

(Gray & Corbally 2014). It has been designed to emulate the process of classifying by a human classifier. First, a rough spectral type is assigned, which is then refined by direct comparison with spectra from standard star libraries.

Currently, MKCLASS is able to classify spectra in the violet-green region (3800–5600 Å) in either rectified or flux-calibrated format. Several studies (e.g. Gray & Corbally 2014; Gray et al. 2016; Hümmerich et al. 2018) have shown that, providing input spectra of sufficient signal-to-noise (S/N), the results of MKCLASS compare well with the results of manual classification (precision of 0.6 spectral subclass and half a luminosity class according to Gray & Corbally 2014).

MKCLASS comes with two libraries of MKK standard spectra, which have been acquired with the Gray/Miller (GM) spectrograph on the 0.8 m reflector of the Dark Sky Observatory in North Carolina, USA. *libr18* contains rectified spectra in the spectral range from 3800–4600 Å and a resolution of 1.8 Å that were obtained with a 1200 g mm<sup>-1</sup> grating. *libnor36* boasts flux-calibrated and normalised spectra in the spectral range from 3800–5600 Å and a resolution of 3.6 Å obtained with a 600 g mm<sup>-1</sup> grating. MKCLASS allows for the use of additional spectral libraries tailored to the specific needs of the researcher.

An interesting feature of the MKCLASS code is its ability to identify a set of spectral peculiarities, such as found in CP1 and CP2 stars, barium stars, carbon-rich giants etc. For more information on the MKCLASS code, we refer the reader to Gray & Corbally (2014) and the corresponding website.<sup>3</sup>

### 2.3. Target selection criteria

To select suitable mCP star candidates, we specifically searched for the presence of the tell-tale 5200 Å depression in the LAMOST DR4 spectra of early-type stars. In the following, we pro-

vide background information and detail our selection criteria and the methods employed in the construction of the present sample of stars.

#### 2.3.1. The flux depressions in mCP stars

The first to notice significant flux depressions at 4100 Å, 5200 Å, and 6300 Å in the spectrum of the mCP star HD 221568 was Kodaira (1969). Similar features in the ultraviolet region at 1400 Å, 1750 Å, and 2750 Å were later identified and investigated (Jamar 1977, 1978). It was found that these spectral features solely occur in mCP stars. Khan & Shulyak (2007) showed that Fe is the principal contributor to the 5200 Å depression for the whole range of  $T_{\text{eff}}$  of mCP stars, while Cr and Si play a role primarily in the low  $T_{\text{eff}}$  region. Figure 1 shows the 4800 Å to 5700 Å region of the spectra of a non-CP star, a corresponding synthetic spectrum and the newly-identified mCP star LAMOST J025951.09+540337.5 (#78<sup>4</sup>; TYC 3701-157-1), illustrating the 5200 Å depression in the latter object.

To investigate the flux depression at 5200 Å, Maitzen (1976) introduced the narrow-band three-filter  $\Delta a$  system, which samples the depth of this depression by comparing the flux at the center (5220 Å,  $g_2$ ) with the adjacent regions (5000 Å,  $g_1$  and 5500 Å,  $y$ ) using a band-width of 130 Å for  $g_1$  and  $g_2$  and 230 Å for the Strömgren  $y$  filter. The index was introduced as:

$$a = g_2 - (g_1 + y)/2.$$

This quantity is slightly dependent on temperature in the sense that it increases towards lower temperatures. Therefore, the intrinsic peculiarity index had to be defined as:

$$\Delta a = a - a_0(g_1 - y),$$

that is, the difference between the individual  $a$  value and the  $a$  value of non-peculiar stars of the same colour. The locus of the  $a_0$  values for non-peculiar objects was termed the normality line. Virtually all mCP stars have positive  $\Delta a$  values up to +75 mmag (Paunzen et al. 2005). Only extreme cases of CP1 and CP3 stars can exhibit marginally positive  $\Delta a$  values. Be/Ae, B[e] and  $\lambda$  Bootis stars exhibit significant negative values. In summary, it has been shown that the  $\Delta a$  system is an efficient and reliable means of identifying mCP stars.

#### 2.3.2. Sample selection

In the present study, we concentrated on the publicly-available spectra from LAMOST DR4 (Zhao et al. 2012; Luo et al. 2018). As first step, the complete catalogue was cross-matched with the *Gaia* DR2 catalogue (Gaia Collaboration et al. 2018). To identify suitable targets, we exploited the  $G$  versus ( $BP - RP$ ) diagram to set a corresponding limit on the investigated spectral type range (hotter than mid F, i.e. ( $BP - RP$ ) < 0.45 mag). From the remaining objects, apparent supergiants were excluded. As this approach is bound to miss highly-reddened hot objects, we searched the spectral types listed in the DR4 VizieR online catalogue<sup>5</sup> (Luo et al. 2018) for additional early-type (B-, A-, and F-type) targets, which were also included into the analysis.

Only spectra with a S/N of more than 50 in the Sloan  $g$  band were considered for further analysis. This cut was deemed necessary because a lower S/N renders the detection of mCP star

<sup>4</sup> The numbers given behind the identifiers refer to the internal identification number and facilitate easy identification in the tables.

<sup>5</sup> <http://cdsarc.u-strasbg.fr/viz-bin/cat/V/153>

<sup>3</sup> <http://www.appstate.edu/~grayro/mkclass/>

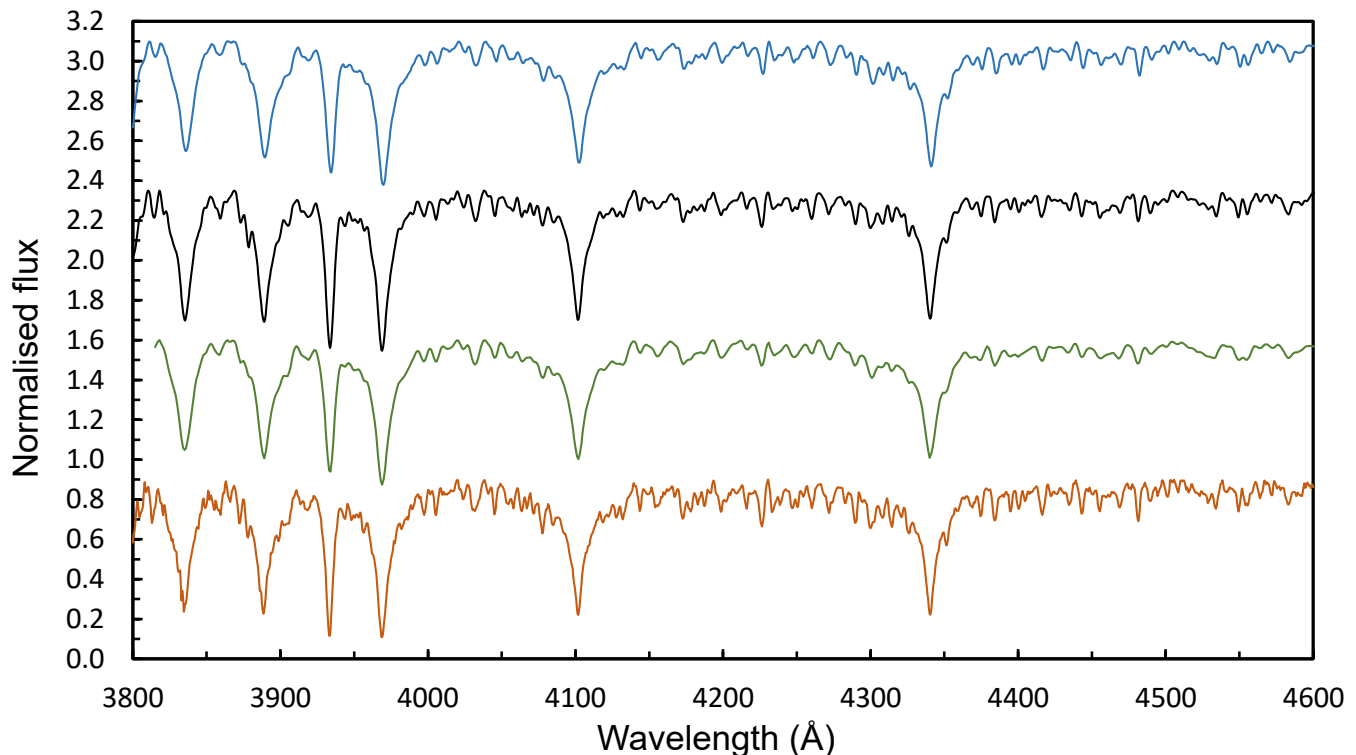


**Fig. 3.** Blue-violet region of (from top to bottom) the F0 V standard spectra from the *liblamost*, *libsynth*, *libnor36*, and *libr18* standard libraries.

features difficult (Paunzen et al. 2011). If more than one spectrum was available for a single object, only the spectrum with the highest Sloan *g* band S/N was included into the analysis.

From the remaining spectra, suitable candidates were selected by the presence of the tell-tale 5200 Å depression. To calculate synthetic  $\Delta a$  values, all spectra were normalised to the flux at 4030 Å. This guarantees that the large absolute flux differences introduced by the apparent visual magnitude do not cause any numerical biases in the final magnitudes. The filter curves of  $g_1$ ,  $g_2$ , and  $y$  as defined in Kupka et al. (2003) were then folded with the spectra and the corresponding magnitudes calculated. All objects with a significant positive  $\Delta a$  index were visually inspected for the presence of a 5200 Å depression in order to sort out glitches in the spectra or contamination by other objects such as cool stars with strong features in the 5200 Å range.

Figure 2 illustrates this process by providing sample LAMOST DR4 spectra of mCP stars showing 5200 Å flux depressions of various strengths. Also shown is the ‘impostor’ LAMOST J001159.88+435908.5 (GSC 02794-00977). This object is actually a mid to late K star whose 5200 Å region is dominated by absorption lines of the Mg I triplet at 5167 Å, 5173 Å, and 5184 Å, which leads to a significantly positive  $\Delta a$  value and highlights the need for setting a limit on the investigated spectral type range via the above described colour-colour cut.

In this way, a list of 1002 mCP star candidates was compiled. This collection of stars is referred to in the following as the ‘final sample’. We here emphasise that our sample is obviously biased towards mCP stars with conspicuous flux depressions at 5200 Å. However, not all mCP stars show significant 5200 Å depressions, in particular in low-resolution spectra, and such objects will have been missed by the imposed selection criteria. On the other hand, early-type stars with significant 5200 Å depressions are nearly

always mCP stars; therefore, the chosen approach should be well suited to collecting a pure sample of mCP stars.

### 3. Spectral classification

Spectral classification is an important tool in astrophysics, which allows for the easy identification of astrophysically interesting objects. Furthermore, it enables to place stars in the Hertzsprung-Russell diagram, thus enabling the derivation of physical parameters. However, in the era of large survey projects such as LAMOST, RAVE, or SDSS/SEGUE, which produce a multitude of stellar spectra, human manual classification is no longer able to cope with the amount of data and the need for automatic classification has arisen. For the present study, we chose to employ a modified version of the MKCLASS code (cf. Section 2.2) that has been specifically tailored to the needs of our project. More details are provided in this section, which details the spectral classification workflow.

#### 3.1. Spectral classification with the MKCLASS code

As deduced from an investigation of the program code, the current version of the MKCLASS code (v1.07) is able to identify the following spectral features, which are important in the detection of CP2 stars: the blend at 4077 Å (which may contain contributions from Si II 4076 Å, Sr II 4077 Å, and Cr II 4077 Å), the blend at 4130 Å (due to enhanced Si II 4128/30 Å and/or Eu II 4130 Å), and the Eu II 4205 Å line. On a significant detection of these features, the following output is created: ‘Sr’ (4077 Å), ‘Si’ (4130 Å), ‘Eu’ (4205 Å). As other elements besides Sr and Si contribute to the blends at 4077 Å and 4130 Å, the output may be misleading in some cases. Nevertheless, this allows a robust de-

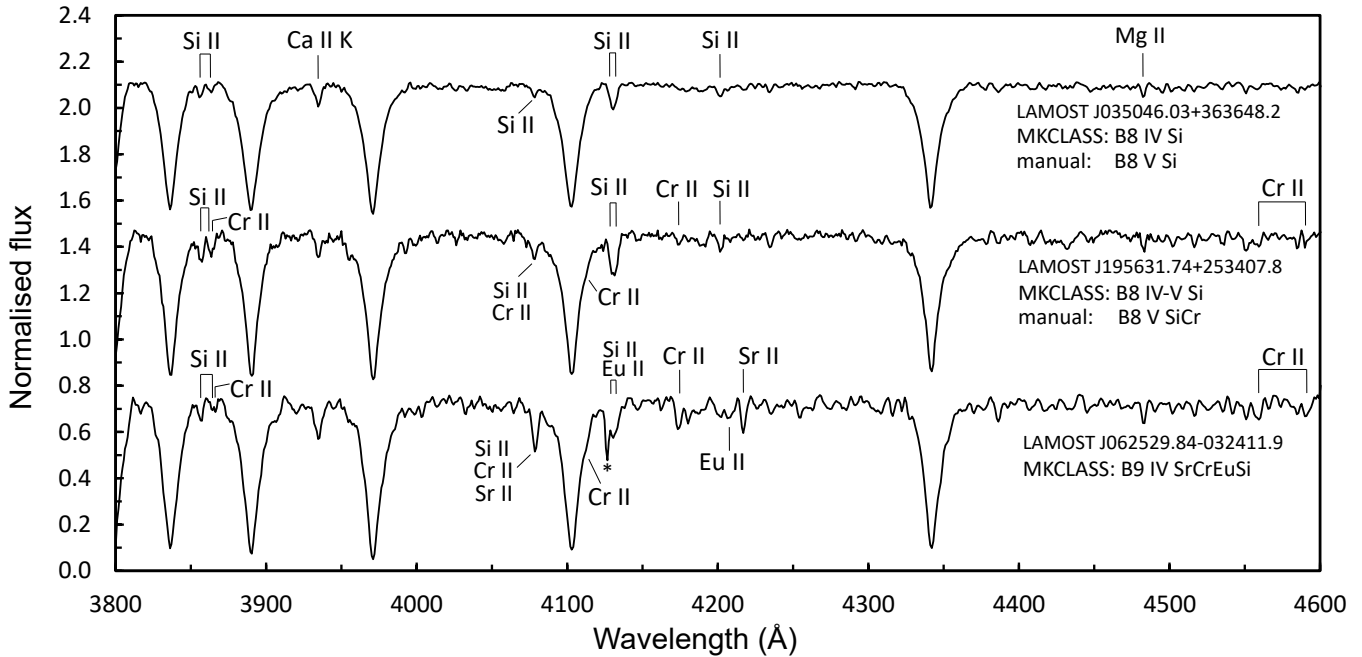


**Fig. 4.** Showcase of three newly identified ‘hot’ mCP stars, illustrating the blue-violet region of the LAMOST DR4 spectra of (from top to bottom) LAMOST J035046.03+363648.2 (#151; Gaia DR2 220081859486642816), LAMOST J195631.74+253407.8 (#929; Gaia DR2 2026771741029840128), and LAMOST J062529.84-032411.9 (#576; TYC 4789-2924-1). MKCLASS final types and, where available, manual types derived in the present study are indicated. Some prominent lines of interest are identified. The asterisk marks the position of a ‘glitch’ in the spectrum of LAMOST J062529.84-032411.9.

tection of mCP stars (e.g. Hümmerich et al. 2018) and is a good starting point for further investigations.

To suit the special needs of our project, which is solely concerned with the identification and classification of mCP stars among a sample of early-type candidate stars, we opted to refine the MKCLASS peculiarity identification routine. The code was therefore altered to probe several additional lines, with the advantage that the new version is now able to more robustly identify traditional mCP star peculiarities. In addition, we enabled the identification of Cr peculiarities and, to some extent, He peculiarities, which are relevant to the classification of mCP stars. The choice of lines was dictated by the resolution and quality of the input material (i.e. LAMOST DR4 spectra), in particular concerning the availability of neighbouring continuum flux to probe a certain line and the numerous line blends due to the low resolution. We therefore stress that the resulting version of the MKCLASS code, which is referred to hereafter as MKCLASS\_mCP, has been created specifically for identifying and classifying mCP stars in LAMOST low-resolution spectra. Applying the code to spectra of other resolutions will require a corresponding update of the peculiarity classification routine and, perhaps, an update and enlargement of the employed standard star libraries (see below). Table 1 lists the lines and blends identified by MKCLASS\_mCP, as well as the spectral range in which the corresponding features are searched for. We note that at the resolution of the employed LAMOST spectra, all these lines are, to some extent, blended with other absorption lines. Nevertheless, the listed ions generally constitute the main contributors to these blends in mCP stars.

A sample output of MKCLASS\_mCP is provided in column five of Table 2. Further information on the interpretation of this output is provided below; a discussion of the accuracy of the derived classifications is provided in Section 3.2.

**Table 1.** Absorption lines and blends identified by the modified version of the MKCLASS code (MKCLASS\_mCP) and used in the identification and classification of mCP stars in the present study. The columns denote: (1) Blend/line. (2) Wavelength (Å). (3) Spectral range in which the corresponding feature was probed.

(1)	(2)	(3)
Blend/line	Wavelength (Å)	SpT_range
(Si II/Cr II/Sr II)	4076/77	B7–F5
(Si II/Eu II)	4128/30	B3–F2
Si II	3856	B3–F2
Si II	4200	B3–A2
Si II	5041	B3–F2
Si II	5056	B3–F2
Si II	6347	B3–F2
Si II	6371	B3–F2
Cr II	3866	B7–F2
Cr II	4172	B7–F2
Sr II	4216	B7–F2
Eu II	4205	B7–F2
He I	4009	B0–A0
He I	4026	B0–A0
He I	4144	B0–A0
He I	4387	B0–A0

We note that the Si II line at 5041 Å increases significantly with temperature type; therefore, different detection limits were applied depending on the investigated temperature range. Furthermore, the Si II 6347/71 Å lines were found to show a significant scatter in MKK standard stars. However, at the resolution of



the LAMOST spectra, the red Si II lines are a readily detectable and outstanding feature of strong Si stars and contribute significantly to an unambiguous detection of Si peculiarity, in particular as the corresponding lines in the blue-violet region are difficult to detect because of continuum flux issues (3856/62 Å) and blending issues (4076 Å and 4128/30 Å).

As has been described in Section 2.2, MKCLASS is a computer program that emulates the workflow of a human classifier in the traditional MKK spectral classification process, which involves comparing the input spectrum to a set of standard star spectra. It is therefore imperative to carefully select standard star libraries that match the input spectra in resolution and calibration-wise. MKCLASS comes with the two standard libraries *libr18* and *libnor36* (cf. Section 2.2), which, unfortunately, do not match the spectral resolution of the LAMOST low-resolution spectra. Furthermore, as far as we are aware of, a standard library based on LAMOST spectra does not exist.

In the framework of the LAMOST-*Kepler* project, Gray et al. (2016) presented MKK spectral classifications of more than 100 000 LAMOST spectra of about 80 000 objects situated in the *Kepler* field. The authors solved the above-mentioned issue by degrading the flux-calibrated LAMOST spectra to a resolution of  $R \sim 1100$  and truncating them to the 3800–5600 Å region in order to enable the use of MKCLASS with the flux-calibrated *libnor36* library (cf. also the MKCLASS documentation). Here we follow their approach, but we also searched for alternative methods, as degrading spectra obviously results in loss of information. This, however, is detrimental to the identification of the often subtle chemical peculiarities of our sample stars.

We synthesised a library of spectra using the program SPEC-TRUM<sup>6</sup> (Gray & Corbally 1994) and ATLAS9 model atmospheres (Castelli & Kurucz 2003), which is referred to hereafter as the *libsynth* library. Only dwarf spectra (luminosity class V) were synthesised because no models were available to reproduce the subtle differences in surface gravity among early-type giant stars. Furthermore, we collected a set of LAMOST standard star spectra (the *liblamost* library) by carefully choosing a grid of suitable high S/N spectra from the list presented by Gray et al. (2016). Only dwarf and giant spectra were chosen, as not enough suitable spectra of higher luminosity class objects were available to build up a corresponding grid. We note, however, that it has been well confirmed that mCP stars are generally main-sequence objects (cf. Netopil et al. 2017, and references therein, and Sections 1, 3.2, and 4.2); therefore, we do not expect that the absence of spectra of higher luminosity class objects in these two libraries significantly affects our results – in particular as the *libr18* and *libnor36* libraries boast corresponding spectra of all luminosity classes.

The stars and corresponding LAMOST spectrum identifiers of the *liblamost* library are given in the Appendix in Table C.1. Although it contains a very suitable grid of dwarf spectra, we note that the *liblamost* library is far from being a perfect set of standard star spectra (a corresponding quality flag that estimates the suitability of a spectrum as a standard is also provided in Table C.1). It contains a fast rotator and some spectra show ‘impurities’ not expected in MKK standards. These shortcomings will lead to increased uncertainties in the derivation of the temperature and luminosity classes. However, the library consists of spectra obtained with the same instrument – and hence, importantly, of the same resolution as our input spectra – and was extremely valuable in the identification of chemical pecu-

liarities. We nevertheless explicitly caution against using the *liblamost* library as a standard star library out of the context of the present investigation. We also emphasise the need for a standard star library based on LAMOST low-resolution spectra, which will greatly facilitate further research based on this excellent data source. The *liblamost* library may very well serve as a starting point; this, however, is beyond the scope of the present investigation.

In the following, an overview over the employed spectral libraries is presented. As an example, Figure 3 illustrates the F0V standard spectra from the corresponding libraries. We note that the *libsynth* and *liblamost* libraries only contain spectra in the approximate spectral type range of our sample stars.

- *libr18*: spectral range from 3800–4600 Å, resolution of 1.8 Å ( $R \sim 2200$ ), normalised and rectified spectra; all luminosity classes (Ia–V)
- *libnor36*: spectral range from 3800–5600 Å, resolution of 3.6 Å ( $R \sim 1100$ ), flux-calibrated and normalised spectra; all luminosity classes (Ia–V)
- *libsynth*: spectral range from 3800–4600 Å, smoothed to a resolution of 3.0 Å and an output spacing of 0.5 Å, flux-calibrated and normalised synthetic spectra; only dwarf spectra (luminosity class V); spectral types B5 to F5
- *liblamost*: spectral range from 3800–5600 Å, resolution  $R \sim 1800$ , flux-calibrated and normalised spectra; only dwarf and giant spectra (luminosity classes V and III); spectral types B3 to G0

mCP stars may exhibit peculiar Ca II K profiles and line strengths (Faraggiana 1987; Gray & Corbally 2009; Ghazaryan et al. 2018) as well as generally enhanced metal-lines. Several authors have therefore adopted a notation that indicates separate spectral types as derived from the Ca II K line (the k-type), the hydrogen lines (the h-type), and the general strength of the metal-lines (the m-type), in the same way as is usually done for CP1 stars. The MKCLASS code also assigns k/h/m-types in cases where discrepant spectral types are derived from the corresponding features. As mCP stars are prone to exhibiting marked Ca and He deficiencies (e.g. Gray & Corbally 2009; Ghazaryan et al. 2018) and often enhanced metal-lines, the hydrogen-line profile is a better indicator of the actual effective temperature (Gray & Corbally 2009). Where they have been derived by the code (or by manual classification), k/h/m types are listed in the present study.

For most stars, only minor differences in temperature and luminosity types were found between the results from the different spectral libraries. In cases where the same spectral type was derived more than once, the most common spectral type was adopted (cf. Table 2). If no common classifications existed, spectral types were favoured in the order *liblamost* > *libsynth* > *libnor36* > *libr18*. In the case of strong differences between the derived classifications, the corresponding spectra were visually inspected and the best fitting type was chosen.

To determine significant chemical peculiarities from the ‘raw’ MKCLASS\_mCP output, the number of detections  $N_{\text{det}}$  of the peculiar strength of a given line with the different standard star libraries ( $0 \leq N_{\text{det}} \leq 4$ ) was counted, which provides an estimation of significance. Obviously,  $N_{\text{det}} = 4$  is a very robust detection;  $N_{\text{det}} < 2$  detections, on the other hand, have to be viewed with caution. Furthermore, we required that the identification of overabundances cannot be based on a single strong line (with the exception of the Cr II 4172 Å line in the identification of a Cr peculiarity; see below).

<sup>6</sup> <http://www.appstate.edu/~grayro/spectrum/spectrum.html>

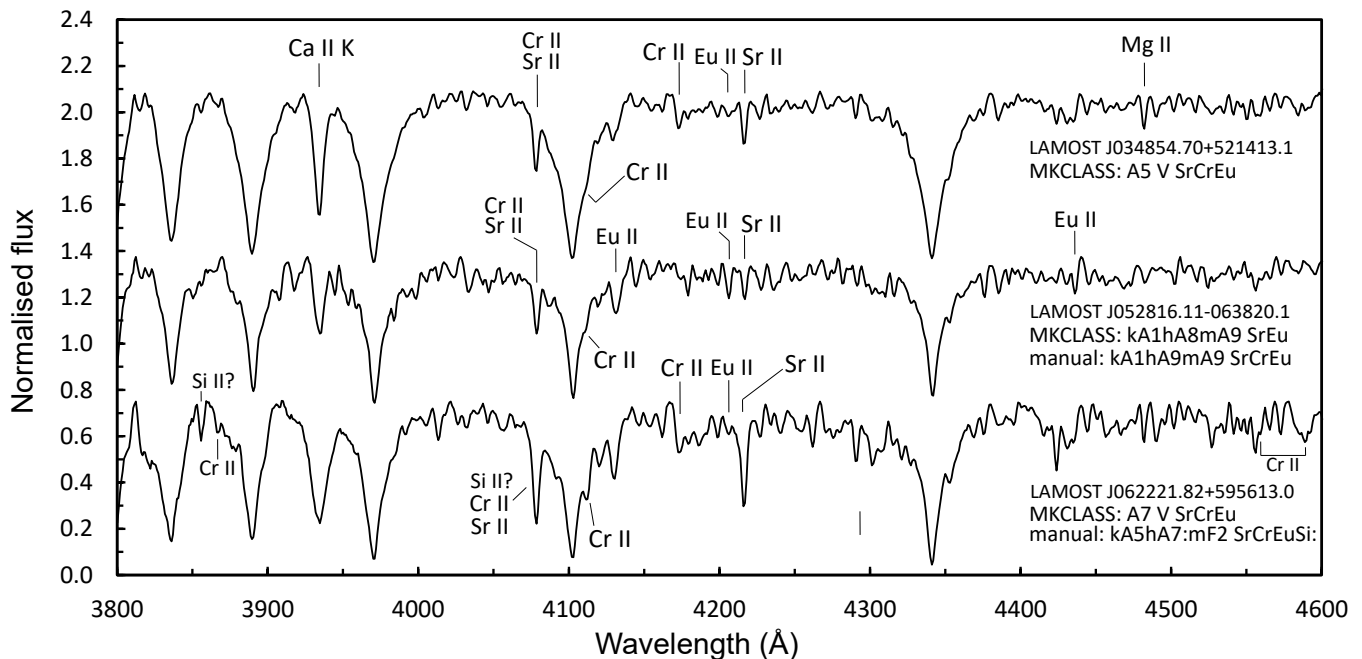


**Fig. 5.** Showcase of three newly identified ‘cool’ mCP stars, illustrating the blue-violet region of the LAMOST DR4 spectra of (from top to bottom) LAMOST J034854.70+521413.1 (#150; Gaia DR2 251609324623302400), LAMOST J052816.11-063820.1 (#344; TYC 4765-708-1), and LAMOST J062221.82+595613.0 (#561; TYC 3776-269-1). MKCLASS final types and, where available, manual types derived in the present study are indicated. Some prominent lines of interest are identified.

To come up with an approach that forms a compromise between spurious detections and overly high thresholds required a good amount of experimentation and experience in comparing the results of manual and automatic classification. Table 3 lists the conditions found to work best with the input material and our methodological approach.  $N_{\text{det}}(\lambda)$  is the number of detections of a peculiarly strong line at the specified wavelength (Å). For instance, a Cr peculiarity was flagged when (a) a strong Cr II 4172 Å line was detected with a least two different standard star libraries **or** (b) a strong Cr II 3866 Å line **and** a strong Cr II 4172 Å line were detected at least once **or** (c) a strong blend at 4077 Å was detected at least twice **and** a strong Cr II 4172 Å line was detected at least once.

Following the conventions of the MKK system, the peculiarity types ‘Si’, ‘Cr’, ‘Sr’, and ‘Eu’ were flagged according to the conditions given in Table 3 and attached to the temperature and luminosity types in the final spectral classification. Several stars in our sample that were not assigned any of the above mentioned peculiarity types nevertheless show strong blends at 4077 Å and/or 4130 Å. In these cases, we decided to add the non-standard suffixes ‘bl4077’ and ‘bl4130’ to the derived spectral types (e.g. ‘B8 IV bl4130’) if the corresponding blends had been detected at least twice. In these objects, apart from the strong blends, the peculiarities are either too subtle to have passed our significance criteria, no other significant features are present, or the code failed to identify them for some reason. Manual classification is necessary to throw more light on this matter (cf. Section 4.4).

In addition, we opted to probe the He I lines at 4009 Å, 4026 Å, 4144 Å, and 4387 Å to identify CP2 stars with weak He I lines and He-peculiar objects. The corresponding detection thresholds for all four standard star libraries were determined using the He lines of 626 apparently chemically-normal B stars with spectra boasting  $S/N > 100$ . The number of detections as

‘weak’ or ‘strong’ of the He lines with the different standard star libraries was counted and the results across all lines and libraries were added up to yield  $N_{\text{det}}(\text{He-wk})$  and  $N_{\text{det}}(\text{He-st})$ . He-weakness and He-overabundance were assumed when  $N_{\text{det}}(\text{He-wk}) > 2$  and  $N_{\text{det}}(\text{He-st}) > 2$ , respectively. In this way, we identified 55 mCP stars with weak He I lines and three mCP stars with apparently strong He I lines. As expected, these are mostly B7–B9 Si CP2 stars, which are notorious for their weak He lines, and mid-B type stars (likely He-peculiar objects). Interestingly, in three mid-B type stars, both weak and strong He I lines were identified, which strongly suggests He peculiarity. The corresponding suffixes ‘He-wk’ and ‘He-st’ were added to the derived spectral types. Several He-peculiar objects are discussed in Section 4.6.

In this way, peculiarities were identified in all but 36 stars from our sample, which highlights the efficiency of the chosen approach. The (mostly low S/N) spectra of the remaining objects were investigated manually and searched for the presence of chemical peculiarities. Most of these objects show subtle or complicated peculiarities that failed to meet the imposed significance criteria. Corresponding peculiarity types were manually added to the final spectral types. The remaining objects are a ‘mixed bag’ containing stars with enhanced metal-lines and strong flux depressions that nevertheless lack the traditional Si, Cr, Sr, Eu peculiarities and several He-peculiar objects. Appropriate comments were added to the tables, in which manually-derived peculiarity types and all further additions that are not directly based on the MKCLASS\_mCP output are highlighted.

### 3.2. Evaluation

As a test of the validity of our approach, we manually classified a sample of ten randomly chosen stars and compared our results with the final spectral types derived in the described man-

**Table 2.** Spectral classifications derived by manual classification and the MKCLASS\_mCP code. The columns denote: (1) Internal identification number. (2) LAMOST identifier. (3) Spectral type derived by manual classification. (4) MKCLASS\_mCP final type. (5) MKCLASS\_mCP output using the standard star libraries *libr18*, *libnor36*, *libsynth*, and *liblamost*.

(1)	(2)	(3)	(4)	(5)
No.	LAMOST ID	SpT_manual	SpT_MKCLASS_mCP	Output using <i>libr18/libnor36/libsynth/liblamost</i>
142	J034541.53+275631.8	kA3hA6mA6 SrCrEu	A6 V SrCrEu	kA4hA4mA8 bl4077 bl4130 Sr4216 Cr4172 Eu4205 A6 V bl4077 bl4130 Sr4216 Eu4205 A6 V bl4077 bl4130 Sr4216 Eu4205 A5 IV–V bl4077 bl4130 Sr4216
151	J035046.03+363648.2	B8 V Si	B8 IV Si	B6 IV–V Si5041 Si5056 Si6347 bl4130 B8 IV Si6347 bl4130 B8 IV Si5041 Si5056 Si6347 bl4130 B7 IV Si5041 Si5056 Si6347 bl4077 bl4130
232	J043201.64+471447.8	A2 V SrCrEu(Si)	A1 V SrCrEu	kA2hA6mA8 bl4077 Sr4216 Cr4172 Eu4205 A1 IV–V bl4077 bl4130 Sr4216 kA2hA3mA6 bl4077 bl4130 Sr4216 Cr4172 A1 V bl4077 bl4130 Sr4216
306	J051844.95+380605.3	B9 V SrCrEuSi	B9 IV SrCr	kB9hA0mA2 bl4077 bl4130 Sr4216 Cr4172 B9.5 III–IV bl4077 bl4130 Sr4216 Cr4172 kB9.5hA1mA3 bl4077 bl4130 Sr4216 Cr3866 Cr4172 B9 IV bl4077 bl4130 Sr4216 Cr4172
344	J052816.11-063820.1	kA1hA9mA9 SrCrEu	kA1hA8mA9 SrEu	A1 II–III bl4077 bl4130 Sr4216 Eu4205 kA2hA5mA9 bl4077 bl4130 Sr4216 Eu4205 kA1hA9mA8 bl4077 bl4130 Sr4216 Eu4205 kA1hA8mA9 Si3856 bl4077 bl4130 Sr4216 Eu4205
561	J062221.82+595613.0	kA5hA7:mF2 SrCrEuSi:	A7 V SrCrEu	A8 mA4 metal weak kA6hA8mF3 bl4077 bl4130 Sr4216 Cr3866 kA5hA7mF1 bl4077 bl4130 Sr4216 Cr3866 Cr4172 Eu4205 A7 V bl4077 bl4130 Sr4216 Cr4172
596	J062909.51+023823.8	B8 V Si	B8 IV–V Si	B8 IV–V Si5041 Si5056 Si6347 Si6371 bl4130 B8 IV–V Si5041 Si5056 Si6347 Si6371 bl4130 B8 IV Si5041 Si5056 Si6347 Si6371 bl4130 B8 IV–V Si5041 Si5056 Si6347 Si6371 bl4077 bl4130
724	J065511.76+115158.3	A7 V SrCrEu	A7 V SrEu	A8 V bl4077 bl4130 Sr4216 Eu4205 A9 V bl4077 bl4130 Sr4216 Eu4205 A7 V Si6347 bl4077 bl4130 Sr4216 Eu4205 A7 V bl4077 bl4130 Sr4216
732	J065647.94+242958.8	A0 V SiSrCr	B9.5 V Sr	kB9hA7mA5 Sr4216 Cr3866 Eu4205 B9.5 IV–V bl4077 bl4130 kB9.5hA3mA3 bl4077 Sr4216 B9.5 V bl4077 bl4130
929	J195631.74+253407.8	B8 V SiCr	B8 IV–V Si	B8 V Si5041 Si5056 Si6347 Si6371 bl4077 bl4130 B8 IV–V Si5056 Si6347 Si6371 bl4077 bl4130 B8 IV–V Si5041 Si5056 Si6347 Si6371 bl4077 bl4130 A0 II–III Si5056 Si6347 Si6371 bl4077 bl4130

**Table 3.** Conditions employed to flag the presence of an overabundance from the ‘raw’ MKCLASS\_mCP output. The columns denote: (1) Overabundant ion. (2) Condition(s) required to be met for a detection to be deemed significant.

(1)	(2)
Ion	condition(s)
<b>Si II</b>	$(N_{\text{det}}(3856) + N_{\text{det}}(4200) + N_{\text{det}}(5041) + N_{\text{det}}(5056) + N_{\text{det}}(6347) + N_{\text{det}}(6371)) > 1$
<b>Cr II</b>	$N_{\text{det}}(4172) > 1$ OR $(N_{\text{det}}(3866) > 0 \text{ AND } N_{\text{det}}(4172) > 0)$ OR $(N_{\text{det}}(4077) > 1 \text{ AND } N_{\text{det}}(4172) > 0)$
<b>Sr II</b>	$(N_{\text{det}}(4077) > 0 \text{ AND } N_{\text{det}}(4216) > 0)$
<b>Eu II</b>	$(N_{\text{det}}(4130) > 2 \text{ AND } N_{\text{det}}(4205) > 0)$

ner from the MKCLASS\_mCP output, which, for convenience, are termed hereafter the ‘MKCLASS final types’. In addition, we visually inspected the spectra of about 100 further stars to check for the presence of peculiarly strong lines and evaluate the reliability of the classifications. The results from the manual classification are shown in Table 2 and highlight the good agreement between the manually- and automatically-derived (hydrogen-line) temperature types. In general, we estimate the uncertainty of the derived temperature types to be  $\pm 1$  subclass. This, however, increases to about  $\pm 2$  subclasses towards later and more pecu-

liar mCP stars for which the classification is notoriously difficult and, for the most extreme objects, unreliable. Figures 4 and 5 showcase, respectively, three ‘hot’ mCP stars and three ‘cool’ mCP stars, which have been newly identified as such in the present study. MKCLASS final types and, where available, manual types from Table 2 are indicated.

There is also a generally good agreement in regard to the derived peculiarity types. However, with our approach, we obviously missed the presence of peculiarities in several objects (Table 2). A further investigation of these stars shows that this has been mostly due to either the imposed significance criteria, weak or complicated peculiarities, or the absence of continuum flux to probe certain lines (or a combination thereof). A good case in point is LAMOST J065647.94+242958.8 (#732; TYC 1898-1408-1), whose blue-violet spectrum is shown in the upper panel of Figure 6. It shows enhanced Si II lines at 3856/62 Å, 4128/31 Å, and 4200 Å. Furthermore, strong Cr II lines are present at 3866 Å, 4111 Å, 4172 Å, 4559 Å, and 4588 Å. The blend at around 4077 Å is notoriously difficult to interpret and can contain contributions from Si II, Cr II, and Sr II. The strong Sr II line at 4216 Å, however, indicates the presence of a Sr peculiarity. Consequently, we have classified this star as A0 V SiSrCr. The MKCLASS\_mCP code missed the rather subtle Si and Cr peculiarities (MKCLASS final type: B9.5 V Sr).



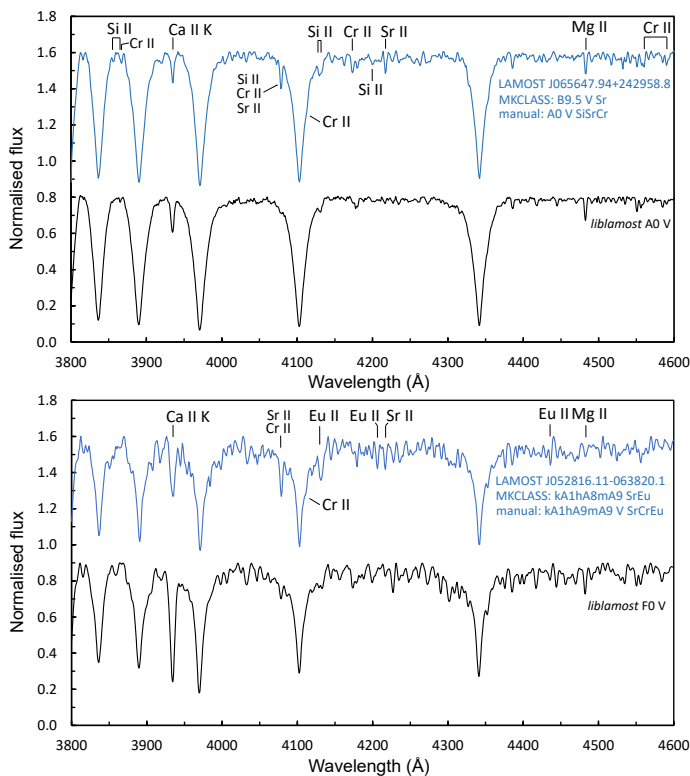


**Fig. 6.** Upper panel shows a comparison of the blue-violet spectra of the mCP star LAMOST J065647.94+242958.8 (#732; TYC 1898-1408-1; manual type: A0 V SiSrCr; MKCLASS final type: B9.5 V Sr) to the *liblamost* A0 V standard spectrum. Lower panel illustrates a comparison of the blue-violet spectra of the mCP star LAMOST J052816.11-063820.1 (#344; TYC 4765-708-1; manual type: kA1hA9mA9 SrCrEu; MKCLASS final type: kA1hA8mA9 SrEu) to the *liblamost* F0 V standard spectrum. Some prominent lines of interest are indicated. We note the weak Ca II K line with a peculiar profile and the unusual profile of the H $\epsilon$  line in LAMOST J052816.11-063820.1.

The bottom panel of Figure 6 illustrates the case of LAMOST J052816.11-063820.1 (#344; TYC 4765-708-1; also shown in Figure 5), a cool CP2 star that may serve as a warning and an example illustrating the difficulty of classifying the more extreme mCP stars, which may possess peculiarities that render their spectra difficult to match to any standard star (Gray & Corbally 2009). The star exhibits a weak Ca II K line with a peculiar profile. While the hydrogen-line profile points to a late A-type star, the broad K line is that of an early A-type star and reasonably matched by that of an A1 V standard. As CP2 stars are prone to exhibiting marked Ca deficiencies (e.g. Gray & Corbally 2009; Ghazaryan et al. 2018), the hydrogen-line profile is a better indicator of the actual effective temperature than the K line strength (Gray & Corbally 2009), hence LAMOST J052816.11-063820.1 is obviously a late-type mCP star. However, while the H $\gamma$ , H $\delta$ , H $\delta$ , and H $\epsilon$  lines are reasonably well matched by that of an A9 V star, the H $\epsilon$  line exhibits an unusual profile, which makes it difficult to match the hydrogen-line profile to that of any standard star. We also note the unusually weak Mg II line at 4481 Å. The MKCLASS\_mCP code duly assigned final k/h/m-types of A1, A8, and A9; we prefer k/h/m-types of A1, A9, and A9.

The spectrum of LAMOST J052816.11-063820.1 shows strong blends at 4077 Å and 4130 Å, which – judging from the strong lines at 4216 Å (Sr II), 4205 Å (Eu II), and 4435 Å (Eu II) – are mainly caused by overabundances of Sr and Eu. The strong

Cr II lines at 3866 Å and 4111 Å (the bump in the red wing of H $\delta$ ) indicate a Cr overabundance; a corresponding enhanced line at 4172 Å, however, is notably absent. We have classified this star as kA1hA9mA9 V SrCrEu. The MKCLASS\_mCP code duly identified the main peculiarities (MKCLASS final type: kA1hA8mA9 SrEu).

The examples show that the peculiarity types derived in the present investigation are in many cases not exhaustive but rather denote the main peculiarities present. They are still very useful for first orientation and an excellent starting point for more detailed investigations; they are furthermore suited to statistical studies (cf. Section 4.4).

Some cautionary words are necessary in regard to luminosity classification. It is well known that problems with the luminosity classification may arise by the confusion of luminosity criteria and mCP star characteristics or peculiarities. In the early A-type stars, luminosity classification is primarily based on hydrogen-line profiles. The mCP stars, in general, are slow rotators that display narrow lines and hydrogen-line profiles that are easily misinterpreted as belonging to stars of higher luminosity. Indeed, the hydrogen-line profiles of many late B- and early A-type stars of our sample are best matched by standards of luminosity class III although there is no further indication that these stars are in fact giant stars. Additional confusion may arise due to peculiarly strong lines that are also used in luminosity classification. Si II lines, for example, are enhanced in giants and supergiants as well as in several types of mCP stars, which might lead to corresponding misclassifications (Loden & Sundman 1989). This holds especially true for classifications based on photographic plates or low S/N spectra. In regard to CP1 stars, the term ‘anomalous luminosity effect’ has been coined, which describes the perplexing situation that luminosity criteria from different regions of the spectrum indicate different luminosities. This also applies at least partly to mCP stars, which may show strong general enhancements of metal-lines in their spectra that are reminiscent of much cooler stars. Furthermore, while obtaining the hydrogen-line type is fairly straightforward for most mCP stars, the more peculiar objects show distorted atmospheres and unusual and peculiar hydrogen-line profiles that may not match any standard star (Gray & Corbally 2009), which may result in classification errors. Abnormal hydrogen-line profiles are especially observed in cool mCP stars (Kochukhov et al. 2002).

These issues also impact automatic classification routines such as the MKCLASS code and will surely be at the root of the high luminosity classification of many of our sample stars, which should be regarded with caution. It has been well confirmed that mCP stars are generally main-sequence objects (e.g. Netopil et al. 2017 and references therein) and the results from the colour-magnitude diagram (CMD) (Section 4.2) fully support this finding. A detailed analysis of this issue is necessary but beyond the scope of the present investigation.

At this point, we would like to also recall that at least half of the mCP stars are spectroscopic variables, that is, the observed line strengths may vary considerably over the rotation period (e.g. Gray & Corbally 2009), which should always be kept in mind when working with mCP star spectra.

Table A.1 in the Appendix presents the MKCLASS final types along with essential data for our sample stars.

## 4. Discussion

This section discusses properties of our final sample such as magnitude distribution, distances from the Sun, evolutionary

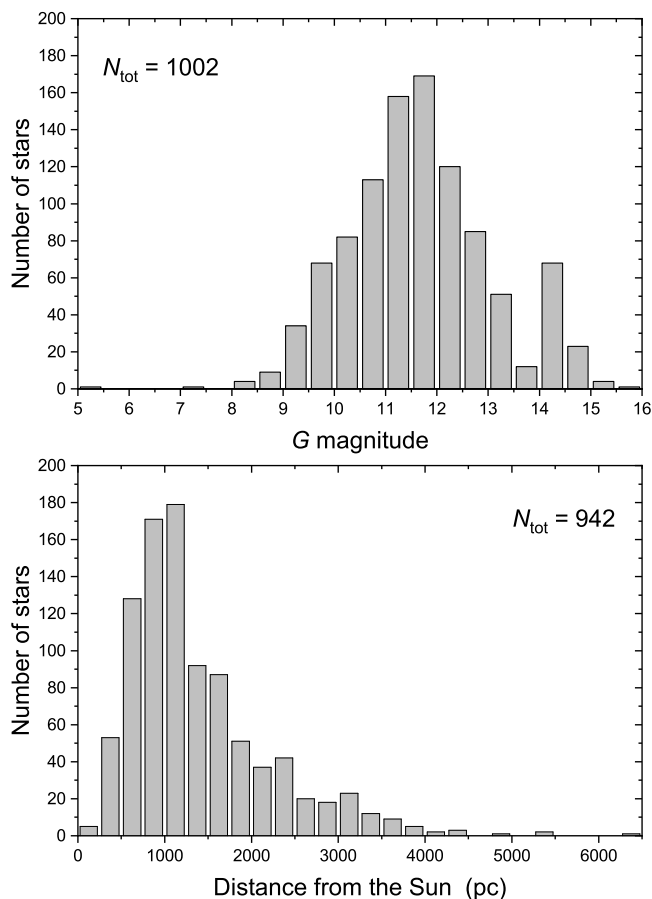


**Fig. 7.** Histograms of the  $G$  magnitudes (upper panel) and distances from the Sun (lower panel). For the construction of the latter, only stars with absolute parallax errors less than 25 % were employed.

status, and their distribution in space, and discusses interesting objects such as the eclipsing binary system LAMOST J034306.74+495240.7.

#### 4.1. Magnitudes and distances from the Sun

In Figure 7, we present the histograms of the  $G$  magnitudes and the distances from the Sun of our sample stars. The magnitude distribution peaks between 11th and 12th magnitude, which corresponds to a distance of about 1 kpc for the investigated range of spectral types. While our sample contains only a few new mCP stars within 500 pc around the Sun, there is a significant number of objects beyond 2 kpc, which might help to shed more light on the Galactic radial metallicity gradient (Netopil et al. 2016) and its influence on the formation and evolution of CP stars.

In summary, our sample is a perfect extension to the mCP stars listed in the catalogue of Renson & Manfroid (2009), which are on the average closer and brighter, peaking at 9th magnitude.

#### 4.2. Evolutionary status

In the following sections, we investigate the evolutionary status of our sample stars in the  $(BP - RP)_0$  versus  $M_{G,0}$  and mass versus fractional age on the main sequence spaces. We caution that, due to the imposed selection criteria (cf. Section 2.3.2), our

sample is biased towards stars showing a conspicuous 5200 Å flux depression in the low-resolution LAMOST spectra. Therefore, our results, while being based on a statistically significant sample size, have to be viewed with caution and their general validity needs to be tested by a more extended sample selected via different methodological approaches.

##### 4.2.1. Colour-magnitude diagram

To investigate the astrophysical properties of our sample stars in a CMD, we employed the homogeneous Gaia DR2 photometry from Arenou et al. (2018). Most of our sample stars are situated within the Galactic disk farther than 500 pc from the Sun; therefore, interstellar reddening (absorption) cannot be neglected. Because hardly any objects have Strömgren-Crawford indices available (Paunzen 2015), we relied on the published reddening map by Green et al. (2018). To interpolate within this map, parallaxes were directly converted to distances. To limit the error of the absorption values to 0.1 mag, only objects with relative parallax errors of at most 25 % (942 in total) were used. The transformation of the reddening values was performed using the relations:

$$E(B - V) = 0.76E(BP - RP) = 0.40A_G. \quad (1)$$

These relations already take into account the conversion to extinction in different bands using the coefficients as listed in Green et al. (2018).

In Figure 8, we present the CMD of our sample stars together with PARSEC isochrones (Bressan et al. 2012) for solar metallicity  $[Z] = 0.020$ . We favour this value because it has been shown to be consistent with recent results of Helioseismology (Vagnozzi 2019). Also included is the reddening vector according to an uncertainty of 0.1 mag for  $E(B - V)$ . About 20 stars are situated below the zero-age main sequence (ZAMS) to such an extent that it cannot be explained by errors in the reddening estimation. Inconsistent photometry or binarity might possibly have led to the observed positions but, with the available data, we are unable to shed more light on this matter.

The stars LAMOST J061609.42+265703.2 (#537;  $M_{G,0} = +7.78$  mag,  $(BP - RP)_0 = +0.840$  mag), LAMOST J064757.48+105648.2 (#678;  $M_{G,0} = +7.75$  mag,  $(BP - RP)_0 = +1.721$  mag), and LAMOST J202943.73+384756.6 (#943;  $M_{G,0} = +3.61$  mag,  $(BP - RP)_0 = +1.180$  mag) are not plotted in the CMD because they lie outside the chosen boundaries. The available spectra clearly confirm that they are mCP stars. We double-checked the identifications in the Gaia DR2 and LAMOST catalogues and searched for nearby objects on the sky that might have influenced the photometry, albeit with negative results. In the case of LAMOST J202943.73+384756.6, we strongly suspect that binarity might be at the root of the observed outlying position. Its spectrum has an unusual black-body curve, and its spectral energy distribution (SED) looks like the superposition of two objects, with a clearly visible infrared excess. However, we are unable to explain the reasons behind the observed inconsistent photometry for the other two stars.

From the distribution of stars in Figure 8, we conclude that the majority of our sample stars is between 100 Myr and 1 Gyr old. There are only a few very young stars and an accumulation of objects older than 300 Myr.

The here employed isochrones have been calculated for stars of standard composition, that is, chemically normal stars, assuming solar metallicity  $[Z] = 0.020$ . As the chemical bulk composition of mCP stars is unknown, however, the choice of the

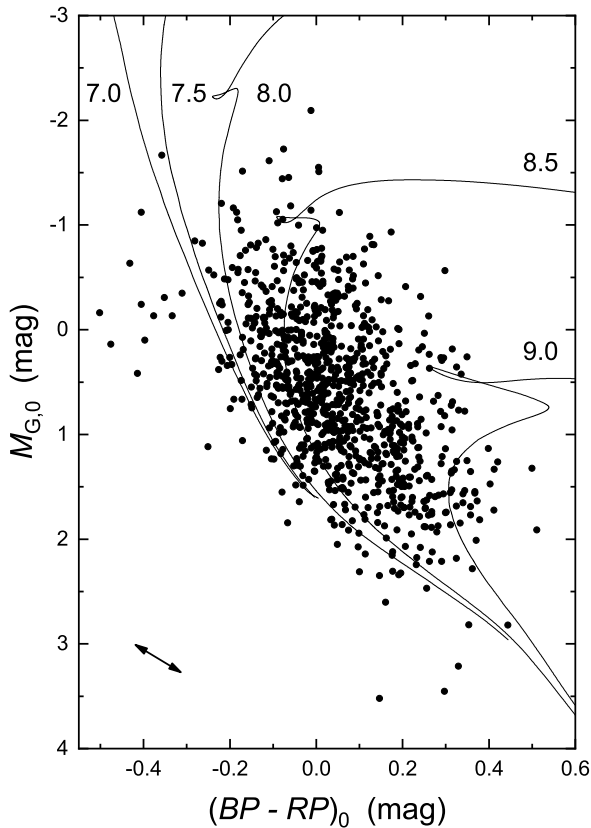


**Fig. 8.**  $(BP - RP)_0$  versus  $M_{G,0}$  diagram of our sample stars, together with PARSEC isochrones for solar metallicity  $[Z] = 0.020$  (listed are the logarithmic ages). The arrow indicates the reddening vector for the maximum expected error due to the employed reddening map and the parallax error.

right chemical composition for the theoretical tracks remains an open question (cf. e.g. the discussion in Bagnulo et al. 2006). The main question is whether the apparent overabundances encountered at the surface are representative for the whole stellar interior. If diffusion is assumed as the main mechanism (in line with most theoretical studies), the overall abundance will be close to solar because corresponding underabundances are expected in the stellar interior. All current isochrone calculations are based on assuming a  $[Z]$  value for the whole star; it is currently not possible to consider different  $[Z]$  values for different layers of the stellar atmosphere. A detailed discussion of the influence of  $[Z]$  on the determination of age on the main sequence is provided in the following section.

#### 4.2.2. Mass versus age on the main sequence

To examine the evolutionary status of our sample stars in more detail, we investigated the distribution of mass ( $M$ ) versus age on the main sequence. Age on the main sequence ( $\tau$ ) is here defined as the fraction of life spent on the main sequence, with the ZAMS corresponding to  $\tau = 0\%$  and the terminal-age main sequence (TAMS) to  $\tau = 100\%$ . Only objects with absolute parallax errors less than 25% were considered in this process. We again used PARSEC isochrones (Bressan et al. 2012) for solar metallicity  $[Z] = 0.020$  and  $7.0 < \log t < 10.0$  (step size: 0.025). Bearing in mind the observational errors, the chosen step size is

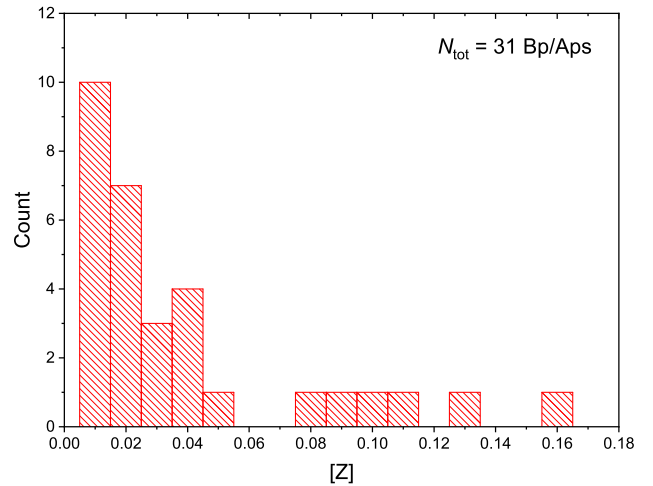


**Fig. 9.** Distribution of  $[Z]$  values for the CP2 stars from the Ghazaryan et al. (2018) catalogue with a least three measurements of C, N, O and S.

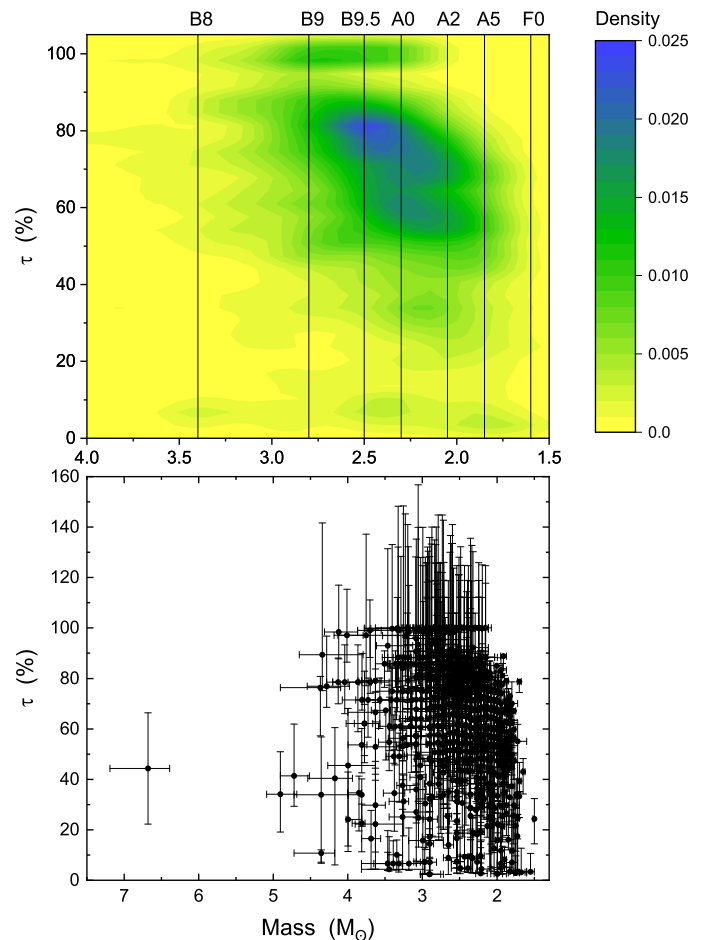


**Fig. 10.** Mass versus fractional age on the main sequence ( $\tau$ ) distribution assuming solar metallicity  $[Z] = 0.020$  for the 903 sample stars fulfilling the imposed accuracy criteria. Upper panel shows a density plot for masses up to  $4 M_{\odot}$ . The position of the spectral types has been based on the information given in Pecaut & Mamajek (2013).

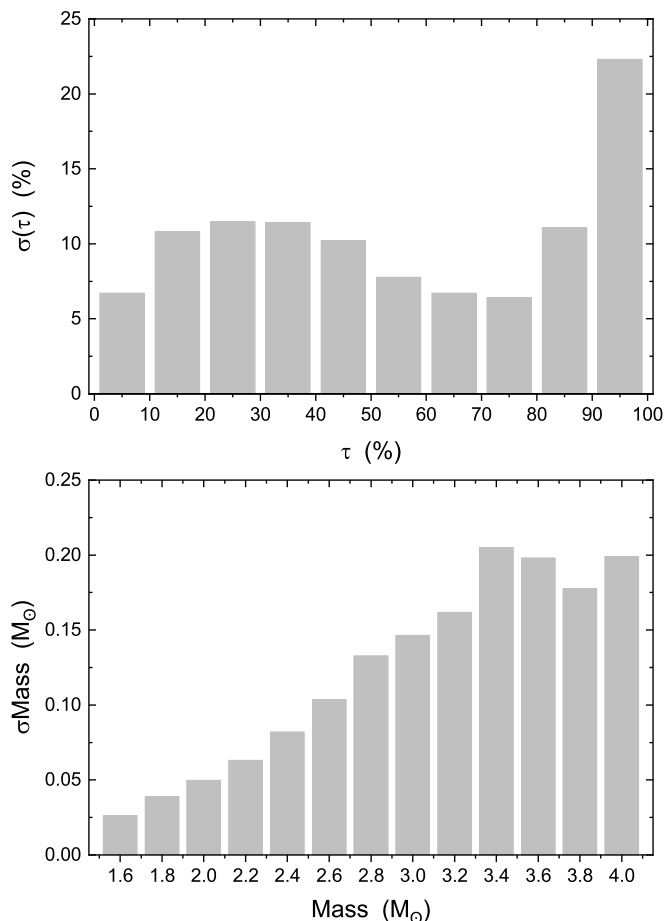


**Fig. 11.** Distributions of errors for the derived fractional ages on the main sequence ( $\tau$ ; upper panel) and masses (lower panel) assuming solar metallicity  $[Z] = 0.020$ .

sufficient not to run into numerical inaccuracies due to the grid being too coarse. We did not interpolate within the grid but always selected the point with minimal Euclidean distance to the observed value in the  $(BP - RP)_0$  versus  $M_{G,0}$  space. Only grid points representing the main sequence (flagged “1” in the corresponding isochrones) were used. As next step, we discarded all data points with a distance of more than 0.05 mag between observed value and theoretical grid point, which guarantees the exclusion of points below the ZAMS and above the TAMS. In this way, masses and ages were derived for 903 sample stars fulfilling the imposed accuracy criteria.

As final step, the lifetime on the main sequence was calculated for a given mass using the upper envelope of the isochrone grid. With this parameter, the fractional lifetime of a star on the main sequence can be easily calculated. To compute upper and lower limits for  $\tau$  and  $M$ , the full error ellipse was taken into account. This procedure is described in more detail in Kochukhov & Bagnulo (2006).

Table B.1 lists the derived masses and fractional ages on the main sequence for solar metallicity  $[Z] = 0.020$ , which are graphically represented in Figure 10. The density plot in the upper panel clearly shows that there are only very few stars in our sample younger than  $\tau < 20\%$ . Most stars have a relative age of  $\tau \geq 60\%$ .

To check the reliability of our results, we have investigated the error distribution of the age and mass estimates in detail.

This analysis was done for solar metallicity. We have investigated the influence of the assumed metallicity in a second step. For this, masses were binned in  $0.2 M_{\odot}$  and ages in 10% intervals. Sizes have been chosen to guarantee the availability of a significant number of data points in each bin. Figure 11 illustrates the corresponding histograms. The absolute errors of the masses increase linearly until  $M = 3.4 M_{\odot}$  and then flatten out, which means that the relative error stays constant over the whole investigated mass range. The situation is different for the derived ages; up to  $\tau \leq 90\%$ , absolute errors remain almost constant. Relative errors obtained for younger stars, therefore, are significantly larger than for old ones. This, however, does not impact our conclusions (see below). The significant increase of the errors for the last age bin is due to the higher density of isochrones in this region; furthermore, taking the error ellipse into account, some stars may be located above the TAMS.

In order to evaluate the effect of the chosen metallicity on our results, we have investigated the  $[Z]$  distribution for CP2 stars from the Ghazaryan et al. (2018) catalogue with a least three measurements of C, N, O, and S. These light elements were chosen because they contribute the most to the derived  $[Z]$  values. They appear significantly underabundant in most CP2 stars, which therefore show lower  $[Z]$  values than chemically normal stars (Figure 9). For most objects, we find  $[Z]$  values in the range from about 0.008 to 0.060. From the reference source, we were not able to estimate the errors of the derived  $[Z]$  values, which mainly depend on the errors of the individual abundance determinations; these, however, are mostly not available.

We emphasise that all available isochrones use scaled abundances according to the abundance pattern of the Sun. Whether this approximation can also be applied to CP stars remains at the present time unknown (cf. Figure 1 of Ghazaryan et al. 2018). On the basis of open cluster members, Bagnulo et al. (2006) investigated the influence of the overall metallicity on the error of the age determination for CP2 stars, using metallicities of  $[Z] = 0.020$  (solar) and  $[Z] = 0.008$ , as derived from the corresponding host clusters. As clusters with  $[Z] > 0.020$  are very rare in the Milky Way (Netopil et al. 2016), no isochrones for metallicities exceeding solar metallicity were considered in their study.

When estimating  $\tau$ , we have to consider two effects, which are illustrated in Figure 12. As is well known, lines of constant  $\tau$  are not distributed equally across the main sequence (Figure 12, upper panel). For a constant value of  $(BP - RP)_0$ , they are much tighter in terms of  $M_{G,0}$  for the first  $\sim 70\%$  of the main-sequence lifetime. The total interval of  $M_{G,0}$  from ZAMS to TAMS spans about 2.6 mag, whereas the intervals covered to  $\tau = 25\%$  and  $\tau = 50\%$  amount to only 0.3 mag and 0.7 mag, respectively.

The lower panel of Figure 12 explores the impact of isochrones of different metallicity on the positions of the ZAMS and TAMS. The magnitude differences between the positions of the ZAMS are nearly constant and amount to 0.4 mag, which corresponds to an age difference of about 30% at the ZAMS. This means that a ZAMS star of solar metallicity ( $[Z] = 0.020$ ) would have already spent 30% of its main-sequence lifetime for  $[Z] = 0.008$  but would be situated 0.4 mag below the ZAMS for  $[Z] = 0.060$ . This illustrates the dilemma elicited by the lack of knowledge of the overall metallicity of mCP stars and the resulting loss of accuracy, as clearly demonstrated by Bagnulo et al. (2006). The uncertainty is largest for stars near the ZAMS and has to be considered together with the distribution of errors for a given distinct metallicity (Figure 11). However, because individual  $[Z]$  values and their errors are unavailable for our sample

stars, we are not able to provide reliable estimations of the contribution to the computed errors.

Figure 13 illustrates the mass versus  $\tau$  distributions for all three investigated isochrones. The majority of our sample stars is situated in the rather narrow spectral range from B8 to A0 (cf. Section 4.4). However, there is also a lesser but significant amount of stars with spectral types between A5 and F0. Any calibrated mass distribution should represent these results to some extent. The lower-metallicity isochrone ( $[Z] = 0.008$ ) yields mainly old ( $\tau > 75\%$ ) and cooler (later than spectral type A0) stars; no young stars are present. On the other hand, adopting the isochrone for  $[Z] = 0.060$  results in a quite homogeneous age and mass distribution. However, there is a lack of stars cooler than A5, in conflict with the observations. Overall, as expected, none of the employed isochrones is suitable to reproduce the observed distribution of spectral types. Nevertheless, assuming solar metallicity offers the best compromise, with most stars situated in the late B-type realm and a tail of objects extending down to spectral type F0.

To further tackle this important problem, a modern and detailed abundance analysis of the light elements is needed. The current available data are rare and mainly based on the assumption of local thermodynamical equilibrium (Roby & Lambert 1990). For the relevant spectral type domain, almost all suitable spectral lines (i.e. lines of sufficient strength) are situated in the spectral region redwards of  $6000 \text{ \AA}$ . Unfortunately, the medium-resolution spectra of the LAMOST survey, which should be sufficient in terms of resolution, do not cover a significant amount of the specified spectral region (Zhang et al. 2020).

Finally, diffusion calculations for light elements are needed to estimate the influence of the magnetic field and to what extent the observed surface abundances are representative of the stellar composition. Until now, however, because of the lack of corresponding observations, such calculations are not available (Stift & Alecian 2012). Therefore, in the following, we have adopted the results for solar metallicity ( $[Z] = 0.020$ ) as best approximation. Assuming isochrones for lower  $[Z]$  values would lead to the derivation of older fractional ages (cf. Figure 13).

Hubrig et al. (2000) put forth the hypotheses that mCP stars with masses  $M < 3 M_{\odot}$  are concentrated towards the centre of the main-sequence band and that magnetic fields only appear in stars that have completed about 30% of their lifetime on the main sequence. In their investigation of the evolutionary status of mCP stars, Kochukhov & Bagnulo (2006) demonstrated that mCP stars with  $M > 3 M_{\odot}$  are distributed homogeneously among the main sequence. They further identified 22 young ( $\tau < 30\%$ ) mCP stars among their sample stars with  $M \leq 3 M_{\odot}$ , thereby rejecting the proposal of Hubrig et al. (2000) that all observably magnetic low-mass CP stars have completed a significant fraction of their main-sequence lifetime. That very young (ZAMS to 25% on the main sequence) mCP stars do exist has been unambiguously demonstrated by several studies on the basis of members of open clusters (cf. e.g. Bagnulo et al. 2003, Pöhl et al. 2003, Landstreet et al. 2007, and Landstreet et al. 2008).

Nevertheless, Kochukhov & Bagnulo (2006) also find an uneven distribution for mCP stars with masses of  $M < 3 M_{\odot}$ , in particular for stars with  $M \leq 2 M_{\odot}$ , which tend to cluster in the centre of the main-sequence band. Confirming their previous results, Hubrig et al. (2007) again found that mCP stars with  $M < 3 M_{\odot}$  are concentrated towards the centre of the main-sequence band.

As is obvious from Figure 10, most of our sample stars are situated in the  $2 \leq M_{\odot} \leq 3$  bin. In agreement with the results of the aforementioned studies, we also find an uneven distribution of the fractional lifetime; however, our sample stars boast a mean

fractional age of  $\tau = 63\%$  (standard deviation of 23%; cf. Figure 14). Young mCP stars, while undoubtedly present, are conspicuously underrepresented in our sample.

In summary, our results strongly suggest an inhomogeneous age distribution among low-mass ( $M < 3 M_{\odot}$ ) mCP stars as hinted at by previous studies. However, we stress that our sample is biased towards mCP stars showing a conspicuous  $5200 \text{ \AA}$  flux depression in the low-resolution LAMOST spectra and has not been selected on the basis of an unbiased, direct detection of a magnetic field. Therefore, our results have to be viewed with caution and their general validity needs to be tested by a more extended sample selected via different methodological approaches. It remains to be sorted out in what way the occurrence of the  $5200 \text{ \AA}$  depression is connected with this result, in particular why this feature is apparently much more prominent in older stars. Several studies have shown that the  $5200 \text{ \AA}$  depression increases with magnetic field strength and the atmospheric metal content (e.g. Kochukhov et al. 2005; Khan & Shulyak 2006).

Our analysis has been based on a statistically significant sample of mCP stars. Furthermore, due to the applied methods, it is not impacted by potential error sources that have been proposed to influence the results of former studies, such as a displacement of stars from the ZAMS by the application of negative Lutz-Kelker corrections or incorrect  $T_{\text{eff}}$  values caused by the anomalous flux distributions of mCP stars (cf. e.g. the discussions in Kochukhov & Bagnulo 2006 and Netopil et al. 2008). Even if the here derived error margins had been significantly underestimated, which we see no reason to believe, the general conclusion would hold. However, we caution that individual  $[Z]$  values and their errors are not available for our sample stars and that the influence of  $[Z]$  on the derived fractional ages is large.

#### 4.3. Space distribution

To investigate the location of our sample stars in the Galactic [XYZ] plane, the corresponding coordinates were obtained from a conversion of spherical Galactic coordinates (latitude and longitude) to Cartesian coordinates using the distance  $d$  from Bailer-Jones et al. (2018). In this work, the positive X-axis points towards the Galactic centre, the Y-axis is positive in the direction of Galactic rotation and the positive Z-axis points towards the north Galactic pole. Only objects with absolute parallax errors less than 25% were considered in this process. 942 stars satisfied this criterion.

We divided our sample in candidate members of the thin disk (scale height of 350 pc) and the thick disk (1200 pc). The scale heights were taken from Ojha (2001) and Aumer & Binney (2017). Our results are shown in Figure 15. From the sample of 942 stars, 797 objects likely belong to the thin disk and 135 objects to the thick disk. The remaining ten stars qualify for being members of the halo population and are thus worth a closer look.

As a first step, we checked the spectra of the halo star candidates and confirmed that all objects exhibit the typical spectral features of mCP stars and a clearly visible flux depression. For the calculation of the total spatial velocity  $v_{\text{tot}}$ , the radial velocity (RV) is needed. Data from the LAMOST survey include automatically measured RV information of the spectra (Anguiano et al. 2018). We checked the reliability of these values for mCP stars, that is, the spectral range from late B- to early F-type objects, by searching for common entries with the RV catalogue of Kharchenko et al. (2007). In total, 11 stars were found that are common to both our sample and this catalogue. Some of these objects boast more than one spectrum in LAMOST



**Table 4.** Kinematic and astrometric data for the ten stars of our sample with a height larger than 1200 pc above the Galactic plane. The columns denote: (1) Internal identification number. (2) LAMOST ID. (3) MKCLASS final type. (4) X-coordinate towards the Galactic centre. (5) Y-coordinate in direction of Galactic rotation. (6) Z-coordinate towards the north Galactic pole. (7) Radial velocity ( $R_V$ ) taken from LAMOST DR4. (8) Standard deviation of  $R_V$ . (9) Total spatial velocity ( $v_{\text{tot}}$ ). (10) Standard deviation of  $v_{\text{tot}}$ .

(1)	(2)	(3)	(4)	(5)	(6)	(7)	(8)	(9)	(10)
No.	LAMOST_ID	SpT_final	X (pc)	Y (pc)	Z (pc)	$R_V$ (km s $^{-1}$ )	$\sigma_{R_V}$ (km s $^{-1}$ )	$v_{\text{tot}}$ (km s $^{-1}$ )	$\sigma_{v_{\text{tot}}}$ (km s $^{-1}$ )
816	J073950.01+201812.7	B9 IV–V SrCrEu	–3305	–1170	+1239	+71	4	74	7
859	J091053.70+285032.7	A9 V SrCrEu	–1592	–496	+1487	–24	9	44	11
870	J104323.95+045214.3	A1 IV–V CrEu	–440	–875	+1265	+23	3	30	4
873	J114130.23+403822.7	B9 IV–V CrEuSi	–480	+125	+1380	–43	5	98	16
875	J122139.23+383309.5	kA2hA4mA7 bl4077 bl4130	–346	+202	+1732	–42	1	133	10
876	J122746.05+113635.3	B8 IV Si (He-wk)	+142	–665	+2298	+182	5	292	39
879	J140422.54+044357.9	kA4hA7mF0 SrCrEu	+703	–202	+1355	–55	15	200	23
880	J150331.87+093125.4	A8 V SrCrEu	+1233	+213	+1736	–38	5	312	33
881	J155549.85+401144.4	B8 IV Si	+1491	+3070	+4063	+90	5	96	10
895	J181156.38+523411.4	B7 IV–V Si	+635	+3869	+2002	–6	5	147	31

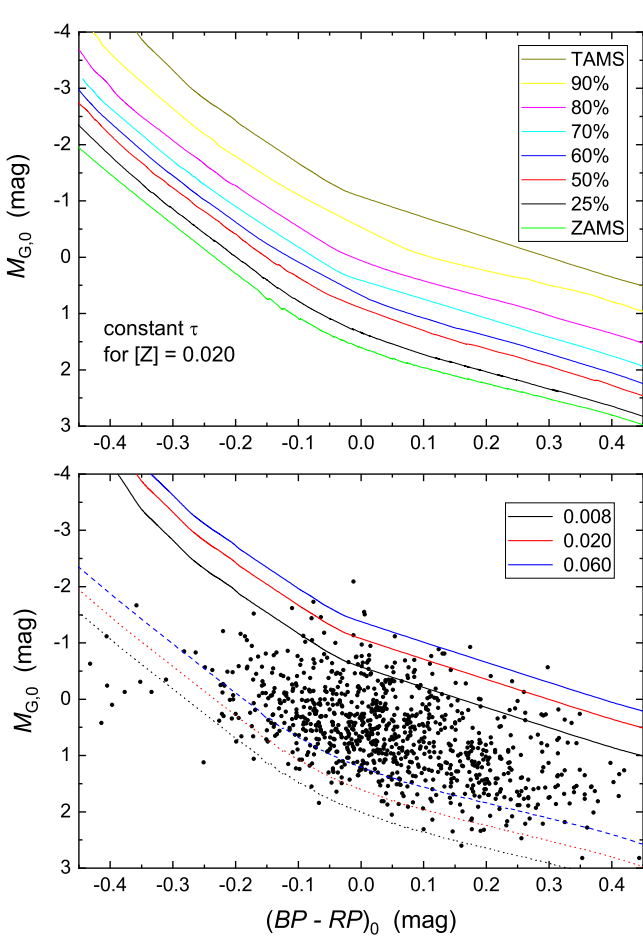


**Fig. 12.** Lines of constant fractional ages on the main sequence ( $\tau$ ) for solar metallicity  $[Z] = 0.020$  (upper panel). Lower panel shows the positions of the ZAMS and TAMS for isochrones with  $[Z] = 0.008$ , 0.020, and 0.060. Values have been chosen to cover the main range of  $[Z]$  values found for CP2 stars (Figure 9).

DR4; in these cases, mean RV values were calculated. Comparing the RV values from both sources, we find a mean difference of  $+2.4 \text{ km s}^{-1}$ , which lends confidence that the LAMOST RVs are useful in a statistical sense. However, we caution that an external uncertainty we cannot account for is introduced by the

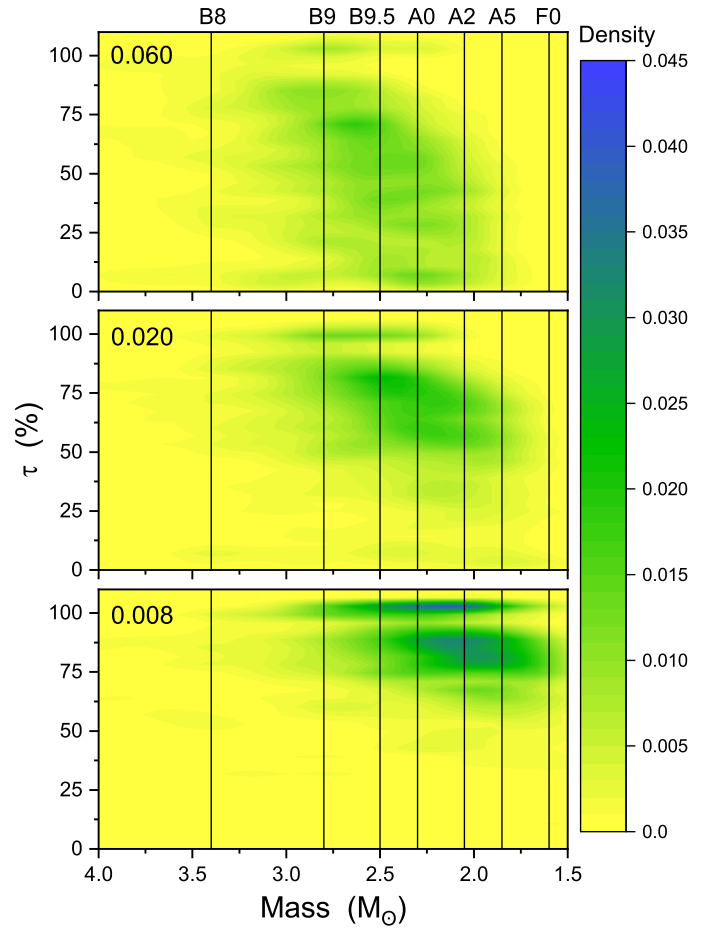


**Fig. 13.** Mass versus fractional age on the main sequence ( $\tau$ ) distributions for isochrones with  $[Z] = 0.008$ , 0.020, and 0.060, illustrating the differences in the derived mass and age distributions.

spot-induced RV variations of mCP stars that can reach up to  $\pm 50 \text{ km s}^{-1}$  (Polosukhina et al. 1999).

The space velocities were calculated following the formulae of Johnson & Soderblom (1987). The final values are listed in Table 4. Stars of the halo population show  $v_{\text{tot}} > 180 \text{ km s}^{-1}$  as compared to the local standard of rest (Venn et al. 2004). We therefore conclude that the



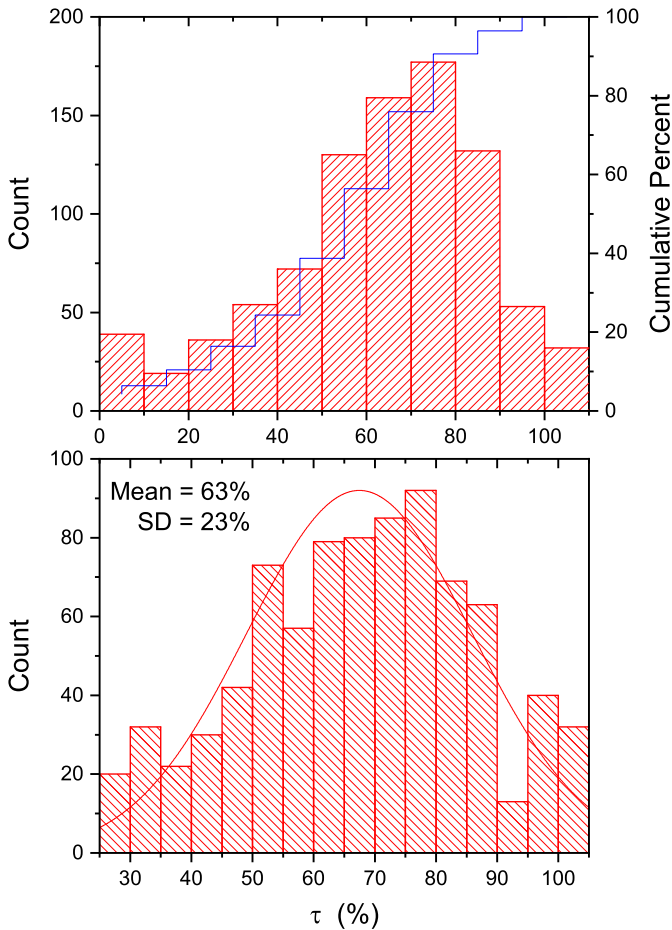


**Fig. 14.** Distribution of fractional ages on the main sequence ( $\tau$ ) among the 903 sample stars fulfilling our accuracy criteria.

stars LAMOST J122746.05+113635.3 (#876; Gaia DR2 3907547639444408064) and LAMOST J150331.87+093125.4 (#880; Gaia DR2 1167894108493926016) are kinematically true halo objects, which is of considerable interest as no halo CP2 stars have been discovered so far. Considering the error, the star LAMOST J140422.54+044357.9 (#879) does not satisfy this criterion.

Beers et al. (1996) identified LAMOST J122746.05+113635.3 as candidate field horizontal-branch star. Its spectrum, however, is that of a Si CP2 star (Figure 16). There are very strong Si II lines at 3856/62 Å, 4128/31 Å, 4200 Å, 5041/56 Å, and 6347/71 Å. In addition, the He I lines are weak, which is commonly observed in CP2 stars. It has consequently been classified as B8 IV Si (He-wk) by the MKCLASS\_mCP code. Almost all blue horizontal-branch stars, on the other hand, are metal-weak and their spectra rather resemble that of  $\lambda$  Bootis stars (Gray & Corbally 2009). We feel therefore safe in rejecting the proposed horizontal-branch classification.

In summary, according to the available evidence, LAMOST J122746.05+113635.3 and LAMOST J150331.87+093125.4 are bona-fide CP2 stars whose distances and kinematical properties are in agreement with halo stars. If confirmed, they would be the first CP2 halo objects known and therefore of great interest.

LAMOST J155549.85+401144.4 (#881; Gaia DR2 1382933122321062912) is another interesting object because it is listed in the catalogue of hot subdwarfs by Geier et al.

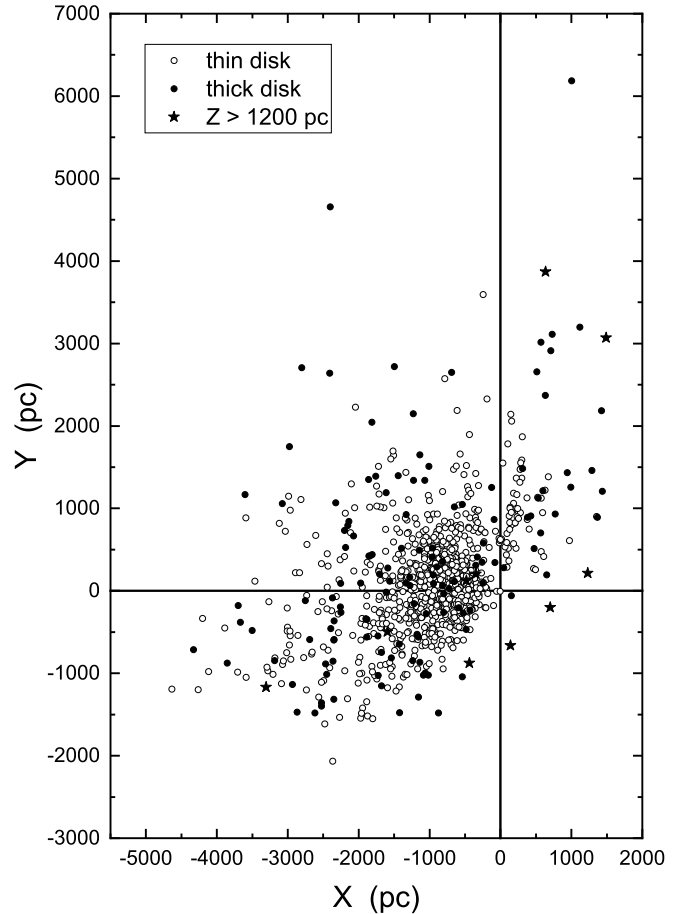


**Fig. 15.** Distribution of the 942 stars with absolute parallax errors less than 25% in the [XY] plane. Stars were divided in probable members of the thin and thick disk according to the scale heights given in Ojha (2001); Aumer & Binney (2017). Ten stars have Z values larger than 1200 pc and might be Halo objects.

(2017). The location in the  $(BP - RP)_0$  versus  $M_{G,0}$  diagram (Figure 8), however, does not support this classification. The same is true for the spectrum, which is that of a classical Si CP2 star (MKCLASS final type: B8 IV Si). We note that the occurrence of abundance anomalies in hot subdwarfs has been well established; for example, Wild & Jeffery (2018) identified two hot subdwarfs with effective temperatures of about 37 000 K and enrichments of 1.5 to 3 dex in heavy metals. This, however, is very different from what we see in LAMOST J155549.85+401144.4, which is significantly cooler than that ( $\sim 14\,000$  K) and shows the abundance pattern of a CP2 star. The current evidence, therefore, points to it being no subdwarf but a Si CP2 star.

Although the LAMOST survey is avoiding dense regions such as star clusters, we searched for possible cluster members among our sample stars. To this end, the positions, diameter, proper motions, distances and their errors of star clusters from Kharchenko et al. (2013) and Cantat-Gaudin et al. (2018) were employed and we searched for matches within  $3\sigma$  of these parameters. In total, seven matches in six open clusters were found, which are listed in Table 5. Judging from a comparison of the ages derived from Figure 8 and the cluster ages, all objects seem to be true cluster members.

**Table 5.** Open cluster members among our sample stars. The columns denote: (1) Internal identification number. (2) LAMOST ID. (3) Open cluster.

(1)	(2)	(3)
No.	LAMOST_ID	Open cluster
203	J041641.15+511253.2	NGC 1528
269	J045933.63+395715.8	Alessi 2
317	J052059.29+351123.5	Gulliver 8
497	J060815.12+045107.6	NGC 2168
502	J060827.84+204832.0	NGC 2168
675	J064741.02+072458.8	Collinder 115
868	J095855.77-044413.8	Collinder 359

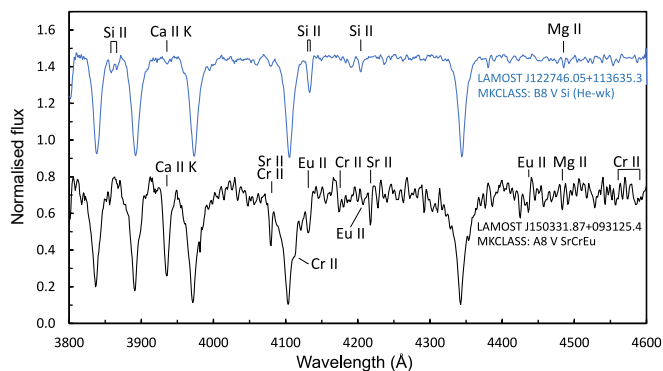


**Fig. 16.** Blue-violet spectra of the proposed halo stars LAMOST J122746.05+113635.3 (#876; MKCLASS final type B8 IV Si (He-wk); upper spectrum) and LAMOST J150331.87+093125.4 (#880; MKCLASS final type A8 V SrCrEu; lower spectrum). Some prominent lines of interest are indicated.

#### 4.4. Peculiarity type distribution

Figure 17 explores the distribution of Si, Cr, Sr, and Eu peculiarities versus hydrogen-line spectral type for the 876 stars of our sample with unambiguous identifications (i.e. without the stars in which only strong 4077 Å and/or 4130 Å blends or no traditional peculiarities were identified). Stars with hydrogen-line types of B9.5 are not listed separately but included under spectral type B9. The number of stars per spectral type bin varies considerably, with the B8–A0 stars forming the vast majority of our sample. Nevertheless, some tentative trends can be identified, although the interpretation towards the low temperature end is severely hampered by the small number statistics for objects later than A9:

- Si peculiarities are present between spectral types B4 and F0. They play a dominant role in stars with spectral types earlier than B9, strongly decreasing in importance in later-type objects. Except for He peculiarities (which are not shown in the plot), Si peculiarities are the only chemical peculiarities identified in objects earlier than B8.
- Cr peculiarities set in at spectral type B8 and form an important part of the peculiarity mix between spectral types B9 and A9.
- Sr and Eu peculiarities set in at spectral type B8 and increase in strength towards later types.

This is in good agreement with the expectations and the literature. It is well known that Si peculiarities are present throughout a wide range of effective temperatures in mCP stars (e.g.

Renson & Manfroid 2009). The hottest stars with Eu peculiarities from the Renson & Manfroid (2009) catalogue are of spectral type B8, which holds true also for the vast majority of stars with Cr and Sr peculiarities, with the exception of only three objects (HD 35502, spectral type B6 Sr Cr Si; HD 167288, spectral type B7 Si Cr; HD 213918, spectral type B7 Si Sr). Likewise, the work of Ghazaryan et al. (2018) contains atomic data for Eu, Cr, and Sr from effective temperatures of, respectively, 12 900 K (~B8), 14 700 K (~B6), and 13 300 K (~B8) downwards. The good agreement of the peculiarity type ‘blue borders’ between the present work and the literature provides independent proof of the reliability of the here derived spectral types.

Figure 18 illustrates the distribution of stars in which only strong blends at 4077 Å and/or 4130 Å were identified. Again, stars with hydrogen-line types of B9.5 are included under spectral type B9. These stars were not assigned Si, Cr, Sr, and Eu types with the here employed workflow because, apart from the strong blends, the peculiarities are either too subtle to have passed our significance criteria, no other significant features are present or the code failed to identify them for some reason (cf. Section 3.1).

Manual classification is necessary to throw more light on what elements contribute to the observed blends. Nevertheless, the distribution of the 4130 Å blend identifications, in particular for objects earlier than B9, is in general agreement with the distribution of Si peculiarities. We therefore expect that most of the ‘bl4130’ stars in our sample will turn out to be Si stars. No similar predictions can be made for the ‘bl4077’ stars from the available data.

#### 4.5. Comparison with samples from the literature

The following sections compare our results with the works of Renson & Manfroid (2009), Skiff (2014), and Qin et al. (2019). We further note that 22 of our sample stars are contained in the sample of strongly magnetic Ap stars of Scholz et al. (2019). As the authors do not list spectral types, a direct comparison of results was not possible. The stars common to both samples are identified in Table A.1.

##### 4.5.1. Comparison with the compilations of Renson & Manfroid (2009) and Skiff (2014)

Our final sample contains 59 mCP stars or candidates that are also included in the catalogue of Renson & Manfroid (2009). This low level of coincidence (6.65 %) is expected because the Renson & Manfroid (2009) sample mostly consists of bright stars (peaking at around 9th magnitude) for which there are no LAMOST spectra available.

Table 6 gives a comparison of the spectral types from the present study, the RM09 catalogue, and the compilation of Skiff (2014). For most stars, there is a good general agreement between the different sources. For example, for the 46 stars that have at least one other detailed literature classification listing the temperature subtype, the determined hydrogen-line types agree within  $\pm 2$  subclasses, which seems reasonable considering the inhomogeneous source material behind the literature classifications and the inherent difficulties in classifying mCP stars. For several stars, our results provide a first detailed classification; furthermore, we confirm several doubtful objects as mCP stars and show that some suspected CP1 stars are in fact mCP stars. A more detailed investigation into this matter will be the topic of an upcoming study that will be concerned with a new classi-

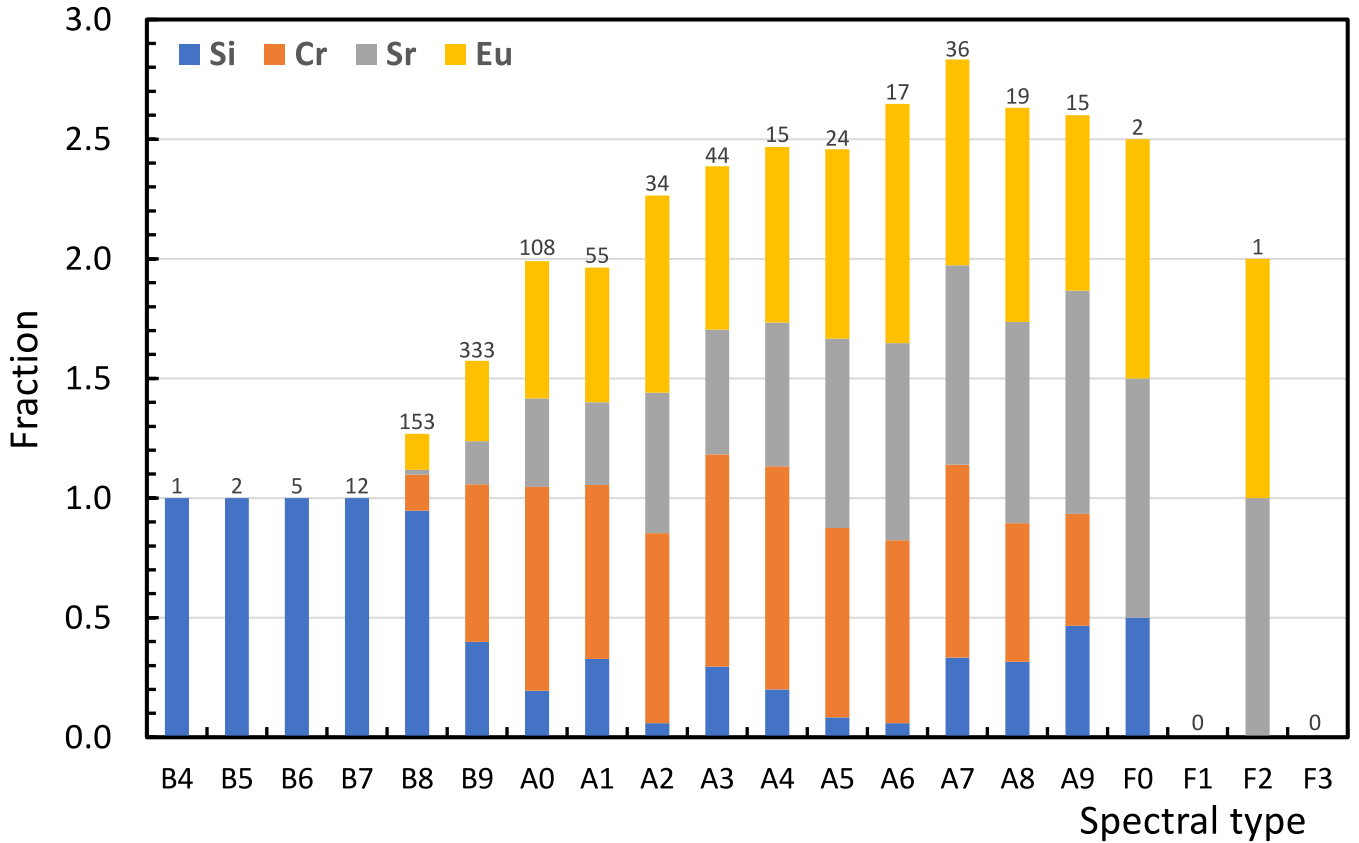


**Fig. 17.** Fractional distribution of chemical peculiarities versus hydrogen-line spectral type for the 876 stars with unambiguous peculiarity type identifications. The numbers above the bars indicate the number of objects in the corresponding spectral type bin. Because a single object may have multiple peculiarities, fractions may exceed 1.

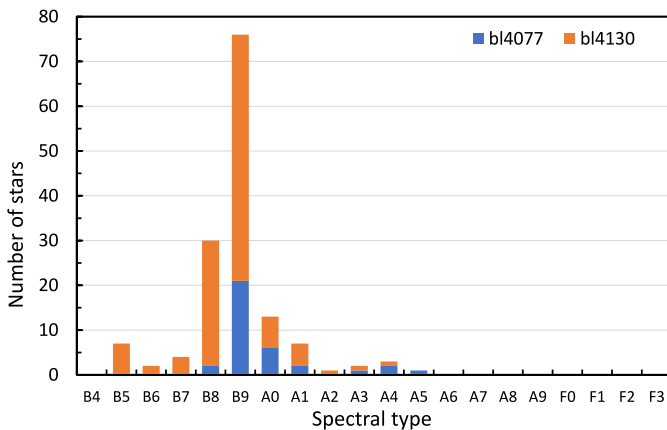


**Fig. 18.** Distribution of stars in which only strong blends at 4077 Å and/or 4130 Å were identified.

fication of stars in the RM09 catalogue based on homogeneous spectroscopic material.

#### 4.5.2. Comparison with the sample of Qin et al. (2019)

Qin et al. (2019) searched for CP1 stars in low resolution spectra of early-type stars from LAMOST DR5 and compiled a catalogue of 9372 CP1 stars. Because cooler CP2 stars may ex-

hibit similar spectral features (Ca deficiency, overabundance of Fe-group elements), the authors expect a contamination of their sample by these objects. To identify potential CP2 stars among the CP1 star candidates, they used the 4077 Å blend as reference line, which may contain contributions from Si II, Cr II, and Sr II. Synthetic spectra with overabundances of Sr, Cr, Eu, and Si of 2.0 dex were computed for different effective temperatures and the equivalent widths of the 4077 Å blend were calculated and compared for both the templates and the observed spectra. If the equivalent width of the observed 4077 Å feature ( $EW_{4077\_obs}$ ) exceeded that of the corresponding templates ( $EW_{4077\_temp}$ ), a star was flagged as a CP2 star candidate. In this way, Qin et al. (2019) flagged 1131 stars within their sample of CP1 star candidates as CP2 star candidates. From a cursory investigation of about 20 randomly chosen objects, several bona-fide CP2 stars have indeed been found among the objects with high values of  $(EW_{4077\_obs} - EW_{4077\_temp})$ , in line with the expectations of Qin et al. (2019). However, the incidence of CP2 stars seems to drop rather sharply towards lower values of  $(EW_{4077\_obs} - EW_{4077\_temp})$ . We assume that this is because a strong 4077 Å feature alone, while often helpful, is an insufficient criterion for identifying CP2 stars.

Only 45 objects are common to both our sample and the Qin et al. (2019) catalogue. Of these stars, about 70% (31 objects) were flagged as CP2 star candidates. Table 7 compares the Qin et al. (2019) k/h/m spectral types to the final types derived in the present study for all objects common to both lists. In general,

the agreement between the derived spectral types is poor. With the here employed methodology, different k/h/m-types were assigned to only 21 of these stars. A detailed investigation of the stars common to both lists, in particular a comparison of the automatically derived classifications to manually derived spectral types and an investigation of the source(s) of the observed discrepancies, is beyond the scope of the present paper but might be beneficial to both studies and help with the refinement of the employed algorithms.

On first glance, the low level of coincidence between the Qin et al. (2019) catalogue and the here presented sample of mCP seems surprising. We have identified several reasons for this, which are related to the different approaches and goals of both studies.

Qin et al. (2019) explicitly searched for CP1 stars. CP2 stars were identified as a contaminant and corresponding candidates were subsequently identified. Because they searched for CP2 star candidates within their sample of CP1 star candidates, that is, among objects with pronounced differences between k and h spectral types, their sample will not contain any CP2 stars that do not share these characteristics. However, early-type CP2 stars generally do not show significant (if any) differences between k and h types; this phenomenon is mostly restricted to late-type CP2 stars. Thus, we assume that the Qin et al. (2019) subsample of CP2 star candidates is biased towards late-type CP2 stars.<sup>7</sup> This is further corroborated by the fact that, in agreement with the expectations for identifying CP1 stars, Qin et al. (2019) constrained their search to objects with  $6500\text{ K} < T_{\text{eff}} < 11\,000\text{ K}$ . In fact, their final catalogue contains only 11 objects with  $T_{\text{eff}} > 10\,000\text{ K}$ . Thus, only very few stars hotter than spectral type A0 are present in their sample.

Our study follows a very different approach and is concerned with the identification of mCP stars that were selected among early-type targets by the presence of a significant  $5200\text{ \AA}$  flux depression. The spectra of CP1 stars, on the other hand, generally do not show this feature (Paunzen et al. 2005). However, not all mCP stars distinctly show a  $5200\text{ \AA}$  depression either, in particular in low-resolution spectra. Therefore, we will have missed any such mCP stars, which might have found their way into the Qin et al. (2019) candidate sample. Most important, however, is that the majority of our sample stars is situated in the spectral range of B8 to A0 ( $9700\text{ K} < T_{\text{eff}} < 12\,500\text{ K}$ ), which renders them mostly incompatible with the candidate sample of Qin et al. (2019).

In summary, the above mentioned issues, combined with the fact that the incidence of CP2 stars seems to drop rather sharply towards lower values of  $(EW_{4077_{\text{obs}}} - EW_{4077_{\text{temp}}})$  in the CP2 star candidate subsample of Qin et al. (2019) and the different source material ( $\sim 9.0$  million spectra in DR5 vs.  $\sim 7.6$  million spectra in DR4), illustrate that no significant overlap between both samples is to be expected. We would like to again stress that it never was the intention of Qin et al. (2019) to collect a pure sample of CP2 stars. Their subsample of candidates, however, is a valuable starting point for further investigations. As a spin-off of the present study, we intend to investigate the Qin et al. (2019) CP2 star candidates to confirm or reject their status as mCP stars. It is clear that investigations based on a broader analysis of LAMOST early-type spectra (i.e. also including stars without conspicuous  $5200\text{ \AA}$  flux depressions) will lead to the discovery of many more mCP stars in the future.

<sup>7</sup> Although not statistically significant, it is interesting to note that all stars from the Qin et al. (2019) candidate sample we were able to confirm as CP2 stars were indeed late-type CP2 stars.

#### 4.6. The mid-B type mCP stars - He-peculiar objects?

23 stars of our sample have MKCLASS final types earlier than B7. More than half of these objects were classified as showing peculiarly weak He I lines ('He-wk'). Interestingly, three stars were identified as showing both weak and strong ('He-st') He I lines, which strongly suggests He peculiarity. Besides that, only Si overabundances and strong  $4130\text{ \AA}$  blends were identified in several of these objects. As He-rich stars are generally hotter than spectral type B4 (Gray & Corbally 2009) and therefore not expected to contribute to our sample, we consider these objects good candidates for He-weak (CP4) stars.

Figure 19 showcases the spectra of five mid-B type stars. The hydrogen-line profiles and the prominent C II  $4267\text{ \AA}$  lines corroborate the classifications, although we manually derived slightly different temperature types in two cases. LAMOST J014940.99+534134.2 (#37; TYC 3684-1139-1) and LAMOST J062348.46+034201.1 (#567; HD 256582) are He-weak stars with Si overabundances. LAMOST J062307.91+264642.0 (#565; Gaia DR2 3432273606513132544) is also certainly He-weak but does not fit any of the standard subclasses of the He-weak stars (the 'hot' Si stars, i.e. Si stars with hotter temperatures than the classical Si CP2 stars; the P Ga stars; the Sr Ti stars; cf. Gray & Corbally 2009). It is here classified as B4 V HeB7 (R. O. Gray, personal communication).

LAMOST J055023.89+261330.2 (#421; TYC 1866-861-1) boasts a rather noisy spectrum (g band S/N of 79) that is, apart from the hydrogen lines, basically a 'smattering' of metal-lines, without any particularly outstanding features – except for the strong C II  $4267\text{ \AA}$  and the weak Mg II  $4481\text{ \AA}$  lines that support its classification as a mid B-type object. This is also supported by the colour index  $(BP - RP)_0 = -0.182\text{ mag}$ . The He I lines, then, seem to be curiously absent from its spectrum, so the star may be related to the CP4 stars, although the metal-lines seem way too strong to support this interpretation. We here tentatively classify it as B4: V HeB9. The star shows a strong flux depression at  $5200\text{ \AA}$ , and, according to data from the SuperWASP archive (Butters et al. 2010), is a periodic photometric variable with a period of about 11.5 d. It certainly merits a closer look – this, however, is beyond the scope of the present investigation.

The He lines of LAMOST J052118.97+320805.7 (#318; HD 242764) do not look weak for its temperature type but have broad profiles suggesting rapid rotation. This, however, is not supported by the hydrogen-line profile, which almost exactly matches that of the B4 V standard. The presence of a number of unidentified metal-lines (which do show evidence for rotational broadening, but not to the extent the He I lines imply) and the conspicuous  $5200\text{ \AA}$  depression suggest that this star is indeed chemically peculiar, although it also does not fit into any of the standard mid-B peculiarity subtypes. It has been classified as B4 Vpn in the present study (R. O. Gray, personal communication).

Additional proof that this star is indeed chemically peculiar comes from its periodic photometric variability with a period of about 5.1 d in SuperWASP data and the conspicuous  $5200\text{ \AA}$  flux depression in its spectrum. Incidentally, the star is listed with a spectral type of B8 Si Sr in the Renson & Manfroid (2009) catalogue, which is not supported by the available LAMOST spectrum. We were unable to get at the root of this classification; however, the star is listed as B9 in the Henry Draper extension (Cannon 1931) and was classified as B5p by Chargeishvili (1988). Further He-peculiar objects and candidates can be gleaned from Table A.1.

**Table 6.** Comparison of the spectral types derived in this study, the RM09 catalogue, and the compilation of Skiff (2014). The columns denote: (1) Internal identification number. (2) Identification number from the RM09 catalogue. (3) LAMOST identifier. (4) Spectral type, as derived in this study. (5) Spectral type from the RM09 catalogue. An asterisk (\*) or a question mark (?) in parantheses behind the spectral type denote, respectively, well-known CP2 stars and CP2 stars of doubtful nature. (6) Spectral type from the compilation of Skiff (2014). (7) Corresponding reference from the compilation by Skiff (2014).

(1) No.	(2) ID_RM09	(3) ID_LAMOST	(4) SpT_final	(5) SpT_RM09	(6) SpT_Skiff	(7) Ref_Skiff
14	1236	J004947.16+525208.2	B9 V CrEuSi (He-wk)	B9 Si	ApSi	Bidelman (1998)
19	1543	J010007.84+045339.3	kB8hA3mA6 Cr	A0 Si Cr (?)	A0/2	Hou et al. (2015)
22	1680	J010651.35+154426.9	kA1hA7mA7 SrCrEu	A3	A3p	Nassau & Macrae (1955)
33	2210	J013055.87+452155.7	kA1hA3mA4 SrCr	A0 Sr	A0pSrCr?	Floquet (1975)
38	2750	J015059.58+540259.1	B8 IV bl4130	B8 Si	B8IIIpSi	Grenier et al. (1999)
61	3660	J022120.02+280415.6	A8 V SrEuSi	A2 Sr Eu	ApSrEu	Bidelman (1983)
77	4580	J025945.31+541941.5	kB7hA7mA6 CrEuSi	A2 Si Cr Eu	B9pSi	Grenier et al. (1999)
80	4740	J030350.21+463718.3	A8 V SrCrEuSi	Sr Eu	ApSrEu Sr vstrong	Bidelman (1985)
83	4820	J030633.66+025615.7	B9.5 IV-V CrEu	A2 Cr Eu (?)	A2pCrEu Sr 4077A weak	Drilling & Pesch (1973)
130	5750	J034000.57+444858.4	kA0hA1mA3 (Si)	A0	n/a	n/a
132	5800	J034112.38+453031.7	A1 V SrCrEu	Sr Eu	ApSrEu	Bidelman (1985)
134	5850	J034229.41+353820.9	A0 IV-V bl4077 bl4130	A1 Sr	A1pSr	Guetter (1977)
138	5860	J034417.13+494336.6	B8 IV-V CrSi	A0 Cr Eu (?)	ApCrEu:	Bidelman (1985)
180	6530	J040642.34+454640.8	kB9hA2mA6 CrSi	A0 Si	ApSi	Bidelman (1985)
228	7210	J042736.18+063643.1	A2 IV-V SrCrEu	A0 Sr Cr Eu	ApSrCrEu	Bidelman & MacConnell (1973)
241	7740	J044407.32-005639.0	F0 V SrEuSi	F0 Sr Eu	FpSrEu	Bidelman & MacConnell (1973)
252	7960	J045121.11+093555.8	A0 V SrCrEuSi	A0 Sr Cr Eu	ApSrCrEu	Bidelman & MacConnell (1973)
275	8140	J050210.72+464600.0	B8 III-IV Si	Si	ApSi	Bidelman (1985)
318	8872	J052118.97+320805.7	B4 Vpn	B8 Si Sr	B9	Cannon (1931)
325	8938	J052259.54+343944.9	B9.5 V Cr	B9 Si Cr Sr	A0/2	Hou et al. (2015)
334	9082	J052616.48+331544.2	B8 IV-V bl4130	A0 Si Sr	A2	Cannon (1931)
343	9200	J052812.16+415006.4	kA0hA3mA7 Si	B5 Si	ApSi	Bidelman (1983)
351	9295	J053025.32+332639.6	A6 V SrEu	A1-	A7	Cannon (1931)
360	9350	J053239.91+434307.5	B8 IV Si	B9 Si	B8pSi	Floquet (1975)
371	9740	J053504.75-012406.5	kA0hA2mA4 CrEu	A2 Cr Eu	A0pSi	Giesekeing (1983)
393	10107	J054102.12+332331.1	B7 IV Si (He-wk)	B9 Si (?)	n/a	n/a
403	10323	J054630.44+273518.1	B9 V CrEu	B8 Si (?)	n/a	n/a
411	10375	J054819.92+333516.9	kA4hA9mF1 SrCrEuSi	A5 Si Sr	A7	Cannon (1931)
409	10385	J054757.12+235011.8	B9.5 II-III EuSi	B9 Si Sr	B8	Cannon (1931)
418	10447	J055002.80+234023.9	B9 IV bl4130	B9 Si Cr	B9	Cannon (1931)
428	10460	J055121.05+420610.5	B8 IV Si	A Si	ApSi	Bidelman (1983)
436	10536	J055237.95+274922.8	A6 V SrCrEu	A2-	n/a	n/a
445	10602	J055422.76+305401.8	B8 III bl4130	A0-	A2	Cannon (1931)
470	10900	J060045.94-035344.3	A0 IV-V Si	A0 Cr Eu	A0VpSi	Grenier et al. (1999)
476	10915	J060227.33+282943.9	B8 III-IV EuSi (He-wk)	A0 Si	A3	Cannon (1931)
475	10917	J060225.92+244628.5	B8 IV Si	B9 Si	B8/9.5IV/VSi:	Clausen & Jensen (1979)
560	11800	J062155.55+001812.2	B8 III Si	A0 Si Sr	A0pSi	Grenier et al. (1999)
564	11810	J062257.61+231625.8	A1 IV-V SrCrEu	A2 Sr	ApSr	Bidelman (1983)
597	12200	J062914.34+004257.0	B7 III-IV Si	B9 Si	ApSi	Bidelman & MacConnell (1973)
604	12300	J063035.50+035245.3	A1 IV-V SrCr	A2 Sr Eu	ApSrEu	Bidelman & MacConnell (1973)
611	12360	J063218.45+032146.3	B9 III-IV Si (He-wk)	B9 Si	ApSi	Bidelman & MacConnell (1973)
627	12630	J063744.29+195655.1	kA1hA7mF4 SrCrSi	A Sr Eu	ApSrEu	Bidelman (1983)
630	12690	J063752.90+091516.7	B8 IV Si	B9 Si	ApSi	Bidelman & MacConnell (1973)
715	13790	J065403.63+221545.2	A6 IV SrCrEu	A2 Sr Eu	ApSrEu	Bond (1972)
721	13980	J065458.31+040826.9	kA1hA3mA6 SrCrEu	A2 Sr Cr Eu	FpSrCrEu	Bidelman & MacConnell (1973)
753	14520	J070252.77+023700.0	kB9hA9mA7 SrSi	A2 Si	ApSi	Bidelman & MacConnell (1973)
763	14740	J070617.23+101601.6	B9 IV EuSi	A0 Si	ApSi	Bidelman & MacConnell (1973)
774	15123	J071337.30+040720.7	B8 IV CrEuSi	B9 Si	n/a	n/a
792	15650	J072118.92+223422.7	B9 V bl4077	Sr (?)	ApSr	Bidelman (1983)
827	17490	J074851.40+001619.1	kB8hA3mA3 CrEu	Cr Eu	ApCrEu	Bidelman & MacConnell (1973)
829	17540	J074959.61+013517.8	kA1hA3mA7 SrCrEuSi	Sr Cr Eu	ApSrCrEu	Bidelman & MacConnell (1973)
830	17630	J075041.80-060338.3	A2 IV SrCrEu	A0 Cr Eu	FpCrEu	Bidelman & MacConnell (1973)
838	18380	J080339.87-082141.0	kB9hA3mA8 SrCrEu	A0 Cr Eu	ApCrEu	Bidelman & MacConnell (1973)
867	24620	J095644.95-021719.5	kA2hA3mA6 SrCrEu	A2 Sr Eu Cr	ApSrCrEu	Bidelman (1981)
873	29280	J114130.23+403822.7	B9 IV-V CrEuSi	A0- (?)	A0m:	Slettebak & Stock (1959)
877	31550	J122855.36+255446.3	B9 V CrEu	A0 Sr Cr Eu (*)	B8pSiCrSr	Sato & Kuji (1990)
967	59010	J222549.96+343851.0	B8 IV EuSi	A0 Si (?)	ApSi:	Bidelman (1985)
980	60185	J230905.79+523711.2	B8 IV EuSi	B8 Si	ApSi	Bidelman (1998)
1001	61520	J235740.51+470001.7	B9 IV CrSi	B8 (?)	n/a	n/a

#### 4.7. The eclipsing binary system LAMOST J034306.74+495240.7

The star LAMOST J034306.74+495240.7 (#135; TYC 3321-881-1) was identified as an eclipsing binary system in ASAS-SN data (Jayasinghe et al. 2019). It is listed in the International Variable Star Index of the AAVSO (VSX; Watson 2006) under the designation ASASSN-V J034306.74+495240.8 and with a period of 5.1431 d. We have analyzed the available ASAS-SN data for this star and derive a period of  $5.1435 \pm 0.0012$  d and

an epoch of primary minimum at  $HJD\ 2457715.846 \pm 0.002$ . The light curve is shown in Figure 20 and illustrates that the orbit is slightly eccentric, the secondary minimum occurs at an orbital phase of  $\varphi = 0.46$ . In addition, there is evidence for out-of-eclipse variability in agreement with rotational modulation on one component of the system.

Two spectra are available for this star in LAMOST DR4. The first spectrum ('spectrum1') was obtained on 23 October 2015 (MJD 57318; observation median UTC 17:33:00; g band S/N:

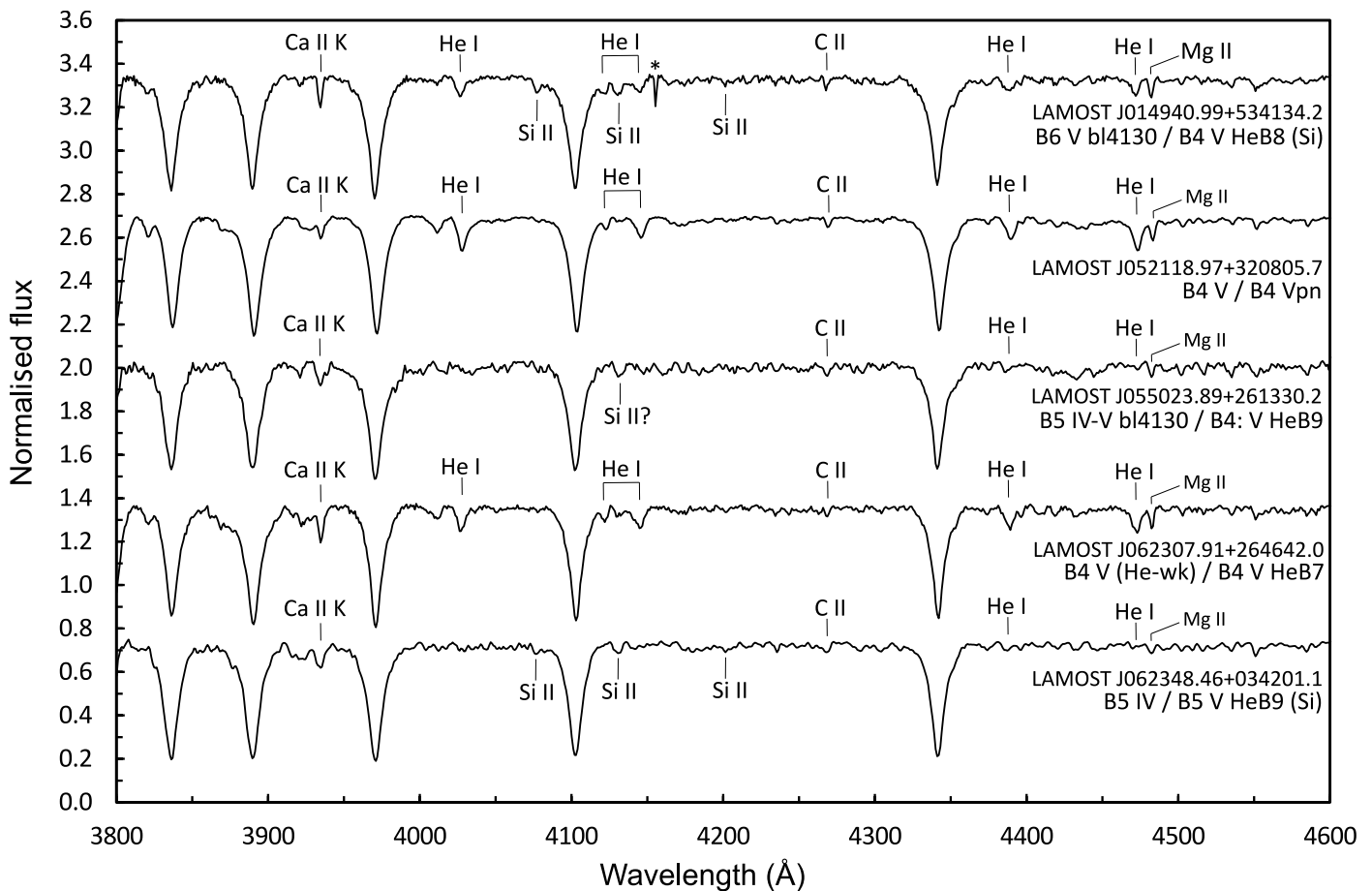


**Fig. 19.** Showcase of five newly identified peculiar mid-B type stars, illustrating the blue-violet region of the LAMOST DR4 spectra of (from top to bottom) LAMOST J014940.99+534134.2 (#37; TYC 3684-1139-1), LAMOST J052118.97+320805.7 (#318; HD 242764), LAMOST J055023.89+261330.2 (#421; TYC 1866-861-1), LAMOST J062307.91+264642.0 (#565; Gaia DR2 3432273606513132544), and LAMOST J062348.46+034201.1 (#567; HD 256582). MKCLASS final types and manual types derived in the present study are indicated. Some prominent lines of interest are identified. The asterisk marks the position of a 'glitch' in the spectrum of LAMOST J014940.99+534134.2.

258), which corresponds to an orbital phase of  $\varphi = 0.890$ . The second spectrum ('spectrum2') was taken on 19 January 2016 (MJD 57406; observation median UTC 11:46:00; *g* band S/N: 207), which corresponds to an orbital phase of  $\varphi = 0.952$ . Therefore, both spectra were taken during maximum light, and we find no significant difference between them. Both show a strong flux depression at 5200 Å and enhanced Si II lines at 3856/62 Å, 4128/31 Å, 4200 Å, 5041/56 Å, and 6347/71 Å. We have analyzed the spectrum with the highest S/N (spectrum1) and derive a spectral type of B9 III Si. Figure 21 compares the blue-violet part of both spectra to the liblamost B9 III standard, whose hydrogen-line profile provides a good fit to the observed ones.

In summary, we conclude that at least one component of the LAMOST J034306.74+495240.7 system is a Si CP2 star. It is, therefore, of great interest because mCP stars in eclipsing binaries are exceedingly rare (Renson & Manfroid 2009; Niemczura et al. 2017; Kochukhov et al. 2018; Skarka et al. 2019) and accurate parameters for the components can be derived via an orbital solution of the system. We strongly encourage further studies of this interesting object.

#### 4.8. The SB2 system LAMOST J050146.85+383500.8

Figure 22 illustrates the peculiar spectrum of LAMOST J050146.85+383500.8 (#272; HD 280281), which we suspect to

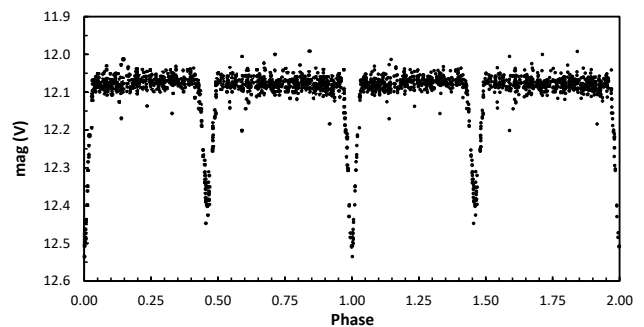


**Fig. 20.** ASAS-SN light curve of the eclipsing binary system LAMOST J034306.74+495240.7 (#135; TYC 3321-881-1). The data have been folded with the orbital period of  $P_{\text{orb}} = 5.1435 \pm 0.0012$  d.

be a blend of two different stars. This becomes especially obvious in the profile of the H $\gamma$  line (Figure 23).

To further investigate this matter, we employed the VO Sed Analyzer tool VOSA<sup>8</sup> v6.0 (Bayo et al. 2008) to fit the SED to the available photometry. For comparison, we used a Kurucz ODFNEW/NOVER model (Castelli et al. 1997) with  $T_{\text{eff}} = 12\,500$  K, which corresponds to a spectral type of B8.

<sup>8</sup> <http://svo2.cab.inta-csic.es/theory/vosa/>



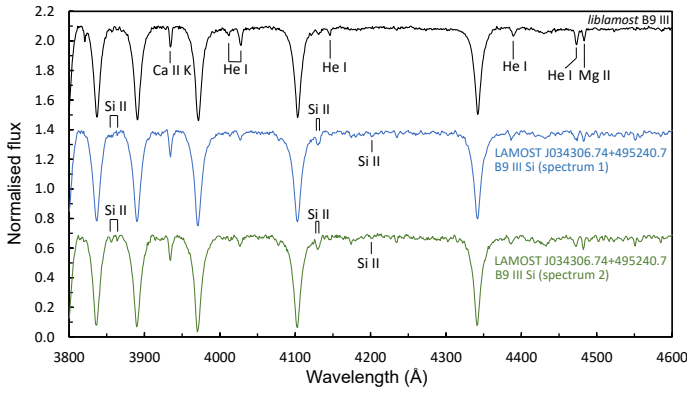


**Fig. 21.** Comparison of the blue-violet spectra of the eclipsing binary system LAMOST J034306.74+495240.7 (#135; TYC 3321-881-1) to the *liblamost* B9 III standard spectrum (upper spectrum). Some prominent lines of interest are indicated.

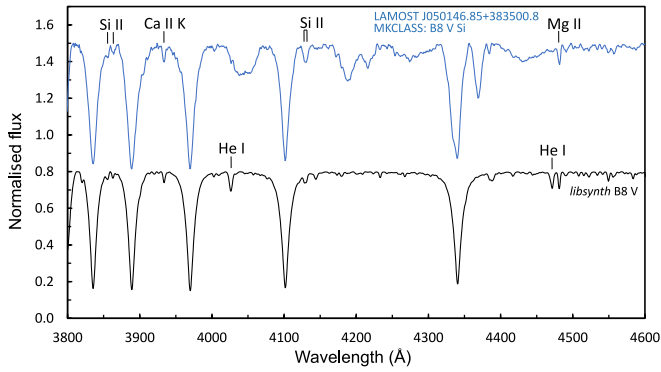


**Fig. 22.** Comparison of the blue-violet spectra of the proposed SB2 system LAMOST J050146.85+383500.8 (#272; HD 280281; MKCLASS final type B8 V Si) to the *libsynth* B8 V standard spectrum (upper spectrum). Some prominent lines of interest are indicated.

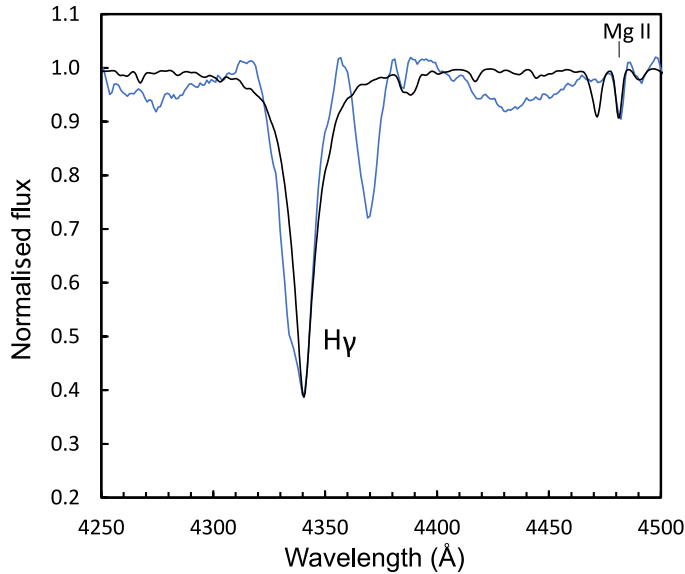


**Fig. 23.** Close-up view of the H $\gamma$  region of the proposed SB2 system LAMOST J050146.85+383500.8 (blue spectrum) and the *libsynth* B8 V standard (black spectrum), illustrating the peculiar profile of the H $\gamma$  line indicative of binarity.

**Table 7.** Comparison of the spectral types derived in this study to the catalogue of Qin et al. (2019). The columns denote: (1) Internal identification number. (2) LAMOST identifier. (3) Spectral type, as derived in this study. (4) Spectral type from Qin et al. (2019). (5) Ap\_flag from Qin et al. (2019). A value of 1 indicates that the star is a CP2 star candidate.

(1)	(2)	(3)	(4)	(5)
No.	ID_LAMOST	SpT_final	SpT_Qin	Ap_flag
2	J000834.32+321205.4	A2 IV SrCrEu	kA2hA7mA7	1
12	J003425.61+452108.7	kA1hA7mA9 SrEuSi	kA2hA3mA5	1
25	J011435.00+534757.2	A1 IV–V SrCrEuSi	kA1hA5mA5	1
29	J012028.54+480545.6	kA4hA7mA8 SrCrEu	kA5hA6mA7	1
30	J012122.31+442826.2	kA3hA7mA8 CrEu	kA5hA5mA7	1
35	J014508.87+322430.3	kA1hA6mA7 SrCrEu	kA1hA5mA5	1
68	J023936.01+540059.5	kA2hA5mA7 CrEu	kA6hA5mA5	0
70	J024243.57+453720.4	A1 V SrCrEuSi	kA6hA6mA7	1
106	J032333.76+510336.6	A2 V CrEuSi	kA3hA6mA7	0
218	J042235.95+411448.9	A1 IV SrCrEuSi	kA6hA5mA7	1
235	J043752.46+533259.6	B9.5 V CrSi	kA0hA1mA5	1
244	J044446.24+513129.2	A9 V SrEu	kA5hA5mF0	0
246	J044713.47+540515.5	A2 IV CrEu	kA6hA6mF0	0
252	J045121.11+093555.8	A0 V SrCrEuSi	kA2hA1mA6	1
259	J045508.24+204943.7	kA2hA4mA7 SrCrEu	kA6hA5mA7	1
286	J050925.66+512444.9	A3 III–IV CrEu	kA5hA6mA7	0
330	J052459.98-064651.8	A0 IV–V Si	kA3hA5mA7	1
332	J052552.24+344817.3	A0 V CrEu	kA1hA1mA5	1
344	J052816.11-063820.1	kA1hA9mA9 SrCrEu	kA2hA7mA6	1
387	J053840.17+413754.0	kA1hA7mA9 SrCrEuSi	kA3hA6mA7	1
423	J055045.30+372809.0	kA2hA4mA7 SrCrEu	kA6hA5mA7	1
427	J055110.67+360517.0	B9.5 V SrCr	kA1hA1mA5	1
441	J055333.92+180202.9	F2 V SrEu	kA7hA7mF5	0
483	J060356.06+213033.2	A8 V SrEu	kA5hA6mF0	0
542	J061743.05+595315.3	A1 IV Eu	kA3hA6mA7	1
570	J062449.08+190854.0	kA2hA3mA7 SrCrEu	kA3hA5mF0	1
571	J062449.21+161325.7	A0 V Cr	kA1hA1mA5	0
627	J063744.29+195655.1	kA1hA7mF4 SrCrSi	kA2hA6mA7	1
643	J064158.41+223927.2	A5 IV SrCrEu	kA1hA6mA7	0
689	J064907.51+114600.1	kA1hA7mA8 SrCr	kA2hA6mA5	0
690	J064947.96+202510.8	kA3hA5mA7 bl4077 bl4130	kA7hA7mA7	0
770	J070907.08+441114.7	B9.5 V CrEu	kA1hA6mA5	1
773	J071258.59+065952.3	A2 IV SrCrEu	kA3hA6mA7	1
775	J071413.88+142449.5	A3 III–IV SrCrEu	kA6hA5mA7	1
779	J071550.38+063655.9	A1 IV SrCrEuSi	kA2hA5mA7	1
814	J073548.83+123225.1	kA1hA9mA8 SrEu	kA6hA7mA7	1
828	J074919.49+051551.8	kA1hA9mA9 SrCrEu	kA2hA7mA5	1
831	J075220.93+113710.6	kA5hA6mA9 SrCrEu	kA5hA6mA7	0
848	J082137.47+064401.0	A1 IV SrCrEu	kA2hA5mA5	1
850	J082326.74+072116.4	kA3hA7mF1 SrCrEu	kA2hA6mA7	0
853	J083539.12+002150.4	kA2hA3mA6 SrCrEu	kA3hA1mA7	0
861	J092233.23+072519.4	kA3hA6mA9 SrCrEu	kA6hA5mA7	1
879	J140422.54+044357.9	kA4hA7mF0 SrCrEu	kA6hA6mA7	1
899	J185127.99+262012.1	A0 IV–V Cr	kA0hA1mA7	1
909	J192524.14+431911.5	kA3hA7mA9 SrCrEu	kA6hA5mA5	1

We emphasise that a change of  $T_{\text{eff}}$  of about 2000 K in either direction will not impact our conclusions. Figure 24 illustrates the results of the fitting process. The flux model was fitted to either match the ultraviolet or the optical wavelength region. In any case, the discrepancies are readily visible and it is obvious that the observed flux distribution of LAMOST J050146.85+383500.8 cannot be fitted with a single star flux model. We note that it is well known that CP2 stars show a ‘blueing’ effect (Maitzen 1980), which leads to observed flux discrepancies due to stronger absorption in the ultraviolet than in chemically normal stars. However, a slight shift in the ultraviolet region will not alter our conclusions.

Because the features of the companion star are readily visible in the available LAMOST spectrum, we conclude that its absolute magnitude must be similar to the B-type main-sequence component. We therefore assume that it is a supergiant star with a progenitor of higher mass. Such a combination of components is quite unusual among mCP stars; in order to put further constraints on this spectroscopic binary system, orbital elements

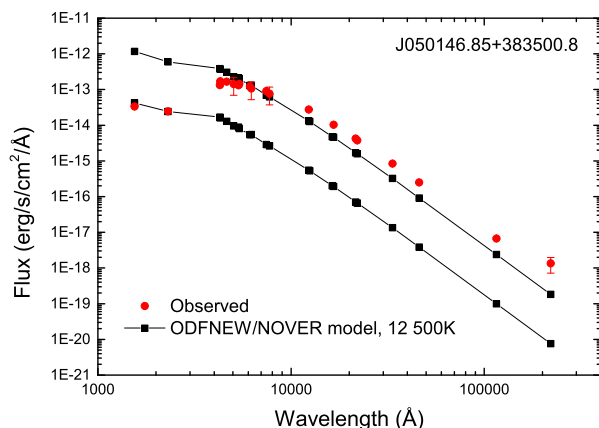


**Fig. 24.** Comparison of the SED of LAMOST J050146.85+383500.8 (red dots) to a Kurucz ODFNEW/NOVER model with  $T_{\text{eff}} = 12\,500\text{ K}$  (black squares). The model was forced to either fit the ultraviolet (lower model) or optical flux (upper model). The discrepancies are clearly visible, the star’s SED cannot be fitted with a single star flux model.

or the analysis of light-travel time effects are needed. LAMOST J050146.85+383500.8, therefore, is an interesting target for follow-up studies.

## 5. Conclusions

We carried out a search for mCP stars in the publicly available spectra of LAMOST DR4. Suitable candidates were selected by searching for the presence of the characteristic 5200 Å flux depression. In consequence, our sample is biased towards mCP stars with conspicuous flux depressions at 5200 Å. Spectral classification was carried out with a modified version of the MKCLASS code (MKCLASS\_mCP) and, for a subsample of stars, by manual classification. We evaluated our results by spot-checking with manually derived spectral types and comparison to samples from the literature.

The main findings of the present investigation are summarised in the following:

- We identified 1002 mCP stars, most of which are new discoveries. There are only 59 common entries with the catalogue of Renson & Manfroid 2009. With our work, we significantly increase the sample size of known Galactic mCP stars, paving the way for future in-depth statistical studies.
- To suit the special needs of our project, we updated the current version (v1.07) of the MKCLASS code to probe several additional lines, with the advantage that the new version (here termed MKCLASS\_mCP) is now able to more robustly identify traditional mCP star peculiarities, including Cr peculiarities and, to some extent, He peculiarities.
- mCP star peculiarities (Si, Cr, Sr, Eu, strong blends at 4077 Å and/or 4130 Å) were identified in all but 36 stars of our sample, highlighting the efficiency of the chosen approach and the peculiarity identification routine. The remaining objects (mostly mCP stars with weak or complicated peculiarities and He-peculiar objects) were manually searched to locate the presence of peculiarities.
- Comparisons between manually derived spectral types and the MKCLASS\_mCP final types indicate a good agreement between the derived temperature and peculiarity types. This is further corroborated by a comparison with spectral types

from the Renson & Manfroid (2009) and Skiff (2014) catalogues and the good agreement of the peculiarity type versus spectral type distribution between this study and the literature. However, with our approach, we missed the presence of certain peculiarities in several objects. The peculiarity types presented here are therefore not exhaustive. They nevertheless form a sound basis for statistical and further studies.

- Our sample stars are between 100 Myr and 1 Gyr old, with the majority having masses between  $2 M_{\odot}$  and  $3 M_{\odot}$ . We investigated the evolutionary status of 903 mCP stars, deriving a mean fractional age on the main sequence of  $\tau = 63\%$  (standard deviation of 23%). Young mCP stars, while undoubtedly present, are conspicuously underrepresented in our sample. Our results could be considered as strong evidence for an inhomogeneous age distribution among low-mass ( $M < 3 M_{\odot}$ ) mCP stars, as hinted at by previous studies. However, we caution that our sample has not been selected on the basis of an unbiased, direct detection of a magnetic field. Therefore, our results have to be viewed with caution and their general validity needs to be tested by a more extended sample selected via different methodological approaches.
- The mCP stars LAMOST J122746.05+113635.3 (#876) and LAMOST J150331.87+093125.4 (#880) boast distances and kinematical properties in agreement with halo stars. If confirmed, they would be the first CP2 halo objects known and therefore of special interest.
- We identified LAMOST J034306.74+495240.7 (#135; TYC 3321-881-1) as an eclipsing binary system ( $P_{\text{orb}} = 5.1435 \pm 0.0012\text{ d}$ ) hosting a Si CP2 star component (spectral type B9 III Si). This is of great interest because mCP stars in eclipsing binaries are exceedingly rare.
- The star LAMOST J050146.85+383500.8 was identified as an SB2 system likely comprising of a Si CP2 star and a supergiant.

Future investigations will be concerned with an in-depth study of the new mCP stars identified in this work, particularly with regard to their photometric variability, along with further development and refinement of the approach for identifying and classifying mCP stars in large spectroscopic databases using the MKCLASS code.

*Acknowledgements.* We thank the referee for his thoughtful report that helped to significantly improve the paper. This work has been supported by the DAAD (project No. 57442043). The Guo Shou Jing Telescope (the Large Sky Area Multi-Object Fiber Spectroscopic Telescope, LAMOST) is a National Major Scientific Project built by the Chinese Academy of Sciences. Funding for the project has been provided by the National Development and Reform Commission. LAMOST is operated and managed by National Astronomical Observatories, Chinese Academy of Sciences. This work presents results from the European Space Agency (ESA) space mission Gaia. Gaia data are being processed by the Gaia Data Processing and Analysis Consortium (DPAC). Funding for the DPAC is provided by national institutions, in particular the institutions participating in the Gaia MultiLateral Agreement (MLA). The Gaia mission website is <https://www.cosmos.esa.int/gaia>. The Gaia archive website is <https://archives.esac.esa.int/gaia>.

## References

- Anguiano, B., Majewski, S. R., Allende-Prieto, C., et al. 2018, *A&A*, 620, A76
- Arenou, F., Luri, X., Babusiaux, C., et al. 2018, *A&A*, 616, A17
- Aumer, M. & Binney, J. 2017, *MNRAS*, 470, 2113
- Aurière, M., Wade, G. A., Silvester, J., et al. 2007, *A&A*, 475, 1053
- Babcock, H. W. 1947, *ApJ*, 105, 105
- Bagnulo, S., Landstreet, J. D., Lo Curto, G., Szeifert, T., & Wade, G. A. 2003, *A&A*, 403, 645
- Bagnulo, S., Landstreet, J. D., Mason, E., et al. 2006, *A&A*, 450, 777
- Bailer-Jones, C. A. L., Rybizki, J., Fousneau, M., Mantelet, G., & Andrae, R. 2018, *AJ*, 156, 58
- Bayo, A., Rodrigo, C., Barrado Y Navascués, D., et al. 2008, *A&A*, 492, 277
- Beers, T. C., Wilhelm, R., Doinidis, S. P., & Mattson, C. J. 1996, *ApJS*, 103, 433
- Bidelman, W. P. 1981, *AJ*, 86, 553
- Bidelman, W. P. 1983, *AJ*, 88, 1182
- Bidelman, W. P. 1985, *AJ*, 90, 341
- Bidelman, W. P. 1998, *PASP*, 110, 270
- Bidelman, W. P. & Keenan, P. C. 1951, *ApJ*, 114, 473
- Bidelman, W. P. & MacConnell, D. J. 1973, *AJ*, 78, 687
- Bond, H. E. 1972, *PASP*, 84, 446
- Braithwaite, J. & Spruit, H. C. 2004, *Nature*, 431, 819
- Bressan, A., Marigo, P., Girardi, L., et al. 2012, *MNRAS*, 427, 127
- Butters, O. W., West, R. G., Anderson, D. R., et al. 2010, *A&A*, 520, L10
- Cannon, A. J. 1931, *Annals of Harvard College Observatory*, 100, 61
- Cantat-Gaudin, T., Jordi, C., Vallenari, A., et al. 2018, *A&A*, 618, A93
- Castelli, F., Gratton, R. G., & Kurucz, R. L. 1997, *A&A*, 318, 841
- Castelli, F. & Kurucz, R. L. 2003, in *IAU Symposium*, Vol. 210, *Modelling of Stellar Atmospheres*, ed. N. Piskunov, W. W. Weiss, & D. F. Gray, A20
- Chargeishvili, K. B. 1988, *Abastumanskaia Astrofizicheskaia Observatoriia Byulleten*, 65, 18
- Clausen, J. V. & Jensen, K. S. 1979, in *IAU Colloq. 47: Spectral Classification of the Future*, Vol. 9, 479
- Cui, X.-Q., Zhao, Y.-H., Chu, Y.-Q., et al. 2012, *Research in Astronomy and Astrophysics*, 12, 1197
- Drilling, J. S. & Pesch, P. 1973, *AJ*, 78, 48
- Faraggiana, R. 1987, *Ap&SS*, 134, 381
- Floquet, M. 1975, *A&AS*, 21, 25
- Gaia Collaboration, Brown, A. G. A., Vallenari, A., et al. 2018, *A&A*, 616, A1
- Geier, S., Østensen, R. H., Nemeth, P., et al. 2017, *A&A*, 600, A50
- Ghazaryan, S., Alecian, G., & Hakobyan, A. A. 2018, *MNRAS*, 480, 2953
- Giesecking, F. 1983, *A&A*, 118, 102
- Gray, R. O. & Corbally, C. J. 1994, *AJ*, 107, 742
- Gray, R. O. & Corbally, C. J. 2009, *Stellar Spectral Classification* (Princeton, NJ: Princeton Univ. Press)
- Gray, R. O. & Corbally, C. J. 2014, *The Astronomical Journal*, 147, 80
- Gray, R. O., Corbally, C. J., De Cat, P., et al. 2016, *AJ*, 151, 13
- Green, G. M., Schlafly, E. F., Finkbeiner, D., et al. 2018, *MNRAS*, 478, 651
- Grenier, S., Baylac, M. O., Rolland, L., et al. 1999, *A&AS*, 137, 451
- Guetter, H. H. 1977, *AJ*, 82, 598
- Hou, W., Luo, A., Yang, H., et al. 2015, *MNRAS*, 449, 1401
- Hubrig, S., North, P., & Mathys, G. 2000, *ApJ*, 539, 352
- Hubrig, S., North, P., & Schöller, M. 2007, *Astronomische Nachrichten*, 328, 475
- Hümmerich, S., Mikulášek, Z., Paunzen, E., et al. 2018, *A&A*, 619, A98
- Jamar, C. 1977, *A&A*, 56, 413
- Jamar, C. 1978, *A&A*, 70, 379
- Jayasinghe, T., Stanek, K. Z., Kochanek, C. S., et al. 2019, *MNRAS*, 486, 1907
- Johnson, D. R. H. & Soderblom, D. R. 1987, *AJ*, 93, 864
- Jones, T. J., Wolff, S. C., & Bonsack, W. K. 1974, *ApJ*, 190, 579
- Kepler Mission Team. 2009, *VizieR Online Data Catalog*, V/133
- Khan, S. A. & Shulyak, D. V. 2006, *A&A*, 448, 1153
- Khan, S. A. & Shulyak, D. V. 2007, *A&A*, 469, 1083
- Kharchenko, N. V., Piskunov, A. E., Schilbach, E., Röser, S., & Scholz, R. D. 2013, *A&A*, 558, A53
- Kharchenko, N. V., Scholz, R. D., Piskunov, A. E., Röser, S., & Schilbach, E. 2007, *Astronomische Nachrichten*, 328, 889
- Kochukhov, O. 2017, *A&A*, 597, A58
- Kochukhov, O. & Bagnulo, S. 2006, *A&A*, 450, 763
- Kochukhov, O., Bagnulo, S., & Barklem, P. S. 2002, *ApJ*, 578, L75
- Kochukhov, O., Johnston, C., Alecian, E., & Wade, G. A. 2018, *MNRAS*, 478, 1749
- Kochukhov, O., Khan, S., & Shulyak, D. 2005, *A&A*, 433, 671
- Kodaira, K. 1969, *ApJ*, 157, L59
- Krtićka, J., Janík, J., Marková, H., et al. 2013, *A&A*, 556, A18
- Krtićka, J., Mikulášek, Z., Henry, G. W., et al. 2009, *A&A*, 499, 567
- Kupka, F., Paunzen, E., & Maitzen, H. M. 2003, *MNRAS*, 341, 849
- Landstreet, J. D., Bagnulo, S., Andretta, V., et al. 2007, *A&A*, 470, 685
- Landstreet, J. D., Silaj, J., Andretta, V., et al. 2008, *A&A*, 481, 465
- Loden, L. O. & Sundman, A. 1987, *Journal of Astrophysics and Astronomy*, 8, 351
- Loden, L. O. & Sundman, A. 1989, *Journal of Astrophysics and Astronomy*, 10, 183
- Luo, A. L., Zhao, Y. H., Zhao, G., & et al. 2018, *VizieR Online Data Catalog*, 5153, 0
- Maitzen, H. M. 1976, *A&A*, 51, 223
- Maitzen, H. M. 1980, *A&A*, 89, 230
- Michaud, G. 1970, *ApJ*, 160, 641
- Molnar, M. R. 1973, *ApJ*, 179, 527
- Morgan, W. W. 1933, *ApJ*, 77, 330
- Moss, D. 2004, in *IAU Symposium*, Vol. 224, *The A-Star Puzzle*, ed. J. Zverko, J. Ziznovsky, S. J. Adelman, & W. W. Weiss, 245–252
- Murphy, S. J. & Paunzen, E. 2017, *MNRAS*, 466, 546
- Nassau, J. J. & Macrae, D. A. 1955, *ApJ*, 121, 32
- Netopil, M., Paunzen, E., Heiter, U., & Soubiran, C. 2016, *A&A*, 585, A150
- Netopil, M., Paunzen, E., Hümmerich, S., & Bernhard, K. 2017, *MNRAS*, 468, 2745
- Netopil, M., Paunzen, E., Maitzen, H. M., North, P., & Hubrig, S. 2008, *A&A*, 491, 545
- Niemczura, E., Hümmerich, S., Castelli, F., et al. 2017, *Scientific Reports*, 7, 5906
- Ojha, D. K. 2001, *MNRAS*, 322, 426
- Paunzen, E. 2015, *A&A*, 580, A23
- Paunzen, E., Netopil, M., Pintado, O. I., & Rode-Paunzen, M. 2011, *Astronomische Nachrichten*, 332, 77
- Paunzen, E., Stütz, C., & Maitzen, H. M. 2005, *A&A*, 441, 631
- Pecaut, M. J. & Mamajek, E. E. 2013, *ApJS*, 208, 9
- Pöhl, H., Maitzen, H. M., & Paunzen, E. 2003, *A&A*, 402, 247
- Polosukhina, N., Kurtz, D., Hack, M., et al. 1999, *A&A*, 351, 283
- Preston, G. W. 1974, *ARA&A*, 12, 257
- Przybylski, A. 1966, *Nature*, 210, 20
- Qin, L., Luo, A. L., Hou, W., et al. 2019, *ApJS*, 242, 13
- Renson, P. & Manfroid, J. 2009, *A&A*, 498, 961
- Richer, J., Michaud, G., & Turcotte, S. 2000, *ApJ*, 529, 338
- Roby, S. W. & Lambert, D. L. 1990, *ApJS*, 73, 67
- Sato, K. & Kuji, S. 1990, *A&AS*, 85, 1069
- Scholz, R. D., Chojnowski, S. D., & Hubrig, S. 2019, *A&A*, 628, A81
- Sikora, J., David-Uraz, A., Chowdhury, S., et al. 2019, *MNRAS*, 487, 4695
- Skarka, M., Kabáth, P., Paunzen, E., et al. 2019, *MNRAS*, 487, 4230
- Skiff, B. A. 2014, *VizieR Online Data Catalog*, B/mk
- Skrutskie, M. F., Cutri, R. M., Stiening, R., et al. 2006, *AJ*, 131, 1163
- Slettebak, A. & Stock, J. 1959, *Astronomische Abhandlungen der Hamburger Sternwarte*, 5, 105
- Smalley, B., Antoci, V., Holdsworth, D. L., et al. 2017, *MNRAS*, 465, 2662
- Stibbs, D. W. N. 1950, *MNRAS*, 110, 395
- Stift, M. J. & Alecian, G. 2012, *MNRAS*, 425, 2715
- Vagnozzi, S. 2019, *Atoms*, 7
- Venn, K. A., Irwin, M., Shetrone, M. D., et al. 2004, *AJ*, 128, 1177
- Watson, C. L. 2006, *Society for Astronomical Sciences Annual Symposium*, 25, 47
- Wild, J. F. & Jeffery, C. S. 2018, *MNRAS*, 473, 4021
- Wolff, S. C. 1983, *The A-stars : problems and perspectives*
- Wolff, S. C. & Wolff, R. J. 1971, *AJ*, 76, 422
- Zhang, B., Liu, C., Li, C.-Q., et al. 2020, *Research in Astronomy and Astrophysics*, 20, 51
- Zhao, G., Zhao, Y.-H., Chu, Y.-Q., Jing, Y.-P., & Deng, L.-C. 2012, *Research in Astronomy and Astrophysics*, 12, 723

## Appendix A: Essential data for our sample stars

Table A.1 lists essential data for our sample stars. It is organised as follows:

- Column 1: Internal identification number.
- Column 2: LAMOST identifier.
- Column 3: Alternativ identifier (HD number, TYC identifier, or GAIA DR2 number).
- Column 4: Right ascension (J2000). Positional information was taken from GAIA DR2 (Gaia Collaboration et al. 2018; Arenou et al. 2018).
- Column 5: Declination (J2000).
- Column 6: MKCLASS final type, as derived in this study.<sup>9</sup> All further additions to the spectral type that are not directly based on the MKCLASS\_mCP output are highlighted using italics. For an easy identification, manually altered spectral types are indicated by asterisks.
- Column 7: Sloan *g* band S/N of the analysed spectrum.
- Column 8: *G* mag (GAIA DR2).
- Column 9: *G* mag error.
- Column 10: Parallax (GAIA DR2).
- Column 11: Parallax error.
- Column 12: Dereddened colour index  $(BP - RP)_0$  (GAIA DR2).
- Column 13: Colour index error.
- Column 14: Absorption in the *G* band,  $A_G$ .
- Column 15: Intrinsic absolute magnitude in the *G* band,  $M_{G,0}$ .
- Column 16: Absolute magnitude error.

Tables A.1, B.1, and C.1 are available at the CDS.<sup>10</sup>

## Appendix B: Masses and fractional ages on the main sequence

## Appendix C: LAMOST Standard Star Library

<sup>9</sup> We note that, as in the Renson & Manfroid (2009) catalogue, the 'p' denoting peculiarity was omitted from the spectral classifications.

<sup>10</sup> <http://cdsarc.u-strasbg.fr/viz-bin/cat/J/A+A/640/A40>

**Table A.1.** Essential data for our sample stars, sorted by increasing right ascension. The columns denote: (1) Internal identification number. (2) LAMOST identifier. (3) Alternativ identifier (HD number, TYC identifier or GAIA DR2 number). (4) Right ascension (J2000; GAIA DR2). (5) Declination (J2000; GAIA DR2). (6) Spectral type, as derived in this study. (7) Sloan  $g$  band S/N ratio of the analysed spectrum. (8)  $G$  mag (GAIA DR2). (9)  $G$  mag error. (10) Parallax (GAIA DR2). (11) Parallax error. (12) Dereddened colour index  $(BP - RP)_0$  (GAIA DR2). (13) Colour index error. (14) Absorption in the  $G$  band,  $A_G$ . (15) Intrinsic absolute magnitude in the  $G$  band,  $M_{G,0}$ . (16) Absolute magnitude error.

(1)	(2)	(3)	(4)		(5)	(6)	(7)	(8)	(9)	(10)	(11)	(12)	(13)	(14)	(15)	(16)
No.	ID_LAMOST	ID_alt	RA(J2000)	Dec(J2000)	SpT_final	S/N $_g$	$G$ mag	$e_G$ mag	$\pi$ (mas)	$e_\pi$	$(BP - RP)_0$	$e_{(BP - RP)_0}$	$A_G$	$M_{G,0}$	$e_{M_{G,0}}$	
1	J000700.42+053333.6	TYC 7-1183-1	00 07 00.30	+05 33 33.64	A0 IV-V SrCrEuSi	369	10.5972	0.0005	+1.579	0.056	+0.238	0.002	0.15	+1.44	0.09	
2	J000834.32+321205.4	TYC 2263-195-1	00 08 34.32	+32 12 05.48	A2 IV SrCrEu	166	11.6306	0.0005	+1.355	0.046	+0.325	0.003	0.11	+2.18	0.09	
3	J000840.99+580213.2	Gaia DR2 422492913555750912	00 08 41.00	+58 02 13.21	A0 Ib-II bl4077	105	14.1363	0.0025	+0.152	0.023	-0.012	0.012	1.18	-1.14	0.33	
4	J001137.65+473203.2	TYC 3251-1665-1	00 11 37.73	+47 32 02.75	B9 V Cr	173	10.7570	0.0008	+0.955	0.058	+0.054	0.003	0.17	+0.49	0.14	
5	J001345.60+562953.5	TYC 3661-1153-1	00 13 45.84	+56 29 53.60	B9 IV-V CrSi (He-wk)	241	10.3974	0.0006	+1.176	0.031	-0.030	0.002	0.62	+0.13	0.08	
6	J001407.53+553052.8	TYC 3657-780-1	00 14 07.53	+55 30 52.89	B9 IV-V Eu	264	11.0914	0.0011	+0.912	0.046	-0.016	0.003	0.62	+0.27	0.12	
7	J002343.42+535755.9	Gaia DR2 419523991644430208	00 23 43.43	+53 57 55.92	B9 IV-V bl4077 bl4130	111	12.8617	0.0004	+0.283	0.033	+0.010	0.002	0.77	-0.65	0.26	
8	J002454.57+385413.2	Gaia DR2 379258467075146112	00 24 54.58	+38 54 13.24	A8 V SrCrEu	122	12.5838	0.0003	+0.745	0.064	+0.239	0.002	0.16	+1.78	0.19	
9	J002616.49+562735.1	TYC 3661-142-1	00 26 16.50	+56 27 35.14	kA3hA7mF2 Si	59	11.7673	0.0004	+0.803	0.040	-0.048	0.002	0.48	+0.81	0.12	
10	J003312.88+543141.3	TYC 3658-79-1	00 33 12.64	+54 31 41.33	B8 V Si	560	10.2213	0.0006	+1.081	0.051	-0.085	0.002	0.37	+0.02	0.11	
11	J003318.47+571616.8 <sup>a</sup>	TYC 3662-378-1	00 33 18.47	+57 16 16.79	B9 IV-V Si	338	10.6583	0.0009	+1.105	0.053	-0.082	0.003	0.61	+0.26	0.12	
12	J003425.61+452108.7	Gaia DR2 389018591278583552	00 34 25.58	+45 21 09.21	kA1hA7mA9 SrEuSi	64	14.1081	0.0005	+0.347	0.039	+0.222	0.015	0.17	+1.64	0.25	
13	J004555.55+553553.8	TYC 3659-1537-1	00 45 55.53	+55 35 53.73	kA0hA3mA6 SrEu	332	10.5123	0.0004	+1.602	0.055	+0.058	0.002	0.24	+1.30	0.09	
14	J004947.16+525208.2	HD 232285	00 49 46.83	+52 52 08.24	B9 V CrEuSi (He-wk)	285	9.3967	0.0004	+2.214	0.064	+0.049	0.001	0.45	+0.67	0.08	
15	J005002.58+434300.5	TYC 2810-568-1	00 50 02.59	+43 43 00.55	B9 V SrEu	232	11.8448	0.0005	+0.752	0.048	-0.029	0.003	0.13	+1.10	0.15	
16	J005535.39+433430.0	TYC 2810-1634-1	00 55 35.40	+43 34 30.04	kB9.5hA1mA3 Eu	296	11.6205	0.0013	+0.475	0.073	-0.048	0.005	0.17	-0.17	0.34	
17	J005604.18+453914.9	TYC 3262-1253-1	00 56 04.19	+45 39 14.95	A5 V SrEu	164	11.6601	0.0004	+0.837	0.051	+0.222	0.002	0.23	+1.05	0.14	
18	J005937.83+532354.0	TYC 3668-724-1	00 59 37.83	+53 23 53.93	B9 IV-V Si	199	11.7537	0.0007	+0.649	0.066	+0.052	0.002	0.43	+0.39	0.22	
19	J010007.84+045339.3	HD 5844	01 00 07.85	+04 53 39.46	kB8hA3mA6 Cr	293	9.7105	0.0009	+1.189	0.118	+0.106	0.003	0.11	-0.02	0.22	
20	J010159.03+505149.9	Gaia DR2 404326915576637184	01 01 59.02	+50 51 49.99	kA3hA7mA8 SrCrEu	190	13.4949	0.0005	+0.457	0.032	+0.267	0.003	0.37	+1.43	0.16	
21	J010522.41+501031.3 <sup>a</sup>	TYC 3271-1597-1	01 05 22.42	+50 10 29.60	B9 V Cr	367	10.4967	0.0006	+0.968	0.054	+0.038	0.002	0.31	+0.12	0.13	
22	J010651.35+154426.9	HD 6590	01 06 51.17	+15 44 26.92	kA1hA7mA7 SrCrEu	416	9.9956	0.0009	+1.277	0.067	+0.262	0.004	0.29	+0.24	0.12	
23	J011154.28+563254.7	TYC 3677-2219-1	01 11 54.20	+56 32 54.70	B9.5 IV-V CrEu	142	10.9232	0.0004	+1.285	0.035	-0.086	0.002	0.48	+0.99	0.08	
24	J011430.72+432537.2	TYC 2812-530-1	01 14 30.73	+43 25 37.19	A9 V Sr	187	11.0312	0.0007	+1.098	0.044	+0.398	0.003	0.10	+1.13	0.10	
25	J011435.00+534757.2	Gaia DR2 410353407527493504	01 14 35.00	+53 47 57.22	A1 IV-V SrCrEuSi	115	12.1234	0.0003	+1.025	0.046	+0.205	0.002	0.68	+1.50	0.11	
26	J011524.23+515128.5	TYC 3276-520-1	01 15 24.26	+51 51 28.85	A0 V SrCr	452	11.2142	0.0012	+1.519	0.072	+0.068	0.003	0.40	+1.72	0.11	
27	J011627.87+250924.1	TYC 1750-2062-1	01 16 27.88	+25 09 24.15	B8 III-IV Si	140	12.5959	0.0007	+0.210	0.057	-	-	-	-	-	
28	J011816.48+514639.8	TYC 3276-500-1	01 18 16.41	+51 46 40.53	B9 IV-V CrEuSi	409	10.7842	0.0006	+1.368	0.063	-0.012	0.003	0.34	+1.13	0.11	
29	J012028.54+480545.6	TYC 3269-867-1	01 20 28.55	+48 05 45.63	kA4hA7mA8 SrCrEu	300	11.3762	0.0006	+0.935	0.055	+0.214	0.002	0.29	+0.94	0.14	
30	J012122.31+442826.2	Gaia DR2 397601443468210944	01 21 22.30	+44 28 26.12	kA3hA7mA8 CrEu	152	12.2442	0.0014	+0.520	0.050	+0.316	0.007	0.14	+0.69	0.21	
31	J012220.76+532354.4	TYC 3670-871-1	01 22 20.76	+53 23 54.43	B9 IV Si	298	11.0429	0.0032	+0.985	0.054	+0.069	0.013	0.52	+0.49	0.13	
32	J013031.12+454021.1	TYC 3278-454-1	01 30 31.13	+45 40 21.16	B9 IV CrEuSi	233	11.1469	0.0025	+0.853	0.082	-0.088	0.006	0.10	+0.70	0.21	
33	J013055.87+452155.7	TYC 3278-614-1	01 30 55.88	+45 21 55.77	kA1hA3mA4 SrCr	734	9.2923	0.0006	+1.037	0.077	+0.112	0.003	0.14	-0.77	0.17	
34	J014016.31+422946.5	TYC 2823-1986-1	01 40 16.31	+42 29 46.52	B9 V Cr	113	12.5656	0.0007	+0.476	0.067	-0.081	0.005	0.13	+0.82	0.31	
35	J014508.87+322430.3	Gaia DR2 305411761460144896	01 45 08.88	+32 24 30.39	kA1hA6mA7 SrCrEu	109	14.2946	0.0005	+0.382	0.054	+0.241	0.003	0.13	+2.08	0.31	
36	J014905.86+543820.9	Gaia DR2 408536189683896960	01 49 05.87	+54 38 21.00	kA0hA5mA6 Cr	187	12.4605	0.0005	+0.615	0.045	+0.125	0.004	0.23	+1.17	0.17	
37	J014940.99+534134.2	TYC 3684-1139-1	01 49 41.00	+53 41 34.26	B4 V HeB8 (Si)*	154	12.4184	0.0007	+0.327	0.038	-0.010	0.005	0.45	-0.46	0.26	
38	J015059.58+540259.1	HD 11140	01 50 59.78	+54 03 02.16	B8 IV bl4130	691	8.5498	0.0006	+1.015	0.071	-0.110	0.004	0.20	-1.62	0.16	
39	J015458.39+541849.0	TYC 3684-2153-1	01 54 58.39	+54 18 49.09	B9 V Cr	367	11.3345	0.0014	+0.872	0.064	+0.116	0.005	0.20	+0.84	0.17	
40	J015545.33+543748.2	TYC 3688-1164-1	01 55 45.33	+54 37 48.21	B9.5 III-IV Si	152	11.8995	0.0005	+0.940	0.048	-0.004	0.003	0.41	+1.35	0.12	
41	J015559.12+563558.0	Gaia DR2 504860387608173184	01 55 59.13	+56 35 58.06	B9.5 II-III Si	139	14.0054	0.0004	+0.408	0.027	+0.031	0.004	0.53	+1.53	0.15	
42	J015628.29+534409.9	TYC 3684-1671-1	01 56 28.30	+53 44 09.94	B9.5 IV bl4130	336	11.8104	0.0005	+0.413	0.040	-0.052	0.003	0.26	-0.38	0.22	
43	J015654.63+543533.0	Gaia DR2 408394047746449280	01 56 54.64	+54 35 33.06	A1 II-III bl4130	177	12.9211	0.0003	+0.239	0.034	+0.001	0.003	0.40	-0.59	0.32	
44	J015729.58+542137.2	TYC 3684-165-1	01 57 29.77	+54 21 36.51	B8 V Si	496	10.5459	0.0012	+0.642	0.083	-0.054	0.007	0.32	-0.74	0.29	
45	J020004.86+560852.5	TYC 3689-200-1	02 00 04.61	+56 08 51.37	B9 IV Si	538	10.1176	0.0011	+4.935	0.314	+0.146	0.003	0.07	+3.52	0.15	
46	J020024.73+544319.0	Gaia DR2 504415600792977920	02 00 24.73	+54 43 19.06	A1 IV-V SrCr	253	12.3203	0.0005	+0.477	0.037	+0.154	0.003	0.51	+0.21	0.17	
47	J020034.64+451914.2	TYC 3280-1768-1	02 00 34.65	+45 19 14.24	kA1hA3mA6 CrEu	215	11.4997	0.0008	+0.853	0.074	+0.071	0.004	0.13	+1.03	0.19	
48	J020228.03+565629.3	Gaia DR2 505090907095341824	02 02 28.03	+56 56 29.45	kB9.5hA5mA6 Cr	103	14.0315	0.0005	+0.298	0.028	+0.143	0.003	0.58	+0.82	0.21	
49	J020338.02+533204.2	TYC 3685-1684-1	02 03 38.02	+53 32 04.26	B8 V Si	426	11.1758	0.0033	+0.742	0.058	-0.018	0.015	0.27	+0.26	0.18	
50	J020415.91+503019.4	HD 12532	02 04 16.21	+50 30 19.66	B6 III Si	687	9.5114	0.0011	+1.084	0.065	-0.097	0.006	0.29	-0.61	0.14	

**Table A.1.** Essential data for our sample stars, sorted by increasing right ascension. The columns denote: (1) Internal identification number. (2) LAMOST identifier. (3) Alternativ identifier (HD number, TYC identifier or GAIA DR2 number). (4) Right ascension (J2000; GAIA DR2). (5) Declination (J2000; GAIA DR2). (6) Spectral type, as derived in this study. (7) Sloan  $g$  band S/N ratio of the analysed spectrum. (8)  $G$  mag (GAIA DR2). (9)  $G$  mag error. (10) Parallax (GAIA DR2). (11) Parallax error. (12) Dereddened colour index  $(BP - RP)_0$  (GAIA DR2). (13) Colour index error. (14) Absorption in the  $G$  band,  $A_G$ . (15) Intrinsic absolute magnitude in the  $G$  band,  $M_{G,0}$ . (16) Absolute magnitude error.

(1)	(2)	(3)	(4)		(5)	(6)	(7)	(8)	(9)	(10)	(11)	(12)	(13)	(14)	(15)	(16)
No.	ID_LAMOST	ID_alt	RA(J2000)	Dec(J2000)	SpT_final	S/N $_g$	$G$ mag	$e_G$ mag	$\pi$ (mas)	$e_\pi$	$(BP - RP)_0$	$e_{(BP - RP)_0}$	$A_G$	$M_{G,0}$	$e_{M_{G,0}}$	
51	J020417.01+553439.5	Gaia DR2 456542864521078144	02 04 17.04	+55 34 39.35	B9.5 IV Si	169	12.4943	0.0072	–	–	–	–	–	–	–	
52	J020425.19+561142.4	TYC 3689-1567-1	02 04 25.19	+56 11 42.54	B8 V Si	305	11.4011	0.0026	+0.835	0.052	–0.092	0.011	0.48	+0.53	0.14	
53	J020842.44+544442.1	Gaia DR2 456423464428927360	02 08 42.45	+54 44 42.11	B9 III–IV Si	122	13.3649	0.0008	+0.417	0.029	+0.074	0.004	0.54	+0.93	0.16	
54	J020921.65+471008.4	HD 13090	02 09 21.45	+47 10 10.99	B9 III–IV Si	298	9.0616	0.0006	+1.413	0.070	–0.167	0.003	0.26	–0.45	0.12	
55	J021106.70+492548.2	TYC 3289-2552-1	02 11 06.70	+49 25 48.16	B9 III–IV Si	181	12.3874	0.0005	+0.192	0.046	+0.005	0.004	0.36	–1.55	0.52	
56	J021147.71+515247.3	TYC 3293-1775-1	02 11 47.77	+51 52 49.09	B9 III–IV bl4077 bl4130	204	10.6664	0.0015	+0.717	0.037	+0.075	0.006	0.32	–0.38	0.12	
57	J021429.02+553451.3	HD 13592	02 14 28.73	+55 34 53.10	B8 IV–V Si	266	9.5172	0.0005	+1.757	0.051	–0.091	0.002	0.33	+0.41	0.08	
58	J021626.36+442611.8	TYC 2842-681-1	02 16 26.36	+44 26 11.89	B9.5 III–IV EuSi	882	9.3855	0.0008	+1.569	0.074	+0.035	0.005	0.17	+0.20	0.11	
59	J021927.75+420707.6	TYC 2838-1789-1	02 19 27.75	+42 07 07.67	B8 IV–V <sup>b</sup>	983	9.4303	0.0005	+1.109	0.083	–0.091	0.003	0.12	–0.47	0.17	
60	J022113.98+381906.4	Gaia DR2 331697064392371584	02 21 13.99	+38 19 06.36	A0 V Cr	136	14.1572	0.0015	+0.369	0.050	+0.042	0.008	0.13	+1.87	0.30	
61	J022120.02+280415.6	HD 14522	02 21 20.03	+28 04 15.86	A8 V SrEuSi	198	8.7493	0.0005	+3.525	0.055	+0.206	0.003	0.23	+1.26	0.06	
62	J022252.38+485816.0	Gaia DR2 355271624484226944	02 22 52.39	+48 58 16.02	kA0hA3mA6 Cr	134	13.3035	0.0004	+0.823	0.135	+0.160	0.003	0.28	+2.60	0.36	
63	J023335.11+530446.3	TYC 3687-654-1	02 33 35.12	+53 04 46.41	B9.5 II–III Si	120	11.6941	0.0007	+0.690	0.039	–0.065	0.003	0.58	+0.31	0.13	
64	J023534.25+520926.0	Gaia DR2 452192028288916096	02 35 34.25	+52 09 26.09	B9.5 II–III Si	169	13.0338	0.0008	+0.402	0.037	+0.002	0.003	0.67	+0.38	0.21	
65	J023800.44+374400.0	Gaia DR2 333718035483431040	02 38 00.45	+37 44 00.04	A0 IV–V bl4077 bl4130	114	12.5399	0.0006	+0.537	0.071	–0.020	0.004	0.15	+1.04	0.29	
66	J023805.20+513946.1	TYC 3308-1326-1	02 38 05.20	+51 39 46.15	B8 IV Si	147	11.8472	0.0013	+0.722	0.039	–0.011	0.006	0.67	+0.47	0.13	
67	J023844.12+510644.1	TYC 3308-1621-1	02 38 44.13	+51 06 44.16	B9.5 IV bl4077 bl4130	110	12.6169	0.0005	+0.551	0.049	+0.017	0.003	0.74	+0.58	0.20	
68	J023936.01+540059.5	Gaia DR2 453949185310404736	02 39 36.02	+54 00 59.65	kA2hA5mA7 CrEu	163	12.3750	0.0009	+1.085	0.030	+0.511	0.007	0.64	+1.91	0.08	
69	J024028.73+473922.8	TYC 3300-2476-1	02 40 28.74	+47 39 22.83	B9 V Cr	116	11.7478	0.0006	+0.823	0.045	+0.089	0.004	0.27	+1.05	0.13	
70	J024243.57+453720.4	TYC 3296-281-1	02 42 42.76	+45 37 20.73	A1 V SrCrEuSi	142	11.9910	0.0006	+1.019	0.037	+0.311	0.003	0.17	+1.86	0.09	
71	J024542.78+555858.9	Gaia DR2 454542577989769472	02 45 42.78	+55 58 59.00	kA0hA4mA6 CrSi	163	11.8698	0.0004	+1.010	0.033	+0.061	0.002	1.02	+0.87	0.09	
72	J025123.15+455720.9	TYC 3297-693-1	02 51 23.16	+45 57 20.94	B9.5 IV–V Cr*	318	11.1158	0.0006	+0.625	0.047	+0.090	0.002	0.33	–0.23	0.17	
73	J025317.44+465342.6	Gaia DR2 437431973738031744	02 53 17.45	+46 53 42.66	kA3hA3mA7 CrEu	135	12.7318	0.0004	+0.458	0.039	+0.208	0.003	0.25	+0.78	0.19	
74	J025507.91+463730.1	Gaia DR2 434413749897657728	02 55 07.91	+46 37 30.19	A0 V SrCr	96	14.5096	0.0004	+0.394	0.034	+0.060	0.002	0.63	+1.86	0.19	
75	J025708.41+241901.3	TYC 1782-825-1	02 57 08.41	+24 19 01.31	A9 V SrEu	170	11.5772	0.0007	+0.938	0.042	+0.237	0.003	0.22	+1.22	0.11	
76	J025716.49+572715.7	TYC 3709-175-1	02 57 16.36	+57 27 15.73	B9 V Eu	221	10.7272	0.0007	+0.870	0.155	–0.840	0.003	3.06	–2.64	0.39	
77	J025945.31+541941.5 <sup>a</sup>	HD 18410	02 59 45.28	+54 19 44.96	kB7hA7mA6 CrEuSi	770	9.0794	0.0012	+2.858	0.035	+0.167	0.006	0.41	+0.95	0.06	
78	J025951.09+540337.5	TYC 3701-157-1	02 59 51.20	+54 03 39.14	B8 III–IV Si	409	10.5057	0.0011	+1.183	0.045	0.000	0.004	1.33	–0.46	0.10	
79	J030339.08+472125.5	Gaia DR2 435816451857186048	03 03 39.08	+47 21 25.54	kA0hA3mA5 CrSi	160	12.1342	0.0006	+0.501	0.032	+0.123	0.005	0.48	+0.15	0.15	
80	J030350.21+463718.3	TYC 3310-1808-1	03 03 50.21	+46 37 18.37	A8 V SrCrEuSi	653	9.8183	0.0003	+1.688	0.040	+0.282	0.002	0.33	+0.63	0.07	
81	J030459.32+351024.5	Gaia DR2 138608975579548544	03 04 59.33	+35 10 24.58	A7 V SrCrEu	130	12.3721	0.0003	+0.831	0.052	+0.340	0.002	0.40	+1.57	0.14	
82	J030614.98+485615.0	TYC 3318-18-1	03 06 14.91	+48 56 17.16	kB9hA5mA3 SrCrEu	431	10.1998	0.0007	+1.257	0.044	+0.039	0.002	0.81	–0.11	0.09	
83	J030633.66+025615.7	TYC 58-1131-1	03 06 33.67	+02 56 15.77	B9.5 IV–V CrEu	301	11.4566	0.0008	+0.808	0.089	+0.019	0.002	0.25	+0.75	0.24	
84	J030655.59+492941.0	Gaia DR2 436280858083105024	03 06 55.59	+49 29 41.04	A0 IV–V Cr	111	12.2319	0.0003	+1.184	0.032	+0.252	0.002	0.89	+1.71	0.08	
85	J030708.46+460837.7	TYC 3310-1240-1	03 07 08.47	+46 08 37.72	B9.5 IV bl4077 bl4130	222	11.0603	0.0012	+1.249	0.048	+0.004	0.006	0.42	+1.12	0.10	
86	J030709.75+535142.4	TYC 3702-136-1	03 07 09.72	+53 51 42.60	B8 III–IV bl4130	194	10.1437	0.0010	+1.434	0.125	–0.142	0.003	1.39	–0.47	0.20	
87	J030759.91+452730.7	TYC 3310-129-1	03 07 59.79	+45 27 30.71	B9 IV bl4130	411	10.6727	0.0009	–	–	–	–	–	–	–	
88	J030837.10+364000.8	Gaia DR2 139337264594236288	03 08 37.11	+36 40 00.81	A0 V Cr	104	14.3423	0.0008	+0.094	0.052	–	–	–	–	–	
89	J030915.26+262955.5	TYC 1791-480-1	03 09 15.27	+26 29 55.58	A3 V Sr	217	11.2401	0.0013	+1.735	0.054	+0.162	0.002	0.45	+1.99	0.08	
90	J030937.10+451010.4	TYC 3310-2246-1	03 09 37.11	+45 10 10.51	A0 V Cr*	136	11.8616	0.0008	+0.594	0.042	+0.074	0.005	0.45	+0.28	0.16	
91	J031043.71+480727.8	Gaia DR2 435920218270165504	03 10 43.72	+48 07 27.87	A0 IV–V SrCrEu	160	12.7285	0.0002	+0.663	0.032	+0.181	0.001	0.66	+1.18	0.11	
92	J031054.55+462725.9	TYC 3310-1345-1	03 10 54.42	+46 27 25.89	kA1hA4mA6 SrCrEu	421	10.6114	0.0011	+1.043	0.067	+0.171	0.004	0.52	+0.19	0.15	
93	J031100.46+443818.2	TYC 2860-145-1	03 11 00.46	+44 38 18.20	A1 II–III Si	246	11.5547	0.0009	–0.513	0.191	–	–	–	–	–	
94	J031111.67+461637.6	TYC 3310-2115-1	03 11 11.68	+46 16 37.67	B9.5 IV–V CrEu	185	12.2008	0.0014	+0.725	0.038	+0.111	0.006	0.47	+1.03	0.12	
95	J031142.28+080707.6	HD 19846	03 11 42.05	+08 07 07.60	B9 IV–V Eu	695	8.5098	0.0007	+3.773	0.057	–0.414	0.004	0.98	+0.42	0.06	
96	J031244.57+113233.7	TYC 651-963-1	03 12 44.56	+11 32 34.00	B9.5 IV Cr	154	10.0352	0.0009	+1.951	0.047	+0.024	0.003	0.67	+0.81	0.07	
97	J031315.28+331930.4	Gaia DR2 137397859224918016	03 13 15.29	+33 19 30.48	A0 V CrEu	190	12.0185	0.0005	+1.345	0.057	+0.232	0.003	0.42	+2.24	0.11	
98	J031536.60+430106.0	TYC 2856-451-1	03 15 36.63	+43 01 03.49	B8 IV Si*	297	10.0378	0.0007	+1.417	0.068	–0.080	0.003	0.35	+0.44	0.12	
99	J031714.31+565041.4	TYC 3710-812-1	03 17 14.32	+56 50 41.40	B8 IV CrSi (He-wk)	247	11.0567	0.0005	+0.903	0.038	–0.185	0.002	1.96	–1.12	0.10	
100	J031722.65+490836.3	TYC 3319-464-1	03 17 22.36	+49 08 36.59	B9.5 IV–V CrEu	276	9.6825	0.0009	+2.436	0.041	+0.048	0.004	0.66	+0.96	0.06	



**Table A.1.** Essential data for our sample stars, sorted by increasing right ascension. The columns denote: (1) Internal identification number. (2) LAMOST identifier. (3) Alternativ identifier (HD number, TYC identifier or GAIA DR2 number). (4) Right ascension (J2000; GAIA DR2). (5) Declination (J2000; GAIA DR2). (6) Spectral type, as derived in this study. (7) Sloan  $g$  band S/N ratio of the analysed spectrum. (8)  $G$  mag (GAIA DR2). (9)  $G$  mag error. (10) Parallax (GAIA DR2). (11) Parallax error. (12) Dereddened colour index  $(BP - RP)_0$  (GAIA DR2). (13) Colour index error. (14) Absorption in the  $G$  band,  $A_G$ . (15) Intrinsic absolute magnitude in the  $G$  band,  $M_{G,0}$ . (16) Absolute magnitude error.

(1)	(2)	(3)	(4)		(5)	(6)	(7)	(8)	(9)	(10)	(11)	(12)	(13)	(14)	(15)	(16)
No.	ID_LAMOST	ID_alt	RA(J2000)	Dec(J2000)	SpT_final	S/N $_g$	$G$ mag	$e_G$ mag	pi(mas)	$e_{pi}$	$(BP - RP)_0$	$e_{(BP - RP)_0}$	$A_G$	$M_{G,0}$	$e_{M_{G,0}}$	
101	J032020.62+485347.2	TYC 3319-1872-1	03 20 20.63	+48 53 47.20	B5 III-IV bl4130	306	11.3562	0.0012	+0.956	0.041	+0.089	0.003	0.99	+0.27	0.11	
102	J032111.38+530600.5	TYC 3703-715-1	03 21 11.38	+53 06 00.52	B8 IV-V EuSi	154	11.3153	0.0015	+0.467	0.199	-	-	-	-	-	
103	J032122.27+445902.7	TYC 2873-3205-1	03 21 22.28	+44 59 00.12	B9.5 V bl4077 bl4130	209	9.9483	0.0006	+2.086	0.058	+0.001	0.002	0.32	+1.22	0.08	
104	J032224.63+441318.6	TYC 2873-1033-1	03 22 24.64	+44 13 18.62	A8 V SrCr	165	11.4434	0.0012	+1.370	0.077	+0.301	0.002	0.39	+1.74	0.13	
105	J032252.44+320514.7	Gaia DR2 124329274471999232	03 22 52.45	+32 05 14.71	A0 V SrCrEuSi	220	11.8053	0.0003	+0.718	0.067	+0.221	0.002	0.60	+0.49	0.21	
106	J032333.76+510336.6	Gaia DR2 442651497173870080	03 23 33.76	+51 03 36.63	A2 V CrEuSi	107	12.9872	0.0006	+0.880	0.031	+0.313	0.002	1.34	+1.37	0.09	
107	J032343.27+442245.4	Gaia DR2 241472445889902080	03 23 43.27	+44 22 45.50	A0 Ib-II EuSi	108	14.6248	0.0041	+0.243	0.036	+0.010	0.02	0.41	+1.14	0.33	
108	J032413.45+525937.5	TYC 3703-669-1	03 24 13.45	+52 59 37.59	B7 V bl4130	124	11.5487	0.0016	+0.747	0.034	-0.074	0.006	1.56	-0.64	0.11	
109	J032611.50+495758.8	TYC 3320-16-1	03 26 11.50	+49 57 58.83	B8 V Si	136	12.2755	0.0006	+0.591	0.040	-0.056	0.003	0.84	+0.30	0.16	
110	J032719.03+142144.4	Gaia DR2 41984099888203392	03 27 19.04	+14 21 44.25	B9 V CrEu	186	12.7108	0.0004	+0.473	0.045	-0.018	0.004	0.61	+0.47	0.21	
111	J032747.71+453527.0	TYC 3312-1515-1	03 27 47.72	+45 35 27.10	B9 III-IV Cr	104	11.9996	0.0010	+0.712	0.039	+0.024	0.004	0.51	+0.75	0.13	
112	J032823.89+542139.1	TYC 3703-2-1	03 28 23.90	+54 21 39.08	B9.5 V SrCr	179	11.5554	0.0006	+1.048	0.059	+0.024	0.002	1.58	+0.08	0.13	
113	J032856.39+475618.4	TYC 3316-892-1	03 28 56.69	+47 56 20.09	B9 IV-V bl4130	463	9.6703	0.0005	+1.448	0.048	-0.037	0.002	0.69	-0.22	0.09	
114	J032939.33+060540.8	TYC 63-463-1	03 29 39.35	+06 05 40.82	B9 V CrEuSi	303	11.5663	0.0007	+1.036	0.038	-0.038	0.003	0.71	+0.93	0.09	
115	J033003.45+563459.0	Gaia DR2 448609132207300096	03 30 03.45	+56 34 58.99	A1 IV-V CrEu	148	11.9160	0.0004	+1.603	0.042	+0.074	0.002	1.39	+1.55	0.08	
116	J033053.47+550051.2	TYC 3707-124-1	03 30 53.18	+55 00 51.27	B9 IV-V CrEu	258	9.9624	0.0015	+2.276	0.055	-0.101	0.006	0.86	+0.89	0.07	
117	J033221.41+472318.3	TYC 3316-1385-1	03 32 21.19	+47 23 17.08	B9 V bl4130	216	10.2552	0.0006	+2.000	0.043	-0.191	0.002	1.10	+0.66	0.07	
118	J033228.57+433038.0	TYC 2874-2420-1	03 32 28.58	+43 30 38.26	B8 III-IV EuSi	146	11.1063	0.0026	+0.635	0.066	+0.048	0.008	0.43	-0.31	0.23	
119	J033325.39+452124.0	TYC 3312-694-1	03 33 25.32	+45 21 24.29	A0 V SrCr	324	11.2030	0.0009	+1.128	0.051	+0.179	0.002	0.60	+0.87	0.11	
120	J033341.86+542708.3	TYC 3720-422-1	03 33 41.87	+54 27 08.35	B8 III-IV EuSi	180	11.4739	0.0006	+0.979	0.034	-0.006	0.003	1.50	-0.07	0.09	
121	J033348.98+334153.1	HD 278822	03 33 48.99	+33 41 53.05	B6 III-IV Si	256	9.9195	0.0005	+1.706	0.066	-0.004	0.002	1.21	-0.13	0.10	
122	J033359.91+564753.9	Gaia DR2 448596934500298880	03 33 59.92	+56 47 53.88	A0 II-III EuSi	145	12.1883	0.0040	+0.515	0.204	-	-	-	-	-	
123	J033512.23+490936.7	Gaia DR2 249686244426935296	03 35 12.24	+49 09 36.76	B9.5 II-III CrSi	120	12.7989	0.0007	+0.487	0.038	+0.106	0.003	0.76	+0.48	0.18	
124	J033546.83+512723.7	TYC 3325-152-1	03 35 46.83	+51 27 23.73	B9 V Cr	111	11.6677	0.0008	+1.249	0.037	-0.761	0.003	3.16	-1.01	0.08	
125	J033611.64+582252.1	TYC 3728-990-1	03 36 11.65	+58 22 52.22	B8 III-IV Si	109	12.0052	0.0006	+0.854	0.066	-0.352	0.003	1.97	-0.31	0.17	
126	J033620.54+575723.8	TYC 3724-886-1	03 36 20.55	+57 57 23.90	B8 IV-V Si	160	11.9796	0.0003	+1.021	0.036	+0.189	0.001	1.30	+0.72	0.09	
127	J033648.54+571248.6	Gaia DR2 448982588204437120	03 36 48.54	+57 12 48.62	B9.5 V Cr	142	11.9229	0.0004	+1.106	0.044	+0.239	0.002	1.50	+0.64	0.10	
128	J033726.54+523401.6	TYC 3716-278-1	03 37 26.55	+52 34 01.65	A6 V SrCrEu	149	11.5672	0.0007	+1.715	0.033	+0.373	0.002	1.10	+1.63	0.07	
129	J033742.76+494930.0	Gaia DR2 249729468977400832	03 37 42.77	+49 49 30.06	B9 III-IV Si	104	13.3761	0.0003	+0.373	0.025	-0.034	0.002	1.18	+0.05	0.15	
130	J034000.57+444858.4	TYC 2875-2489-1	03 40 00.58	+44 48 58.26	kA0hA1mA3 (Si)*	771	9.8025	0.0007	+1.479	0.769	-	-	-	-	-	
131	J034036.63+455233.0	TYC 3313-1894-1	03 40 36.45	+45 52 32.95	kA0hA2mA5 Cr	216	10.5868	0.0007	+0.318	0.458	-	-	-	-	-	
132	J034112.38+453031.7	TYC 3313-1037-1	03 41 12.10	+45 30 31.79	A1 V SrCrEu	336	9.7342	0.0004	+2.202	0.054	+0.036	0.001	0.56	+0.88	0.07	
133	J034114.89+483916.7	TYC 3317-108-1	03 41 14.90	+48 39 16.70	A0 IV-V Sr	118	11.9607	0.0008	+0.933	0.035	+0.155	0.003	0.81	+1.00	0.10	
134	J034229.41+353820.9	HD 22961	03 42 29.42	+35 38 20.93	A0 IV-V bl4077 bl4130	800	9.5145	0.0003	+3.312	0.039	-0.251	0.001	1.00	+1.12	0.06	
135	J034306.74+495240.7	TYC 3321-881-1	03 43 06.74	+49 52 40.80	B9 III Si*	258	11.9711	0.0006	+0.475	0.038	+0.085	0.002	1.06	-0.70	0.18	
136	J034312.35+581724.9	Gaia DR2 449154489978207488	03 43 12.35	+58 17 25.02	A1 IV SrCr	154	11.8213	0.0005	+1.151	0.029	-0.058	0.002	1.44	+0.68	0.07	
137	J034411.65+500117.8	TYC 3321-374-1	03 44 11.34	+50 01 17.86	B7 IV-V Si	481	9.6221	0.0005	+1.555	0.039	-0.218	0.002	0.82	-0.24	0.07	
138	J034417.13+494336.6	TYC 3321-1539-1	03 44 17.38	+49 43 34.76	B8 IV-V CrSi	457	9.6305	0.0006	+1.238	0.041	-0.101	0.002	0.86	-0.77	0.09	
139	J034458.31+464848.7	TYC 3313-1279-1	03 44 58.31	+46 48 48.78	B9 III-IV Si	389	11.3576	0.0011	+1.024	0.052	+0.116	0.004	0.65	+0.76	0.12	
140	J034514.32+294335.4	HD 281193	03 45 14.32	+29 43 35.50	A4 IV CrEuSi	136	9.9949	0.0005	+2.384	0.085	+0.115	0.002	0.45	+1.43	0.09	
141	J034525.09+523642.2	TYC 3716-571-1	03 45 25.09	+52 36 42.26	A1 IV-V CrEu	237	11.8307	0.0005	+1.304	0.040	+0.255	0.002	1.01	+1.40	0.08	
142	J034541.53+275631.8	TYC 1807-159-1	03 45 41.41	+27 56 31.86	kA3hA6mA6 SrCrEu* <sup>d</sup>	259	10.5867	0.0008	+1.279	0.088	+0.195	0.003	0.22	+0.90	0.16	
143	J034543.16+583801.1	Gaia DR2 473184522761462400	03 45 43.17	+58 38 01.09	A0 IV bl4130	129	14.3359	0.0002	+0.434	0.025	+0.228	0.002	1.19	+1.33	0.13	
144	J034550.78+592754.7	Gaia DR2 474041145398913024	03 45 50.78	+59 27 54.74	B9 IV Eu	129	12.2978	0.0017	+0.964	0.030	+0.299	0.008	1.08	+1.13	0.08	
145	J034614.32+514056.5	Gaia DR2 251478379660219904	03 46 14.33	+51 40 56.51	B8 V Si (He-wk)	152	12.3500	0.0009	+0.794	0.036	+0.097	0.005	1.15	+0.70	0.11	
146	J034704.76+305136.2	HD 281171	03 47 04.77	+30 51 36.04	A4 IV-V Sr	164	11.0769	0.0009	+1.616	0.099	+0.314	0.002	0.77	+1.35	0.14	
147	J034731.69+394858.2	HD 275801	03 47 31.70	+39 48 58.31	B9 IV-V Cr	238	11.4844	0.0007	+0.800	0.056	+0.073	0.003	0.57	+0.43	0.16	
148	J034828.34+460128.5	TYC 3326-2034-1	03 48 28.35	+46 01 28.77	A0 II-III CrEu	395	11.1605	0.0024	-0.534	0.518	-	-	-	-	-	
149	J034834.07+391150.8	TYC 2863-759-1	03 48 34.07	+39 11 50.92	A0 III-IV Eu	194	11.7411	0.0008	+1.146	0.043	+0.101	0.004	0.81	+1.23	0.10	
150	J034854.70+521413.1	Gaia DR2 251609324623302400	03 48 54.70	+52 14 13.13	A5 V SrCrEu	147	12.8362	0.0003	+0.999	0.031	+0.267	0.002	1.07	+1.76	0.08	

**Table A.1.** Essential data for our sample stars, sorted by increasing right ascension. The columns denote: (1) Internal identification number. (2) LAMOST identifier. (3) Alternativ identifier (HD number, TYC identifier or GAIA DR2 number). (4) Right ascension (J2000; GAIA DR2). (5) Declination (J2000; GAIA DR2). (6) Spectral type, as derived in this study. (7) Sloan  $g$  band S/N ratio of the analysed spectrum. (8)  $G$  mag (GAIA DR2). (9)  $G$  mag error. (10) Parallax (GAIA DR2). (11) Parallax error. (12) Dereddened colour index  $(BP - RP)_0$  (GAIA DR2). (13) Colour index error. (14) Absorption in the  $G$  band,  $A_G$ . (15) Intrinsic absolute magnitude in the  $G$  band,  $M_{G,0}$ . (16) Absolute magnitude error.

(1)	(2)	(3)	(4)		(5)	(6)	(7)	(8)	(9)	(10)	(11)	(12)	(13)	(14)	(15)	(16)
No.	ID_LAMOST	ID_alt	RA(J2000)	Dec(J2000)	SpT_final	S/N $_g$	$G$ mag	$e_G$ mag	$\pi$ (mas)	$e_\pi$	$(BP - RP)_0$	$e_{(BP - RP)_0}$	$A_G$	$M_{G,0}$	$e_{M_{G,0}}$	
151	J035046.03+363648.2	Gaia DR2 220081859486642816	03 50 46.04	+36 36 48.27	B8 V Si* <sup>d</sup>	129	12.4742	0.0004	+0.384	0.048	-0.119	0.003	0.51	-0.11	0.27	
152	J035222.92+325344.1	HD 279137	03 52 22.93	+32 53 44.13	B9 IV (Cr)*	138	10.8883	0.0006	+1.439	0.055	-0.031	0.002	0.47	+1.21	0.10	
153	J035238.56+284808.0	Gaia DR2 167014411808069504	03 52 38.57	+28 48 08.01	B9.5 III CrEu	84	14.3013	0.0008	+0.070	0.049	-	-	-	-	-	
154	J035323.41+511945.5	Gaia DR2 251273492539058560	03 53 23.42	+51 19 45.51	B9 III bl4130	136	12.4213	0.0007	+0.455	0.590	-	-	-	-	-	
155	J035328.65+401211.4	Gaia DR2 230000141564434432	03 53 28.65	+40 12 11.46	B9 IV-V CrSi	248	11.7017	0.0008	+1.274	0.033	+0.058	0.003	1.08	+1.15	0.08	
156	J035402.92+483618.9	Gaia DR2 246983193871427072	03 54 02.92	+48 36 18.93	B8 IV-V EuSi	124	12.0396	0.0007	+0.886	0.036	+0.070	0.005	1.19	+0.59	0.10	
157	J035458.95+524755.5	TYC 3717-914-1	03 54 58.84	+52 47 54.37	B9 IV Si	370	10.7480	0.0005	+1.066	0.056	-0.264	0.002	1.71	-0.83	0.13	
158	J035502.04+422421.6	Gaia DR2 231448438897036800	03 55 02.05	+42 24 21.67	A0 II-III bl4077 bl4130	117	14.2345	0.0006	+0.355	0.029	+0.017	0.003	1.00	+0.98	0.18	
159	J035508.23+444208.1	TYC 2876-1121-1	03 55 08.23	+44 42 08.23	B9.5 II-III bl4130	203	12.1215	0.0003	+0.401	0.042	+0.013	0.002	0.92	-0.78	0.23	
160	J035601.03+473843.6	TYC 3330-2807-1	03 56 01.04	+47 38 43.68	B8 IV Si (He-wk)	457	10.1658	0.0019	+1.490	0.120	-0.065	0.005	0.93	+0.10	0.18	
161	J035642.77+513747.2	TYC 3339-770-1	03 56 42.77	+51 37 47.19	A0 IV-V Cr	343	11.2870	0.0009	+1.030	0.050	+0.150	0.002	0.94	+0.41	0.12	
162	J035700.35+240805.7	HD 283172	03 57 00.36	+24 08 05.79	B9 V CrSi	243	11.3804	0.0009	+0.928	0.079	-0.052	0.004	0.31	+0.91	0.19	
163	J035716.27+344839.6	HD 279178	03 57 16.27	+34 48 39.65	A7 V SrCrEu	250	11.4612	0.0006	+1.230	0.041	+0.198	0.002	0.48	+1.43	0.09	
164	J035738.10+522745.9	TYC 3339-300-1	03 57 38.11	+52 27 45.89	B9.5 III-IV Si	297	11.2969	0.0008	+0.825	0.048	-0.047	0.002	1.37	-0.49	0.14	
165	J035752.06+580323.1	TYC 3725-1418-1	03 57 52.06	+58 03 23.11	B9.5 II-III Si	136	12.4059	0.0004	+0.453	0.040	+0.041	0.003	1.27	-0.58	0.20	
166	J035828.16+555117.3	Gaia DR2 468737788503660288	03 58 28.16	+55 51 17.35	A0 III-IV CrEu	176	12.2127	0.0005	+1.135	0.032	+0.148	0.002	1.09	+1.40	0.08	
167	J035945.29+331757.7	TYC 2361-392-1	03 59 45.30	+33 17 57.72	B8 IV Si	141	12.6797	0.0003	+0.409	0.039	+0.025	0.002	0.71	+0.03	0.21	
168	J040009.29+584106.1	Gaia DR2 470056824500164608	04 00 09.29	+58 41 06.16	B9 IV Cr	117	12.4413	0.0002	+0.845	0.032	+0.082	0.001	1.59	+0.49	0.10	
169	J040023.62+462840.7	HD 25010	04 00 23.62	+46 28 40.69	B8 IV-V Si	358	10.3137	0.0006	+1.381	0.051	-0.144	0.002	1.08	-0.06	0.09	
170	J040207.61+511231.9	Gaia DR2 250653299261292800	04 02 07.62	+51 12 31.91	B9 IV EuSi	112	12.5781	0.0004	+0.873	0.040	+0.124	0.002	1.24	+1.04	0.11	
171	J040213.87+370957.1 <sup>a</sup>	HD 279277	04 02 13.74	+37 09 57.15	B9 V CrEuSi	311	10.6138	0.0004	+1.863	0.047	+0.003	0.001	0.88	+1.09	0.07	
172	J040217.66+340724.2	Gaia DR2 170944650483159040	04 02 17.66	+34 07 24.23	A2 V SrCrEu	82	14.6761	0.0005	+0.207	0.035	+0.177	0.003	0.50	+0.76	0.37	
173	J040229.46+571905.4	TYC 3726-229-1	04 02 29.47	+57 19 05.39	B8 IV Si	428	9.7835	0.0006	+1.495	0.037	+0.002	0.002	0.60	+0.06	0.07	
174	J040245.51+485337.9	Gaia DR2 247227942587888768	04 02 45.53	+48 53 37.91	B9 IV Si	102	12.9425	0.0004	+0.643	0.034	+0.002	0.002	1.52	+0.46	0.12	
175	J040305.44+444943.7	TYC 2889-238-1	04 03 05.44	+44 49 43.80	B9 III-IV Si	225	11.4741	0.0010	+0.720	0.036	+0.035	0.003	1.01	-0.24	0.12	
176	J040314.83+534717.4	TYC 3718-527-1	04 03 14.83	+53 47 17.46	B9 II-III Si	212	11.5850	0.0006	+0.556	0.031	-0.064	0.001	1.76	-1.46	0.13	
177	J040452.41+484841.1	Gaia DR2 247167984843330304	04 04 52.42	+48 48 41.20	A2 IV CrEu	108	12.9807	0.0006	+1.050	0.026	+0.158	0.002	1.21	+1.87	0.07	
178	J040508.94+484944.7	TYC 3335-1943-1	04 05 08.94	+48 49 44.59	B8 III-IV EuSi	256	10.0895	0.0008	+1.075	0.050	-0.182	0.003	1.30	-1.05	0.11	
179	J040511.96+471903.3	Gaia DR2 245917015488631552	04 05 11.97	+47 19 03.46	A0 II-III Cr	224	12.2341	0.0002	+0.600	0.040	+0.109	0.002	1.26	-0.13	0.15	
180	J040642.34+454640.8 <sup>a</sup>	HD 25706	04 06 42.35	+45 46 40.89	kB9hA2mA6 CrSi	774	10.1112	0.0004	+1.769	0.049	+0.026	0.001	0.60	+0.75	0.08	
181	J040654.80+210519.9	HD 284143	04 06 54.80	+21 05 19.99	B9 V CrEu	505	10.7260	0.0010	+1.717	0.076	-0.001	0.002	0.68	+1.22	0.11	
182	J040715.76+310107.8	HD 281582	04 07 15.76	+31 01 07.97	kA5hA8mF0 CrEuSi	485	9.9505	0.0006	+2.677	0.145	+0.184	0.002	0.74	+1.35	0.13	
183	J040723.45+553340.0	TYC 3722-782-1	04 07 23.45	+55 33 40.03	A0 IV-V Cr	294	11.1627	0.0010	+0.779	0.038	+0.130	0.002	1.43	-0.81	0.12	
184	J040728.92+415903.9	Gaia DR2 231940401634554112	04 07 28.93	+41 59 04.10	B9 IV-V CrSi	119	12.7525	0.0006	+0.674	0.042	+0.193	0.004	0.91	+0.98	0.15	
185	J040755.56+534052.7	Gaia DR2 275908565958715776	04 07 55.57	+53 40 52.74	B8 III-IV Si	123	12.7288	0.0007	+0.465	0.030	-0.116	0.003	1.43	-0.37	0.15	
186	J040809.35+485644.1	TYC 3336-1400-1	04 08 09.34	+48 56 44.04	B8 III-IV Si	124	11.5957	0.0009	+0.580	0.041	+0.015	0.002	1.36	-0.95	0.16	
187	J040821.16+540119.2	TYC 3718-2-1	04 08 21.17	+54 01 19.32	A2 IV-V SrCrEu	266	10.7801	0.0006	+2.044	0.043	+0.007	0.002	1.08	+1.25	0.07	
188	J040832.16+243436.8	HD 283428	04 08 32.17	+24 34 36.77	A9 V SrCrEuSi	219	11.1143	0.0016	+0.959	0.104	+0.349	0.003	0.77	+0.26	0.24	
189	J041056.36+534031.0	Gaia DR2 275238001306676480	04 10 56.37	+53 40 31.31	kB9.5hA3mA3 SrCrSi	146	12.2253	0.0003	+1.245	0.034	+0.120	0.002	1.00	+1.70	0.08	
190	J041107.47+433904.3	Gaia DR2 232179030014210048	04 11 07.47	+43 39 04.39	B8 IV SiCr*	132	12.6631	0.0006	+0.386	0.043	+0.009	0.003	1.01	-0.41	0.24	
191	J041121.82+545540.8	TYC 3722-714-1	04 11 21.74	+54 55 40.82	B8 III-IV (Cr)*	297	10.9217	0.0006	+1.690	0.067	+0.246	0.002	1.90	+0.16	0.10	
192	J041207.40+235857.2	HD 283516	04 12 07.43	+23 58 57.45	B9 V CrEu	474	9.8901	0.0010	+2.825	0.048	+0.188	0.003	0.67	+1.48	0.06	
193	J041222.48+504917.9	Gaia DR2 271636757126607104	04 12 22.49	+50 49 17.99	B9.5 IV Eu	102	12.9139	0.0003	+0.799	0.032	+0.039	0.001	1.45	+0.97	0.10	
194	J041403.70+494110.7 <sup>a</sup>	TYC 3336-982-1	04 14 03.71	+49 41 10.76	B9.5 II-III Si	185	11.8594	0.0009	+0.864	0.043	+0.100	0.004	1.07	+0.47	0.12	
195	J041431.97+480234.3	TYC 3332-443-1	04 14 31.98	+48 02 34.36	B8 III-IV Si	195	11.9233	0.0034	+0.892	0.043	+0.161	0.014	1.43	+0.25	0.12	
196	J041448.39+484252.7	TYC 3332-853-1	04 14 48.39	+48 42 52.82	B9.5 II-III bl4130	272	11.0196	0.0022	+0.889	0.049	-0.152	0.006	1.57	-0.81	0.13	
197	J041459.31+532400.8	TYC 3719-75-1	04 14 59.32	+53 24 00.80	B9 III-IV Si	110	11.9190	0.0003	+0.883	0.042	+0.015	0.002	1.13	+0.52	0.12	
198	J041506.01+414635.1	Gaia DR2 228782565577949952	04 15 06.02	+41 46 35.11	A0 III-IV bl4077 bl4130	120	12.7046	0.0004	+0.587	0.131	+0.288	0.002	1.28	+0.27	0.49	
199	J041530.27+511305.8	TYC 3340-685-1	04 15 30.28	+51 13 05.80	B9 V Cr	270	11.6996	0.0008	+0.944	0.048	+0.060	0.003	0.61	+0.96	0.12	
200	J041550.17+494027.7	Gaia DR2 270578717700916096	04 15 50.18	+49 40 27.79	A4 III-IV bl4077	151	12.1442	0.0003	+1.101	0.040	+0.201	0.002	0.94	+1.42	0.09	

**Table A.1.** Essential data for our sample stars, sorted by increasing right ascension. The columns denote: (1) Internal identification number. (2) LAMOST identifier. (3) Alternativ identifier (HD number, TYC identifier or GAIA DR2 number). (4) Right ascension (J2000; GAIA DR2). (5) Declination (J2000; GAIA DR2). (6) Spectral type, as derived in this study. (7) Sloan  $g$  band S/N ratio of the analysed spectrum. (8)  $G$  mag (GAIA DR2). (9)  $G$  mag error. (10) Parallax (GAIA DR2). (11) Parallax error. (12) Dereddened colour index  $(BP - RP)_0$  (GAIA DR2). (13) Colour index error. (14) Absorption in the  $G$  band,  $A_G$ . (15) Intrinsic absolute magnitude in the  $G$  band,  $M_{G,0}$ . (16) Absolute magnitude error.

(1)	(2)	(3)	(4)	(5)	(6)	(7)	(8)	(9)	(10)	(11)	(12)	(13)	(14)	(15)	(16)
No.	ID_LAMOST	ID_alt	RA(J2000)	Dec(J2000)	SpT_final	S/N <sub>g</sub>	G mag	e_G mag	pi (mas)	e_pi	$(BP - RP)_0$	$e_{(BP - RP)_0}$	$A_G$	$M_{G,0}$	$e_{M_{G,0}}$
201	J041607.68+511955.5	TYC 3340-1041-1	04 16 07.69	+51 19 55.51	B8 IV Si	250	11.7336	0.0004	+0.794	0.040	-0.122	0.002	0.81	+0.42	0.12
202	J041619.00+291523.7	HD 281818	04 16 19.00	+29 15 23.79	B9 V EuSi	366	10.0161	0.0005	+1.715	0.052	-0.031	0.001	1.08	+0.11	0.08
203	J041641.15+511253.2	TYC 3340-629-1	04 16 41.15	+51 12 53.21	B8 IV CrSi	230	12.1156	0.0007	+0.780	0.042	-0.006	0.003	0.78	+0.80	0.13
204	J041706.53+462439.2	TYC 3328-2095-1	04 17 06.53	+46 24 39.27	B9 IV bl4130	122	12.1136	0.0009	+1.021	0.043	-0.104	0.004	0.93	+1.23	0.10
205	J041744.73+403036.1	Gaia DR2 227872964522959616	04 17 44.73	+40 30 36.22	A0 IV SrCrEu	198	11.9723	0.0007	+1.144	0.066	+0.052	0.002	1.15	+1.11	0.14
206	J041748.47+534201.4	TYC 3719-604-1	04 17 48.48	+53 42 01.60	B9 IV-V Si	108	11.7587	0.0012	+1.201	0.035	-0.015	0.005	2.10	+0.05	0.08
207	J041813.52+525506.4	TYC 3719-599-1	04 18 13.39	+52 55 06.39	B8 III-IV bl4130	267	10.8985	0.0008	+1.365	0.109	-0.036	0.003	1.11	+0.46	0.18
208	J041819.79+414611.3	Gaia DR2 228744980321896448	04 18 19.79	+41 46 11.37	kB9.5hA1mA3 Si	112	14.2355	0.0015	+0.273	0.039	+0.049	0.007	1.06	+0.36	0.31
209	J041827.05+204500.5	HD 284335	04 18 27.05	+20 45 00.57	B9 IV-V Sr	290	11.4504	0.0011	+0.958	0.096	+0.008	0.003	0.81	+0.55	0.22
210	J041834.97+224205.5	HD 284308	04 18 35.08	+22 42 04.40	kA3hA5mA9 SrCrEu	381	10.5200	0.0005	+1.627	0.048	+0.205	0.002	0.54	+1.04	0.08
211	J041920.40+530457.5	Gaia DR2 275289094232992384	04 19 20.41	+53 04 57.52	B9.5 III-IV Si	111	12.9156	0.0006	+0.447	0.040	+0.085	0.003	1.56	-0.40	0.20
212	J041946.03+471655.3	Gaia DR2 257920070391100032	04 19 46.04	+47 16 55.41	B9.5 III-IV Si	108	12.5751	0.0010	+0.532	0.044	+0.050	0.005	1.77	-0.57	0.19
213	J041952.45+401551.1	TYC 2882-1513-1	04 19 52.45	+40 15 51.20	A0 IV-V SrCrEu	168	11.8203	0.0006	+0.917	0.051	+0.098	0.002	1.19	+0.44	0.13
214	J042104.15+033648.2	Gaia DR2 3283347848906203520	04 21 04.15	+03 36 48.20	B8 III-IV Si	189	13.1678	0.0005	+0.397	0.049	-0.114	0.004	0.62	+0.54	0.27
215	J042113.88+441145.3	TYC 2891-1625-1	04 21 13.88	+44 11 45.21	A1 V SrCrEu	135	10.6491	0.0004	+1.561	0.048	+0.117	0.001	0.67	+0.94	0.08
216	J042200.91+402507.7	HD 276286	04 22 00.92	+40 25 07.89	B9 V Eu	246	11.1562	0.0013	+1.747	0.064	-0.045	0.003	1.11	+1.26	0.09
217	J042235.21+515224.6	TYC 3341-92-1	04 22 35.22	+51 52 24.60	B8 III bl4130	303	10.5483	0.0003	+0.300	0.449	-	-	-	-	-
218	J042235.95+411448.9	TYC 2883-63-1	04 22 35.95	+41 14 48.97	A1 IV SrCrEuSi	178	12.4050	0.0003	+0.883	0.046	+0.235	0.002	0.82	+1.31	0.12
219	J042248.93+474138.0	TYC 3333-1433-1	04 22 48.92	+47 41 38.03	A0 II Eu	308	11.4005	0.0033	-0.520	0.272	-	-	-	-	-
220	J042304.38+405451.5	HD 276275	04 23 04.39	+40 54 51.60	B7 IV Si	494	10.6030	0.0004	+1.035	0.052	-0.045	0.001	0.78	-0.10	0.12
221	J042344.60+350740.4	HD 279836	04 23 44.60	+35 07 40.35	A2 IV SrEu	347	10.2024	0.0005	+2.755	0.053	+0.249	0.003	0.76	+1.64	0.07
222	J042410.70+540958.6	Gaia DR2 275497417325069696	04 24 10.70	+54 09 58.66	B9 IV bl4077 bl4130	113	12.7648	0.0008	+0.777	0.036	+0.013	0.004	1.55	+0.66	0.11
223	J042441.72+424439.2	Gaia DR2 228514770078270976	04 24 41.74	+42 44 39.13	B9 IV-V CrEu (He-wk)	117	12.5875	0.0007	+0.738	0.058	+0.203	0.005	0.78	+1.15	0.18
224	J042521.99+232323.1	HD 284427	04 25 21.99	+23 23 21.54	A0 IV-V SrCrEu	516	10.6442	0.0005	+1.508	0.051	+0.134	0.001	1.03	+0.51	0.09
225	J042602.49+540804.0	TYC 3719-1063-1	04 26 02.49	+54 08 04.14	B9.5 IV-V CrEu	236	10.7222	0.0006	+1.105	0.041	-0.155	0.002	1.20	-0.26	0.09
226	J042613.51+435333.7	Gaia DR2 253399226476443136	04 26 13.52	+43 53 33.71	B9 IV-V Cr	101	14.7966	0.0014	+0.297	0.035	+0.255	0.006	1.17	+0.99	0.26
227	J042616.93+331258.7	HD 282086	04 26 16.93	+33 12 58.76	B9 III-IV CrEuSi	266	11.2353	0.0016	+0.841	0.082	+0.021	0.006	0.66	+0.20	0.22
228	J042736.18+063643.1	HD 28238	04 27 35.96	+06 36 43.13	A2 IV-V SrCrEu	506	9.0822	0.0005	+2.864	0.059	+0.188	0.002	0.23	+1.13	0.07
229	J042920.21+501901.0	Gaia DR2 270820296720663168	04 29 20.22	+50 19 01.07	B9 IV-V CrEu	125	12.5741	0.0007	+0.893	0.043	+0.055	0.003	1.25	+1.08	0.12
230	J043045.19+484742.5	TYC 3350-370-1	04 30 45.19	+48 47 42.58	B8 IV-V Si (He-wk)	225	11.4279	0.0011	+0.882	0.034	+0.029	0.003	1.01	+0.15	0.10
231	J043150.95+220725.7	Gaia DR2 145046852381708288	04 31 50.95	+22 07 25.72	A4 V SrCrEu	106	13.8300	0.0003	+0.578	0.032	+0.199	0.002	1.04	+1.60	0.13
232	J043201.64+471447.8	TYC 3346-66-1	04 32 01.64	+47 14 48.00	A2 V SrCrEu(Si)* <sup>d</sup>	419	10.2635	0.0005	+2.500	0.061	+0.257	0.004	0.86	+1.39	0.07
233	J043315.40+404158.8	Gaia DR2 179844097595682944	04 33 15.41	+40 41 58.88	B6 IV (He-wk)	110	14.2200	0.0004	+0.286	0.034	+0.042	0.003	1.02	+0.47	0.26
234	J043459.73+222805.5	Gaia DR2 145126399472110848	04 34 59.73	+22 28 05.72	kB8hA3mA6 CrSi	106	13.0972	0.0006	+0.687	0.024	+0.016	0.004	0.98	+1.30	0.09
235	J043752.46+533259.6	Gaia DR2 273642674351866240	04 37 52.47	+53 32 59.65	B9.5 V CrSi	323	12.4731	0.0003	+1.247	0.041	+0.027	0.002	1.65	+1.30	0.09
236	J043814.39+542341.7	Gaia DR2 273828667913353728	04 38 14.40	+54 23 41.77	B9 IV-V CrSi	219	12.5861	0.0007	+0.862	0.036	+0.054	0.005	1.24	+1.03	0.10
237	J044015.93+215631.3	HD 284592	04 40 15.93	+21 56 31.52	B9 V CrEu	472	11.0040	0.0013	+1.057	0.049	+0.053	0.004	0.85	+0.28	0.11
238	J044108.28+481631.3	Gaia DR2 257474944280221824	04 41 08.29	+48 16 31.38	B8 IV CrSi (He-wk)	213	11.8758	0.0007	+0.834	0.052	+0.117	0.002	1.51	-0.03	0.15
239	J044214.27+353207.5	Gaia DR2 174309701521387008	04 42 14.28	+35 32 07.61	B8 III bl4130	103	12.4460	0.0004	+1.007	0.039	+0.076	0.002	2.11	+0.35	0.10
240	J044313.88+532544.2	TYC 3733-622-1	04 43 13.88	+53 25 44.22	B8 IV-V Cr(Si)*	548	11.2241	0.0012	+1.166	0.044	+0.107	0.002	1.14	+0.42	0.10
241	J044407.32-005639.0	TYC 4735-654-1	04 44 07.16	-00 56 39.02	F0 V SrEuSi	346	10.1724	0.0003	+1.015	0.053	+0.098	0.001	0.11	+0.09	0.12
242	J044433.39+540720.9	TYC 3733-47-1	04 44 33.40	+54 07 20.92	A1 II Si	280	11.4320	0.0009	+1.153	0.041	-0.043	0.003	0.91	+0.83	0.09
243	J044441.74+263924.0	Gaia DR2 154343223195896704	04 44 41.74	+26 39 24.09	B9 IV-V Cr	112	11.5960	0.0009	+1.623	0.049	+0.218	0.002	1.24	+1.41	0.08
244	J044446.24+513129.2	TYC 3355-141-1	04 44 46.15	+51 31 29.31	A9 V SrEu	376	10.9987	0.0020	+1.882	0.181	+0.411	0.004	0.65	+1.72	0.21
245	J044605.51+435344.1	TYC 2905-208-1	04 46 05.52	+43 53 44.09	B9.5 IV-V CrEu	236	11.2435	0.0014	+1.161	0.058	+0.079	0.003	0.93	+0.64	0.12
246	J044713.47+540515.5	TYC 3733-133-1	04 47 13.51	+54 05 15.68	A2 IV CrEu	465	9.6125	0.0005	+1.718	0.051	-0.068	0.003	0.70	+0.08	0.08
247	J044715.48+573746.4	TYC 3741-236-1	04 47 15.45	+57 37 45.45	B9.5 IV-V Si	370	10.9459	0.0015	+0.953	0.060	+0.020	0.004	0.83	+0.01	0.15
248	J044741.43+230820.9	TYC 1831-1868-1	04 47 41.44	+23 08 20.96	B8 III-IV EuSi	126	12.1933	0.0013	+0.457	0.046	+0.065	0.005	0.81	-0.32	0.23
249	J044758.11+070009.4	TYC 96-157-1	04 47 58.12	+07 00 09.43	B9 V CrSi (He-wk)	196	11.0805	0.0006	+1.197	0.057	-0.098	0.003	0.23	+1.24	0.11
250	J045038.83+544917.1	Gaia DR2 273444865338468736	04 50 38.84	+54 49 17.23	B8 IV-V Si (He-wk)	120	12.3142	0.0005	+0.686	0.043	+0.250	0.003	1.46	+0.03	0.14

**Table A.1.** Essential data for our sample stars, sorted by increasing right ascension. The columns denote: (1) Internal identification number. (2) LAMOST identifier. (3) Alternative identifier (HD number, TYC identifier or GAIA DR2 number). (4) Right ascension (J2000; GAIA DR2). (5) Declination (J2000; GAIA DR2). (6) Spectral type, as derived in this study. (7) Sloan  $g$  band S/N ratio of the analysed spectrum. (8)  $G$  mag (GAIA DR2). (9)  $G$  mag error. (10) Parallax (GAIA DR2). (11) Parallax error. (12) Dereddened colour index  $(BP - RP)_0$  (GAIA DR2). (13) Colour index error. (14) Absorption in the  $G$  band,  $A_G$ . (15) Intrinsic absolute magnitude in the  $G$  band,  $M_{G,0}$ . (16) Absolute magnitude error.

(1)	(2)	(3)	(4)		(5)	(6)	(7)	(8)	(9)	(10)	(11)	(12)	(13)	(14)	(15)	(16)
No.	ID_LAMOST	ID_alt	RA(J2000)	Dec(J2000)	SpT_final	S/N <sub>g</sub>	$G$ mag	$e_G$ mag	$\pi$ (mas)	$e_\pi$	$(BP - RP)_0$	$e_{(BP - RP)_0}$	$A_G$	$M_{G,0}$	$e_{M_{G,0}}$	
251	J045109.07+433556.5	TYC 2906-2149-1	04 51 09.11	+43 35 56.83	A1 II-III Si	188	11.7949	0.0015	+0.663	0.071	+0.030	0.029	0.60	+0.30	0.24	
252	J045121.11+093555.8	HD 287173	04 51 21.12	+09 35 55.81	A0 V SrCrEuSi	564	9.9255	0.0003	+2.219	0.061	+0.135	0.001	0.54	+1.12	0.08	
253	J045131.08+395823.5	HD 277044	04 51 31.08	+39 58 23.66	B9 V bl4130	102	11.3158	0.0011	+0.770	0.052	+0.058	0.002	0.59	+0.16	0.15	
254	J045148.66+435755.1	TYC 2906-368-1	04 51 48.67	+43 57 55.18	B9.5 II-III Si	170	12.3508	0.0008	+0.421	0.035	+0.095	0.004	0.72	-0.25	0.19	
255	J045150.13+594602.0	TYC 3745-269-1	04 51 50.14	+59 46 02.00	B9 V CrEu	250	11.4013	0.0008	+1.577	0.035	+0.005	0.003	1.26	+1.13	0.07	
256	J045220.67+405034.9	HD 277028	04 52 20.69	+40 50 34.94	B9 V SrCr	210	10.7310	0.0007	+0.526	0.258	-	-	-	-	-	
257	J045231.56+521715.1	TYC 3356-1085-1	04 52 31.56	+52 17 15.04	A5 IV SrCrEu	193	10.3405	0.0004	+2.302	0.049	+0.314	0.002	0.62	+1.53	0.07	
258	J045316.36+244251.8	HD 283952	04 53 16.37	+24 42 51.77	B9.5 V C*	216	10.7801	0.0005	+1.271	0.045	+0.123	0.002	0.70	+0.60	0.09	
259	J045508.24+204943.7	Gaia DR2 3411724520166949120	04 55 08.24	+20 49 43.69	kA2hA4mA7 SrCrEu	147	14.0406	0.0003	+0.756	0.037	+0.353	0.002	0.62	+2.82	0.12	
260	J045538.72+243458.6	HD 283960	04 55 38.72	+24 34 58.70	A0 IV CrEu	124	11.3335	0.0008	+1.584	0.044	+0.294	0.002	0.76	+1.57	0.08	
261	J045637.95+380626.6	HD 280235	04 56 37.95	+38 06 26.74	kB9hA1mA4 bl4130	322	10.0614	0.0004	+1.265	0.047	+0.143	0.002	1.09	-0.52	0.09	
262	J045708.30+543307.3	Gaia DR2 273280733165163264	04 57 08.30	+54 33 07.13	A0 IV Si	151	12.2942	0.0003	+0.835	0.040	+0.224	0.002	0.84	+1.06	0.12	
263	J045713.44+383741.1	HD 280230	04 57 13.44	+38 37 41.23	B9.5 IV bl4077 bl4130	128	11.3683	0.0009	+1.293	0.063	-0.042	0.003	1.21	+0.71	0.12	
264	J045741.74+405440.1	HD 277264	04 57 41.74	+40 54 40.26	B8 III-IV Si	150	10.6503	0.0007	+0.947	0.064	-0.148	0.003	0.55	-0.02	0.15	
265	J045747.66+560121.5	TYC 3738-1376-1	04 57 47.66	+56 01 21.53	B9.5 IV CrEu	245	10.8983	0.0023	+1.538	0.045	+0.018	0.005	1.74	+0.09	0.08	
266	J045808.28+465625.9	TYC 3348-2776-1	04 58 08.28	+46 56 25.90	B9 IV-V CrEuSi	176	11.5823	0.0006	+0.998	0.042	+0.109	0.003	0.80	+0.78	0.10	
267	J045914.82+410335.6	HD 277256	04 59 14.82	+41 03 35.61	B7 III bl4130	427	9.2353	0.0005	+0.787	0.043	-0.076	0.003	0.44	-1.73	0.13	
268	J045926.29+535030.4	TYC 3743-1043-1	04 59 26.17	+53 50 30.51	B9 V CrEu	292	10.9138	0.0009	+1.475	0.050	+0.081	0.003	0.64	+1.12	0.09	
269	J045933.63+395715.8	TYC 2898-2642-1	04 59 33.58	+39 57 15.94	A0 IV-V SrCr	168	11.9263	0.0006	+0.734	0.044	+0.114	0.019	0.93	+0.32	0.14	
270	J050143.90+440946.2	Gaia DR2 205566588012912896	05 01 43.91	+44 09 46.35	B9 IV Cr	109	12.1255	0.0005	+1.844	0.915	-	-	-	-	-	
271	J050144.01+584923.4	TYC 3746-1604-1	05 01 44.02	+58 49 23.39	B8 III-IV Si	573	9.9912	0.0005	+1.061	0.045	-0.117	0.002	0.98	-0.86	0.10	
272	J050146.85+383500.8	HD 280281	05 01 46.85	+38 35 00.81	B8 V Si* c	104	10.9424	0.0010	+1.253	0.041	+0.109	0.004	0.90	+0.53	0.09	
273	J050205.88+403800.1	Gaia DR2 200809138640147072	05 02 05.89	+40 38 00.15	kA1hA3mA3 CrSi	102	14.6777	0.0006	+0.279	0.035	+0.039	0.004	0.84	+1.07	0.28	
274	J050209.22+395941.4	HD 277411	05 02 09.23	+39 59 41.35	B7 IV Si (He-wk) (He-st)	186	11.1530	0.0027	+0.897	0.070	-0.045	0.009	0.46	+0.46	0.18	
275	J050210.72+464600.0	TYC 3344-79-1	05 02 10.72	+46 46 00.07	B8 III-IV Si	241	9.7607	0.0006	+1.177	0.049	-0.164	0.002	0.87	-0.76	0.10	
276	J050230.72+582514.3	TYC 3746-2118-1	05 02 30.72	+58 25 14.33	A0 IV CrEu	193	11.0443	0.0005	+1.357	0.043	+0.214	0.002	0.80	+0.90	0.08	
277	J050435.61+530749.4	TYC 3734-376-1	05 04 35.61	+53 07 49.42	B7 V Si	189	11.1216	0.0014	+1.259	0.039	+0.336	0.005	1.20	+0.42	0.08	
278	J050453.61+403735.7	TYC 2899-621-1	05 04 53.62	+40 37 35.71	B5 IV-V bl4130 (He-wk)	135	11.2878	0.0014	+0.832	0.055	-0.089	0.004	0.55	+0.34	0.15	
279	J050519.16+412323.4	Gaia DR2 201277766811826176	05 05 19.16	+41 23 23.42	B8 IV-V Si (He-wk)	136	11.6903	0.0011	+0.731	0.043	-0.080	0.006	0.46	+0.55	0.14	
280	J050537.89+554553.8	TYC 3738-363-1	05 05 37.98	+55 45 52.99	B8 IV-V bl4130	217	10.9355	0.0009	+1.375	0.041	+0.188	0.003	1.03	+0.60	0.08	
281	J050731.60+570017.2	TYC 3743-386-1	05 07 31.62	+57 00 17.15	kB9.5hA7mA6 CrEu	316	10.4902	0.0012	-3.275	1.147	-	-	-	-	-	
282	J050748.68+385804.4	HD 277595	05 07 48.69	+38 58 04.42	B8 V bl4130	296	9.5146	0.0006	+1.347	0.067	-0.124	0.003	0.57	-0.41	0.12	
283	J050813.24+404513.2	HD 277537	05 08 13.26	+40 45 13.17	B9 III Si*	340	10.3210	0.0005	+1.075	0.050	-0.157	0.001	0.59	-0.11	0.11	
284	J050839.79+422835.6	TYC 2903-225-1	05 08 39.80	+42 28 35.59	B7 V Si	96	11.7575	0.0006	+0.835	0.041	+0.031	0.004	0.47	+0.90	0.12	
285	J050900.01+493815.1	TYC 3353-1331-1	05 09 00.01	+49 38 15.12	B9 V Cr (He-wk)	249	11.6302	0.0009	+0.840	0.047	-0.006	0.004	0.99	+0.26	0.13	
286	J050925.66+512444.9	TYC 3357-906-1	05 09 25.66	+51 24 44.98	A3 III-IV CrEu	164	11.1055	0.0019	+1.398	0.051	+0.108	0.004	0.59	+1.25	0.09	
287	J050952.91+424828.1	TYC 2903-279-1	05 09 52.91	+42 48 28.22	A0 V SrCrEu	81	11.8222	0.0009	+0.973	0.049	-0.035	0.003	0.66	+1.10	0.12	
288	J051003.60+382125.9	TYC 2896-2008-1	05 10 03.61	+38 21 26.03	A0 V SrCrEu	110	12.2482	0.0005	+0.903	0.041	+0.077	0.004	0.73	+1.30	0.11	
289	J051013.62+420718.3	HD 277634	05 10 13.63	+42 07 18.31	kA0hA1mA3 Eu	573	9.6076	0.0009	+3.674	0.703	+0.146	0.003	0.09	+2.35	0.42	
290	J051205.75+491307.8	TYC 3353-348-1	05 12 05.75	+49 13 07.81	A2 V Sr	189	11.3847	0.0007	+1.528	0.044	-0.039	0.003	0.66	+1.64	0.08	
291	J051322.65+385958.7	HD 277821	05 13 22.65	+38 59 58.78	B9 IV-V bl4077 bl4130	219	11.4385	0.0007	+0.815	0.065	-0.096	0.004	0.67	+0.32	0.18	
292	J051327.91+573333.0	TYC 3743-2168-1	05 13 27.87	+57 33 33.11	B9 V Cr	179	11.4714	0.0005	+0.940	0.036	+0.093	0.002	0.88	+0.46	0.10	
293	J051506.10+321121.3	Gaia DR2 180672678389101952	05 15 06.11	+32 11 21.39	A0 IV-V SrCr	121	11.9559	0.0004	+0.677	0.043	+0.291	0.002	0.81	+0.29	0.15	
294	J051510.44+330047.9 <sup>a</sup>	HD 241843	05 15 10.44	+33 00 47.98	B9 IV-V CrEu	226	10.2085	0.0010	+1.345	0.051	+0.070	0.003	0.58	+0.27	0.10	
295	J051523.41+183519.5	TYC 1287-1240-1	05 15 23.42	+18 35 19.61	B8 IV Sr	114	12.8452	0.0005	+0.398	0.046	-0.138	0.003	1.05	-0.20	0.25	
296	J051539.57+360321.9	Gaia DR2 186913304529270016	05 15 39.57	+36 03 22.00	A0 V SrCr	101	14.2619	0.0004	+0.408	0.042	+0.176	0.005	1.39	+0.92	0.23	
297	J051540.30+370025.0	HD 280682	05 15 40.31	+37 00 25.17	B8 IV Si	198	10.9237	0.0012	+1.427	0.103	+0.064	0.007	0.53	+1.17	0.16	
298	J051709.99+214859.0	Gaia DR2 3414598991456199168	05 17 09.99	+21 48 59.20	B9 V Cr	108	14.5263	0.0010	+0.325	0.031	+0.127	0.004	1.15	+0.94	0.21	
299	J051711.10+365831.6	TYC 2402-795-1	05 17 11.11	+36 58 31.75	B9.5 IV-V SrCr	187	11.9807	0.0007	+0.832	0.043	+0.072	0.005	0.63	+0.95	0.12	
300	J051717.29+362615.5	HD 280802	05 17 17.21	+36 26 15.55	B8 IV Si (He-wk)	360	10.7389	0.0008	+0.927	0.062	-0.130	0.005	0.56	+0.01	0.15	

**Table A.1.** Essential data for our sample stars, sorted by increasing right ascension. The columns denote: (1) Internal identification number. (2) LAMOST identifier. (3) Alternativ identifier (HD number, TYC identifier or GAIA DR2 number). (4) Right ascension (J2000; GAIA DR2). (5) Declination (J2000; GAIA DR2). (6) Spectral type, as derived in this study. (7) Sloan *g* band S/N ratio of the analysed spectrum. (8) *G* mag (GAIA DR2). (9) *G* mag error. (10) Parallax (GAIA DR2). (11) Parallax error. (12) Dereddened colour index  $(BP - RP)_0$  (GAIA DR2). (13) Colour index error. (14) Absorption in the *G* band,  $A_G$ . (15) Intrinsic absolute magnitude in the *G* band,  $M_{G,0}$ . (16) Absolute magnitude error.

(1)	(2)	(3)	(4)	(5)	(6)	(7)	(8)	(9)	(10)	(11)	(12)	(13)	(14)	(15)	(16)
No.	ID_LAMOST	ID_alt	RA(J2000)	Dec(J2000)	SpT_final	S/N <sub>g</sub>	<i>G</i> mag	<i>e</i> <sub><i>G</i> mag</sub>	pi (mas)	<i>e</i> <sub>pi</sub>	$(BP - RP)_0$	<i>e</i> <sub><math>(BP - RP)_0</math></sub>	$A_G$	$M_{G,0}$	<i>e</i> <sub><math>M_{G,0}</math></sub>
301	J051725.85+364904.8	HD 280795	05 17 25.86	+36 49 04.87	A0 IV–V SrCr	204	11.4545	0.0007	+0.696	0.041	+0.139	0.003	0.69	–0.03	0.14
302	J051800.77+184058.1	TYC 1287-1110-1	05 18 00.77	+18 40 58.19	B9 V Cr	333	11.3538	0.0010	+0.970	0.059	+0.325	0.003	0.93	+0.36	0.14
303	J051812.81+370758.9	TYC 2402-1131-1	05 18 12.82	+37 07 58.99	B9.5 IV–V CrEuSi	305	11.7380	0.0008	+0.864	0.044	–0.021	0.003	0.53	+0.89	0.12
304	J051813.83+374532.4	Gaia DR2 187175946071857408	05 18 13.84	+37 45 32.51	kA1hA5mA3 SrCrSi	132	12.9961	0.0005	+0.691	0.073	+0.166	0.002	0.51	+1.68	0.23
305	J051816.22+380429.4	HD 280761	05 18 16.24	+38 04 29.53	B9 V CrSi	160	11.8640	0.0006	+0.943	0.042	–0.044	0.004	0.44	+1.29	0.11
306	J051844.95+380605.3	Gaia DR2 187564730808766848	05 18 44.96	+38 06 05.33	B9 V SrCrEuSi* <sup>d</sup>	116	14.0374	0.0011	+0.418	0.028	+0.187	0.005	1.28	+0.87	0.15
307	J051852.91+133356.6	TYC 711-1863-1	05 18 52.92	+13 34 01.78	B9.5 IV–V Cr	991	7.4031	0.0009	+5.273	0.107	–0.071	0.006	0.31	+0.70	0.07
308	J051854.92+124446.8	Gaia DR2 3387793447726005376	05 18 54.93	+12 44 46.91	A1 IV–V CrEu	120	14.4398	0.0006	+0.476	0.030	+0.215	0.004	1.34	+1.49	0.15
309	J051857.75+412255.9	Gaia DR2 195073398794823040	05 18 57.75	+41 22 55.85	B9 IV CrSi	105	14.1977	0.0004	+0.290	0.039	–0.063	0.004	1.21	+0.30	0.30
310	J051922.65+451350.7	TYC 3358-659-1	05 19 22.66	+45 13 50.77	B8 III–IV (CrSi)*	252	11.1642	0.0012	+0.565	0.059	–0.139	0.005	0.71	–0.78	0.23
311	J051956.20+392118.6	Gaia DR2 187964609445409536	05 19 56.21	+39 21 18.67	B9.5 III–IV Cr	133	14.3460	0.0012	+0.329	0.030	+0.101	0.007	0.96	+0.97	0.20
312	J051957.65+334802.5	Gaia DR2 181253976444979456	05 19 57.64	+33 48 02.55	B8 V bl4130	149	11.9283	0.0004	+0.378	0.063	+0.054	0.003	0.94	–1.12	0.36
313	J052001.14+490915.4	HD 34439	05 20 01.18	+49 09 18.40	B8 IV EuSi (He-wk)	531	9.0140	0.0014	+2.172	0.056	–0.067	0.006	0.28	+0.42	0.07
314	J052016.52+351301.6	HD 280950	05 20 16.53	+35 13 01.89	B5 V bl4130 (He-wk) (He-st)	189	10.8196	0.0010	+0.901	0.063	–0.311	0.005	0.94	–0.35	0.16
315	J052043.33+380212.5	Gaia DR2 187568815318517760	05 20 43.34	+38 02 12.55	A1 II Si	103	13.4429	0.0006	+0.495	0.029	+0.022	0.003	1.40	+0.52	0.14
316	J052043.38+335022.0	Gaia DR2 181243187487128960	05 20 43.39	+33 50 21.17	B8 IV Si	153	12.0607	0.0011	+0.813	0.049	–0.084	0.006	0.68	+0.94	0.14
317	J052059.29+351123.5	HD 280948	05 20 59.29	+35 11 23.58	B9.5 III bl4130	200	10.2693	0.0016	+1.571	0.056	+0.074	0.007	0.55	+0.70	0.09
318	J052118.97+320805.7	HD 242764	05 21 18.98	+32 08 05.85	B4 V <sub>pm</sub> *	488	9.8145	0.0022	+0.885	0.066	–0.174	0.009	0.50	–0.95	0.17
319	J052128.61+401445.8	HD 278068	05 21 28.62	+40 14 45.81	B8 IV–V SiCr*	286	11.2981	0.0015	+0.849	0.111	–0.177	0.007	0.70	+0.24	0.29
320	J052143.28+354353.0	Gaia DR2 183754437683161216	05 21 43.28	+35 43 53.04	A0 III Eu	199	12.4640	0.0017	+0.550	0.052	+0.011	0.007	1.38	–0.21	0.21
321	J052220.03+132145.8	TYC 712-2078-1	05 22 20.03	+13 21 45.89	B9 V SrCr	269	10.7849	0.0007	+1.147	0.047	+0.135	0.003	0.80	+0.28	0.10
322	J052237.24+324258.3	TYC 2394-214-1	05 22 37.25	+32 42 58.40	B9 IV–V CrSi	149	12.2183	0.0006	+0.724	0.041	–0.039	0.005	0.59	+0.93	0.13
323	J052244.67+345827.3	TYC 2398-315-1	05 22 44.68	+34 58 27.34	B6 IV Si	372	11.4327	0.0017	+0.777	0.058	–0.204	0.008	0.96	–0.07	0.17
324	J052254.93+134638.7 <sup>a</sup>	HD 243096	05 22 54.93	+13 46 38.79	A1 IV bl4130	250	11.0763	0.0008	+1.185	0.047	+0.189	0.002	0.67	+0.78	0.10
325	J052259.54+343944.9	HD 281056	05 22 59.55	+34 39 44.94	B9 V V Cr	191	10.6012	0.0010	+0.794	0.047	+0.052	0.003	0.58	–0.48	0.14
326	J052329.37+423212.0	Gaia DR2 195256707998564480	05 23 29.38	+42 32 12.11	B9 V CrEu	109	14.6622	0.0008	+0.238	0.032	–0.087	0.005	1.12	+0.43	0.30
327	J052422.19+383106.2	Gaia DR2 187644204884340480	05 24 22.19	+38 31 06.29	B8 III Si (He-wk)	103	14.2274	0.0014	+0.373	0.031	+0.109	0.006	1.16	+0.93	0.19
328	J052454.62+434145.3	Gaia DR2 207372260984327936	05 24 54.64	+43 41 45.36	B9.5 III–IV bl4130	107	12.8217	0.0004	+0.672	0.043	+0.158	0.003	0.86	+1.10	0.15
329	J052454.90+370932.6	TYC 2415-423-1	05 24 54.91	+37 09 32.67	B8 III–IV EuSi	116	11.3825	0.0008	+0.677	0.043	+0.054	0.003	1.18	–0.65	0.15
330	J052459.98-064651.8	TYC 4765-1018-1	05 24 59.99	–06 46 51.83	A0 IV–V Si	227	11.8359	0.0004	+1.310	0.048	+0.233	0.002	0.25	+2.17	0.09
331	J052510.60+440918.0	TYC 2921-1065-1	05 25 10.60	+44 09 18.02	B9.5 IV–V Eu	148	12.3953	0.0004	+0.874	0.060	–0.078	0.003	0.96	+1.14	0.16
332	J052552.24+344817.3	Gaia DR2 182850540345232256	05 25 52.24	+34 48 17.36	B9 V CrEu	136	13.1048	0.0004	+0.728	0.029	+0.143	0.003	0.87	+1.55	0.10
333	J052602.25+075254.0	TYC 700-1067-1	05 26 02.26	+07 52 54.03	A0 V CrEu	342	11.2510	0.0013	+1.319	0.052	–0.045	0.005	0.62	+1.23	0.10
334	J052616.48+331544.2	HD 243492	05 26 16.49	+33 15 44.26	B8 IV–V bl4130	256	10.6016	0.0005	+0.842	0.042	+0.044	0.003	0.58	–0.35	0.12
335	J052621.99+491939.9	TYC 3367-968-1	05 26 22.00	+49 19 39.89	kA1hA3mA7 SrCrEu	299	10.6318	0.0012	+1.512	0.146	+0.235	0.005	0.40	+1.13	0.22
336	J052643.64+341450.5	Gaia DR2 182629916466102784	05 26 43.64	+34 14 50.55	B7 IV–V Si	136	13.0085	0.0012	+0.452	0.042	–0.139	0.005	0.80	+0.49	0.21
337	J052658.34+155131.6	Gaia DR2 3390885033905554176	05 26 58.34	+15 51 31.72	A7 V SrCrEu	149	14.3652	0.0016	+0.382	0.035	+0.291	0.006	1.07	+1.21	0.21
338	J052718.48-012726.1	Gaia DR2 3220192038446213760	05 27 18.48	–01 27 26.16	A0 IV–V CrEu	108	13.3183	0.0005	+0.571	0.034	+0.033	0.003	0.29	+1.81	0.14
339	J052739.41+533935.4	TYC 3748-1827-1	05 27 39.32	+53 39 36.63	A0 III–IV SrCrEu	385	10.7348	0.0007	+1.074	0.045	+0.020	0.004	0.86	+0.03	0.10
340	J052748.30+453546.1	TYC 3359-1802-1	05 27 48.30	+45 35 46.14	B8 IV Si	308	10.1747	0.0011	+1.363	0.067	–0.169	0.005	0.66	+0.19	0.12
341	J052800.13+351644.0	Gaia DR2 183262612388074496	05 28 00.14	+35 16 44.03	A2 III–IV SrCrEu	124	12.8995	0.0009	+0.677	0.038	+0.171	0.004	1.01	+1.05	0.13
342	J052805.24+343638.8	Gaia DR2 182664997758510848	05 28 05.26	+34 36 38.91	B8 III–IV Si	102	13.3388	0.0015	+0.493	0.034	+0.142	0.008	0.98	+0.82	0.16
343	J052812.16+415006.4	HD 278204	05 28 11.99	+41 50 06.46	kA0hA3mA7 Si	247	10.3252	0.0007	+1.173	0.066	–0.141	0.002	0.39	+0.28	0.13
344	J052816.11-063820.1	TYC 4765-708-1	05 28 16.10	–06 38 20.07	kA1hA9mA9 SrCrEu* <sup>d</sup>	358	10.7380	0.0005	+2.685	0.041	+0.444	0.007	0.06	+2.82	0.06
345	J052818.84+414932.6	HD 278203	05 28 18.85	+41 49 32.69	A0 IV–V CrEu	186	10.3076	0.0006	+0.917	0.294	–	–	–	–	–
346	J052823.82+491141.0	Gaia DR2 213505989678368640	05 28 23.83	+49 11 41.06	A0 II–III bl4130	109	13.2444	0.0004	+0.273	0.022	+0.027	0.004	0.76	–0.33	0.18
347	J052900.00+403426.0	Gaia DR2 193909630159512576	05 29 00.01	+40 34 26.05	B9.5 IV–V Cr	171	11.3729	0.0007	+0.444	0.658	–	–	–	–	–
348	J052945.57+440142.2	Gaia DR2 195762479048137344	05 29 45.57	+44 01 42.23	A2 IV–V SrCrEu	194	12.3760	0.0002	+0.784	0.051	+0.178	0.002	0.69	+1.16	0.15
349	J052947.73+420240.7	HD 278201	05 29 47.74	+42 02 40.67	B9 V Cr	283	10.9859	0.0010	+0.900	0.056	–0.432	0.004	1.39	–0.63	0.14
350	J052950.88+172629.8	TYC 1301-1038-1	05 29 50.88	+17 26 29.80	B9 IV bl4077 bl4130	272	11.8268	0.0005	+0.725	0.041	+0.126	0.003	0.69	+0.44	0.13

**Table A.1.** Essential data for our sample stars, sorted by increasing right ascension. The columns denote: (1) Internal identification number. (2) LAMOST identifier. (3) Alternativ identifier (HD number, TYC identifier or GAIA DR2 number). (4) Right ascension (J2000; GAIA DR2). (5) Declination (J2000; GAIA DR2). (6) Spectral type, as derived in this study. (7) Sloan  $g$  band S/N ratio of the analysed spectrum. (8)  $G$  mag (GAIA DR2). (9)  $G$  mag error. (10) Parallax (GAIA DR2). (11) Parallax error. (12) Dereddened colour index  $(BP - RP)_0$  (GAIA DR2). (13) Colour index error. (14) Absorption in the  $G$  band,  $A_G$ . (15) Intrinsic absolute magnitude in the  $G$  band,  $M_{G,0}$ . (16) Absolute magnitude error.

(1)	(2)	(3)	(4)	(5)	(6)	(7)	(8)	(9)	(10)	(11)	(12)	(13)	(14)	(15)	(16)
No.	ID_LAMOST	ID_alt	RA(J2000)	Dec(J2000)	SpT_final	S/N $_g$	$G$ mag	$e_G$ mag	$\pi$ (mas)	$e_\pi$	$(BP - RP)_0$	$e_{(BP - RP)_0}$	$A_G$	$M_{G,0}$	$e_{M_{G,0}}$
351	J053025.32+332639.6	HD 244168	05 30 25.32	+33 26 39.77	A6 V SrEu	161	10.9158	0.0003	+3.246	0.432	+0.329	0.002	0.26	+3.21	0.29
352	J053049.15+393224.7	Gaia DR2 190785028567285888	05 30 49.16	+39 32 24.77	A2 IV CrEu	134	12.7920	0.0007	+0.729	0.056	+0.113	0.004	0.83	+1.27	0.17
353	J053049.19+195827.1	Gaia DR2 3401277205495091200	05 30 49.20	+19 58 27.18	A1 IV–V CrEu	111	14.3678	0.0006	+0.383	0.037	+0.283	0.004	0.71	+1.58	0.22
354	J053125.46+414645.6	TYC 2918-328-1	05 31 25.47	+41 46 45.59	B9.5 V SrCr	197	11.1567	0.0008	+0.833	0.063	–0.065	0.002	0.76	+0.00	0.17
355	J053139.66+380231.5	TYC 2910-488-1	05 31 39.67	+38 02 31.45	B8 III–IV Si	451	10.1420	0.0011	+1.601	0.113	–0.143	0.002	0.74	+0.42	0.16
356	J053204.19+103549.6	TYC 705-856-1	05 32 04.19	+10 35 49.65	B9 V Cr	173	11.6659	0.0009	+0.642	0.057	+0.191	0.004	0.57	+0.13	0.20
357	J053207.60+351630.3	TYC 2411-667-1	05 32 07.60	+35 16 30.34	B8 IV–V Si	200	11.2139	0.0008	+0.882	0.048	–0.071	0.004	0.47	+0.47	0.13
358	J053229.49+171430.2	Gaia DR2 3397273059024206720	05 32 29.50	+17 14 30.22	B9.5 IV–V SrCrEu	108	13.2816	0.0006	+0.592	0.027	+0.189	0.004	0.80	+1.34	0.11
359	J053231.77+441954.0	Gaia DR2 195863638416486144	05 32 31.77	+44 19 54.12	B8 III–IV SiCrEu*	132	13.1000	0.0005	+0.339	0.040	+0.012	0.004	0.62	+0.13	0.26
360	J053239.91+434307.5	HD 36259	05 32 39.89	+43 43 04.20	B8 IV Si	218	9.0375	0.0007	+1.856	0.072	–0.221	0.003	0.50	–0.12	0.10
361	J053259.46+161128.3	Gaia DR2 3396880529075737984	05 32 59.47	+16 11 28.40	B8 III–IV Si (He-wk)	200	12.4956	0.0019	+0.641	0.040	+0.010	0.008	0.95	+0.58	0.14
362	J053315.94+351856.0	TYC 2412-64-1	05 33 15.95	+35 18 56.08	A0 IV–V CrEu	145	11.8044	0.0006	+0.903	0.055	+0.161	0.003	0.40	+1.18	0.14
363	J053318.54+201332.6	TYC 1305-145-1	05 33 18.55	+20 13 32.66	B9.5 IV–V SrCr	171	11.5245	0.0010	+1.000	0.038	+0.049	0.006	0.68	+0.85	0.10
364	J053320.79+333114.5	Gaia DR2 3449103487404273408	05 33 20.80	+33 31 14.51	B8 IV–V Si	124	12.9540	0.0012	+0.577	0.038	–0.130	0.005	1.20	+0.56	0.15
365	J053333.97+303009.2	Gaia DR2 3446277502000268672	05 33 33.97	+30 30 09.30	B8 III–IV bl4130	133	12.3690	0.0012	+0.668	0.045	–0.074	0.006	1.34	+0.16	0.15
366	J053343.13+360821.5	Gaia DR2 183230593411140864	05 33 43.13	+36 08 21.52	B8 III–IV bl4130	135	14.2961	0.0012	+0.363	0.037	+0.055	0.004	1.42	+0.68	0.22
367	J053347.07+132207.4	TYC 713-421-1	05 33 47.07	+13 22 07.45	B9.5 III–IV SrEuSi	233	11.0293	0.0013	+1.803	0.296	+0.103	0.004	0.87	+1.44	0.36
368	J053355.06+325544.2	Gaia DR2 3448859872559385600	05 33 55.07	+32 55 44.17	A0 IV CrEu	116	12.9827	0.0009	+0.628	0.028	–0.018	0.005	1.20	+0.78	0.11
369	J053401.24+284902.2	TYC 1860-166-1	05 34 01.25	+28 49 02.22	B9.5 V SrCr	126	11.4276	0.0005	+0.977	0.051	+0.229	0.003	1.05	+0.32	0.12
370	J053439.95-015728.1	HD 290693	05 34 39.84	–01 57 28.19	A0 III CrEuSi	385	10.5331	0.0024	+1.019	0.072	+0.024	0.01	0.38	+0.20	0.16
371	J053504.75-012406.5	TYC 4766-330-1	05 35 04.54	–01 24 06.58	kA0hA2mA4 CrEu	559	9.4159	0.0008	+2.288	0.058	+0.042	0.004	0.30	+0.91	0.07
372	J053509.30+350554.4	TYC 2412-450-1	05 35 09.31	+35 05 54.47	B9 IV–V bl4130	126	12.1210	0.0009	+0.586	0.050	–0.046	0.004	0.96	0.00	0.19
373	J053510.70+165914.2	Gaia DR2 3397038996190150528	05 35 10.71	+16 59 14.29	B9.5 IV–V SrCr	205	12.5486	0.0017	+0.628	0.055	+0.271	0.004	0.85	+0.68	0.20
374	J053526.26+175705.1	Gaia DR2 3397700288010818688	05 35 26.26	+17 57 05.17	B9 IV bl4077 bl4130	186	12.6681	0.0007	+0.663	0.046	+0.036	0.005	0.90	+0.88	0.16
375	J053531.48+305432.1	TYC 2404-1071-1	05 35 31.48	+30 54 32.17	B8 IV–V Si	180	12.0381	0.0007	+0.906	0.076	–0.149	0.005	1.08	+0.75	0.19
376	J053531.81+211856.3	TYC 1309-1089-1	05 35 31.81	+21 18 56.30	B9 IV CrSi	167	11.8327	0.0003	+0.669	0.047	+0.024	0.003	0.80	+0.16	0.16
377	J053542.47+145443.0	Gaia DR2 3395789302442225792	05 35 42.47	+14 54 43.00	B9.5 III–IV Si	128	14.4888	0.0005	+0.374	0.033	+0.091	0.005	1.20	+1.16	0.20
378	J053551.11+450901.3	TYC 3359-2146-1	05 35 51.10	+45 09 01.24	B9 V Cr	305	11.5348	0.0008	+0.623	0.050	+0.188	0.004	0.52	–0.01	0.18
379	J053554.49+210229.6	Gaia DR2 3402868160162970496	05 35 54.50	+21 02 29.71	A3 III–III SrCrEuSi	138	12.1587	0.0005	+0.885	0.039	+0.500	0.003	0.57	+1.32	0.11
380	J053601.89+324756.5	Gaia DR2 3448827853582010112	05 36 01.89	+32 47 56.56	B9 III EuSi	112	14.3607	0.0006	+0.315	0.032	+0.151	0.004	1.31	+0.54	0.23
381	J053636.38+305520.4 <sup>a</sup>	HD 245261	05 36 36.39	+30 55 20.53	B9.5 V CrSi	172	11.0049	0.0009	+1.777	0.068	–0.047	0.004	0.77	+1.48	0.10
382	J053749.62+541330.7	TYC 3749-702-1	05 37 49.63	+54 13 30.76	B9 V Cr	177	11.7930	0.0008	+0.914	0.041	+0.159	0.004	0.63	+0.97	0.11
383	J053755.64+493047.3	Gaia DR2 214241180701977216	05 37 55.64	+49 30 47.40	B9.5 II–III Si	132	12.0179	0.0007	+0.395	0.039	+0.084	0.004	0.48	–0.48	0.22
384	J053815.61+193035.7	TYC 1306-837-1	05 38 15.61	+19 30 35.84	B8 IV Si	162	11.3036	0.0017	+0.718	0.063	–0.002	0.008	0.77	–0.19	0.20
385	J053821.15+143839.3	Gaia DR2 3347684564918451328	05 38 21.15	+14 38 39.43	B9 IV–V SrCr	183	11.7856	0.0003	+0.823	0.049	+0.026	0.003	0.87	+0.50	0.14
386	J053836.41+242850.6	Gaia DR2 3428723146028987392	05 38 36.41	+24 28 50.69	kB7hB9mA1 Si	154	12.2723	0.0005	+0.592	0.048	+0.024	0.003	1.22	–0.09	0.18
387	J053840.17+413754.0	Gaia DR2 192886156629653504	05 38 40.18	+41 37 54.05	kA1hA7mA9 SrCrEuSi	114	12.2659	0.0006	+0.912	0.041	+0.256	0.003	0.44	+1.63	0.11
388	J053901.26+540638.5	TYC 3749-888-1	05 39 00.93	+54 06 38.55	A7 V SrCrEuSi	253	9.7068	0.0006	+2.456	0.048	+0.222	0.003	0.63	+1.02	0.07
389	J053909.24+461117.3	TYC 3360-1477-1	05 39 09.24	+46 11 17.34	B9 IV–V Sr	227	11.6665	0.0006	+0.981	0.057	+0.074	0.005	0.65	+0.97	0.14
390	J053912.12+480622.4	Gaia DR2 210874235579559808	05 39 12.12	+48 06 22.34	B9 IV–V Cr	132	12.2815	0.0004	+0.627	0.034	+0.223	0.002	0.79	+0.48	0.13
391	J054027.66+333102.4	Gaia DR2 3448584552275686144	05 40 27.66	+33 31 02.67	kB9.5hA2mA4 Eu	116	14.6747	0.0035	+0.322	0.035	+0.186	0.014	1.00	+1.21	0.24
392	J054044.78+243154.9	Gaia DR2 3428700842260487040	05 40 44.79	+24 31 55.06	A5 IV SrCrEu	194	11.9913	0.0008	+0.967	0.065	+0.056	0.004	1.12	+0.80	0.15
393	J054102.12+332331.1	TYC 2408-1757-1	05 41 02.13	+33 23 31.10	B7 IV Si (He-wk)	197	11.2705	0.0025	+0.564	0.068	–0.176	0.01	0.73	–0.71	0.27
394	J054123.41+253043.2	HD 246255	05 41 23.29	+25 30 42.93	B9.5 IV–V SrCr	243	10.4934	0.0006	+1.521	0.065	+0.078	0.004	0.30	+1.11	0.10
395	J054301.11+383843.2	Gaia DR2 189854704291739648	05 43 01.12	+38 38 43.22	B9 IV–V Cr	122	11.8730	0.0010	+1.181	0.070	+0.047	0.006	0.86	+1.38	0.14
396	J054402.53+181251.3	HD 246892	05 44 02.61	+18 12 51.39	B9.5 II–III EuSi	329	10.8254	0.0013	+0.817	0.082	–0.025	0.006	0.47	–0.08	0.22
397	J054418.27+382207.0	Gaia DR2 189926408770237184	05 44 18.28	+38 22 07.12	A0 III–IV SrCr	119	12.3646	0.0007	–0.291	0.124	–	–	–	–	–
398	J054543.05+350259.7	TYC 2413-643-1	05 45 43.05	+35 02 59.76	A0 IV–V SrCr	133	11.8787	0.0006	+1.118	0.050	–0.018	0.004	0.69	+1.43	0.11
399	J054547.46+400703.6	TYC 2915-1913-1	05 45 47.46	+40 07 03.69	kA1hA3mA7 SrCrEuSi	192	11.9338	0.0003	+1.011	0.037	+0.123	0.003	0.67	+1.29	0.09
400	J054548.96+222854.3	HD 247241	05 45 48.96	+22 28 55.30	B9 V SrCrEu	469	10.3016	0.0005	+1.342	0.090	–0.009	0.002	0.52	+0.42	0.15



**Table A.1.** Essential data for our sample stars, sorted by increasing right ascension. The columns denote: (1) Internal identification number. (2) LAMOST identifier. (3) Alternativ identifier (HD number, TYC identifier or GAIA DR2 number). (4) Right ascension (J2000; GAIA DR2). (5) Declination (J2000; GAIA DR2). (6) Spectral type, as derived in this study. (7) Sloan  $g$  band S/N ratio of the analysed spectrum. (8)  $G$  mag (GAIA DR2). (9)  $G$  mag error. (10) Parallax (GAIA DR2). (11) Parallax error. (12) Dereddened colour index  $(BP - RP)_0$  (GAIA DR2). (13) Colour index error. (14) Absorption in the  $G$  band,  $A_G$ . (15) Intrinsic absolute magnitude in the  $G$  band,  $M_{G,0}$ . (16) Absolute magnitude error.

(1)	(2)	(3)	(4)		(5)	(6)	(7)		(8)	(9)	(10)	(11)	(12)	(13)	(14)	(15)	(16)
No.	ID_LAMOST	ID_alt	RA(J2000)	Dec(J2000)	SpT_final	S/N $_g$	$G$ mag	$e_G$ mag	pi (mas)	$e_{pi}$	$(BP - RP)_0$	$e_{(BP - RP)_0}$	$A_G$	$M_{G,0}$	$e_{M_{G,0}}$		
401	J054613.99+245550.4	Gaia DR2 3428625182116541952	05 46 14.00	+24 55 50.41	A9 V SrCrEuSi	107	12.2017	0.0002	+0.555	0.041	+0.154	0.003	0.90	+0.02	0.17		
402	J054622.23+204640.9	Gaia DR2 3399995204999449984	05 46 22.23	+20 46 40.82	B8 IV Si	94	12.0309	0.0010	+0.851	0.038	+0.155	0.005	0.40	+1.28	0.11		
403	J054630.44+273518.1	TYC 1870-1407-1	05 46 30.45	+27 35 18.16	B9 V CrEu	137	11.5944	0.0004	+0.962	0.053	-0.020	0.004	0.72	+0.79	0.13		
404	J054634.75+370200.6	TYC 2417-826-1	05 46 34.76	+37 02 00.61	B8 IV Si	140	11.9319	0.0007	+0.625	0.051	-0.053	0.004	0.83	+0.08	0.18		
405	J054724.36+171922.7	Gaia DR2 3398036734272024704	05 47 24.37	+17 19 22.81	B9 IV-V SrCr	195	11.9193	0.0026	+0.582	0.052	+0.109	0.013	0.65	+0.09	0.20		
406	J054732.61+121608.0	TYC 723-950-1	05 47 32.62	+12 16 08.07	B5 V HeB9*	110	12.8837	0.0014	+0.430	0.038	-0.019	0.006	0.73	+0.32	0.20		
407	J054750.69+115742.3	TYC 723-750-1	05 47 50.70	+11 57 42.35	B9 IV-V CrSi	223	11.6513	0.0007	+0.538	0.044	+0.033	0.004	0.58	-0.27	0.18		
408	J054754.48+413621.3	TYC 2919-515-1	05 47 54.49	+41 36 21.36	B9 IV-V Cr	321	11.4195	0.0008	+0.920	0.048	+0.108	0.004	0.91	+0.33	0.12		
409	J054757.12+235011.8	TYC 1862-1494-1	05 47 57.13	+23 50 11.83	B9.5 II-III EuSi	281	10.3040	0.0006	+1.009	0.055	-0.031	0.003	0.42	-0.10	0.13		
410	J054807.07+210619.0	HD 247724	05 48 07.08	+21 06 19.08	B7 IV bl4130	522	9.6286	0.0005	+0.971	0.061	-0.135	0.003	0.39	-0.83	0.14		
411	J054819.92+333516.9 <sup>a</sup>	TYC 2409-1922-1	05 48 19.77	+33 35 16.98	kA4hA9mF1 SrCrEuSi	200	10.4505	0.0006	+1.729	0.086	+0.052	0.002	0.58	+1.06	0.12		
412	J054822.35+103530.7	TYC 719-303-1	05 48 22.36	+10 35 30.78	B9 V Cr	112	11.3847	0.0007	+0.829	0.041	+0.129	0.005	0.67	+0.31	0.12		
413	J054826.28+304929.2	TYC 2405-268-1	05 48 26.29	+30 49 29.21	B8 III Eu	123	11.6907	0.0017	+0.487	0.055	-0.007	0.007	0.88	-0.76	0.25		
414	J054844.18+522027.9	TYC 3372-485-1	05 48 44.19	+52 20 27.92	A1 V CrEu	198	12.0289	0.0003	+0.829	0.035	+0.202	0.002	0.54	+1.08	0.10		
415	J054850.62+350217.4	TYC 2413-1-1	05 48 50.46	+35 02 17.46	kB8hA0mA1 CrEu	156	10.3198	0.0006	+1.416	0.066	-0.066	0.002	0.60	+0.48	0.11		
416	J054928.70+404455.7	Gaia DR2 191842273418923776	05 49 28.70	+40 44 55.73	B9 V SrCr	204	12.4174	0.0006	+0.505	0.040	+0.036	0.004	0.57	+0.36	0.18		
417	J054952.18+352212.6	TYC 2413-441-1	05 49 52.19	+35 22 12.66	B8 IV Si	259	10.9698	0.0005	+0.971	0.044	-0.103	0.002	0.72	+0.18	0.11		
418	J055002.80+234023.9	HD 248072	05 50 02.80	+23 40 23.97	B9 IV bl4130	349	10.5259	0.0015	+1.124	0.134	-0.103	0.006	0.48	+0.30	0.26		
419	J055002.87+235548.0	TYC 1862-2027-1	05 50 02.87	+23 55 48.06	A1 IV-V Cr	186	11.6992	0.0006	+1.081	0.072	-0.005	0.004	0.52	+1.35	0.15		
420	J055019.83+214937.6	Gaia DR2 3424216763262732544	05 50 19.83	+21 49 37.69	B9.5 III-IV EuSi	240	11.5652	0.0009	+0.950	0.038	-0.050	0.005	0.67	+0.78	0.10		
421	J055023.89+261330.2	TYC 1866-861-1	05 50 23.89	+26 13 30.29	B4: V HeB9*	79	11.5523	0.0015	+0.612	0.052	-0.182	0.009	1.03	-0.55	0.19		
422	J055026.09+314751.1	Gaia DR2 3444961073046795392	05 50 26.09	+31 47 51.20	B9 III Si*	62	14.1948	0.0009	+0.252	0.051	-0.045	0.006	0.79	+0.41	0.44		
423	J055045.30+372809.0	TYC 2417-126-1	05 50 45.30	+37 28 09.07	kA2hA4mA7 SrCrEu	133	11.8874	0.0004	+1.534	0.059	+0.279	0.003	0.89	+1.93	0.10		
424	J055054.75+410356.0	TYC 2916-1788-1	05 50 54.75	+41 03 56.09	B8 IV Si (He-wk)	454	11.0859	0.0008	+0.677	0.063	-0.110	0.005	0.50	-0.26	0.21		
425	J055105.53+411410.9	Gaia DR2 192253357627486592	05 51 05.53	+41 14 10.94	A1 V SrCrEu	169	13.0171	0.0008	+0.548	0.039	+0.186	0.003	0.55	+1.16	0.16		
426	J055108.25+531610.8 <sup>a</sup>	TYC 3750-928-1	05 51 08.26	+53 16 10.89	A2 IV-V SrCrEu	261	11.5413	0.0004	+1.375	0.037	+0.250	0.002	0.35	+1.88	0.08		
427	J055110.67+360517.0	TYC 2418-790-1	05 51 10.68	+36 05 17.01	B9.5 V SrCr	116	12.0787	0.0003	+0.854	0.039	+0.314	0.003	0.78	+0.96	0.11		
428	J055121.05+420610.5	HD 38943	05 51 20.74	+42 06 10.53	B8 IV Si	352	9.0962	0.0011	+1.422	0.057	-0.046	0.007	0.36	-0.50	0.10		
429	J055143.67+205025.1	HD 248458	05 51 43.67	+20 50 25.09	B9 IV-V bl4130	288	9.9889	0.0007	+0.566	0.277	-	-	-	-	-		
430	J055154.28+350352.9	TYC 2414-679-1	05 51 54.29	+35 03 52.95	A3 III-IV SrCrEu	105	12.4204	0.0005	+0.964	0.042	+0.333	0.006	0.50	+1.85	0.11		
431	J055157.54+410439.7	TYC 2916-2241-1	05 51 57.55	+41 04 39.72	A1 IV-V Cr	119	11.5408	0.0006	+0.708	0.059	+0.080	0.004	0.61	+0.18	0.19		
432	J055207.96+242953.9	Gaia DR2 3428136865813370880	05 52 07.97	+24 29 53.96	B9 IV CrSi	116	14.4510	0.0008	+0.198	0.041	-0.406	0.006	2.06	-1.12	0.45		
433	J055218.79+331852.7	TYC 2410-2403-1	05 52 18.79	+33 18 52.82	B9.5 V Cr	226	11.2003	0.0006	+0.852	0.037	+0.087	0.003	0.56	+0.30	0.11		
434	J055219.99+261909.7	TYC 1871-116-1	05 52 19.99	+26 19 09.70	B9 IV-V bl4130	173	11.1083	0.0018	+1.085	0.074	-0.134	0.005	0.67	+0.62	0.16		
435	J055237.04+154023.8	TYC 1312-2862-1	05 52 37.04	+15 40 23.90	B8 IV-V Si	184	11.7179	0.0010	+0.721	0.040	-0.099	0.009	0.36	+0.64	0.13		
436	J055237.95+274922.8	TYC 1871-1738-1	05 52 37.95	+27 49 22.78	A6 V SrCrEu	120	11.4405	0.0005	+1.285	0.045	+0.197	0.003	0.38	+1.60	0.09		
437	J055254.41+310240.3	Gaia DR2 3444843223443216000	05 52 54.41	+31 02 40.36	A0 III-IV CrSi	18	14.2614	0.0005	+0.380	0.028	+0.063	0.003	0.64	+1.52	0.17		
438	J055300.15+411220.9	TYC 2916-1620-1	05 53 00.15	+41 12 20.96	A1 IV-V SrCr	160	11.2609	0.0008	+0.830	0.048	+0.218	0.002	0.52	+0.34	0.14		
439	J055308.38+254739.9	TYC 1867-2207-1	05 53 08.39	+25 47 39.95	B8 III-IV EuSi	116	10.9895	0.0006	+0.875	0.074	-0.066	0.006	0.63	+0.07	0.19		
440	J055321.75+302915.8	TYC 2406-1980-1	05 53 21.76	+30 29 15.91	A1 V SrCrEu	103	12.0275	0.0005	+1.333	0.048	+0.114	0.003	0.51	+2.14	0.09		
441	J055333.92+180202.9	HD 248844	05 53 33.92	+18 02 02.96	F2 V SrEu	182	10.3666	0.0004	+0.561	0.155	-	-	-	-	-		
442	J055346.74+144708.2	Gaia DR2 3347180885513452160	05 53 46.74	+14 47 08.17	B9.5 IV-V CrEu	111	12.2860	0.0013	+0.649	0.043	+0.020	0.007	0.44	+0.91	0.15		
443	J055409.86+165428.3	HD 248975	05 54 09.87	+16 54 28.42	B8 IV Si	157	10.7329	0.0007	+0.820	0.068	-0.122	0.002	0.27	+0.03	0.19		
444	J055411.43+304113.3	Gaia DR2 3444069098537504512	05 54 11.43	+30 41 13.53	B8 IV-V Si	114	11.5208	0.0004	+0.766	0.041	+0.011	0.003	0.56	+0.38	0.13		
445	J055422.76+305401.8	HD 248874	05 54 22.76	+30 54 01.90	B8 III bl4130	253	10.0389	0.0012	+0.812	0.058	-0.092	0.003	0.71	-1.13	0.16		
446	J055422.96+415825.7	TYC 2920-1365-1	05 54 22.96	+41 58 25.69	B9 V CrEu	409	9.9528	0.0009	+1.443	0.057	+0.014	0.003	0.29	+0.46	0.10		
447	J055426.04+241129.6	Gaia DR2 3427914867543706496	05 54 26.05	+24 11 29.74	B9 V Cr	118	14.1450	0.0004	+0.378	0.032	+0.066	0.003	1.12	+0.91	0.19		
448	J055449.32+263732.6	TYC 1871-1008-1	05 54 49.33	+26 37 32.73	A0 IV-V SrCrEu	135	11.5552	0.0003	+1.153	0.051	+0.022	0.004	0.63	+1.24	0.11		
449	J055504.38+262725.6	TYC 1871-1483-1	05 55 04.38	+26 27 25.64	B8 IV-V SrSi	57	11.1396	0.0008	+0.789	0.041	-0.108	0.004	0.82	-0.19	0.12		
450	J055507.06+121347.0	TYC 724-1180-1	05 55 07.07	+12 13 47.04	B9.5 II-III SrSi	260	11.3687	0.0010	+0.574	0.063	-0.090	0.005	0.36	-0.20	0.24		

**Table A.1.** Essential data for our sample stars, sorted by increasing right ascension. The columns denote: (1) Internal identification number. (2) LAMOST identifier. (3) Alternativ identifier (HD number, TYC identifier or GAIA DR2 number). (4) Right ascension (J2000; GAIA DR2). (5) Declination (J2000; GAIA DR2). (6) Spectral type, as derived in this study. (7) Sloan *g* band S/N ratio of the analysed spectrum. (8) *G* mag (GAIA DR2). (9) *G* mag error. (10) Parallax (GAIA DR2). (11) Parallax error. (12) Dereddened colour index  $(BP - RP)_0$  (GAIA DR2). (13) Colour index error. (14) Absorption in the *G* band,  $A_G$ . (15) Intrinsic absolute magnitude in the *G* band,  $M_{G,0}$ . (16) Absolute magnitude error.

(1)	(2)	(3)	(4)	(5)	(6)	(7)	(8)	(9)	(10)	(11)	(12)	(13)	(14)	(15)	(16)
No.	ID_LAMOST	ID_alt	RA(J2000)	Dec(J2000)	SpT_final	S/N <sub><i>g</i></sub>	<i>G</i> mag	<i>e</i> <sub><i>G</i></sub> mag	pi (mas)	<i>e</i> <sub>pi</sub>	$(BP - RP)_0$	<i>e</i> <sub><math>(BP - RP)_0</math></sub>	$A_G$	$M_{G,0}$	<i>e</i> <sub><math>M_{G,0}</math></sub>
451	J055519.77+154335.4	TYC 1312-2891-1	05 55 19.77	+15 43 35.47	B9 V Cr	164	10.8051	0.0010	+1.094	0.068	-0.024	0.005	0.31	+0.69	0.14
452	J055523.13+150002.5	HD 249209	05 55 23.13	+15 00 02.59	B8 IV CrSi	227	10.9644	0.0013	+0.499	0.075	+0.001	0.005	0.43	-0.97	0.33
453	J055529.24+393248.5	TYC 2916-1265-1	05 55 29.25	+39 32 48.53	kB8hA3mA3 CrSi	120	11.4179	0.0005	+0.961	0.047	-0.026	0.004	0.55	+0.79	0.12
454	J055534.89+281813.2	Gaia DR2 3431156738919784320	05 55 34.90	+28 18 13.28	B9 III-IV Si	159	12.3021	0.0004	+0.404	0.058	+0.016	0.004	0.80	-0.46	0.32
455	J055539.90+171036.9	Gaia DR2 3349797452608779520	05 55 39.91	+17 10 36.91	A0 IV-V CrEu	112	14.0679	0.0009	+0.469	0.028	+0.189	0.005	0.69	+1.73	0.14
456	J055545.19+195746.3	TYC 1320-1062-1	05 55 45.19	+19 57 46.32	B9.5 III-IV Si	161	11.4597	0.0004	+0.778	0.040	+0.000	0.003	0.61	+0.30	0.12
457	J055557.19+275828.0	TYC 1871-1862-1	05 55 57.19	+27 58 28.00	A0 IV-V Cr	109	12.2417	0.0009	+0.645	0.069	+0.178	0.004	0.78	+0.51	0.24
458	J055604.42+160937.1	TYC 1312-1184-1	05 56 04.42	+16 09 37.11	B8 IV-V Si	260	11.2583	0.0009	+0.977	0.051	-0.151	0.006	0.49	+0.71	0.12
459	J055618.50+210706.3	TYC 1324-209-1	05 56 18.51	+21 07 06.39	B5 III-IV bl4130 (He-wk)	125	11.5927	0.0008	+0.561	0.050	-0.028	0.004	0.86	-0.52	0.20
460	J055625.41+295741.2	TYC 1875-195-1	05 56 25.42	+29 57 41.22	B6 IV-V bl4130 (He-wk) (He-st)	158	12.0124	0.0004	+0.699	0.051	-0.044	0.004	0.53	+0.70	0.16
461	J055629.24+120153.3	TYC 724-1222-1	05 56 29.25	+12 01 53.34	B9 V SrCr	221	11.5961	0.0008	+0.814	0.040	+0.016	0.005	0.37	+0.77	0.12
462	J055657.30+265341.3	Gaia DR2 3430777686586008576	05 56 57.30	+26 53 41.38	B9 III-IV EuSi	101	12.4593	0.0015	+0.368	0.038	+0.012	0.006	0.83	-0.54	0.23
463	J055703.71+463318.7	TYC 3361-532-1	05 57 03.68	+46 33 17.57	B9 V Cr	456	10.8254	0.0009	+1.029	0.049	+0.003	0.004	0.30	+0.58	0.12
464	J055719.01+124008.6	Gaia DR2 3343641424444963072	05 57 19.01	+12 40 08.67	A1 III-IV CrEuSi	147	12.1762	0.0002	+0.844	0.040	+0.367	0.003	0.25	+1.56	0.11
465	J055730.88+295306.9	TYC 1875-271-1	05 57 30.88	+29 53 06.89	B9 IV-V SrCr	117	11.6520	0.0013	+0.629	0.043	+0.039	0.006	0.56	+0.08	0.16
466	J055739.82+160140.8	Gaia DR2 3348827404175942656	05 57 39.83	+16 01 40.94	A0 IV-V Cr	165	12.0056	0.0009	+0.735	0.045	+0.084	0.007	0.53	+0.81	0.14
467	J055940.19+284225.7	TYC 1875-2529-1	05 59 40.19	+28 42 25.72	B9 III-IV Si	118	12.1002	0.0021	+0.503	0.059	+0.035	0.011	0.64	-0.04	0.26
468	J060020.24+154701.5	TYC 1313-1569-1	06 00 20.25	+15 47 01.54	B9 V bl4077 bl4130	152	11.8799	0.0012	+0.825	0.043	-0.073	0.005	0.61	+0.85	0.12
469	J060040.60+100410.1	TYC 721-2348-1	06 00 40.60	+10 04 10.11	B9.5 V CrEu	207	11.9664	0.0005	+0.766	0.039	+0.028	0.004	0.43	+0.96	0.12
470	J060045.94+035344.3	HD 40759	06 00 45.73	-03 53 44.41	A0 IV-V Si	702	8.5214	0.0006	+2.326	0.055	-0.142	0.002	0.42	-0.07	0.07
471	J060106.34+042123.3	Gaia DR2 3024207178875434496	06 01 06.35	-04 21 23.33	kA1hA5mA8 SrCrEu	152	11.7624	0.0005	+0.726	0.041	+0.237	0.003	0.87	+0.19	0.13
472	J060136.47+293812.0	Gaia DR2 3437677014671183744	06 01 36.47	+29 38 12.09	B8 IV Si	56	13.1481	0.0014	+0.334	0.047	+0.033	0.006	0.61	+0.16	0.31
473	J060155.40+280356.1	TYC 1872-1819-1	06 01 55.40	+28 03 56.11	B8 IV Si	247	11.6929	0.0004	+0.623	0.073	-0.002	0.004	0.33	+0.33	0.26
474	J060202.24+282202.0	Gaia DR2 3431346134097961216	06 02 02.24	+28 22 02.03	B9 IV-V SrEu	56	12.7638	0.0015	+0.272	0.045	-0.063	0.009	0.62	-0.68	0.36
475	J060225.92+244628.5	HD 40833	06 02 25.92	+24 46 28.52	B8 IV Si	535	9.2072	0.0019	+1.321	0.071	-0.181	0.008	0.39	-0.58	0.13
476	J060227.33+282943.9	HD 250515	06 02 27.33	+28 29 43.95	B8 III-IV EuSi (He-wk)	298	10.1046	0.0017	+0.557	0.051	+0.006	0.007	0.34	-1.51	0.20
477	J060241.10+231013.0	TYC 1864-1494-1	06 02 41.11	+23 10 13.23	B9 III-IV Si	308	11.3684	0.0004	+0.992	0.041	-0.334	0.004	1.49	-0.13	0.10
478	J060258.76+160557.2	HD 250765	06 02 58.76	+16 05 57.19	B9.5 IV Cr	295	10.4195	0.0008	+0.913	0.091	-0.128	0.002	0.65	-0.43	0.22
479	J060315.94+143510.2	TYC 729-949-1	06 03 15.95	+14 35 10.35	B9 IV-V CrEu	169	11.4316	0.0010	+0.752	0.077	-0.074	0.006	0.72	+0.09	0.23
480	J060343.72+013555.5	TYC 130-1391-1	06 03 43.73	+01 35 55.60	kB7hB9mA0 bl4130 (He-wk)	184	11.8978	0.0012	+0.825	0.036	+0.027	0.004	0.87	+0.61	0.11
481	J060347.88+412532.7	TYC 2933-1919-1	06 03 47.89	+41 25 32.80	A0 IV-V SrCrEuSi	173	12.3304	0.0005	+0.856	0.038	+0.185	0.003	0.59	+1.40	0.11
482	J060354.12+162915.5	TYC 1313-470-1	06 03 54.11	+16 29 15.68	B9 V Cr	111	11.9379	0.0007	+1.077	0.041	-0.031	0.005	0.71	+1.39	0.10
483	J060356.06+213033.2	TYC 1325-1708-1	06 03 56.06	+21 30 33.21	A8 V SrEu	386	10.9242	0.0017	+1.771	0.065	+0.113	0.004	0.36	+1.81	0.09
484	J060410.32+462824.4	TYC 3374-1710-1	06 04 10.33	+46 28 24.46	B9 III Si	110	12.9083	0.0006	+0.397	0.065	+0.019	0.003	0.37	+0.53	0.36
485	J060418.34+413658.0	TYC 2933-1569-1	06 04 18.22	+41 36 58.04	A1 IV-V CrSi	244	10.7932	0.0006	+1.123	0.055	+0.054	0.003	0.43	+0.62	0.12
486	J060431.41+350633.1	TYC 2427-1223-1	06 04 31.41	+35 06 33.14	B8 III CrSi (He-wk)	194	12.4054	0.0013	+0.405	0.042	+0.074	0.007	0.86	-0.42	0.23
487	J060453.02+205450.7	TYC 1325-259-1	06 04 53.02	+20 54 50.74	B8 III Si	398	10.6130	0.0007	+0.800	0.050	-0.140	0.003	0.67	-0.55	0.15
488	J060453.41+161322.1	TYC 1313-1527-1	06 04 53.41	+16 13 22.18	A0 IV Cr	143	11.4692	0.0008	+1.047	0.038	+0.169	0.003	0.58	+0.99	0.09
489	J060516.22+120731.9	TYC 725-1158-1	06 05 16.23	+12 07 31.94	B9 V SrCr	211	11.5435	0.0004	+0.713	0.042	+0.075	0.003	0.45	+0.36	0.14
490	J060518.19+125728.6	Gaia DR2 3342783113882464256	06 05 18.20	+12 57 28.63	B9 IV-V SrCr	149	12.8004	0.0016	+0.510	0.053	-0.127	0.007	1.04	+0.30	0.23
491	J060543.16+215523.2	Gaia DR2 3423437827993940608	06 05 43.17	+21 55 23.33	B8 III-IV Cr	102	14.3544	0.0010	+0.298	0.039	+0.004	0.006	1.30	+0.42	0.29
492	J060620.10+142624.2	Gaia DR2 3345279181372314624	06 06 20.11	+14 26 24.28	B9 V SrCrEu	108	13.1161	0.0010	+1.091	0.062	+0.256	0.003	0.84	+2.47	0.13
493	J060621.79+212433.8 <sup>a</sup>	HD 251556	06 06 21.80	+21 24 35.74	B9.5 III-IV Cr	386	10.2064	0.0009	+1.455	0.080	-0.172	0.003	0.36	+0.66	0.13
494	J060707.31+232405.2	Gaia DR2 3425366680625960064	06 07 07.32	+23 24 05.25	A0 IV-V CrEu	112	14.2870	0.0005	+0.529	0.032	+0.187	0.004	0.99	+1.91	0.14
495	J060732.16+221707.0	Gaia DR2 3423564130094727552	06 07 32.17	+22 17 06.95	B8 II-III EuSi	183	12.7663	0.0023	+0.569	0.173	-	-	-	-	-
496	J060809.53+240945.0	HD 252026	06 08 09.53	+24 09 45.05	B8 III-IV Si	449	9.9815	0.0007	+1.122	0.047	-0.104	0.003	0.51	-0.28	0.10
497	J060815.12+045107.6	TYC 139-1180-1	06 08 15.12	+04 51 07.68	B9 IV-V Eu	282	11.4279	0.0017	+1.153	0.081	-0.037	0.008	0.43	+1.30	0.16
498	J060820.34+005411.7	Gaia DR2 3122985452386853632	06 08 20.35	+00 54 11.73	B5 IV Si (He-wk)	185	12.6323	0.0006	+0.270	0.043	+0.011	0.018	0.46	-0.68	0.35
499	J060820.77-025507.5	HD 294640	06 08 20.77	-02 55 07.60	A1 IV-V Sr	248	10.6258	0.0004	+1.571	0.040	+0.137	0.006	0.29	+1.32	0.07
500	J060821.41+502149.8	HD 233211	06 08 21.10	+50 21 49.80	kB9hA3mA2 bl4077 bl4130	676	9.3215	0.0009	+2.094	0.051	+0.017	0.007	0.33	+0.60	0.07

**Table A.1.** Essential data for our sample stars, sorted by increasing right ascension. The columns denote: (1) Internal identification number. (2) LAMOST identifier. (3) Alternativ identifier (HD number, TYC identifier or GAIA DR2 number). (4) Right ascension (J2000; GAIA DR2). (5) Declination (J2000; GAIA DR2). (6) Spectral type, as derived in this study. (7) Sloan  $g$  band S/N ratio of the analysed spectrum. (8)  $G$  mag (GAIA DR2). (9)  $G$  mag error. (10) Parallax (GAIA DR2). (11) Parallax error. (12) Dereddened colour index  $(BP - RP)_0$  (GAIA DR2). (13) Colour index error. (14) Absorption in the  $G$  band,  $A_G$ . (15) Intrinsic absolute magnitude in the  $G$  band,  $M_{G,0}$ . (16) Absolute magnitude error.

(1)	(2)	(3)	(4)	(5)	(6)	(7)	(8)	(9)	(10)	(11)	(12)	(13)	(14)	(15)	(16)
No.	ID_LAMOST	ID_alt	RA(J2000)	Dec(J2000)	SpT_final	S/N $_g$	$G$ mag	$e_G$ mag	pi (mas)	$e_{pi}$	$(BP - RP)_0$	$e_{(BP - RP)_0}$	$A_G$	$M_{G,0}$	$e_{M_{G,0}}$
501	J060822.66+233735.4	TYC 1877-408-1	06 08 22.67	+23 37 35.48	B9.5 IV-V CrSi	475	10.6377	0.0010	+1.183	0.208	-0.088	0.003	0.45	+0.56	0.38
502	J060827.84+204832.0	Gaia DR2 3375272518547111680	06 08 27.84	+20 48 32.12	B9 IV CrEuSi	119	12.3687	0.0003	+0.890	0.071	-0.082	0.003	0.93	+1.18	0.18
503	J060851.09+424158.2	TYC 2933-1518-1	06 08 50.81	+42 41 58.24	B9 III-IV bl4130	444	9.8528	0.0009	+0.838	0.054	-0.089	0.003	0.49	-1.02	0.15
504	J060853.81+465924.7	Gaia DR2 963466378309113856	06 08 53.81	+46 59 24.79	A1 IV-V Cr	130	12.9117	0.0017	+0.487	0.081	+0.181	0.007	0.24	+1.11	0.37
505	J060905.54+114858.8	TYC 738-220-1	06 09 05.54	+11 48 58.81	B9 V Cr	285	11.9801	0.0004	+1.015	0.060	+0.043	0.004	0.48	+1.54	0.14
506	J060940.01+035028.3	Gaia DR2 3317252389461940480	06 09 40.01	+03 50 28.34	A0 IV SrCrEu	127	13.2614	0.0004	+0.609	0.052	+0.170	0.002	0.64	+1.54	0.19
507	J061001.31+325315.5	TYC 2424-327-1	06 10 01.31	+32 53 15.58	B9 V CrEu	129	9.6521	0.0005	+1.997	0.043	-0.001	0.003	0.26	+0.89	0.07
508	J061029.25+053152.4	TYC 4791-807-1	06 10 29.25	-05 31 52.45	B9 IV-V bl4077 bl4130	284	11.2667	0.0011	+1.209	0.044	-0.476	0.003	1.54	+0.14	0.09
509	J061030.89+032858.7	TYC 135-1133-1	06 10 30.68	+03 28 58.71	B9 V CrEu	391	9.0991	0.0015	+2.092	0.084	-0.377	0.007	0.84	-0.13	0.10
510	J061054.63+240801.2	TYC 1877-112-1	06 10 54.63	+24 08 01.29	A0 IV CrEu	259	11.3950	0.0007	+0.996	0.042	+0.012	0.004	0.71	+0.67	0.10
511	J061058.53+165733.8	TYC 1318-495-1	06 10 58.53	+16 57 33.83	B9 IV-V Eu	203	11.6046	0.0008	+1.264	0.051	-0.066	0.004	1.62	+0.49	0.10
512	J061102.36+244423.8	TYC 1881-1149-1	06 11 02.36	+24 44 23.80	B9 V CrEu	394	10.9938	0.0019	+1.123	0.061	-0.019	0.007	0.63	+0.62	0.13
513	J061114.05+035146.8	HD 42510	06 11 13.84	+03 51 46.57	B9.5 II-III EuSi	436	9.0517	0.0022	+2.119	0.040	-0.209	0.012	0.68	+0.01	0.06
514	J061124.59+124504.9	TYC 738-699-1	06 11 24.60	+12 45 05.01	A0 IV-V CrEu	635	10.4730	0.0013	+1.465	0.049	+0.036	0.008	0.46	+0.84	0.09
515	J061143.19+152832.1	Gaia DR2 3345733932510678656	06 11 43.20	+15 28 32.13	B9.5 V CrEu	129	13.0875	0.0012	+0.720	0.038	-0.052	0.005	1.07	+1.30	0.13
516	J061143.58+025133.3	Gaia DR2 3316930743654985344	06 11 43.59	+02 51 33.35	A9 V SrSi	132	13.0664	0.0006	+0.898	0.030	+0.324	0.005	1.15	+1.68	0.09
517	J061143.92+254734.6	Gaia DR2 3426811541984219520	06 11 43.92	+25 47 34.58	B9 IV-V Cr	109	13.2418	0.0009	+0.356	0.034	+0.034	0.005	0.79	+0.21	0.21
518	J061222.36+240733.9	Gaia DR2 3425476524411862144	06 12 22.37	+24 07 33.91	A8 V SrCrEu	137	12.1788	0.0006	+0.762	0.077	+0.330	0.004	0.82	+0.77	0.22
519	J061229.08+184051.4	TYC 1318-680-1	06 12 29.08	+18 40 51.35	B9.5 V CrSi	328	11.7449	0.0003	+0.627	0.037	+0.082	0.003	0.45	+0.29	0.14
520	J061308.61+342342.1	TYC 2428-1351-1	06 13 08.60	+34 23 42.02	B8 IV-V Si	349	11.4852	0.0011	+1.688	0.302	+0.177	0.007	0.32	+2.31	0.39
521	J061312.69+013350.3	Gaia DR2 3122955177158513920	06 13 12.70	+01 33 50.39	A0 V Cr	149	13.1708	0.0010	+1.066	0.409	-	-	-	-	-
522	J061328.54+405514.0	TYC 2930-111-1	06 13 28.54	+40 55 14.07	B9.5 II-III SiCrSr*	306	11.2009	0.0006	+0.537	0.047	-0.040	0.004	0.30	-0.45	0.20
523	J061329.24+041213.9	TYC 139-2019-1	06 13 29.24	+04 12 13.94	B9.5 V SrCr	267	11.8412	0.0004	+0.995	0.067	+0.199	0.003	0.81	+1.02	0.15
524	J061331.98+135352.9	Gaia DR2 3344392730186495744	06 13 31.99	+13 53 52.94	A0 II Eu	151	13.4168	0.0008	+0.316	0.023	-0.282	0.006	1.76	-0.85	0.17
525	J061338.27+085719.7	TYC 5362-1436-1	06 13 38.27	-08 57 19.67	A7 IV-V SrCrEu	286	10.4517	0.0007	+1.598	0.071	+0.193	0.002	0.26	+1.21	0.11
526	J061341.68+114751.7	Gaia DR2 3331844210134383104	06 13 41.68	+11 47 51.69	B9 III bl4130	106	12.6200	0.0004	+0.610	0.067	-0.049	0.005	0.87	+0.68	0.24
527	J061342.52+263829.6	TYC 1885-92-1	06 13 42.52	+26 38 29.65	B8 III-IV Si	102	10.8684	0.0011	+0.985	0.056	+0.109	0.006	0.56	+0.27	0.13
528	J061350.63+203015.3	TYC 1322-443-1	06 13 50.63	+20 30 15.49	kA0hA2mA4 bl4130	156	11.9459	0.0004	-1.529	0.211	-	-	-	-	-
529	J061413.62+112022.5	TYC 738-1510-1	06 14 13.63	+11 20 22.53	kA2hA3mA6 SrCrEu	104	11.9757	0.0007	+0.998	0.049	+0.000	0.004	0.73	+1.25	0.12
530	J061434.73+050332.4	TYC 139-1241-1	06 14 34.73	+05 03 32.42	B9.5 IV-V Cr	208	12.1693	0.0013	+0.744	0.040	+0.191	0.006	0.76	+0.77	0.13
531	J061436.66+142939.5	Gaia DR2 3344825319290434176	06 14 36.67	+14 29 39.62	B9 V Cr	227	12.2346	0.0003	+0.580	0.068	+0.002	0.004	0.80	+0.26	0.26
532	J061444.86+234440.8	TYC 1877-792-1	06 14 44.86	+23 44 40.89	A8 V SrCrEu	622	9.7436	0.0005	+2.486	0.050	+0.263	0.004	0.14	+1.58	0.07
533	J061455.11+245214.3	TYC 1881-912-1	06 14 55.13	+24 52 14.32	A6 V SrEuSi	274	11.6812	0.0076	-7.091	1.137	-	-	-	-	-
534	J061455.58+032317.5	TYC 135-1270-1	06 14 55.58	+03 23 17.54	B8 IV Si	212	12.0688	0.0007	+0.711	0.041	-0.083	0.003	1.50	-0.17	0.13
535	J061502.38+184511.7	Gaia DR2 3373847718978934656	06 15 02.39	+18 45 11.77	B9 IV-V Cr	178	12.6224	0.0003	+0.518	0.046	+0.110	0.003	1.23	-0.04	0.20
536	J061558.32+135157.3	Gaia DR2 3344570095153338880	06 15 58.33	+13 51 57.37	B5 III-IV bl4130 (He-wk)	148	13.2180	0.0028	+0.487	0.030	-0.032	0.013	1.03	+0.62	0.14
537	J061609.42+265703.2	TYC 1885-208-1	06 16 09.42	+26 57 03.15	B8 IV-V bl4130	192	11.5715	0.0009	+17.732	1.692	+0.840	0.004	0.03	+7.78	0.21
538	J061623.52+330303.3	TYC 2424-369-1	06 16 23.52	+33 03 03.38	B8 IV-V Si (He-wk)	253	10.7561	0.0008	+1.035	0.051	-0.120	0.005	0.61	+0.22	0.12
539	J061638.39+125441.1	Gaia DR2 3332085625956573696	06 16 38.40	+12 54 41.16	B8 III-IV Si	114	13.5954	0.0005	+0.267	0.028	-0.020	0.003	1.39	-0.66	0.23
540	J061713.35+232351.5	TYC 1878-263-1	06 17 13.36	+23 23 51.52	A1 V Cr	259	11.7869	0.0005	+0.867	0.039	+0.171	0.004	0.71	+0.77	0.11
541	J061734.94+252253.8	Gaia DR2 3426033706226654848	06 17 34.96	+25 22 53.92	B8 IV-V CrSi	103	14.4724	0.0009	+0.218	0.033	+0.041	0.005	1.00	+0.17	0.33
542	J061743.05+595315.3	TYC 3776-815-1	06 17 43.07	+59 53 15.31	A1 IV Eu	148	11.3202	0.0006	+1.339	0.054	+0.260	0.002	0.18	+1.77	0.10
543	J061802.68+263156.6	Gaia DR2 3432912006155737216	06 18 02.69	+26 31 56.64	A0 IV SrCrEu	207	12.3734	0.0003	+0.497	0.036	+0.295	0.003	0.59	+0.27	0.17
544	J061817.58+265109.6	HD 254625	06 18 17.58	+26 51 09.74	A1 II Si	462	10.5653	0.0012	+0.999	0.053	-0.122	0.005	0.68	-0.12	0.12
545	J061826.24+211412.3	TYC 1327-1335-1	06 18 26.24	+21 14 12.45	B8 IV-V Si	269	11.3062	0.0008	+0.752	0.067	-0.129	0.006	0.63	+0.06	0.20
546	J061845.15+190925.3	Gaia DR2 3373922661868123136	06 18 45.15	+19 09 25.37	B9 IV bl4130	135	14.0601	0.0008	+0.484	0.031	+0.203	0.005	0.79	+1.70	0.15
547	J061909.30+503741.3	TYC 3387-281-1	06 19 09.35	+50 37 41.34	A1 IV-V SrCr	335	10.7271	0.0006	+1.050	0.039	+0.079	0.003	0.25	+0.58	0.10
548	J061911.91+224143.5	Gaia DR2 3377043763061518592	06 19 11.92	+22 41 43.59	B4 IV Si	101	14.1343	0.0005	+0.558	0.035	+0.349	0.004	1.62	+1.25	0.15
549	J061913.90+185953.3	Gaia DR2 3373905516358940160	06 19 13.91	+18 59 53.45	B9 IV-V Cr	133	14.3685	0.0011	+0.296	0.033	+0.067	0.007	0.99	+0.74	0.24
550	J061914.21+362331.9	TYC 2433-657-1	06 19 14.21	+36 23 31.78	B8 IV Si (He-wk)	292	11.6573	0.0006	+0.667	0.061	-0.082	0.006	0.92	-0.14	0.20

**Table A.1.** Essential data for our sample stars, sorted by increasing right ascension. The columns denote: (1) Internal identification number. (2) LAMOST identifier. (3) Alternative identifier (HD number, TYC identifier or GAIA DR2 number). (4) Right ascension (J2000; GAIA DR2). (5) Declination (J2000; GAIA DR2). (6) Spectral type, as derived in this study. (7) Sloan  $g$  band S/N ratio of the analysed spectrum. (8)  $G$  mag (GAIA DR2). (9)  $G$  mag error. (10) Parallax (GAIA DR2). (11) Parallax error. (12) Dereddened colour index  $(BP - RP)_0$  (GAIA DR2). (13) Colour index error. (14) Absorption in the  $G$  band,  $A_G$ . (15) Intrinsic absolute magnitude in the  $G$  band,  $M_{G,0}$ . (16) Absolute magnitude error.

(1)	(2)	(3)	(4)	(5)	(6)	(7)	(8)	(9)	(10)	(11)	(12)	(13)	(14)	(15)	(16)
No.	ID_LAMOST	ID_alt	RA(J2000)	Dec(J2000)	SpT_final	S/N <sub>g</sub>	$G$ mag	$e_G$ mag	$\pi$ (mas)	$e_\pi$	$(BP - RP)_0$	$e_{(BP - RP)_0}$	$A_G$	$M_{G,0}$	$e_{M_{G,0}}$
551	J061925.97+204122.2	TYC 1327-257-1	06 19 25.96	+20 41 22.36	B9 IV–V Si	253	11.6463	0.0005	+0.760	0.046	−0.093	0.004	0.74	+0.31	0.14
552	J061951.56+283916.8	Gaia DR2 3433772034704740736	06 19 51.57	+28 39 16.95	B9 III–IV bl4130	120	14.6401	0.0010	+0.292	0.050	+0.062	0.008	0.55	+1.42	0.38
553	J062020.91+252606.8	HD 255238	06 20 20.92	+25 26 06.84	kB9.5hA1mA4 Si	173	10.6242	0.0010	+0.905	0.060	−0.163	0.006	0.46	−0.06	0.15
554	J062024.70+212536.0	Gaia DR2 3375964901637225728	06 20 24.71	+21 25 36.05	B9.5 IV Si	102	14.4288	0.0006	+0.299	0.033	+0.012	0.004	1.11	+0.70	0.24
555	J062031.37+300340.5	Gaia DR2 3437010199527628544	06 20 31.38	+30 03 40.52	B9.5 III–IV CrEu	142	14.2571	0.0012	+0.223	0.046	+0.017	0.01	0.77	+0.22	0.45
556	J062040.02+131611.9	HD 255467	06 20 40.02	+13 16 11.91	kB9hA9mA8 Si	726	9.9884	0.0006	+1.450	0.064	−0.174	0.003	0.31	+0.48	0.11
557	J062044.63+023859.6	Gaia DR2 3124629943825342464	06 20 44.64	+02 38 59.72	B8 III Si	105	12.4587	0.0003	+0.425	0.036	+0.114	0.004	1.05	−0.45	0.19
558	J062119.45+050555.7	TYC 140-743-1	06 21 19.46	+05 05 55.71	B6 IV Si	247	11.5244	0.0007	+0.700	0.052	−0.072	0.006	0.49	+0.26	0.17
559	J062136.92+181258.0	Gaia DR2 3370712190994249984	06 21 36.93	+18 12 58.10	B9 IV bl4130	111	14.7557	0.0011	+0.197	0.036	−0.249	0.006	1.79	−0.57	0.40
560	J062155.55+001812.2	HD 44456	06 21 55.42	+00 18 15.17	B8 III Si	128	8.4953	0.0014	+2.162	0.187	−0.158	0.008	0.41	−0.24	0.19
561	J062221.82+595613.0	TYC 3776-269-1	06 22 21.84	+59 56 13.02	<i>kA5hA7:mF2 SrCrEuSi</i> * <sup>d</sup>	343	10.4744	0.0004	+1.221	0.051	+0.313	0.001	0.19	+0.72	0.10
562	J062226.08+443003.8	TYC 2939-1176-1	06 22 26.39	+44 30 03.31	B8 IV Si	384	9.2839	0.0019	+1.835	0.073	−0.110	0.009	0.26	+0.35	0.10
563	J062248.54+144850.5	Gaia DR2 3368707433400422784	06 22 48.56	+14 48 50.48	B9 IV–V Cr	109	14.4736	0.0010	+0.365	0.031	+0.004	0.004	1.38	+0.91	0.19
564	J062257.61+231625.8	TYC 1878-882-1	06 22 57.62	+23 16 25.80	A1 IV–V SrCrEu	355	10.4559	0.0010	+1.351	0.062	+0.038	0.004	0.31	+0.80	0.11
565	J062307.91+264642.0	Gaia DR2 3432273606513132544	06 23 07.92	+26 46 42.04	B4 V <i>HeB7</i> *	127	14.1786	0.0009	+0.235	0.029	−0.108	0.005	0.58	+0.46	0.27
566	J062348.44+043007.6	Gaia DR2 3131479759532254720	06 23 48.45	+04 30 07.63	A8 V SrCrEu	105	11.9647	0.0003	+0.830	0.049	+0.170	0.002	0.70	+0.86	0.14
567	J062348.46+034201.1	HD 256582	06 23 48.53	+03 42 03.78	B5 V <i>HeB9</i> *	174	9.8823	0.0024	+1.416	0.046	+0.070	0.008	1.33	−0.69	0.09
568	J062407.76+264155.1	Gaia DR2 3432227461384464640	06 24 07.76	+26 41 55.20	B9 II–III ( <i>Mg 4481 wk</i> )* <sup>b</sup>	158	14.2335	0.0015	+0.128	0.033	−	−	−	−	−
569	J062427.61+213544.0	Gaia DR2 3376311041641501056	06 24 27.62	+21 35 44.07	A0 V Cr	134	14.5286	0.0005	+0.311	0.035	+0.163	0.003	0.80	+1.19	0.25
570	J062449.08+190854.0	Gaia DR2 3372372797150109184	06 24 49.09	+19 08 54.09	kA2hA3mA7 SrCrEu	142	12.6717	0.0008	+0.790	0.050	+0.340	0.003	0.51	+1.65	0.15
571	J062449.21+161325.7	Gaia DR2 3368971595367574016	06 24 49.21	+16 13 25.76	A0 V Cr	138	13.4502	0.0008	+0.283	0.032	+0.260	0.006	0.84	−0.13	0.25
572	J062451.14+152611.6	Gaia DR2 3368854978416307712	06 24 51.14	+15 26 11.77	B9 V CrEu	140	14.4909	0.0010	+0.280	0.034	−0.041	0.005	1.19	+0.54	0.27
573	J062511.12+160439.7	Gaia DR2 3368966334029514368	06 25 11.13	+16 04 39.83	B9.5 II ( <i>Si</i> ) ( <i>Mg 4481 wk</i> )*	112	14.6802	0.0006	+0.183	0.055	−	−	−	−	−
574	J062513.47+151050.2	Gaia DR2 3368834603091499520	06 25 13.49	+15 10 50.30	B9 V Cr	101	14.9111	0.0005	+0.260	0.032	−0.114	0.003	1.47	+0.51	0.27
575	J062529.19+160620.2	Gaia DR2 3368966166529044864	06 25 29.20	+16 06 20.32	kA2hA3mA5 SrCrEu	103	15.2312	0.0013	+0.286	0.067	+0.177	0.007	0.92	+1.59	0.51
576	J062529.84+032411.9	TYC 4789-2924-1	06 25 29.85	−03 24 11.99	B9 IV SrCrEuSi	123	12.1564	0.0007	+0.657	0.037	+0.095	0.004	0.41	+0.84	0.13
577	J062551.25+240212.8	Gaia DR2 3383424984952243712	06 25 51.26	+24 02 12.82	A5 IV–V SrCrEu	174	14.2458	0.0006	−0.032	0.050	−	−	−	−	−
578	J062614.15+164334.9	Gaia DR2 3369553099579973760	06 26 14.16	+16 43 34.93	B8 IV EuSi (He-wk)	170	14.2085	0.0004	+0.356	0.031	+0.144	0.004	0.64	+1.33	0.19
579	J062620.51+221542.7	Gaia DR2 3376407420706899712	06 26 20.52	+22 15 42.79	B9 IV bl4130	114	14.8829	0.0011	+0.133	0.063	−	−	−	−	−
580	J062630.83+171904.2	Gaia DR2 3369749151948057088	06 26 30.84	+17 19 04.35	B8 III–IV <sup>b</sup>	104	15.0172	0.0014	+0.146	0.046	−	−	−	−	−
581	J062638.98+233156.4	Gaia DR2 3377346055741625728	06 26 38.99	+23 31 56.49	B9.5 III <i>SiCrEu</i> *	175	14.4967	0.0004	+0.287	0.054	+0.074	0.003	0.86	+0.93	0.41
582	J062650.31+244510.6	HD 45148	06 26 50.33	+24 45 13.62	B9.5 IV Cr (He-wk)	772	9.2370	0.0010	+1.762	0.058	+0.005	0.004	0.21	+0.26	0.09
583	J062700.73+153645.9	Gaia DR2 3368872776760586880	06 27 00.74	+15 36 45.99	A0 II–III Si	119	14.5403	0.0013	+0.232	0.036	−0.109	0.006	1.33	+0.04	0.34
584	J062708.44+174403.3	Gaia DR2 3369777468670711936	06 27 08.45	+17 44 03.38	<i>B5 Vp HeB9</i> *	112	14.4438	0.0013	+0.168	0.031	+0.039	0.006	0.89	−0.31	0.40
585	J062710.47+260440.0	Gaia DR2 3431947665737506432	06 27 10.47	+26 04 40.06	kA1hA7mA3 CrEu	125	12.8741	0.0007	+0.401	0.036	+0.163	0.004	0.56	+0.33	0.20
586	J062715.76+174930.0	Gaia DR2 3369802340824496768	06 27 15.77	+17 49 30.08	B9.5 IV bl4130	111	14.9602	0.0005	+0.271	0.034	+0.050	0.004	0.80	+1.32	0.28
587	J062723.33+212713.3	HD 257383	06 27 23.25	+21 27 13.40	B9 V Sr	627	10.8046	0.0008	+1.063	0.038	−0.092	0.004	0.41	+0.53	0.09
588	J062753.43+360317.1	TYC 2434-1050-1	06 27 53.43	+36 03 17.17	A0 IV–V SrCr	301	11.5878	0.0008	+0.778	0.054	+0.009	0.006	0.40	+0.64	0.16
589	J062759.86+172007.8	Gaia DR2 3369705210141630848	06 27 59.87	+17 20 07.91	B9.5 III–IV Cr	115	14.8257	0.0005	+0.221	0.041	+0.119	0.005	1.14	+0.41	0.40
590	J062811.89+551959.8	Gaia DR2 997612807125070080	06 28 11.89	+55 19 59.94	B9.5 V Cr	32	12.7973	0.0004	+0.604	0.040	+0.029	0.004	0.23	+1.47	0.15
591	J062829.47+233423.0	Gaia DR2 3383342418501312384	06 28 29.48	+23 34 23.01	B9 V SrCr	101	15.1717	0.0010	+0.180	0.040	+0.056	0.007	0.76	+0.68	0.48
592	J062832.29+150924.2	Gaia DR2 3356789109612111360	06 28 32.30	+15 09 24.34	A3 V SrEu	109	14.3911	0.0009	+0.458	0.036	+0.221	0.005	0.75	+1.95	0.18
593	J062833.01+162806.1	Gaia DR2 3369363674342613632	06 28 33.01	+16 28 06.14	B9 IV–V Cr	141	14.5703	0.0007	+0.187	0.033	+0.029	0.004	0.73	+0.19	0.38
594	J062838.72+355224.3	Gaia DR2 942803599885897856	06 28 38.73	+35 52 24.36	B9.5 II–III EuSi	107	14.3985	0.0046	+0.165	0.048	−	−	−	−	−
595	J062842.31+162852.9	Gaia DR2 3369363914860764032	06 28 42.32	+16 28 53.00	B9.5 II–III EuSi	168	14.0127	0.0015	+0.260	0.028	+0.074	0.008	0.64	+0.44	0.24
596	J062909.51+023823.8	Gaia DR2 3124242606494984064	06 29 09.52	+02 38 23.87	B8 V <i>Si</i> * <sup>d</sup>	103	13.3277	0.0005	+0.492	0.031	−0.008	0.003	1.05	+0.74	0.14
597	J062914.34+004257.0	HD 291674	06 29 14.34	+00 42 57.04	B7 III–IV Si	516	9.7606	0.0021	+0.900	0.174	−0.220	0.005	0.74	−1.21	0.42
598	J062921.80+165315.3	Gaia DR2 3369474686357680256	06 29 21.81	+16 53 15.45	B9.5 II–III <i>Si</i> *	106	14.9111	0.0010	+0.136	0.058	−	−	−	−	−
599	J062951.75+151823.7	HD 258289	06 29 51.67	+15 18 23.65	B9 V SrCr	364	10.4909	0.0008	+1.079	0.073	+0.144	0.003	0.55	+0.11	0.15
600	J062951.85+285010.3	TYC 1891-1115-1	06 29 51.85	+28 50 10.34	A8 V SrCrEu	154	11.6738	0.0009	+0.908	0.050	+0.177	0.004	0.36	+1.10	0.13

**Table A.1.** Essential data for our sample stars, sorted by increasing right ascension. The columns denote: (1) Internal identification number. (2) LAMOST identifier. (3) Alternative identifier (HD number, TYC identifier or GAIA DR2 number). (4) Right ascension (J2000; GAIA DR2). (5) Declination (J2000; GAIA DR2). (6) Spectral type, as derived in this study. (7) Sloan  $g$  band S/N ratio of the analysed spectrum. (8)  $G$  mag (GAIA DR2). (9)  $G$  mag error. (10) Parallax (GAIA DR2). (11) Parallax error. (12) Dereddened colour index  $(BP - RP)_0$  (GAIA DR2). (13) Colour index error. (14) Absorption in the  $G$  band,  $A_G$ . (15) Intrinsic absolute magnitude in the  $G$  band,  $M_{G,0}$ . (16) Absolute magnitude error.

(1)	(2)	(3)	(4)	(5)	(6)	(7)	(8)	(9)	(10)	(11)	(12)	(13)	(14)	(15)	(16)
No.	ID_LAMOST	ID_alt	RA(J2000)	Dec(J2000)	SpT_final	S/N $_g$	$G$ mag	$e_G$ mag	$\pi$ (mas)	$e_\pi$	$(BP - RP)_0$	$e_{(BP - RP)_0}$	$A_G$	$M_{G,0}$	$e_{M_{G,0}}$
601	J063007.41+283333.3	TYC 1891-1405-1	06 30 07.42	+28 33 33.38	B9 IV-V bl4077 bl4130	172	11.5882	0.0009	+0.748	0.042	-0.060	0.007	0.34	+0.62	0.13
602	J063021.79+201821.4	TYC 1336-731-1	06 30 21.80	+20 18 21.47	A7 V SrCrEuSi	338	11.7963	0.0003	+0.812	0.042	+0.237	0.002	0.22	+1.12	0.12
603	J063033.69+014424.1	HD 288751	06 30 33.69	+01 44 24.14	B8 IV-V EuSi	245	10.9133	0.0011	+0.927	0.040	-0.076	0.004	0.90	-0.15	0.11
604	J063035.50+035245.3	TYC 154-966-1	06 30 35.66	+03 52 46.65	A1 IV-V SrCr	237	9.7386	0.0013	+1.207	0.121	-0.057	0.003	0.30	-0.15	0.22
605	J063037.14+234154.8	Gaia DR2 3382612239700477568	06 30 37.14	+23 41 54.88	B9 III-IV Cr	134	14.3692	0.0006	+0.103	0.041	-	-	-	-	-
606	J063114.46+184731.8	HD 258682	06 31 14.46	+18 47 31.87	kB9.5hA7mA8 SrCrEuSi	256	10.7497	0.0016	+0.698	0.045	+0.207	0.006	0.38	-0.41	0.15
607	J063115.49+235418.3	Gaia DR2 3382717964615683456	06 31 15.49	+23 54 18.31	A0 IV-V CrEu	145	14.2161	0.0006	+0.292	0.051	+0.057	0.004	0.41	+1.13	0.38
608	J063143.15+222551.2	TYC 1340-1953-1	06 31 43.25	+22 25 50.45	B9 IV-V Si	378	10.6750	0.0007	+0.558	0.097	+0.013	0.003	0.11	-0.70	0.38
609	J063201.93+185013.4	Gaia DR2 3371457591156975232	06 32 01.94	+18 50 13.44	B9 III-IV Si	105	13.4379	0.0005	+0.289	0.026	-0.030	0.003	0.50	+0.25	0.20
610	J063204.44+013000.1	HD 46203	06 32 04.44	+01 30 00.11	B9 V SiCrSr(Eu)*	430	9.8422	0.0007	+1.840	0.090	-0.069	0.003	0.37	+0.79	0.12
611	J063218.45+032146.3	HD 259273	06 32 18.45	+03 21 46.43	B9 III-IV Si (He-wk)	196	9.7120	0.0011	+1.479	0.088	-0.140	0.004	0.29	+0.27	0.14
612	J063232.70+155949.8	TYC 1329-606-1	06 32 32.71	+15 59 49.81	B9 IV bl4077 bl4130	341	11.5922	0.0007	+0.969	0.051	-0.011	0.004	0.64	+0.89	0.12
613	J063238.50+205939.7	HD 259117	06 32 38.50	+20 59 39.79	A0 IV-V SrCr	251	10.0636	0.0005	+0.829	0.036	+0.298	0.003	0.22	-0.57	0.11
614	J063256.06+370834.3	TYC 2434-33-1	06 32 56.07	+37 08 34.33	kB9.5hA2mA5 SrCr	216	11.4857	0.0011	+0.883	0.032	+0.081	0.005	0.29	+0.92	0.09
615	J063257.79+203008.2	Gaia DR2 3372764154568111744	06 32 57.79	+20 30 08.21	A0 IV-V SrCr	154	14.0661	0.0007	+0.191	0.050	-	-	-	-	-
616	J063343.72+582308.2	TYC 3777-1866-1	06 33 43.73	+58 23 08.22	B9.5 IV bl4130	232	11.9755	0.0007	+0.865	0.059	-0.079	0.004	0.11	+1.55	0.16
617	J063351.27+184418.9	TYC 1333-644-1	06 33 51.27	+18 44 18.89	B9 IV-V EuSi	322	9.7858	0.0008	+1.461	0.100	-0.222	0.003	0.34	+0.26	0.16
618	J063355.94+263943.7	HD 259452	06 33 55.95	+26 39 43.74	A0 V SrCrEu	172	9.3243	0.0011	+2.073	0.080	+0.046	0.006	0.19	+0.72	0.10
619	J063516.46+215714.9	TYC 1341-349-1	06 35 16.46	+21 57 15.02	B9 IV-V Eu	287	9.5388	0.0018	+1.243	0.082	-0.080	0.011	0.15	-0.14	0.15
620	J063522.08+335132.9 <sup>a</sup>	TYC 2430-1205-1	06 35 22.08	+33 51 32.79	A6 V SrEu	162	10.9600	0.0072	-	-	-	-	-	-	-
621	J063525.23-011456.2	HD 291918	06 35 25.24	-01 14 56.22	B9 V CrEu	141	11.0443	0.0010	+1.251	0.058	-0.006	0.004	0.42	+1.11	0.11
622	J063546.95+061914.9	Gaia DR2 3131961453001491584	06 35 46.95	+06 19 14.96	B9 IV bl4130	137	11.3376	0.0010	+0.595	0.039	+0.053	0.005	0.53	-0.32	0.15
623	J063627.06+014655.4	TYC 146-1299-1	06 36 27.06	+01 46 55.39	B9 V Cr	350	11.2774	0.0008	+1.304	0.186	+0.034	0.005	0.41	+1.44	0.31
624	J063640.63+315450.6	TYC 2439-607-1	06 36 40.63	+31 54 50.63	B9.5 III-IV SrCrEuSi	242	10.2499	0.0007	+0.243	0.080	-	-	-	-	-
625	J063711.23+220811.9	HD 260562	06 37 11.24	+22 08 11.94	kA0hA1mA3 CrEu	429	11.2945	0.0006	+0.741	0.039	+0.085	0.004	0.16	+0.49	0.13
626	J063739.78+241634.6	Gaia DR2 3383059191177247488	06 37 39.78	+24 16 34.59	A3 IV-V SrCrEu	215	14.2018	0.0012	+0.467	0.080	+0.191	0.01	0.21	+2.34	0.37
627	J063744.29+195655.1 <sup>a</sup>	TYC 1337-1539-1	06 37 44.07	+19 56 55.16	kA1hA7mF4 SrCrSi	811	9.1709	0.0004	+2.662	0.044	+0.128	0.002	0.12	+1.18	0.06
628	J063747.15+053115.8	HD 260964	06 37 47.16	+05 31 15.83	A0 II-III Eu	141	11.4906	0.0040	+0.820	0.041	+0.001	0.018	0.38	+0.68	0.12
629	J063748.65+160915.0	Gaia DR2 3358634738659193344	06 37 48.65	+16 09 14.98	A7 V SrCrEuSi	212	12.2557	0.0005	+0.959	0.048	+0.357	0.004	0.48	+1.69	0.12
630	J063752.90+091516.7	HD 260958	06 37 52.91	+09 15 16.75	B8 IV Si	185	10.0152	0.0008	+1.380	0.064	-0.397	0.004	0.62	+0.10	0.11
631	J063800.46+310256.5	TYC 2435-109-1	06 38 00.46	+31 02 56.49	B9.5 V SrCr	192	10.5260	0.0007	+0.995	0.068	+0.025	0.003	0.20	+0.32	0.16
632	J063814.60+274002.2	TYC 1888-847-1	06 38 14.61	+27 40 02.29	B9 IV Si	127	12.6032	0.0010	+0.403	0.043	-0.020	0.007	0.22	+0.41	0.24
633	J063840.72+203356.8	HD 261041	06 38 40.63	+20 33 56.81	A0 IV-V Cr	561	10.7763	0.0015	+1.295	0.153	+0.036	0.003	0.22	+1.12	0.26
634	J063844.48+172022.5	Gaia DR2 3359006648466147968	06 38 44.49	+17 20 22.59	B9 III-IV Si	162	12.9577	0.0012	+0.324	0.052	+0.021	0.005	0.70	-0.19	0.35
635	J063851.43+252003.8	TYC 1884-766-1	06 38 51.44	+25 20 03.89	B9 IV-V Sr	122	12.2508	0.0008	+0.541	0.085	-0.002	0.009	0.18	+0.74	0.34
636	J063853.85-002541.6	TYC 4799-1663-1	06 38 53.85	-00 25 41.64	B8 III-IV Si (He-wk)	214	11.6562	0.0004	+0.773	0.039	+0.015	0.003	0.73	+0.37	0.12
637	J063920.04+211735.5	Gaia DR2 3378859881392215424	06 39 20.04	+21 17 35.55	B9.5 V SrCr	121	13.1980	0.0009	+0.394	0.028	+0.146	0.005	0.25	+0.92	0.16
638	J063940.37+032443.2	HD 261594	06 39 40.50	+03 24 42.93	A2 IV-V SrCrEu	393	10.4761	0.0004	+1.249	0.044	+0.140	0.002	0.17	+0.79	0.09
639	J064012.77+082519.3	HD 261712	06 40 12.72	+08 25 19.19	B8 IV Si	252	10.6409	0.0014	+1.080	0.045	+0.037	0.006	0.66	+0.15	0.10
640	J064013.40+061645.0	HD 261715	06 40 13.41	+06 16 45.02	B8 IV-V Si (He-wk)	127	11.2513	0.0010	+0.821	0.038	-0.200	0.005	0.56	+0.26	0.11
641	J064039.28+264137.2	TYC 1888-159-1	06 40 39.28	+26 41 37.23	B9 IV Si	188	10.5715	0.0009	+0.760	0.048	-0.057	0.004	0.19	-0.22	0.14
642	J064112.55+240506.5 <sup>a</sup>	TYC 1880-251-1	06 41 12.69	+24 05 03.41	A0 III-IV CrEu	921	8.6497	0.0004	+1.632	0.405	-0.030	0.005	0.10	-0.38	0.54
643	J064158.41+223927.2	Gaia DR2 3379294635162916864	06 41 58.41	+22 39 27.25	A5 IV SrCrEu	111	13.5967	0.0005	+0.553	0.122	+0.371	0.004	0.30	+2.01	0.48
644	J064226.95-181244.1	Gaia DR2 3359462365976011648	06 42 26.95	-18 12 44.23	A2 IV-V SrCrEu	113	14.4136	0.0011	+0.328	0.034	+0.223	0.006	0.39	+1.60	0.23
645	J064233.27+032500.7	Gaia DR2 3127497500212384512	06 42 33.27	+03 25 00.75	B8 III-IV Si	154	12.2114	0.0003	+0.606	0.065	+0.051	0.003	1.30	-0.17	0.24
646	J064257.32+521951.3	TYC 3389-862-1	06 42 57.33	+52 19 51.34	kA4hA6mF2 SrCrEu	213	10.6500	0.0005	+1.194	0.038	+0.200	0.002	0.11	+0.92	0.08
647	J064259.18+270608.9	HD 48119	06 42 59.19	+27 06 08.97	B8 IV Si	486	9.5911	0.0014	+0.974	0.090	-0.158	0.002	0.11	-0.58	0.21
648	J064310.76+484123.3	TYC 3381-73-1	06 43 10.78	+48 41 23.27	B9 V CrSi (He-wk)	104	11.5991	0.0004	+0.453	0.080	+0.167	0.004	0.16	-0.28	0.38
649	J064351.19+233534.8	TYC 1893-186-1	06 43 51.19	+23 35 34.79	B9.5 III-IV Si	165	11.2900	0.0010	+0.384	0.328	-	-	-	-	-
650	J064358.45+033447.0	Gaia DR2 3127517738096930432	06 43 58.46	+03 34 47.06	B8 IV-V Si	126	12.7791	0.0009	+0.513	0.036	-0.003	0.005	0.67	+0.66	0.16

**Table A.1.** Essential data for our sample stars, sorted by increasing right ascension. The columns denote: (1) Internal identification number. (2) LAMOST identifier. (3) Alternative identifier (HD number, TYC identifier or GAIA DR2 number). (4) Right ascension (J2000; GAIA DR2). (5) Declination (J2000; GAIA DR2). (6) Spectral type, as derived in this study. (7) Sloan  $g$  band S/N ratio of the analysed spectrum. (8)  $G$  mag (GAIA DR2). (9)  $G$  mag error. (10) Parallax (GAIA DR2). (11) Parallax error. (12) Dereddened colour index  $(BP - RP)_0$  (GAIA DR2). (13) Colour index error. (14) Absorption in the  $G$  band,  $A_G$ . (15) Intrinsic absolute magnitude in the  $G$  band,  $M_{G,0}$ . (16) Absolute magnitude error.

(1)	(2)	(3)	(4)	(5)	(6)	(7)	(8)	(9)	(10)	(11)	(12)	(13)	(14)	(15)	(16)
No.	ID_LAMOST	ID_alt	RA(J2000)	Dec(J2000)	SpT_final	S/N $_g$	$G$ mag	$e_G$ mag	$\pi$ (mas)	$e_\pi$	$(BP - RP)_0$	$e_((BP - RP)_0)$	$A_G$	$M_{G,0}$	$e_{M_{G,0}}$
651	J064438.75+315333.6	Gaia DR2 937202240976723072	06 44 38.75	+31 53 33.76	A1 V SrCrEuSi	141	12.4186	0.0010	+0.619	0.051	+0.143	0.005	0.21	+1.17	0.18
652	J064441.84+213750.5	Gaia DR2 3378235530585937280	06 44 41.85	+21 37 50.54	A0 II EuSi	132	13.9601	0.0020	+0.202	0.043	-0.088	0.01	0.46	+0.03	0.46
653	J064452.82+055428.4	TYC 159-3043-1	06 44 52.83	+05 54 28.73	B8 IV-V Si	129	11.2374	0.0011	+0.749	0.107	-0.094	0.006	0.74	-0.13	0.31
654	J064505.60+122253.2	Gaia DR2 3352393605721639424	06 45 05.61	+12 22 53.30	A0 IV-V SrCrEu	167	14.0446	0.0010	+0.354	0.048	+0.152	0.012	0.51	+1.28	0.30
655	J064510.75+134157.8	Gaia DR2 3352818979283285504	06 45 10.76	+13 41 57.85	B9 III Si	107	13.4362	0.0005	+0.270	0.032	+0.017	0.003	0.42	+0.17	0.26
656	J064511.33+035210.9	TYC 156-1661-1	06 45 11.34	+03 52 10.93	A3 IV-V SrCr	157	10.3271	0.0006	+1.176	0.047	+0.128	0.002	0.14	+0.54	0.10
657	J064514.05+371344.9	TYC 2448-182-1	06 45 14.06	+37 13 44.93	B9 V Cr	364	10.0004	0.0006	+1.596	0.039	-0.014	0.003	0.23	+0.79	0.07
658	J064524.45-020257.8	HD 292348	06 45 24.46	-02 02 57.87	B9 II-III Si	106	14.3338	0.0011	+0.336	0.040	-0.104	0.007	1.63	+0.33	0.26
659	J064529.41+072552.2	TYC 160-109-1	06 45 29.42	+07 25 52.30	B8 IV Si	211	11.3481	0.0016	+0.883	0.081	+0.035	0.007	0.69	+0.39	0.20
660	J064534.06+234628.3	HD 263149	06 45 34.07	+23 46 28.33	A1 IV SrCrEu	238	11.4281	0.0015	+0.835	0.050	+0.066	0.009	0.17	+0.86	0.14
661	J064540.13+112441.7	TYC 754-688-1	06 45 40.14	+11 24 41.80	B9 III Si	202	12.4162	0.0012	+0.437	0.040	+0.093	0.007	0.82	-0.20	0.20
662	J064545.94+133602.0	HD 48806	06 45 46.04	+13 36 04.80	B9 IV-V bl4130	315	9.2788	0.0010	+1.375	0.081	-0.157	0.004	0.29	-0.32	0.14
663	J064549.02+484330.2	TYC 3394-359-1	06 45 49.02	+48 43 30.22	B8 IV-V bl4130	157	12.0159	0.0005	+0.460	0.046	-0.038	0.004	0.24	+0.09	0.22
664	J064559.17+213252.6	HD 263301	06 45 59.18	+21 32 52.66	B8 III Si	391	10.4364	0.0009	+0.531	0.054	-0.192	0.004	0.23	-1.16	0.23
665	J064601.44+221654.4	Gaia DR2 3379399634225338112	06 46 01.45	+22 16 54.42	A0 IV CrEu	107	14.2917	0.0004	+0.326	0.033	+0.289	0.002	0.58	+1.28	0.22
666	J064614.76+072231.1	Gaia DR2 3133202419371320832	06 46 14.77	+07 22 31.28	B8 IV Si	151	11.9800	0.0008	+0.619	0.053	-0.152	0.005	0.83	+0.11	0.19
667	J064616.91+131936.6	Gaia DR2 3352605777105469696	06 46 16.92	+13 19 36.70	A0 III CrEu*	100	14.5164	0.0005	+0.189	0.067	-	-	-	-	-
668	J064617.26+082858.8	HD 263556	06 46 17.26	+08 28 58.91	B9 II-III bl4077 bl4130	153	11.5982	0.0022	+0.894	0.049	+0.018	0.009	0.82	+0.54	0.13
669	J064628.76+150619.4	HD 263549	06 46 28.76	+15 06 19.50	B9 III-IV Si	267	9.7127	0.0005	+1.003	0.088	-0.195	0.003	0.31	-0.59	0.20
670	J064633.16+020802.9	Gaia DR2 3126413484825266560	06 46 33.16	+02 08 02.95	B9 IV-V bl4130	110	12.9308	0.0043	+0.393	0.109	-	-	-	-	-
671	J064637.59+051616.2	TYC 156-871-1	06 46 37.59	+05 16 16.21	B8 IV bl4130	110	12.9161	0.0004	+0.796	0.040	+0.075	0.003	0.51	+1.91	0.12
672	J064641.00+005717.1	Gaia DR2 3125709934822430720	06 46 41.00	+00 57 17.14	B8 IV Si	101	12.8960	0.0007	+0.461	0.036	-0.034	0.005	1.19	+0.02	0.18
673	J064701.81+102355.5	Gaia DR2 3350836834693773312	06 47 01.82	+10 23 55.53	B8 III-IV bl4130	106	12.7947	0.0004	+0.505	0.040	+0.026	0.004	0.42	+0.89	0.18
674	J064719.79+013513.6	TYC 148-641-1	06 47 19.79	+01 35 13.71	A0 II-III EuSi	143	12.6268	0.0010	+0.533	0.039	+0.040	0.006	0.73	+0.53	0.17
675	J064741.02+072458.8	TYC 160-321-1	06 47 41.04	+07 24 58.84	B9 III-IV Si	150	11.2725	0.0020	+0.575	0.036	+0.001	0.009	0.83	-0.77	0.15
676	J064745.41+583506.1	HD 48560	06 47 45.40	+58 35 06.25	kA1hA2mA5 CrEu	614	9.6569	0.0008	+3.559	0.294	+0.100	0.002	0.10	+2.31	0.19
677	J064748.51+160757.8	HD 263921	06 47 48.51	+16 07 57.83	B9 IV-V Sr	201	10.3096	0.0036	-4.029	0.497	-	-	-	-	-
678	J064757.48+105648.2	Gaia DR2 3350927819280584448	06 47 57.50	+10 56 48.31	kB9.5hA1mA2 Cr	159	15.7093	0.0009	+2.669	0.050	+1.721	0.007	0.09	+7.75	0.06
679	J064758.50+283022.6	TYC 1905-1123-1	06 47 58.50	+28 30 22.64	B9 V Cr	615	10.4109	0.0009	+1.137	0.055	-0.037	0.003	0.11	+0.58	0.12
680	J064758.79+105621.5	Gaia DR2 3350927784920847872	06 47 58.80	+10 56 21.61	kA0hA1mA2 bl4077 bl4130	132	12.8648	0.0007	+0.516	0.032	+0.235	0.003	0.53	+0.90	0.15
681	J064826.33+203755.5	TYC 1343-2249-1	06 48 26.33	+20 37 55.60	B9 IV-V bl4130	376	11.4274	0.0005	+0.764	0.063	-0.067	0.005	0.13	+0.71	0.19
682	J064838.53+025528.9	Gaia DR2 3126572299835661568	06 48 38.53	+02 55 28.98	B8 IV bl4130	118	12.8083	0.0012	+0.460	0.053	+0.073	0.007	0.69	+0.43	0.26
683	J064843.13+115633.2	Gaia DR2 3351576084465603072	06 48 43.13	+11 56 33.21	A0 IV-V SrCrEuSi	203	12.2557	0.0005	+0.857	0.048	+0.217	0.005	0.23	+1.69	0.13
684	J064844.97+131201.4	HD 264269	06 48 44.98	+13 12 01.46	B8 IV-V Si	272	11.5207	0.0007	+0.687	0.043	-0.016	0.005	0.31	+0.40	0.14
685	J064851.39+211245.6	TYC 1343-2670-1	06 48 51.39	+21 12 45.65	B7 III-IV bl4130 (He-wk)	212	11.8405	0.0011	+0.548	0.050	-0.138	0.008	0.10	+0.44	0.20
686	J064853.79+203905.3	Gaia DR2 3377882205098370304	06 48 53.79	+20 39 05.28	kB9.5hA2mA5 SrCrEu	143	13.1255	0.0011	+0.374	0.049	+0.143	0.004	0.09	+0.90	0.29
687	J064859.90+381609.0	HD 49198	06 49 00.10	+38 16 11.27	A0 III-IV CrSi	344	9.2945	0.0010	+2.106	0.077	-0.004	0.005	0.19	+0.72	0.09
688	J064901.28+034633.2	TYC 156-582-1	06 49 01.29	+03 46 33.27	B9 V Cr	114	12.4737	0.0003	+0.600	0.036	-0.020	0.003	0.71	+0.66	0.14
689	J064907.51+114600.1	Gaia DR2 3351558114322467968	06 49 07.52	+11 46 00.17	kA1hA7mA8 SrCr	134	13.5457	0.0022	-1.385	0.314	-	-	-	-	-
690	J064947.96+202510.4	TYC 1339-558-1	06 49 47.97	+20 25 10.82	kA3hA5mA7 bl4077 bl4130	330	9.9263	0.0005	+1.510	0.049	+0.344	0.002	0.04	+0.78	0.09
691	J064959.12+125329.4	TYC 755-771-1	06 49 59.13	+12 53 29.38	A0 IV-V CrSi (He-wk)	292	9.9404	0.0006	+1.715	0.069	-0.109	0.002	0.18	+0.94	0.10
692	J065000.25+293255.8	HD 49522	06 50 00.02	+29 32 57.67	A0 V CrEuSi	142	8.8861	0.0008	+2.934	0.084	-0.026	0.003	0.07	+1.16	0.08
693	J065021.64+433020.7	TYC 2954-959-1	06 50 21.64	+43 30 20.76	B9.5 IV Cr	304	10.7962	0.0006	+0.704	0.064	+0.119	0.003	0.23	-0.19	0.20
694	J065047.40+183257.1	TYC 1335-1780-1	06 50 47.40	+18 32 57.17	B9 III-IV Si	414	11.1338	0.0008	+0.825	0.059	-0.105	0.008	0.08	+0.63	0.16
695	J065119.09+102848.9	Gaia DR2 3158687866251327872	06 51 19.09	+10 28 49.03	B9.5 V CrEu	102	14.1592	0.0006	+0.335	0.036	+0.153	0.005	0.34	+1.44	0.24
696	J065134.66+343547.3	Gaia DR2 940138761657217536	06 51 34.66	+34 35 47.41	B9.5 II-III bl4130	235	14.0506	0.0006	+0.192	0.050	-	-	-	-	-
697	J065135.29+205612.8	HD 265031	06 51 35.12	+20 56 13.26	kB9.5hA2mA5 CrEu	543	9.8695	0.0007	+1.745	0.065	-0.019	0.002	0.14	+0.94	0.10
698	J065141.48+102538.0	TYC 751-2305-1	06 51 41.49	+10 25 38.07	B9 V Cr	276	11.7306	0.0006	+0.597	0.049	+0.079	0.004	0.20	+0.41	0.18
699	J065154.51+104428.0	Gaia DR2 3159071973767160704	06 51 54.52	+10 44 28.07	B9 IV-V bl4130	100	13.4866	0.0009	+0.426	0.047	+0.061	0.008	0.13	+1.51	0.24
700	J065200.81+121952.8	TYC 755-1591-1	06 52 00.82	+12 19 52.80	A0 IV CrEu	312	10.6482	0.0005	+1.385	0.068	+0.101	0.003	0.12	+1.24	0.12



**Table A.1.** Essential data for our sample stars, sorted by increasing right ascension. The columns denote: (1) Internal identification number. (2) LAMOST identifier. (3) Alternativ identifier (HD number, TYC identifier or GAIA DR2 number). (4) Right ascension (J2000; GAIA DR2). (5) Declination (J2000; GAIA DR2). (6) Spectral type, as derived in this study. (7) Sloan *g* band S/N ratio of the analysed spectrum. (8) *G* mag (GAIA DR2). (9) *G* mag error. (10) Parallax (GAIA DR2). (11) Parallax error. (12) Dereddened colour index  $(BP - RP)_0$  (GAIA DR2). (13) Colour index error. (14) Absorption in the *G* band,  $A_G$ . (15) Intrinsic absolute magnitude in the *G* band,  $M_{G,0}$ . (16) Absolute magnitude error.

(1)	(2)	(3)	(4)	(5)	(6)	(7)	(8)	(9)	(10)	(11)	(12)	(13)	(14)	(15)	(16)
No.	ID_LAMOST	ID_alt	RA(J2000)	Dec(J2000)	SpT_final	S/N <sub>g</sub>	<i>G</i> mag	<i>e_G</i> mag	pi (mas)	<i>e_pi</i>	$(BP - RP)_0$	$e_{(BP - RP)_0}$	$A_G$	$M_{G,0}$	$e_{M_{G,0}}$
701	J065205.09+065214.6	Gaia DR2 3132980592900051200	06 52 05.10	+06 52 14.67	B9 V Cr	123	12.5078	0.0004	+0.418	0.049	+0.077	0.004	0.30	+0.32	0.26
702	J065209.98+102634.8	Gaia DR2 3158640655970656256	06 52 09.98	+10 26 34.93	kA1hA8mA8 SrEuSi	141	14.1261	0.0014	+0.300	0.037	+0.075	0.008	0.23	+1.28	0.27
703	J065216.71+205412.6	Gaia DR2 3366259508199396864	06 52 16.71	+20 54 12.63	kA0hA5mA6 CrSi	125	13.2474	0.0005	+0.375	0.033	+0.052	0.004	0.15	+0.97	0.20
704	J065226.21+024001.8	HD 289244	06 52 26.22	+02 40 01.90	kB9.5hA3mA3 CrEu	322	11.2022	0.0010	+0.926	0.035	-0.058	0.004	0.44	+0.60	0.10
705	J065235.59+423715.7	HD 49884	06 52 35.20	+42 37 10.07	B9.5 III Eu	198	8.2392	0.0010	+2.741	0.066	-0.010	0.003	0.13	+0.29	0.07
706	J065302.61+403553.6	TYC 2946-305-1	06 53 02.61	+40 35 53.63	A5 IV-V SrEu	172	11.9586	0.0003	+1.045	0.041	+0.253	0.003	0.17	+1.88	0.10
707	J065310.66+071446.8	TYC 161-1956-1	06 53 10.67	+07 14 46.86	kB9hA1mA2 CrEuSi	161	12.2648	0.0023	+0.315	0.041	+0.110	0.018	0.38	-0.63	0.29
708	J065313.89+103303.3	Gaia DR2 3159021155714729472	06 53 13.90	+10 33 03.39	kA0hA2mA5 Eu	119	13.5618	0.0024	+0.328	0.044	+0.023	0.011	0.21	+0.93	0.29
709	J065318.97+131319.7	Gaia DR2 3353293349829167744	06 53 18.98	+13 13 19.81	kA0hA3mA6 Cr	123	14.4544	0.0006	+0.155	0.048	-	-	-	-	-
710	J065340.20+562055.0	TYC 3775-178-1	06 53 40.19	+56 20 55.05	B9 IV-V Cr	159	12.8888	0.0004	+0.358	0.046	-0.012	0.002	0.12	+0.54	0.29
711	J065356.37+103302.0	Gaia DR2 3159010156299346048	06 53 56.38	+10 33 02.06	kB9.5hA1mA3 CrEu	147	13.1461	0.0018	+0.385	0.033	+0.176	0.009	0.24	+0.83	0.19
712	J065358.16+141845.0	TYC 760-381-1	06 53 58.17	+14 18 45.01	B9.5 IV-V SrCrEu	211	10.8393	0.0007	+1.168	0.046	+0.020	0.004	0.08	+1.09	0.10
713	J065400.61+063645.2	Gaia DR2 3129955905132736768	06 54 00.62	+06 36 45.16	A0 IV-V SrCrEu	153	12.2854	0.0006	+0.856	0.063	+0.147	0.004	0.26	+1.69	0.17
714	J065401.04+213810.3	TYC 1343-673-1	06 54 01.04	+21 38 10.40	kA1hA3mA7 CrEu	229	12.1451	0.0004	+0.565	0.044	+0.199	0.003	0.09	+0.81	0.18
715	J065403.63+221545.2	HD 50403	06 54 03.63	+22 15 45.16	A6 IV SrCrEu	386	9.2694	0.0007	+3.141	0.045	+0.181	0.005	0.05	+1.71	0.06
716	J065404.66+113512.6	HD 265946	06 54 04.60	+11 35 09.65	A0 V Cr	638	9.4015	0.0003	+1.797	0.061	-0.021	0.002	0.12	+0.56	0.09
717	J065414.93+083325.5	TYC 748-1845-1	06 54 14.98	+08 33 23.77	B9.5 II-III Si	271	10.4132	0.0012	+0.920	0.039	-0.045	0.005	0.13	+0.10	0.10
718	J065419.05+053003.4	Gaia DR2 3129541049951592576	06 54 19.06	+05 30 03.45	B9 IV-V SrCr	108	12.6897	0.0003	+1.515	0.320	+0.297	0.003	0.14	+3.45	0.46
719	J065444.54+202931.2	Gaia DR2 3366195672104620544	06 54 44.55	+20 29 31.27	B9 V CrEu	117	13.5516	0.0007	+0.256	0.042	+0.077	0.005	0.19	+0.41	0.36
720	J065444.94+135455.5	HD 266119	06 54 44.95	+13 54 55.56	A1 IV-V Cr	177	10.6473	0.0006	+0.943	0.033	+0.133	0.001	0.16	+0.36	0.09
721	J065458.31+040826.9 <sup>d</sup>	HD 266311	06 54 58.17	+04 08 27.55	kA1hA3mA6 SrCrEu	488	9.7499	0.0006	+1.985	0.049	-0.022	0.003	0.19	+1.04	0.07
722	J065505.83+384426.4	TYC 2942-279-1	06 55 05.83	+38 44 26.49	B8 IV bl130	177	12.1167	0.0007	+0.374	0.065	+0.005	0.005	0.14	-0.16	0.38
723	J065509.34+044322.6	TYC 157-2479-1	06 55 09.35	+04 43 22.67	B8 III Si	165	12.3571	0.0005	+0.404	0.046	+0.086	0.003	0.91	-0.52	0.25
724	J065511.76+115158.3	HD 266267	06 55 11.66	+11 51 56.24	A7 V SrCrEu* <sup>d</sup>	566	10.0083	0.0007	+2.020	0.049	+0.044	0.004	0.15	+1.38	0.07
725	J065518.21+022530.3	Gaia DR2 3126252028414767360	06 55 18.21	+02 25 30.24	B9 II-III Si	195	12.3149	0.0014	+0.363	0.069	-0.041	0.026	1.11	-1.00	0.42
726	J065520.87+120622.7	Gaia DR2 3351433903867696640	06 55 20.88	+12 06 22.71	A5 IV-V SrCrEu	115	12.2659	0.0005	+0.828	0.039	+0.175	0.008	0.43	+1.43	0.11
727	J065544.52+563703.5	HD 50243	06 55 44.53	+56 37 03.52	B9.5 IV-V Cr	592	9.4571	0.0004	+1.766	0.054	-0.008	0.004	0.09	+0.61	0.08
728	J065623.57+281013.1	TYC 1906-481-1	06 56 23.57	+28 10 13.15	A9 V SrEu	196	11.3235	0.0005	+1.313	0.049	+0.378	0.003	0.10	+1.81	0.09
729	J065627.80+031055.9	TYC 153-2297-1	06 56 27.82	+03 10 55.95	B9 III (Cr)*	413	11.1237	0.0060	+1.221	0.334	-	-	-	-	-
730	J065629.15+074030.5	TYC 748-2642-1	06 56 29.15	+07 40 30.49	A1 IV-V CrEu	241	10.4546	0.0006	+1.068	0.062	+0.058	0.001	0.11	+0.49	0.14
731	J065629.87+200101.8	TYC 1352-411-1	06 56 29.86	+20 01 01.81	B8 III-IV Si	420	11.5211	0.0009	+0.586	0.061	-0.101	0.006	0.06	+0.30	0.23
732	J065647.94+242958.8	HD 266617	06 56 47.78	+24 29 58.86	A0 V SiSrCr* <sup>d</sup>	383	10.1910	0.0011	+1.584	0.118	+0.021	0.003	0.06	+1.13	0.17
733	J065649.21+541717.5	TYC 3767-219-1	06 56 49.21	+54 17 17.52	A0 V CrEu	297	11.9272	0.0003	+0.950	0.038	+0.142	0.002	0.07	+1.75	0.10
734	J065707.80+030838.9	TYC 153-2323-1	06 57 07.81	+03 08 38.93	B9.5 IV Eu	274	11.4200	0.0013	+0.683	0.040	+0.081	0.006	0.63	-0.04	0.14
735	J065714.71+073908.9	Gaia DR2 3157064639192846720	06 57 14.71	+07 39 08.95	B9.5 IV EuSi	122	12.1459	0.0005	+0.461	0.040	+0.022	0.003	0.20	+0.27	0.19
736	J065800.69+482950.3	HD 50972	06 58 00.79	+48 29 46.52	B9 V SrCr	468	8.0500	0.0006	+4.334	0.083	+0.001	0.002	0.06	+1.17	0.06
737	J065815.39+021919.6	Gaia DR2 3115727022077258112	06 58 15.40	+02 19 19.63	A5 IV-V SrCrEu	263	11.2521	0.0009	+1.325	0.048	+0.179	0.003	0.22	+1.64	0.09
738	J065826.55+123932.0	TYC 756-1181-1	06 58 26.56	+12 39 32.08	B9 IV bl4077 bl4130	363	10.8823	0.0011	+0.624	0.042	-0.022	0.005	0.11	-0.25	0.15
739	J065834.63+282752.9	Gaia DR2 887381960372791296	06 58 34.63	+28 27 52.88	A0 IV Cr	110	14.1264	0.0007	+0.233	0.031	+0.243	0.004	0.11	+0.86	0.29
740	J065846.62+305342.0	TYC 2437-446-1	06 58 46.65	+30 53 41.09	B8 IV SiCr (He-wk)*	368	10.7901	0.0007	+0.773	0.059	-0.128	0.006	0.17	+0.07	0.17
741	J065847.10+005843.6	TYC 149-2573-1	06 58 47.11	+00 58 43.69	A0 III-IV SrCrEuSi	194	11.7281	0.0007	+0.869	0.039	+0.013	0.004	0.42	+1.00	0.11
742	J065941.01+143418.8	TYC 760-1081-1	06 59 41.00	+14 34 18.83	B9 IV EuSi	174	11.7104	0.0013	+0.577	0.067	-0.046	0.007	0.12	+0.40	0.26
743	J070004.95-010025.7	HD 292968	07 00 04.96	-01 00 25.77	B9 V Cr	205	10.9741	0.0007	+0.819	0.063	-0.042	0.004	0.28	+0.26	0.17
744	J070127.57+142617.6	TYC 761-1749-1	07 01 27.58	+14 26 17.70	B8 III-IV EuSi	192	11.4818	0.0006	+0.675	0.073	-0.047	0.007	0.06	+0.57	0.24
745	J070132.95+033625.8	TYC 166-2723-1	07 01 32.95	+03 36 25.82	B9 IV-V Si	243	11.4821	0.0010	+0.933	0.042	+0.028	0.004	0.43	+0.90	0.11
746	J070133.22+061017.5	TYC 174-2230-1	07 01 33.23	+06 10 17.43	B9 IV bl4130	167	11.2555	0.0011	+0.455	0.047	+0.133	0.004	0.36	-0.81	0.23
747	J070144.69-013353.6	TYC 4814-2326-1	07 01 44.70	-01 33 53.59	B9.5 IV-V SrCrEu	162	12.2465	0.0010	+0.402	0.043	+0.129	0.006	0.36	-0.09	0.24
748	J070155.26+010932.0	Gaia DR2 3113112903122735744	07 01 55.27	+01 09 32.08	B9 V Cr	124	12.8682	0.0003	+0.305	0.041	+0.151	0.002	0.58	-0.29	0.29
749	J070200.78+161738.2	HD 52475	07 02 00.78	+16 17 38.36	B8 IV-V Si	288	10.7487	0.0013	+0.757	0.063	-0.171	0.007	0.07	+0.07	0.19
750	J070211.70+202807.9	TYC 1352-1191-1	07 02 11.73	+20 28 08.91	B9.5 V SrCrEu	380	10.8125	0.0005	+0.976	0.060	+0.037	0.002	0.05	+0.71	0.14

**Table A.1.** Essential data for our sample stars, sorted by increasing right ascension. The columns denote: (1) Internal identification number. (2) LAMOST identifier. (3) Alternative identifier (HD number, TYC identifier or GAIA DR2 number). (4) Right ascension (J2000; GAIA DR2). (5) Declination (J2000; GAIA DR2). (6) Spectral type, as derived in this study. (7) Sloan  $g$  band S/N ratio of the analysed spectrum. (8)  $G$  mag (GAIA DR2). (9)  $G$  mag error. (10) Parallax (GAIA DR2). (11) Parallax error. (12) Dereddened colour index  $(BP - RP)_0$  (GAIA DR2). (13) Colour index error. (14) Absorption in the  $G$  band,  $A_G$ . (15) Intrinsic absolute magnitude in the  $G$  band,  $M_{G,0}$ . (16) Absolute magnitude error.

(1)	(2)	(3)	(4)	(5)	(6)	(7)	(8)	(9)	(10)	(11)	(12)	(13)	(14)	(15)	(16)
No.	ID_LAMOST	ID_alt	RA(J2000)	Dec(J2000)	SpT_final	S/N $_g$	$G$ mag	$e_G$ mag	$\pi$ (mas)	$e_\pi$	$(BP - RP)_0$	$e_{(BP - RP)_0}$	$A_G$	$M_{G,0}$	$e_{M_{G,0}}$
751	J070234.35+152247.8	Gaia DR2 3354031500087825792	07 02 34.36	+15 22 47.89	A8 IV-V Eu	104	12.3900	0.0004	+0.619	0.054	+0.420	0.002	0.09	+1.26	0.20
752	J070237.06+362235.1	Gaia DR2 940040321006131200	07 02 37.07	+36 22 35.22	A7 V SrEu	109	13.1453	0.0005	+0.560	0.030	+0.267	0.003	0.15	+1.74	0.13
753	J070252.77+023700.0	HD 52868	07 02 52.76	+02 36 57.25	kB9hA9mA7 SrSi	524	9.4417	0.0005	+1.504	0.085	-0.071	0.004	0.12	+0.21	0.13
754	J070305.59-020902.4	TYC 4818-265-1	07 03 05.59	-02 09 02.48	B8 II-III CrSi	131	12.3575	0.0010	+0.385	0.041	+0.037	0.005	0.48	-0.19	0.24
755	J070337.20+064533.5	TYC 174-29-1	07 03 37.24	+06 45 33.64	B8 III-IV Si	135	10.9012	0.0007	+1.115	0.059	-0.075	0.005	0.16	+0.98	0.12
756	J070337.25+194115.0	TYC 1352-451-1	07 03 37.25	+19 41 15.02	kA0hA3mA6 Cr	164	12.8146	0.0010	+0.466	0.042	+0.195	0.005	0.08	+1.07	0.20
757	J070343.61+140646.3	HD 52959	07 03 43.61	+14 06 46.33	B8 III-IV bl4130 (He-wk)	316	10.1297	0.0008	+0.636	0.060	+0.174	0.002	0.08	-0.93	0.21
758	J070344.63+183406.1	Gaia DR2 3361785015568548608	07 03 44.63	+18 34 06.17	A9 V SrCrEu	134	13.2150	0.0005	+0.510	0.041	+0.253	0.004	0.05	+1.70	0.18
759	J070439.49+181036.7	TYC 1349-141-1	07 04 39.30	+18 10 36.75	B9 IV-V CrEuSi	186	9.9132	0.0008	+1.628	0.083	-0.054	0.004	0.04	+0.93	0.12
760	J070519.30+350140.9	Gaia DR2 891667783681590656	07 05 19.30	+35 01 41.03	B9 IV-V Cr	126	12.9313	0.0008	+0.356	0.052	-0.078	0.004	0.13	+0.56	0.32
761	J070604.68+145303.0	Gaia DR2 3359757408749990016	07 06 04.69	+14 53 03.08	kA5hA5mA9 SrCrEu	121	14.1791	0.0007	+0.270	0.045	+0.240	0.003	0.08	+1.25	0.36
762	J070613.94+185355.6	Gaia DR2 3361893764140100096	07 06 13.94	+18 53 55.60	B9.5 II-III Si	63	14.9322	0.0030	+0.146	0.047	-	-	-	-	-
763	J070617.23+101601.6	HD 53662	07 06 17.01	+10 16 01.62	B9 IV EuSi	433	8.6716	0.0008	+2.050	0.060	-0.076	0.006	0.03	+0.20	0.08
764	J070709.06+225559.9	TYC 1896-1380-1	07 07 09.07	+22 55 59.91	B9 IV-V CrEu	457	10.5471	0.0013	+0.847	0.044	+0.026	0.006	0.05	+0.14	0.12
765	J070738.03+231201.8	TYC 1896-1388-1	07 07 38.03	+23 12 01.76	A0 V SrCrEu	775	9.2462	0.0007	+1.894	0.055	+0.101	0.002	0.05	+0.58	0.08
766	J070755.64-001724.5	HD 293193	07 07 55.64	-00 17 24.57	B9 IV-V Cr	237	11.4148	0.0006	+0.619	0.045	+0.121	0.004	0.40	-0.02	0.16
767	J070801.31+301921.1	TYC 2438-214-1	07 08 01.31	+30 19 21.16	A0 IV CrEu	125	11.6315	0.0012	+1.136	0.064	+0.229	0.008	0.17	+1.74	0.13
768	J070832.40+034245.5	TYC 167-2919-1	07 08 32.24	+03 42 45.33	B8 III-IV Si	128	10.0628	0.0009	+0.977	0.068	-0.224	0.003	0.27	-0.25	0.16
769	J070837.00+164450.5	Gaia DR2 3360604552396348800	07 08 37.01	+16 44 50.53	B9.5 V Eu	145	14.1492	0.0008	+0.334	0.049	+0.061	0.005	0.36	+1.41	0.32
770	J070907.08+441114.7	Gaia DR2 953130071357647360	07 09 07.09	+44 11 14.80	B9.5 V CrEu	124	13.9893	0.0007	+0.510	0.029	+0.196	0.005	0.20	+2.32	0.13
771	J071043.39+095402.9	TYC 766-268-1	07 10 43.40	+09 54 02.97	A0 V SrCrEu	166	11.2727	0.0011	+1.297	0.043	+0.111	0.005	0.07	+1.77	0.09
772	J071113.33+055418.0	TYC 175-4347-1	07 11 13.34	+05 54 18.04	B9 IV Eu	332	11.5305	0.0008	+0.426	0.048	+0.005	0.005	0.12	-0.44	0.25
773	J071258.59+065952.3	Gaia DR2 3153216623376421120	07 12 58.60	+06 59 52.29	A2 IV SrCrEu	215	12.8113	0.0018	+0.524	0.040	+0.357	0.016	0.06	+1.35	0.17
774	J071337.30+040720.7	HD 55585	07 13 37.48	+04 07 21.46	B8 IV CrEuSi	108	9.8835	0.0024	+1.158	0.069	-0.034	0.012	0.18	+0.03	0.14
775	J071413.88+142449.5	Gaia DR2 3167387374048122496	07 14 13.89	+14 24 49.58	A3 III-IV SrCrEu	111	14.0288	0.0004	+0.336	0.032	+0.310	0.003	0.10	+1.56	0.21
776	J071434.25+064339.7	Gaia DR2 3153147908195304320	07 14 34.25	+06 43 39.78	A0 IV-V CrEu	149	13.6121	0.0005	+0.291	0.043	+0.094	0.005	0.05	+0.88	0.32
777	J071458.67+125333.8	TYC 770-628-1	07 14 58.67	+12 53 34.09	B9 IV-V Cr	100	11.9075	0.0012	+0.501	0.055	+0.107	0.005	0.22	+0.19	0.24
778	J071535.85+054343.4	TYC 176-3306-1	07 15 35.89	+05 43 42.38	B8 IV EuSi	413	10.6533	0.0005	+0.778	0.039	-0.058	0.002	0.11	+0.00	0.12
779	J071550.38+063655.9	TYC 176-2454-1	07 15 50.27	+06 36 55.95	A1 IV SrCrEuSi	390	10.5506	0.0006	+2.092	0.053	+0.269	0.002	0.03	+2.12	0.07
780	J071653.67+050509.4	TYC 172-1501-1	07 16 53.67	+05 05 09.40	B9 IV bl4077 bl4130	211	11.3753	0.0003	+0.461	0.414	-	-	-	-	-
781	J071706.27+205242.5	TYC 1358-1336-1	07 17 06.27	+20 52 42.50	B8 IV Si	638	10.4400	0.0007	+1.058	0.077	-0.068	0.003	0.16	+0.41	0.17
782	J071750.10+173858.9	Gaia DR2 3362024090627348864	07 17 50.11	+17 38 58.94	B9.5 V SrCrEu	105	14.6387	0.0007	+0.352	0.032	+0.176	0.005	0.22	+2.15	0.20
783	J071752.83+134707.8 <sup>a</sup>	TYC 775-1162-1	07 17 52.84	+13 47 07.82	A5 IV-V SrCrEu	317	9.3263	0.0005	+1.361	0.540	-	-	-	-	-
784	J071901.76+150939.2	Gaia DR2 3167825632511004416	07 19 01.76	+15 09 39.24	B8 IV Si	149	14.2154	0.0011	+0.117	0.046	-	-	-	-	-
785	J071954.41+051936.0	TYC 172-1153-1	07 19 54.42	+05 19 36.01	B9 V Cr	252	12.2588	0.0004	+0.515	0.045	+0.018	0.005	0.20	+0.62	0.20
786	J071958.04+084727.9	Gaia DR2 3155230555017333760	07 19 58.04	+08 47 27.99	B9 IV-V SrCrEu	157	13.1321	0.0006	+0.302	0.047	+0.029	0.005	0.06	+0.48	0.34
787	J072000.73-030729.1	Gaia DR2 3060095753805333504	07 20 00.74	-03 07 29.12	B9 IV-V bl4130	126	12.6527	0.0004	+0.381	0.045	-0.012	0.003	0.14	+0.42	0.26
788	J072031.89+022923.7	TYC 168-38-1	07 20 31.89	+02 29 23.78	B9.5 III-IV CrSi	148	12.1178	0.0009	+0.506	0.045	-0.014	0.006	0.12	+0.52	0.20
789	J072040.31-000827.5	Gaia DR2 3110653501771439872	07 20 40.31	-00 08 27.52	kA1hA7mA9 CrSi	62	13.1563	0.0017	+0.472	0.046	+0.087	0.007	0.15	+1.37	0.22
790	J072052.36-015852.8	TYC 4820-842-1	07 20 52.37	-01 58 52.85	B9.5 IV-V SrCrEu	152	12.6771	0.0003	+0.366	0.031	+0.070	0.002	0.13	+0.37	0.19
791	J072104.20-031507.4	Gaia DR2 3059901071523913856	07 21 04.21	-03 15 07.45	B9 IV-V SrEu(Cr)*	142	12.5735	0.0054	+0.512	0.052	+0.034	0.026	0.16	+0.96	0.23
792	J072118.92+223422.7	TYC 1909-1687-1	07 21 18.93	+22 34 22.79	B9 V bl4077	544	10.3131	0.0013	+1.522	0.061	-0.098	0.005	0.15	+1.07	0.10
793	J072134.90-033226.0	TYC 4820-3742-1	07 21 34.90	-03 32 26.00	A1 II-III Si	107	11.8123	0.0008	+0.492	0.038	-0.081	0.005	0.12	+0.15	0.18
794	J072243.21+220430.7	HD 57590	07 22 43.25	+22 04 30.52	B9 IV-V SrEu(Cr)*	906	9.5348	0.0008	+1.185	0.084	-0.044	0.039	0.07	-0.16	0.16
795	J072318.82+082617.7	Gaia DR2 3154962720855355520	07 23 18.82	+08 26 17.78	A3 III-IV CrEu	114	13.3816	0.0006	+0.305	0.031	+0.093	0.005	0.06	+0.75	0.22
796	J072341.49-024106.9	TYC 4821-604-1	07 23 41.49	-02 41 07.02	A2 V CrEu	265	11.6810	0.0010	+0.844	0.044	+0.142	0.004	0.09	+1.23	0.12
797	J072412.26-050025.2	TYC 4825-2009-1	07 24 12.26	-05 00 25.35	B8 II-III bl4130	206	11.6433	0.0008	+0.281	0.042	-0.079	0.018	0.32	-1.44	0.33
798	J072415.37-003247.8	TYC 4817-1116-1	07 24 15.38	-00 32 47.84	B8 III bl4130	138	11.4538	0.0008	+0.368	0.055	-0.059	0.004	0.08	-0.80	0.33
799	J072423.08-003904.7	TYC 4817-1061-1	07 24 23.09	-00 39 04.76	B9 IV-V bl4077 bl4130	222	11.6593	0.0007	+0.547	0.043	-0.024	0.004	0.07	+0.28	0.18
800	J072433.03-001416.4	TYC 4817-1368-1	07 24 33.05	-00 14 16.47	B9.5 V CrEu	229	11.3966	0.0007	+0.561	0.048	+0.031	0.003	0.07	+0.07	0.19

**Table A.1.** Essential data for our sample stars, sorted by increasing right ascension. The columns denote: (1) Internal identification number. (2) LAMOST identifier. (3) Alternativ identifier (HD number, TYC identifier or GAIA DR2 number). (4) Right ascension (J2000; GAIA DR2). (5) Declination (J2000; GAIA DR2). (6) Spectral type, as derived in this study. (7) Sloan  $g$  band S/N ratio of the analysed spectrum. (8)  $G$  mag (GAIA DR2). (9)  $G$  mag error. (10) Parallax (GAIA DR2). (11) Parallax error. (12) Dereddened colour index  $(BP - RP)_0$  (GAIA DR2). (13) Colour index error. (14) Absorption in the  $G$  band,  $A_G$ . (15) Intrinsic absolute magnitude in the  $G$  band,  $M_{G,0}$ . (16) Absolute magnitude error.

(1)	(2)	(3)	(4)	(5)	(6)	(7)	(8)	(9)	(10)	(11)	(12)	(13)	(14)	(15)	(16)
No.	ID_LAMOST	ID_alt	RA(J2000)	Dec(J2000)	SpT_final	S/N <sub>g</sub>	$G$ mag	$e_G$ mag	$\pi$ (mas)	$e_\pi$	$(BP - RP)_0$	$e_{(BP - RP)_0}$	$A_G$	$M_{G,0}$	$e_{M_{G,0}}$
801	J072535.29+072629.2	TYC 177-635-1	07 25 35.30	+07 26 29.23	A0 III-IV Cr	370	11.5436	0.0003	+0.095	0.198	-	-	-	-	-
802	J072551.97-041719.5	TYC 4825-1586-1	07 25 51.98	-04 17 19.38	B9.5 IV CrSi	179	12.1882	0.0005	+0.386	0.044	-0.021	0.004	0.25	-0.13	0.25
803	J072614.34-004443.5	TYC 4817-111-1	07 26 14.34	-00 44 43.58	B5 IV bl4130	209	11.4700	0.0011	+0.567	0.051	-0.131	0.005	0.08	+0.16	0.20
804	J072659.14+121919.4	TYC 772-1162-1	07 26 59.14	+12 19 19.44	A4 IV-V SrCrEu	132	11.3252	0.0006	+0.888	0.048	+0.171	0.003	0.08	+0.99	0.13
805	J072725.86-012818.4	TYC 4817-1586-1	07 27 25.87	-01 28 18.42	B5 IV Si	154	12.1513	0.0011	+0.146	0.041	-	-	-	-	-
806	J072915.84+003208.5	TYC 165-835-1	07 29 15.85	+00 32 08.58	B9 V Cr	312	10.4212	0.0012	+1.207	0.054	+0.024	0.005	0.10	+0.73	0.11
807	J072940.44-045552.0	TYC 4825-1371-1	07 29 40.29	-04 55 52.06	B9 V Cr	342	10.1552	0.0005	+1.063	0.054	-0.050	0.001	0.11	+0.18	0.12
808	J072943.39-042433.4	TYC 4825-1200-1	07 29 43.46	-04 24 33.38	A0 V SrCr	283	10.8594	0.0006	+0.688	0.049	+0.191	0.002	0.05	0.00	0.16
809	J073054.73+101640.1	TYC 768-1345-1	07 30 54.73	+10 16 40.12	B9 IV-V bl4077 bl4130	219	10.9476	0.0015	+0.859	0.060	-0.064	0.004	0.05	+0.57	0.16
810	J073102.16+070734.5	TYC 190-233-1	07 31 02.17	+07 07 34.55	kA3hA5mA7 SrCrEu	104	10.8112	0.0004	+1.393	0.261	+0.198	0.002	0.03	+1.50	0.41
811	J073220.17-024048.1	TYC 4834-617-1	07 32 20.18	-02 40 48.14	kA2hA4mA7 CrEuSi	262	11.0241	0.0010	+1.052	0.065	+0.030	0.005	0.06	+1.08	0.14
812	J073254.94+111314.5	HD 59999	07 32 54.95	+11 13 14.55	B9 V SrCr	289	9.5405	0.0006	+1.814	0.057	+0.018	0.003	0.04	+0.80	0.08
813	J073351.72+242221.8	Gaia DR2 868363467228923904	07 33 51.73	+24 22 21.93	B8 IV-V bl4130 (He-wk)	106	11.5540	0.0006	+0.838	0.048	-0.094	0.007	0.11	+1.07	0.13
814	J073548.83+123225.1	TYC 773-931-1	07 35 48.83	+12 32 25.19	kA1hA9mA8 SrEu	197	11.2239	0.0016	+1.309	0.116	+0.357	0.003	0.04	+1.77	0.20
815	J073949.90-030558.0	TYC 4835-1400-1	07 39 49.96	-03 05 59.49	B7 V Si (He-wk)*	214	10.4654	0.0006	+0.710	0.053	-0.102	0.002	0.14	-0.41	0.17
816	J073950.01+201812.7	Gaia DR2 672828861965623040	07 39 50.01	+20 18 12.75	B9 IV-V SrCrEu	80	15.4476	0.0010	+0.196	0.048	-0.067	0.006	0.06	+1.84	0.53
817	J073953.64-002625.6	TYC 4831-2071-1	07 39 53.65	-00 26 25.63	A8 V SrCrEu	124	11.9413	0.0003	+0.624	0.041	+0.297	0.002	0.10	+0.82	0.15
818	J073953.72+080221.4	TYC 778-1580-1	07 39 53.59	+08 02 21.47	B8 III-IV bl4130	433	10.3616	0.0008	+0.867	0.052	-0.116	0.003	0.07	-0.01	0.14
819	J074104.88-003828.3	TYC 4831-885-1	07 41 04.77	-00 38 28.30	B9 V CrEu (He-wk)	283	10.5274	0.0006	+1.013	0.047	+0.079	0.002	0.05	+0.51	0.11
820	J074354.81+022855.1	TYC 183-266-1	07 43 54.82	+02 28 55.05	A0 V Cr	109	11.3431	0.0008	+0.927	0.064	+0.137	0.002	0.05	+1.13	0.16
821	J074414.88+051124.7	TYC 187-2124-1	07 44 14.89	+05 11 24.73	B8 III-IV Si	294	11.4865	0.0008	+0.614	0.062	-0.148	0.003	0.06	+0.37	0.23
822	J074417.67-043551.0	TYC 4839-894-1	07 44 17.67	-04 35 51.05	B9 V CrEu	477	10.1625	0.0008	+1.007	0.053	-0.094	0.003	0.17	+0.01	0.12
823	J074419.88+523638.9	HD 233446	07 44 19.88	+52 36 38.86	A0 V SrCrEu	497	10.1707	0.0008	+1.824	0.075	+0.083	0.003	0.11	+1.36	0.10
824	J074738.21+052329.6	TYC 188-171-1	07 47 38.22	+05 23 29.70	B9 V Cr	319	11.5441	0.0008	+0.437	0.050	-0.033	0.003	0.06	-0.31	0.25
825	J074744.39+052243.8	TYC 188-247-1	07 47 44.39	+05 22 43.84	B9.5 V CrEuSi	150	10.4210	0.0010	+1.661	0.048	+0.144	0.006	0.04	+1.48	0.08
826	J074830.59+002713.2	TYC 180-954-1	07 48 30.48	+00 27 13.23	B9.5 V SrCrEu	224	10.4835	0.0008	+1.344	0.068	+0.038	0.003	0.06	+1.07	0.12
827	J074851.40+001619.1	TYC 180-1290-1	07 48 51.41	+00 16 19.07	kB8hA3mA3 CrEu	229	9.9138	0.0005	+1.394	0.053	+0.027	0.001	0.13	+0.51	0.10
828	J074919.49+051551.8	TYC 188-700-1	07 49 19.50	+05 15 51.83	kA1hA9mA9 SrCrEu	368	11.1328	0.0007	+1.260	0.052	+0.275	0.002	0.04	+1.60	0.10
829	J074959.61+013517.8	TYC 180-2568-1	07 49 59.62	+01 35 17.83	kA1hA3mA7 SrCrEuSi	261	9.9910	0.0007	+0.884	0.062	+0.049	0.001	0.07	-0.35	0.16
830	J075041.80-060338.3	HD 63843	07 50 41.81	-06 03 38.29	A2 IV SrCrEu	130	10.2188	0.0004	+0.814	0.045	+0.076	0.002	0.34	-0.57	0.13
831	J075220.93+113710.6	Gaia DR2 3150803440165601664	07 52 20.93	+11 37 10.63	kA5hA6mA9 SrCrEu	104	13.2627	0.0003	+0.313	0.032	+0.207	0.002	0.06	+0.68	0.23
832	J075429.74-074804.3	Gaia DR2 3042652727681575936	07 54 29.74	-07 48 04.50	B9 III-IV Si	109	12.7518	0.0006	-2.860	0.543	-	-	-	-	-
833	J075516.94+101951.2	TYC 784-149-1	07 55 16.94	+10 19 51.28	A7 V SrEuSi	229	12.0348	0.0003	+0.436	0.038	+0.315	0.002	0.05	+0.18	0.20
834	J075656.82-054907.8	TYC 4845-1387-1	07 56 56.83	-05 49 07.89	B8 IV-V bl4130 (He-wk)	371	11.2779	0.0017	+0.990	0.067	-0.116	0.004	0.11	+1.15	0.16
835	J075951.17+021610.9	HD 65644	07 59 51.17	+02 16 10.84	B8 IV CrEu	334	9.9878	0.0009	+1.328	0.064	-0.088	0.003	0.05	+0.56	0.12
836	J080112.84+305547.8	TYC 2468-1474-1	08 01 12.85	+30 55 47.81	A3 IV SrCrEu	254	11.4569	0.0029	+1.547	0.901	-	-	-	-	-
837	J080210.08+334820.2	TYC 2476-1457-1	08 02 10.09	+33 48 20.25	kA1hA6mA6 Eu	141	13.0555	0.0011	+0.682	0.049	+0.049	0.006	0.17	+2.05	0.16
838	J080339.87-082141.0	TYC 5413-1871-1	08 03 39.88	-08 21 41.01	kB9hA3mA8 SrCrEu	251	9.4489	0.0006	+1.205	0.055	+0.039	0.002	0.20	-0.34	0.11
839	J080435.19-031900.7	TYC 4850-398-1	08 04 35.19	-03 19 00.74	A0 IV-V SrCr	207	10.0101	0.0008	+1.101	0.087	+0.104	0.002	0.05	+0.17	0.18
840	J080734.82-044027.2	Gaia DR2 3067862055404261120	08 07 34.83	-04 40 27.22	kB9.5hA2mA4 SrCrEu	116	13.0785	0.0009	+0.437	0.040	+0.092	0.004	0.08	+1.20	0.21
841	J081024.89+382402.2	TYC 2973-199-1	08 10 24.68	+38 24 02.31	B8 IV Si	426	9.7665	0.0010	+1.034	0.077	-0.103	0.004	0.08	-0.24	0.17
842	J081025.65-062756.5	TYC 4859-583-1	08 10 25.65	-06 27 56.38	B9 IV-V Cr	175	11.3055	0.0007	+0.526	0.052	-0.002	0.003	0.10	-0.19	0.22
843	J081148.45-075357.2	TYC 5426-304-1	08 11 48.45	-07 53 57.21	B8 IV Si (He-wk)	168	11.1818	0.0013	+0.751	0.067	-0.006	0.003	0.42	+0.14	0.20
844	J081342.91-055347.1	TYC 4855-1556-1	08 13 42.91	-05 35 47.23	kB9.5hA3mA3 SrCrEu	217	10.6418	0.0009	+1.488	0.106	+0.062	0.003	0.08	+1.43	0.16
845	J081445.01+172256.9	TYC 1381-753-1	08 14 44.86	+17 22 57.00	kB9hA5mA5 CrEu	402	10.2896	0.0011	+0.662	0.070	-0.008	0.004	0.14	-0.75	0.24
846	J081930.22+001232.3	TYC 196-522-1	08 19 30.23	+00 12 32.29	B6 III-IV Si	132	11.4510	0.0019	+0.606	0.093	-0.219	0.008	0.06	+0.30	0.34
847	J082002.55+000809.3	Gaia DR2 3077512228440068352	08 20 02.50	+00 08 09.40	kA2hA4mA7 CrEu	225	11.5727	0.0006	+0.596	0.062	+0.157	0.003	0.08	+0.37	0.23
848	J082137.47+064401.0	Gaia DR2 3096854940075299712	08 21 37.48	+06 44 01.06	A1 IV SrCrEu	118	13.3369	0.0003	+0.613	0.027	+0.262	0.002	0.06	+2.21	0.11
849	J082235.26+161149.3	TYC 1378-930-1	08 22 35.27	+16 11 49.30	B8 IV Si (He-wk)	227	11.8453	0.0009	+0.443	0.088	-0.204	0.005	0.08	0.00	0.43
850	J082326.74+072116.4	TYC 209-1570-1	08 23 26.70	+07 21 16.02	kA3hA7mF1 SrCrEu	411	11.1021	0.0008	+1.228	0.067	+0.203	0.002	0.08	+1.47	0.13

**Table A.1.** Essential data for our sample stars, sorted by increasing right ascension. The columns denote: (1) Internal identification number. (2) LAMOST identifier. (3) Alternativ identifier (HD number, TYC identifier or GAIA DR2 number). (4) Right ascension (J2000; GAIA DR2). (5) Declination (J2000; GAIA DR2). (6) Spectral type, as derived in this study. (7) Sloan  $g$  band S/N ratio of the analysed spectrum. (8)  $G$  mag (GAIA DR2). (9)  $G$  mag error. (10) Parallax (GAIA DR2). (11) Parallax error. (12) Dereddened colour index  $(BP - RP)_0$  (GAIA DR2). (13) Colour index error. (14) Absorption in the  $G$  band,  $A_G$ . (15) Intrinsic absolute magnitude in the  $G$  band,  $M_{G,0}$ . (16) Absolute magnitude error.

(1)	(2)	(3)	(4)	(5)	(6)	(7)	(8)	(9)	(10)	(11)	(12)	(13)	(14)	(15)	(16)
No.	ID_LAMOST	ID_alt	RA(J2000)	Dec(J2000)	SpT_final	S/N $_g$	$G$ mag	$e_G$ mag	pi (mas)	$e_{pi}$	$(BP - RP)_0$	$e_{(BP - RP)_0}$	$A_G$	$M_{G,0}$	$e_{M_{G,0}}$
851	J082331.87+491533.9	TYC 3418-1363-1	08 23 31.88	+49 15 33.89	B9 V SrCr	245	10.1705	0.0005	+1.211	0.045	+0.041	0.001	0.11	+0.47	0.09
852	J082706.99+453552.9	HD 71047	08 27 06.71	+45 35 52.93	A5 III-IV Sr	362	9.6733	0.0007	+2.785	0.095	+0.143	0.003	0.06	+1.84	0.09
853	J083539.12+002150.4	TYC 210-1694-1	08 35 39.15	+00 21 50.63	kA2hA3mA6 SrCrEu	220	11.6695	0.0006	+0.605	0.044	+0.150	0.002	0.14	+0.43	0.17
854	J084232.90+211043.9	TYC 1398-1797-1	08 42 32.90	+21 10 43.90	A3 IV SrCrEu	246	12.1062	0.0004	+0.611	0.045	+0.235	0.002	0.11	+0.93	0.17
855	J084546.89+054048.1	HD 74722	08 45 46.71	+05 40 48.09	A8 V SrEu	192	9.4740	0.0004	+1.823	0.058	+0.150	0.002	0.06	+0.72	0.09
856	J084613.37+191508.9	HD 74719	08 46 13.20	+19 15 08.96	B9.5 V SrCr	431	9.7889	0.0007	+1.380	0.065	+0.045	0.003	0.06	+0.43	0.11
857	J085148.85+434402.2	Gaia DR2 913924411585612928	08 51 48.86	+43 44 02.29	B8 IV-V <sup>b</sup>	155	12.3875	0.0003	+0.564	0.050	-0.171	0.003	0.08	+1.06	0.20
858	J091022.04+281832.0	Gaia DR2 698186451960307712	09 10 21.97	+28 18 32.27	B9 V CrEu	158	13.0315	0.0008	+0.273	0.088	-	-	-	-	-
859	J091053.70+285032.7	Gaia DR2 698486305101018240	09 10 53.71	+28 50 32.81	A9 V SrCrEu	139	12.5636	0.0005	+0.375	0.069	+0.262	0.003	0.06	+0.37	0.40
860	J091451.94+082606.5	TYC 819-736-1	09 14 51.95	+08 26 06.73	kA2hA7mA6 SrEu	272	9.8052	0.0007	+2.704	0.062	+0.282	0.008	0.09	+1.87	0.07
861	J092233.23+072519.4	TYC 234-81-1	09 22 33.01	+07 25 19.39	kA3hA6mA9 SrCrEu	422	9.2254	0.0006	+2.718	0.044	+0.412	0.009	0.06	+1.33	0.06
862	J092615.37+280323.0	HD 81416	09 26 15.20	+28 03 23.00	B8 IV SrCrEu	498	10.1268	0.0008	+1.106	0.075	-0.073	0.005	0.08	+0.26	0.16
863	J093551.74+093917.8	TYC 821-367-1	09 35 51.64	+09 39 17.54	B9.5 IV-V CrEuSi	121	11.5541	0.0010	+1.095	0.059	+0.040	0.003	0.08	+1.67	0.13
864	J093915.30+041535.0	Gaia DR2 3824575537075330816	09 39 15.29	+04 15 35.11	A4 IV-V SrCr	138	13.3655	0.0005	+0.429	0.062	+0.193	0.004	0.09	+1.44	0.32
865	J094438.61+312641.5	TYC 2501-808-1	09 44 38.63	+31 26 41.56	B8 IV Si	438	11.2249	0.0014	+0.386	0.108	-	-	-	-	-
866	J094532.52+062723.0	TYC 4901-537-1	09 45 32.52	-06 27 23.04	kB8hA4mA4 Cr	137	12.7837	0.0011	+0.667	0.073	+0.036	0.006	0.10	+1.81	0.24
867	J095644.95+021719.5	HD 86170	09 56 45.18	-02 17 20.43	kA2hA3mA6 SrCrEu	762	8.4143	0.0008	+3.811	0.106	+0.128	0.006	0.09	+1.23	0.08
868	J095855.77+044413.8	Gaia DR2 3822254609763252864	09 58 55.77	-04 44 13.74	B9.5 III-IV Eu	105	13.2069	0.0011	+0.167	0.052	-	-	-	-	-
869	J102027.58+280919.4	Gaia DR2 740907873177225088	10 20 27.63	+28 09 19.32	B9 V CrEu	127	13.7089	0.0007	+0.173	0.049	-	-	-	-	-
870	J104323.95+045214.3	Gaia DR2 3858264955602552320	10 43 23.95	+04 52 14.38	A1 IV-V CrEu	169	12.7714	0.0005	+0.585	0.057	+0.133	0.003	0.05	+1.55	0.22
871	J105734.90+260846.0	TYC 1978-545-1	10 57 34.89	+26 08 45.97	A0 V CrEu	282	11.9675	0.0007	+0.838	0.064	-0.031	0.005	0.10	+1.49	0.17
872	J113813.46+441229.5	TYC 3015-595-1	11 38 13.46	+44 12 29.53	A7 V Sr	460	10.9897	0.0006	+1.419	0.065	+0.204	0.002	0.05	+1.70	0.11
873	J114130.23+403822.7	TYC 3014-2468-1	11 41 30.23	+40 38 22.80	B9 IV-V CrEuSi	201	11.6523	0.0011	+0.620	0.105	-0.150	0.004	0.07	+0.55	0.37
874	J120632.73+521507.9	TYC 3457-908-1	12 06 32.66	+52 15 07.91	B9 V Cr (He-wk)	472	10.8068	0.0009	+0.921	0.086	-0.064	0.003	0.09	+0.54	0.21
875	J122139.23+383309.5	Gaia DR2 1532535594973538688	12 21 39.23	+38 33 09.56	kA2hA4mA7 bl4077 bl4130	83	13.1753	0.0004	+0.527	0.038	+0.299	0.002	0.04	+1.75	0.16
876	J122746.05+113635.3	Gaia DR2 3907547639444408064	12 27 46.01	+11 36 35.95	B8 IV Si (He-wk)	124	12.6834	0.0008	+0.359	0.061	-0.226	0.005	0.08	+0.38	0.37
877	J122855.36+255446.3	HD 108662	12 28 54.70	+25 54 46.27	B9 V CrEu	741	5.2066	0.0033	+13.538	0.225	-0.013	0.01	0.02	+0.84	0.06
878	J133835.32+100716.1	TYC 896-860-1	13 38 35.51	+10 07 16.57	kA3hA7mA9 SrCrEu	473	9.8044	0.0013	+2.107	0.102	+0.320	0.004	0.09	+1.34	0.12
879	J140422.54+044357.9	TYC 319-461-1	14 04 22.55	+04 43 57.79	kA4hA7mF0 SrCrEu	240	12.0595	0.0004	+0.619	0.056	+0.172	0.003	0.06	+0.95	0.20
880	J150331.87+093125.4	Gaia DR2 1167894108493926016	15 03 31.88	+09 31 25.44	A8 V SrCrEu	195	12.6710	0.0004	+0.435	0.046	+0.288	0.002	0.08	+0.78	0.23
881	J155549.85+401144.4	Gaia DR2 1382933122321062912	15 55 49.85	+40 11 44.44	B8 IV Si	113	14.0505	0.0008	+0.126	0.028	-0.213	0.005	0.03	-0.49	0.49
882	J163458.89+004659.8	TYC 382-541-1	16 34 58.89	+00 46 59.82	A0 V CrEu	228	11.5347	0.0008	+1.247	0.070	+0.083	0.002	0.19	+1.83	0.13
883	J165909.90+262236.7	TYC 2067-291-1	16 59 09.91	+26 22 36.74	A6 V CrEu	234	11.2186	0.0007	+1.143	0.035	+0.144	0.003	0.09	+1.42	0.08
884	J170210.51+194917.2	TYC 1530-836-1	17 02 10.51	+19 49 17.27	B9.5 IV-V SrCr	237	12.0212	0.0005	+0.419	0.033	+0.055	0.003	0.17	-0.04	0.18
885	J172937.90+414015.2	TYC 3094-784-1	17 29 37.91	+41 40 15.21	B9 IV-V Cr	71	12.4394	0.0004	+0.841	0.023	+0.099	0.002	0.12	+1.94	0.08
886	J173152.09+393831.0	TYC 3091-119-1	17 31 52.09	+39 38 31.10	B9 V Cr	128	11.6335	0.0005	+0.656	0.028	-0.020	0.003	0.11	+0.60	0.10
887	J173536.70+033738.9	TYC 418-2336-1	17 35 36.71	+03 37 39.22	A2 IV-V Sr	219	10.8839	0.0005	+1.681	0.049	+0.066	0.002	0.35	+1.67	0.08
888	J173844.78+243856.2	TYC 2080-1036-1	17 38 44.79	+24 38 56.21	B8 III Si	118	11.8401	0.0009	+0.431	0.034	-0.122	0.005	0.12	-0.10	0.18
889	J174031.07+102400.8	TYC 997-994-1	17 40 31.07	+10 24 00.86	A6 V SrCrEu	224	11.6382	0.0007	+1.254	0.097	+0.215	0.003	0.36	+1.77	0.18
890	J175134.06+263903.1	TYC 2085-2086-1	17 51 34.06	+26 39 03.11	A0 V Cr	125	12.0794	0.0004	+0.541	0.025	+0.076	0.002	0.09	+0.66	0.11
891	J175822.90+065649.5	Gaia DR2 4475629258450293120	17 58 22.91	+06 56 49.53	kA4hA7mF0 SrCrEu	127	12.9984	0.0005	+0.564	0.031	+0.173	0.002	0.47	+1.29	0.13
892	J175919.34+053509.5	Gaia DR2 4474449821775956608	17 59 19.33	+05 35 09.52	A1 IV-V CrEu	256	12.1289	0.0009	+0.819	0.044	0.000	0.015	0.47	+1.23	0.13
893	J180512.65+125948.8	TYC 1016-588-1	18 05 12.61	+12 59 51.41	A0 IV SrCr	392	10.0765	0.0008	+1.261	0.046	+0.095	0.003	0.36	+0.23	0.09
894	J180615.12+023732.9 <sup>a</sup>	TYC 434-1758-1	18 06 15.07	+02 37 30.78	kB9hA3mA7 CrEuSi	578	10.1759	0.0012	+1.803	0.070	-0.003	0.004	0.18	+1.27	0.10
895	J181156.38+523411.4	Gaia DR2 2125305094015307520	18 11 56.40	+52 34 11.48	B7 IV-V Si	119	13.4058	0.0012	+0.170	0.035	-0.237	0.009	0.08	-0.52	0.45
896	J181409.49+053445.1	TYC 439-340-1	18 14 09.49	+05 34 45.13	A0 IV-V SrCr	155	11.6393	0.0008	+0.577	0.042	+0.123	0.005	0.43	+0.02	0.17
897	J184021.60+273858.7	TYC 2115-1062-1	18 40 21.61	+27 38 58.63	B9.5 V Cr	115	12.4871	0.0003	+0.341	0.031	+0.041	0.002	0.30	-0.15	0.20
898	J184217.44+283421.1	TYC 2120-220-1	18 42 17.44	+28 34 20.95	A1 IV CrEu	122	12.2758	0.0005	+0.839	0.028	+0.179	0.002	0.36	+1.53	0.09
899	J185127.99+262012.1	TYC 2117-2336-1	18 51 28.00	+26 20 12.13	A0 IV-V Cr	175	12.5515	0.0004	+0.543	0.026	+0.100	0.002	0.46	+0.76	0.12
900	J185444.63+482024.8	Gaia DR2 2131718510982169728	18 54 44.62	+48 20 24.80	A4 IV-V CrEu	107	12.7484	0.0004	+0.593	0.034	+0.081	0.003	0.15	+1.47	0.13

**Table A.1.** Essential data for our sample stars, sorted by increasing right ascension. The columns denote: (1) Internal identification number. (2) LAMOST identifier. (3) Alternative identifier (HD number, TYC identifier or GAIA DR2 number). (4) Right ascension (J2000; GAIA DR2). (5) Declination (J2000; GAIA DR2). (6) Spectral type, as derived in this study. (7) Sloan  $g$  band S/N ratio of the analysed spectrum. (8)  $G$  mag (GAIA DR2). (9)  $G$  mag error. (10) Parallax (GAIA DR2). (11) Parallax error. (12) Dereddened colour index  $(BP - RP)_0$  (GAIA DR2). (13) Colour index error. (14) Absorption in the  $G$  band,  $A_G$ . (15) Intrinsic absolute magnitude in the  $G$  band,  $M_{G,0}$ . (16) Absolute magnitude error.

(1)	(2)	(3)	(4)	(5)	(6)	(7)	(8)	(9)	(10)	(11)	(12)	(13)	(14)	(15)	(16)
No.	ID_LAMOST	ID_alt	RA(J2000)	Dec(J2000)	SpT_final	S/N $_g$	$G$ mag	$e_G$ mag	$\pi$ (mas)	$e_\pi$	$(BP - RP)_0$	$e_{(BP - RP)_0}$	$A_G$	$M_{G,0}$	$e_{M_{G,0}}$
901	J185821.27+434926.5	TYC 3131-1074-1	18 58 21.29	+43 49 26.42	A7 V SrCrEu	244	11.4667	0.0006	+1.016	0.029	+0.215	0.003	0.09	+1.41	0.08
902	J190132.50+415158.9 <sup>a</sup>	HD 177128	19 01 32.49	+41 51 59.33	kA1hA4mA6 SrCrEu	629	9.1646	0.0004	+3.155	0.043	+0.114	0.003	0.06	+1.60	0.06
903	J191305.80+500013.3	TYC 3550-977-1	19 13 05.80	+50 00 13.39	A4 IV SrCrEu	204	11.8878	0.0005	+0.965	0.024	+0.090	0.003	0.12	+1.69	0.07
904	J191430.53+402714.1	HD 180374	19 14 30.37	+40 27 16.66	B9 IV - V CrEu	660	8.7984	0.0007	+2.529	0.061	+0.021	0.004	0.08	+0.74	0.07
905	J191837.96+394726.4 <sup>a</sup>	TYC 3125-282-1	19 18 37.97	+39 47 26.33	B9.5 IV - V Cr (He-wk)	254	11.0248	0.0007	+0.839	0.208	+0.145	0.004	0.14	+0.50	0.54
906	J191920.17+444706.6	TYC 3133-70-1	19 19 20.18	+44 47 06.71	B8 IV - V Si	185	11.7006	0.0006	+0.288	0.039	-0.059	0.004	0.18	-1.18	0.30
907	J192135.14+440302.4	TYC 3146-839-1	19 21 35.15	+44 03 02.27	A0 II EuSi	399	10.3730	0.0017	+1.113	0.031	-0.072	0.008	0.15	+0.46	0.08
908	J192151.34+450655.3	TYC 3543-971-1	19 21 51.35	+45 06 55.31	B8 IV Si	213	12.3466	0.0006	+0.271	0.029	-0.076	0.004	0.22	-0.71	0.23
909	J192524.14+431911.5	TYC 3146-198-1	19 25 24.12	+43 19 11.12	kA3hA7mA9 SrCrEu	161	11.8109	0.0004	+1.023	0.029	+0.196	0.003	0.19	+1.67	0.08
910	J192630.17+380251.8	Gaia DR2 2052567864358948736	19 26 30.17	+38 02 51.73	B9 V Si	107	13.6254	0.0004	+0.261	0.030	-0.039	0.003	0.18	+0.53	0.25
911	J192943.77+422930.6	Gaia DR2 2125752389095257088	19 29 43.77	+42 29 30.68	B9 V Cr	170	12.6734	0.0004	+0.371	0.026	+0.001	0.003	0.20	+0.32	0.16
912	J193021.81+465043.2	Gaia DR2 2128347270896190208	19 30 21.78	+46 50 43.22	B9 V CrEu	198	13.0596	0.0004	+0.329	0.031	-0.024	0.003	0.12	+0.52	0.21
913	J193128.34+470548.2	TYC 3560-2289-1	19 31 28.35	+47 05 48.26	F0 V SrEu	395	10.7146	0.0003	+2.156	0.024	+0.361	0.001	0.10	+2.28	0.06
914	J193307.57+270643.1	HD 338514	19 33 07.57	+27 06 42.92	kB9.5hA2mA4 CrEu	102	11.1459	0.0010	+1.146	0.031	-0.031	0.004	0.77	+0.67	0.08
915	J193927.58+471826.3	TYC 3560-3168-1	19 39 27.59	+47 18 26.45	B9 V CrEuSi	661	10.3174	0.0010	+1.265	0.032	-0.031	0.005	0.15	+0.68	0.07
916	J194154.63+380153.1	HD 225429	19 41 54.65	+38 01 53.21	kB8hA3mA6 CrEu	297	9.9751	0.0005	+1.624	0.032	-0.072	0.002	0.17	+0.86	0.07
917	J194334.90+300004.0	HD 332508	19 43 34.86	+30 00 01.96	kA0hA1mA3 EuSi	275	10.3491	0.0010	+0.772	0.035	-0.076	0.004	0.35	-0.56	0.11
918	J194611.22+391333.3	HD 225728	19 46 11.21	+39 13 34.93	B8 V bl4077 bl4130	376	10.3882	0.0006	+1.011	0.155	-0.091	0.002	0.28	+0.14	0.34
919	J194629.20+473750.0 <sup>a</sup>	TYC 3561-1857-1	19 46 29.21	+47 37 50.05	kA5hA7mA9 SrCrEu	352	11.3822	0.0009	+1.144	0.044	+0.368	0.003	0.13	+1.55	0.10
920	J194650.18+280638.9	HD 332756	19 46 50.18	+28 06 38.98	B8 III - IV bl4130	106	11.1576	0.0006	+0.623	0.040	-0.081	0.002	0.51	-0.38	0.15
921	J194925.91+470218.0	Gaia DR2 2086363381465025024	19 49 25.95	+47 02 16.98	B9.5 II - III EuSi	123	12.8462	0.0003	+0.115	0.028	-0.012	0.002	0.24	-2.09	0.54
922	J195042.19+483639.4	TYC 3561-781-1	19 50 42.19	+48 36 39.52	kA5hA6mA9 SrCrEu	307	11.4833	0.0011	+1.042	0.029	+0.403	0.008	0.10	+1.47	0.08
923	J195251.15+403621.4	HD 226339	19 52 51.08	+40 36 21.48	B9 IV Si	412	10.8132	0.0007	+0.970	0.038	-0.195	0.003	0.42	+0.33	0.10
924	J195314.26+445712.4	Gaia DR2 2079301664955979392	19 53 14.26	+44 57 12.41	kB9.5hA5mA2 SrEu	117	13.7325	0.0004	+0.293	0.019	+0.069	0.003	0.71	+0.36	0.15
925	J195341.40+441939.9	Gaia DR2 2079071931443788672	19 53 41.39	+44 19 39.86	A0 V CrEu	210	11.9820	0.0004	+0.805	0.041	+0.041	0.002	0.53	+0.98	0.12
926	J195344.32+414104.1	HD 226421	19 53 44.32	+41 41 04.26	B8 V Si	582	10.1422	0.0006	+0.939	0.032	-0.205	0.002	0.48	-0.48	0.09
927	J195506.34+442900.7	TYC 3149-428-1	19 55 06.35	+44 29 00.69	A5 IV - V SrEu	297	11.9201	0.0002	+1.189	0.022	+0.267	0.002	0.41	+1.89	0.06
928	J195551.27+480759.8	TYC 3562-1452-1	19 55 51.23	+48 07 59.42	B9.5 V Cr	363	10.9518	0.0010	+0.946	0.031	-0.040	0.004	0.31	+0.52	0.09
929	J195631.74+253407.8	Gaia DR2 2026771741029840128	19 56 31.75	+25 34 07.84	B8 V SiCr*	134	12.2836	0.0010	+0.765	0.032	-0.119	0.004	1.76	-0.06	0.10
930	J195644.95+432951.5	TYC 3149-1303-1	19 56 44.96	+43 29 51.42	kB9hA8mA6 Si	261	11.8054	0.0005	+0.709	0.026	-0.137	0.003	0.41	+0.65	0.09
931	J195801.13+251550.6	Gaia DR2 1834595113014285824	19 58 01.13	+25 15 50.65	B9 V Cr	108	13.2872	0.0004	+0.700	0.019	-0.022	0.002	1.66	+0.86	0.08
932	J200227.66+463007.0	TYC 3558-1813-1	20 02 27.66	+46 30 06.91	A2 IV SrEu	469	11.3210	0.0006	+1.643	0.023	+0.290	0.002	0.19	+2.21	0.06
933	J200529.70+440656.7	TYC 3162-162-1	20 05 29.68	+44 06 56.39	A1 III - IV bl4077 bl4130	178	11.8068	0.0004	+0.603	0.033	-0.078	0.002	0.70	+0.01	0.13
934	J200544.86+434645.9	TYC 3162-1336-1	20 05 44.85	+43 46 45.18	B9 V bl4130	188	11.8986	0.0002	+0.635	0.026	+0.086	0.002	0.39	+0.53	0.10
935	J200814.38+464916.2	TYC 3559-1471-1	20 08 14.38	+46 49 15.75	A0 V SrCrEu	444	11.0934	0.0009	+0.940	0.025	+0.104	0.003	0.82	+0.14	0.08
936	J200911.86+445359.0	TYC 3162-277-1	20 09 11.87	+44 53 59.14	B9 III Si	214	11.5085	0.0006	+0.690	0.036	-0.220	0.002	0.98	-0.27	0.12
937	J201138.29+273639.6	HD 333914	20 11 38.26	+27 36 38.24	B7 IV - V Si	308	10.7394	0.0010	+1.032	0.034	-0.055	0.004	0.94	-0.13	0.09
938	J201237.90+513759.1	TYC 3571-735-1	20 12 37.90	+51 37 59.20	B8 IV CrSi	220	11.3409	0.0013	+0.541	0.104	-0.005	0.003	0.22	-0.22	0.42
939	J202056.13+380407.6	HD 229032	20 20 56.23	+38 04 07.29	B7 V Si	279	10.7593	0.0004	+1.156	0.030	-0.405	0.002	1.32	-0.24	0.08
940	J202416.52+434141.9	TYC 3164-1108-1	20 24 16.52	+43 41 41.92	A0 II - III bl4077	231	11.8897	0.0008	+0.804	0.025	-1.219	0.003	3.13	-1.72	0.08
941	J202636.19+424251.0	TYC 3160-232-1	20 26 36.19	+42 42 51.07	B9.5 II Si	136	12.6712	0.0004	+0.498	0.026	-0.095	0.003	1.86	-0.70	0.13
942	J202924.63+411507.6	Gaia DR2 2068000609561250816	20 29 24.63	+41 15 07.68	B8 V bl4077 bl4130	201	12.0036	0.0004	+0.939	0.023	-0.502	0.002	2.03	-0.16	0.07
943	J202943.73+384756.6	Gaia DR2 2064117095834734464	20 29 43.73	+38 47 56.62	B9 II - III Si	171	12.3830	0.0014	+1.898	0.218	+1.180	0.003	0.17	+3.60	0.25
944	J203012.93+413750.4	TYC 3161-1091-1	20 30 12.93	+41 37 50.38	B9 III - IV CrSi	286	11.4399	0.0007	+0.901	0.031	+0.004	0.002	0.90	+0.32	0.09
945	J203252.92+440742.5	TYC 3165-381-1	20 32 52.63	+44 07 42.74	kB9hA0mA2 Si	161	9.5781	0.0004	+1.393	0.040	-0.139	0.002	0.42	-0.13	0.08
946	J203337.82+480113.3	TYC 3577-1410-1	20 33 37.83	+48 01 13.40	B9 III Si	343	11.2524	0.0009	+0.459	0.058	-0.358	0.003	1.23	-1.67	0.28
947	J203813.43+442217.0	TYC 3165-370-1	20 38 13.68	+44 22 18.33	B9 IV - V Cr	405	9.7620	0.0008	+1.839	0.043	-0.103	0.003	0.30	+0.78	0.07
948	J204216.10+360057.0	TYC 2699-2845-1	20 42 16.10	+36 00 57.00	B8 IV bl4130	107	11.3592	0.0007	+0.955	0.039	-0.085	0.002	0.89	+0.37	0.10
949	J204308.71+504709.0	Gaia DR2 2180453470538367488	20 43 08.72	+50 47 09.04	B9.5 III - IV CrSi	141	12.8618	0.0007	+0.615	0.023	+0.052	0.003	1.09	+0.71	0.09
950	J204922.38+372816.3	TYC 2699-981-1	20 49 22.38	+37 28 16.30	B9.5 IV - V SrCr	107	12.4261	0.0002	+0.634	0.027	+0.052	0.001	0.90	+0.54	0.11

**Table A.1.** Essential data for our sample stars, sorted by increasing right ascension. The columns denote: (1) Internal identification number. (2) LAMOST identifier. (3) Alternative identifier (HD number, TYC identifier or GAIA DR2 number). (4) Right ascension (J2000; GAIA DR2). (5) Declination (J2000; GAIA DR2). (6) Spectral type, as derived in this study. (7) Sloan  $g$  band S/N ratio of the analysed spectrum. (8)  $G$  mag (GAIA DR2). (9)  $G$  mag error. (10) Parallax (GAIA DR2). (11) Parallax error. (12) Dereddened colour index  $(BP - RP)_0$  (GAIA DR2). (13) Colour index error. (14) Absorption in the  $G$  band,  $A_G$ . (15) Intrinsic absolute magnitude in the  $G$  band,  $M_{G,0}$ . (16) Absolute magnitude error.

(1)	(2)	(3)	(4)	(5)	(6)	(7)	(8)	(9)	(10)	(11)	(12)	(13)	(14)	(15)	(16)
No.	ID_LAMOST	ID_alt	RA(J2000)	Dec(J2000)	SpT_final	S/N $_g$	$G$ mag	$e_G$ mag	$\pi$ (mas)	$e_\pi$	$(BP - RP)_0$	$e_{(BP - RP)_0}$	$A_G$	$M_{G,0}$	$e_{M_{G,0}}$
951	J205711.99+362112.8	TYC 2700-3067-1	20 57 12.00	+36 21 12.81	B8 IV Si	165	11.0595	0.0006	+0.589	0.045	-0.005	0.003	0.53	-0.62	0.17
952	J205820.49+340411.3	TYC 2696-1529-1	20 58 20.50	+34 04 11.39	B8 IV-V Si	101	11.4910	0.0006	+0.680	0.035	-0.063	0.002	0.35	+0.31	0.12
953	J210327.21+013808.7	Gaia DR2 1729657826308369792	21 03 27.22	+01 38 08.55	A2 IV-V SrEu	252	12.5182	0.0003	+0.950	0.052	+0.177	0.003	0.29	+2.12	0.13
954	J212802.14+395946.6	TYC 3186-2260-1	21 28 02.15	+39 59 46.71	B8 III-IV Si	172	11.8125	0.0004	+0.433	0.031	+0.003	0.002	0.64	-0.65	0.16
955	J213646.10+494739.4	Gaia DR2 1979156634085728384	21 36 46.11	+49 47 39.45	A2 IV-V SrCr	137	14.4306	0.0003	+0.244	0.027	-0.109	0.002	1.52	-0.15	0.25
956	J213710.42+402056.7	TYC 3187-943-1	21 37 10.42	+40 20 56.75	kA1hA6mA7 SrCrEu	298	11.0760	0.0013	-2.540	0.506	-	-	-	-	-
957	J213851.08+414514.0	TYC 3191-1090-1	21 38 50.98	+41 45 16.21	B8 IV Si	846	9.9430	0.0005	+1.545	0.054	-0.206	0.001	0.55	+0.34	0.09
958	J213940.97-044004.9	TYC 5217-1367-1	21 39 40.98	-04 40 04.84	B8 IV Si	143	10.8596	0.0008	+0.608	0.097	-0.172	0.004	0.13	-0.35	0.35
959	J214029.69+432658.6 <sup>a</sup>	TYC 3196-875-1	21 40 29.61	+43 26 58.63	kA1hA7mA8 SrCrEuSi	270	10.7689	0.0004	+1.566	0.038	-0.753	0.002	1.75	-0.01	0.07
960	J214045.49+120849.2	TYC 1128-1649-1	21 40 45.37	+12 08 49.21	B9 V SrCr	429	10.4149	0.0005	+1.530	0.050	-0.039	0.003	0.21	+1.13	0.09
961	J214140.45+082543.9	TYC 1120-1719-1	21 41 40.38	+08 25 43.90	B9 IV-V CrEu	314	10.7778	0.0011	+0.596	0.066	+0.015	0.006	0.09	-0.44	0.24
962	J214337.80+494041.9	Gaia DR2 1978967483714383616	21 43 37.81	+49 40 42.02	kA0hA3mA7 CrSi	122	14.5697	0.0006	+0.398	0.021	-0.199	0.003	1.82	+0.75	0.13
963	J214358.57+430044.4	TYC 3192-676-1	21 43 58.54	+43 00 43.65	kB9.5hA2mA5 CrEu	229	10.8782	0.0007	+1.599	0.030	+0.028	0.003	0.44	+1.46	0.06
964	J214815.98+083232.4	Gaia DR2 2701846248105636480	21 48 15.98	+08 32 32.42	B8 IV-V (Cr)*	117	14.4455	0.0008	+0.277	0.073	-	-	-	-	-
965	J220052.34+411659.6	TYC 3206-1198-1	22 00 52.35	+41 16 59.66	B9 III-IV Si	139	9.6347	0.0005	+1.656	0.040	-0.071	0.002	0.27	+0.46	0.07
966	J220500.91+043900.2	TYC 561-1768-1	22 05 00.91	+04 39 00.30	kA2hA8mA9 SrCrEu	197	11.7202	0.0003	+0.745	0.065	+0.289	0.003	0.15	+0.93	0.20
967	J222549.96+343851.0	HD 212714	22 25 49.67	+34 38 51.06	B8 IV EuSi	181	8.7177	0.0005	+1.459	0.064	-0.046	0.003	0.18	-0.64	0.11
968	J222640.42+545105.7	Gaia DR2 2004936299100544128	22 26 40.43	+54 51 05.87	kB9hA0mA2 bl4130	110	12.8230	0.0004	+0.485	0.027	-0.092	0.002	0.80	+0.45	0.13
969	J223811.04+533238.4	TYC 3983-3022-1	22 38 11.05	+53 32 38.43	A0 II-III CrEu*	224	12.1422	0.0007	+0.652	0.040	-0.015	0.008	0.50	+0.71	0.14
970	J224146.84+521705.7	TYC 3633-2112-1	22 41 46.59	+52 17 05.77	B8 III-IV Si	330	10.1168	0.0008	+0.729	0.033	-0.078	0.002	0.48	-1.05	0.11
971	J224704.08+343418.9	TYC 2744-2279-1	22 47 04.08	+34 34 18.92	A8 V SrEuSi	167	11.7583	0.0006	+1.252	0.042	+0.206	0.002	0.18	+2.07	0.09
972	J224927.99+584130.6	TYC 3996-813-1	22 49 27.99	+58 41 30.63	B8 IV Si (He-wk)	118	11.7313	0.0008	+0.966	0.136	+0.101	0.003	0.97	+0.68	0.31
973	J224939.77+341256.5	TYC 2757-2035-1	22 49 39.78	+34 12 56.60	A9 V SrCrEuSi	205	11.6114	0.0007	+1.036	0.033	+0.344	0.002	0.15	+1.54	0.09
974	J225245.93+531333.8	TYC 3984-1798-1	22 52 45.93	+53 13 33.81	B9 II-III EuSi	235	11.9652	0.0006	+0.408	0.035	-0.038	0.003	0.49	-0.47	0.19
975	J225518.40+560355.8	TYC 3989-187-1	22 55 18.40	+56 03 55.81	B9.5 IV Cr	298	11.0244	0.0008	+1.326	0.034	+0.064	0.003	0.57	+1.06	0.07
976	J225656.56+551017.2	TYC 3989-1590-1	22 56 56.56	+55 10 17.29	B8 III Si	174	11.7430	0.0005	+0.340	0.030	-0.171	0.004	0.91	-1.52	0.20
977	J225737.31+492342.7	Gaia DR2 1985841767843891200	22 57 37.33	+49 23 42.83	B8 IV-V Cr	130	13.3784	0.0006	+0.329	0.025	-0.071	0.003	0.41	+0.55	0.17
978	J225918.13+554247.1	Gaia DR2 2008961233205915776	22 59 18.13	+55 42 47.13	A1 III Cr	127	12.5886	0.0005	+0.598	0.030	+0.104	0.003	0.61	+0.86	0.12
979	J230159.71+575548.7	TYC 3993-58-1	23 01 59.71	+57 55 48.72	B9 V Eu	235	11.5508	0.0008	+0.953	0.031	-0.011	0.004	0.58	+0.87	0.09
980	J230905.79+523711.2	TYC 3998-2321-1	23 09 05.44	+52 37 11.29	B8 IV EuSi	786	9.3047	0.0005	+1.298	0.034	-0.033	0.003	0.33	-0.45	0.08
981	J231037.91+584007.7	TYC 4010-80-1	23 10 37.91	+58 40 07.75	B9.5 IV Cr	129	11.8740	0.0003	+0.638	0.046	-0.004	0.002	1.13	-0.23	0.16
982	J231205.86+550220.0	TYC 4002-294-1	23 12 05.86	+55 02 20.02	B8 III-IV Si	101	11.7994	0.0007	+0.539	0.028	-0.152	0.005	0.57	-0.11	0.12
983	J231211.12+564543.8	TYC 4006-501-1	23 12 11.12	+56 45 43.83	B9.5 V CrEu	134	11.8741	0.0007	+0.769	0.032	+0.060	0.003	0.65	+0.66	0.10
984	J231412.30+232336.9	TYC 2236-1035-1	23 14 12.31	+23 23 36.98	B9 IV V SrCrEu	161	11.2083	0.0013	+0.620	0.059	+0.112	0.002	0.23	-0.06	0.21
985	J231505.60+020916.4	HD 219348	23 15 05.61	+02 09 16.61	A7 V SrCrEu	577	9.7839	0.0004	+2.116	0.074	+0.325	0.004	0.16	+1.26	0.09
986	J231553.45+561845.4	TYC 4006-1320-1	23 15 53.32	+56 18 45.56	kB9.5hA3mA3 EuSi	168	11.0930	0.0049	+1.242	0.136	+0.084	0.007	0.60	+0.96	0.24
987	J232106.34+552607.8	TYC 4003-1466-1	23 21 06.35	+55 26 07.85	A0 IV-V Cr	248	11.3421	0.0007	+1.227	0.035	+0.057	0.002	0.27	+1.51	0.08
988	J232111.01+552314.2	TYC 4003-1670-1	23 21 11.12	+55 23 14.26	B9 IV-V bl4130	252	10.9044	0.0006	+0.917	0.043	-0.043	0.002	0.47	+0.24	0.11
989	J232126.71+551802.8	TYC 4003-1920-1	23 21 26.71	+55 18 02.88	A1 II-III Eu	221	11.6543	0.0006	+0.737	0.032	+0.015	0.003	0.38	+0.61	0.11
990	J232231.75+543933.2	Gaia DR2 1996099008739321088	23 22 31.76	+54 39 33.22	B9.5 V Cr	128	12.2867	0.0003	+0.711	0.027	+0.076	0.002	0.33	+1.21	0.10
991	J232507.50+432535.0	TYC 3242-686-1	23 25 07.22	+43 25 35.58	B8 IV Si (He-wk)	143	9.4734	0.0005	+1.713	0.053	-0.103	0.002	0.40	+0.24	0.08
992	J232524.99+561822.0	TYC 4007-1393-1	23 25 25.11	+56 18 22.51	B9 III-IV Si	207	10.8588	0.0008	+1.093	0.046	-0.021	0.002	0.75	+0.30	0.10
993	J232801.60+555306.9	TYC 4003-1156-1	23 28 01.69	+55 53 06.55	kB9hA3mA3 CrEuSi	244	10.9460	0.0006	+1.525	0.034	+0.049	0.002	0.43	+1.43	0.07
994	J232808.48+564209.1	TYC 4007-911-1	23 28 08.48	+56 42 09.09	kB9hA6mA5 CrEu	138	12.0462	0.0003	+1.010	0.032	+0.097	0.002	0.76	+1.31	0.09
995	J233101.92+564608.8	TYC 4007-1067-1	23 31 02.06	+56 46 09.63	B9 IV-V SrCrEuSi (He-wk)	182	10.7793	0.0007	+0.783	0.032	+0.241	0.003	0.57	-0.32	0.10
996	J233123.69+564325.5	TYC 4007-1207-1	23 31 23.92	+56 43 24.50	B8 IV bl4130	169	10.2869	0.0003	+1.056	0.039	-0.039	0.002	0.49	-0.09	0.10
997	J233539.01+555058.3	TYC 4004-1005-1	23 35 39.01	+55 50 58.30	B8 III-IV CrEuSi (He-wk)	102	11.3755	0.0014	+0.580	0.035	+0.046	0.005	0.48	-0.28	0.14
998	J234055.72+565101.4	TYC 4008-1298-1	23 40 55.73	+56 51 01.41	kB9hA1mA3 Cr	149	11.0877	0.0010	+0.581	0.234	-	-	-	-	-
999	J234915.69+560102.0	TYC 4005-947-1	23 49 15.70	+56 01 02.02	B9 IV-V Cr	267	10.9879	0.0010	+1.154	0.041	-0.049	0.004	0.42	+0.88	0.09
1000	J235351.09+525134.5	TYC 4001-1858-1	23 53 51.03	+52 51 35.48	B9 IV-V SrCrEu	302	10.7189	0.0006	+0.582	0.049	+0.124	0.003	0.44	-0.89	0.19



**Table A.1.** Essential data for our sample stars, sorted by increasing right ascension. The columns denote: (1) Internal identification number. (2) LAMOST identifier. (3) Alternativ identifier (HD number, TYC identifier or GAIA DR2 number). (4) Right ascension (J2000; GAIA DR2). (5) Declination (J2000; GAIA DR2). (6) Spectral type, as derived in this study. (7) Sloan  $g$  band S/N ratio of the analysed spectrum. (8)  $G$  mag (GAIA DR2). (9)  $G$  mag error. (10) Parallax (GAIA DR2). (11) Parallax error. (12) Dereddened colour index  $(BP - RP)_0$  (GAIA DR2). (13) Colour index error. (14) Absorption in the  $G$  band,  $A_G$ . (15) Intrinsic absolute magnitude in the  $G$  band,  $M_{G,0}$ . (16) Absolute magnitude error.

(1) No.	(2) ID_LAMOST	(3) ID_alt	(4) RA(J2000)	(5) Dec(J2000)	(6) SpT_final	(7) S/N $g$	(8) $G$ mag	(9) e_ $G$ mag	(10) pi (mas)	(11) e_pi	(12) $(BP - RP)_0$	(13) e_ $(BP - RP)_0$	(14) $A_G$	(15) $M_{G,0}$	(16) e_ $M_{G,0}$
1001	J235740.51+470001.7	TYC 3643-1589-1	23 57 40.27	+47 00 02.36	B9 IV CrSi	316	9.8410	0.0005	+1.215	0.048	-0.076	0.002	0.21	+0.06	0.10
1002	J235825.56+564224.7	TYC 4009-1911-1	23 58 25.56	+56 42 24.77	B9 III-IV Si	309	11.4611	0.0009	-0.142	0.088	-	-	-	-	-

Notes:

<sup>a</sup> Contained in the sample of strongly magnetic Ap stars of Scholz et al. (2019).

<sup>b</sup> Enhanced metal-lines but no traditional Si, Cr, Sr, or Eu peculiarities present.

<sup>c</sup> Spectrum indicative of an SB2 system (cf. Section 4.8).

<sup>d</sup> Cf. Table 2.

**Table B.1.** Masses ( $M$ ) and fractional ages on the main sequence ( $\tau$ ) for the 903 sample stars fulfilling our accuracy criteria. Values have been calculated assuming solar metallicity  $[Z] = 0.020$ . The columns denote: (1) Internal identification number. (2)  $M (M_{\odot})$ . (3)  $\sigma(M)-$ . (4)  $\sigma(M)+$ . (5)  $\tau$  (%). (6)  $\sigma(\tau)-$ . (7)  $\sigma(\tau)+$ .

(1) No.	(2) $M (M_{\odot})$	(3) $\sigma(M)-$	(4) $\sigma(M)+$	(5) $\tau$ (%)	(6) $\sigma(\tau)-$	(7) $\sigma(\tau)+$
1	1.947	0.038	0.021	62	0	4
2	1.697	0.023	0.023	39	4	7
3	3.325	0.322	0.377	99	25	33
4	2.414	0.067	0.052	73	4	9
5	2.730	0.092	0.008	72	4	9
6	2.584	0.066	0.109	74	8	4
7	2.823	0.169	0.341	100	29	19
8	1.849	0.051	0.050	48	10	9
9	2.470	0.102	0.073	43	9	5
10	2.902	0.056	0.117	68	7	8
11	2.792	0.072	0.110	61	10	12
12	1.899	0.075	0.069	52	11	10
13	2.106	0.023	0.043	44	9	3
14	2.352	0.049	0.013	68	4	4
15	2.356	0.091	0.029	29	10	14
16	2.884	0.164	0.227	80	13	10
17	2.074	0.036	0.055	75	4	4
18	2.455	0.099	0.107	76	4	9
19	2.601	0.259	0.077	89	5	44
20	1.925	0.051	0.068	68	7	0
21	2.615	0.077	0.055	81	5	10
22	2.246	0.088	0.239	100	29	12
23	2.538	0.029	0.044	17	9	10
24	2.001	0.030	0.040	85	5	0
25	1.947	0.040	0.020	56	3	3
26	1.993	0.046	0.029	16	12	11
28	2.266	0.004	0.090	36	11	7
29	2.129	0.055	0.045	76	4	5
30	2.197	0.164	0.104	89	10	37
31	2.404	0.066	0.062	76	8	5
32	2.644	0.106	0.130	35	16	12
33	2.987	0.114	0.127	98	11	12
34	2.538	0.085	0.182	35	30	12
35	1.769	0.070	0.080	30	27	17
36	2.084	0.046	0.055	60	7	4
37	2.994	0.340	0.122	88	5	52
38	4.012	0.218	0.172	97	11	18
39	2.219	0.080	0.070	68	4	8
40	2.219	0.049	0.017	19	6	13
41	2.083	0.045	0.046	21	16	9
42	3.037	0.153	0.118	82	5	10
43	2.765	0.111	0.441	100	37	12
44	3.256	0.433	0.134	88	5	60
46	2.486	0.193	0.062	88	5	36
47	2.174	0.051	0.091	61	13	0
48	2.218	0.089	0.060	72	4	9
49	2.584	0.066	0.154	74	15	4
50	3.266	0.089	0.181	84	13	5
52	2.720	0.071	0.118	45	15	12
53	2.219	0.048	0.046	61	3	7
54	3.492	0.064	0.194	67	20	0
56	2.653	0.107	0.220	100	25	12
57	2.777	0.092	0.058	51	10	10
58	2.562	0.069	0.053	81	5	5
59	3.194	0.141	0.120	79	9	10
60	1.947	0.123	0.136	5	2	17
61	2.006	0.013	0.032	68	7	0
63	2.734	0.089	0.063	61	7	7

**Table B.1.** Masses ( $M$ ) and fractional ages on the main sequence ( $\tau$ ) for the 903 sample stars fulfilling our accuracy criteria. Values have been calculated assuming solar metallicity  $[Z] = 0.020$ . The columns denote: (1) Internal identification number. (2)  $M (M_{\odot})$ . (3)  $\sigma(M)-$ . (4)  $\sigma(M)+$ . (5)  $\tau (\%)$ . (6)  $\sigma(\tau)-$ . (7)  $\sigma(\tau)+$ .

(1) No.	(2) $M (M_{\odot})$	(3) $\sigma(M)-$	(4) $\sigma(M)+$	(5) $\tau (\%)$	(6) $\sigma(\tau)-$	(7) $\sigma(\tau)+$
64	2.518	0.102	0.120	73	8	4
65	2.356	0.137	0.062	34	17	23
66	2.524	0.057	0.061	65	4	8
67	2.416	0.069	0.122	69	7	4
68	1.699	0.025	0.026	79	4	0
69	2.174	0.051	0.045	57	0	7
70	1.774	0.025	0.025	57	6	0
71	2.252	0.033	0.047	64	7	4
72	2.494	0.103	0.320	100	33	12
73	2.202	0.086	0.067	79	4	5
74	1.947	0.073	0.053	7	4	14
75	1.999	0.032	0.041	71	8	0
77	2.130	0.008	0.044	72	8	4
78	2.654	0.000	0.340	100	37	0
79	2.511	0.169	0.037	86	0	35
80	2.232	0.013	0.046	88	5	0
81	1.849	0.035	0.059	72	8	0
82	2.720	0.090	0.072	85	5	10
83	2.356	0.091	0.116	61	10	7
84	1.849	0.025	0.026	54	3	3
85	2.255	0.036	0.048	40	8	8
86	3.420	0.154	0.150	71	11	13
89	1.849	0.029	0.003	16	4	9
90	2.479	0.089	0.068	83	5	5
91	2.047	0.039	0.040	68	7	0
92	2.486	0.240	0.024	88	0	44
94	2.139	0.016	0.041	65	7	0
96	2.302	0.037	0.060	60	7	4
97	1.728	0.004	0.031	18	15	9
98	2.685	0.055	0.107	55	11	3
99	4.130	0.133	0.154	79	9	10
100	2.246	0.028	0.019	56	0	7
101	2.479	0.052	0.053	83	5	5
103	2.219	0.000	0.046	34	9	4
104	1.824	0.050	0.030	58	3	3
105	2.301	0.078	0.106	85	5	5
106	1.947	0.048	0.004	70	0	9
107	2.219	0.090	0.137	43	28	11
108	3.221	0.098	0.069	86	5	10
109	2.734	0.143	0.006	61	7	12
110	2.524	0.062	0.115	65	10	8
111	2.356	0.091	0.014	61	3	7
112	2.600	0.038	0.109	84	9	0
113	2.902	0.077	0.073	81	5	10
114	2.368	0.017	0.120	43	11	3
115	2.038	0.045	0.000	28	6	9
116	2.647	0.065	0.073	14	6	12
117	2.968	0.066	0.116	7	5	0
118	2.547	0.053	0.385	100	37	6
119	2.167	0.038	0.052	76	4	4
120	2.709	0.039	0.102	84	9	0
121	2.753	0.044	0.117	83	9	5
123	2.356	0.078	0.085	81	9	5
126	2.219	0.045	0.046	81	5	0
127	2.254	0.063	0.024	85	0	5
128	1.824	0.018	0.025	73	4	0
129	2.725	0.087	0.115	76	8	5
132	2.265	0.010	0.037	61	7	0

**Table B.1.** Masses ( $M$ ) and fractional ages on the main sequence ( $\tau$ ) for the 903 sample stars fulfilling our accuracy criteria. Values have been calculated assuming solar metallicity  $[Z] = 0.020$ . The columns denote: (1) Internal identification number. (2)  $M (M_{\odot})$ . (3)  $\sigma(M)-$ . (4)  $\sigma(M)+$ . (5)  $\tau (\%)$ . (6)  $\sigma(\tau)-$ . (7)  $\sigma(\tau)+$ .

(1)	(2)	(3)	(4)	(5)	(6)	(7)
No.	$M (M_{\odot})$	$\sigma(M)-$	$\sigma(M)+$	$\tau (\%)$	$\sigma(\tau)-$	$\sigma(\tau)+$
133	2.137	0.050	0.041	69	4	4
135	2.936	0.173	0.178	99	16	19
136	2.507	0.014	0.065	51	8	0
137	3.812	0.000	0.185	34	12	6
138	3.361	0.035	0.086	86	9	5
139	2.251	0.033	0.038	71	0	4
140	2.038	0.045	0.015	42	0	11
141	1.947	0.023	0.021	66	4	4
142	2.167	0.084	0.035	76	0	4
143	1.993	0.046	0.045	63	0	8
144	2.020	0.027	0.048	78	4	5
145	2.298	0.047	0.049	71	4	4
146	1.947	0.048	0.034	74	4	4
147	2.390	0.052	0.103	79	9	0
149	2.081	0.028	0.048	57	12	3
150	1.833	0.034	0.016	52	3	3
151	3.160	0.203	0.117	61	7	16
152	2.282	0.017	0.074	28	10	3
155	2.174	0.045	0.028	48	3	9
156	2.338	0.049	0.076	75	8	4
157	4.722	0.206	0.183	41	12	21
158	2.265	0.054	0.091	51	11	6
159	3.084	0.319	0.163	96	10	40
160	2.795	0.097	0.162	69	11	8
161	2.377	0.061	0.031	83	0	5
162	2.436	0.080	0.107	40	21	7
163	1.967	0.020	0.026	57	3	3
164	3.084	0.124	0.071	85	5	10
165	2.822	0.223	0.262	100	25	26
166	2.002	0.012	0.036	54	6	3
167	2.670	0.132	0.122	81	5	10
168	2.404	0.066	0.051	76	4	5
169	3.266	0.123	0.082	53	6	10
170	2.139	0.056	0.039	65	4	4
171	2.265	0.010	0.016	41	6	8
172	2.219	0.139	0.138	77	4	9
173	2.670	0.055	0.050	81	9	5
174	2.538	0.122	0.047	66	0	12
175	2.764	0.217	0.057	89	5	37
176	3.702	0.150	0.167	99	11	12
177	1.874	0.025	0.019	26	4	9
178	4.040	0.188	0.162	79	12	15
179	2.442	0.100	0.236	100	29	12
180	2.356	0.057	0.014	61	3	7
181	2.219	0.038	0.047	34	13	4
182	1.993	0.031	0.055	59	3	4
184	2.116	0.036	0.058	75	4	0
185	3.198	0.071	0.138	75	12	9
186	3.180	0.179	0.136	98	11	19
187	2.201	0.027	0.019	33	8	4
188	2.338	0.223	0.141	100	16	33
189	1.947	0.023	0.019	30	3	8
190	2.932	0.278	0.061	88	0	44
191	2.341	0.095	0.144	100	21	12
192	1.947	0.023	0.020	56	6	3
193	2.246	0.044	0.019	56	3	3
194	2.356	0.030	0.085	81	9	0
195	2.434	0.188	0.076	88	5	36
196	3.629	0.077	0.236	79	16	5

**Table B.1.** Masses ( $M$ ) and fractional ages on the main sequence ( $\tau$ ) for the 903 sample stars fulfilling our accuracy criteria. Values have been calculated assuming solar metallicity  $[Z] = 0.020$ . The columns denote: (1) Internal identification number. (2)  $M (M_{\odot})$ . (3)  $\sigma(M)-$ . (4)  $\sigma(M)+$ . (5)  $\tau$  (%). (6)  $\sigma(\tau)-$ . (7)  $\sigma(\tau)+$ .

(1) No.	(2) $M (M_{\odot})$	(3) $\sigma(M)-$	(4) $\sigma(M)+$	(5) $\tau$ (%)	(6) $\sigma(\tau)-$	(7) $\sigma(\tau)+$
197	2.467	0.102	0.071	69	4	8
198	2.246	0.172	0.392	100	37	26
199	2.219	0.048	0.046	61	7	4
200	1.966	0.019	0.027	61	3	4
201	2.902	0.064	0.066	38	11	10
202	2.679	0.041	0.103	77	12	0
203	2.356	0.031	0.106	57	9	3
204	2.387	0.031	0.106	9	6	0
205	2.174	0.045	0.057	51	8	3
206	2.670	0.000	0.112	81	13	0
207	2.538	0.024	0.107	66	14	0
208	2.441	0.094	0.174	79	13	5
209	2.472	0.121	0.066	65	4	8
210	2.083	0.003	0.039	72	4	4
211	2.814	0.320	0.088	94	5	46
212	2.821	0.222	0.259	100	25	26
213	2.390	0.064	0.051	79	4	5
214	2.780	0.060	0.188	38	22	10
215	2.174	0.035	0.045	68	4	4
216	2.356	0.091	0.000	10	7	11
218	1.993	0.046	0.045	67	4	4
220	2.825	0.058	0.104	80	9	5
221	1.875	0.026	0.024	56	3	3
222	2.419	0.068	0.001	61	0	12
223	2.040	0.047	0.082	71	8	0
224	2.316	0.000	0.061	82	5	0
225	3.366	0.100	0.090	61	15	7
226	2.083	0.090	0.108	80	9	5
227	2.562	0.107	0.108	81	9	5
228	2.083	0.045	0.004	68	0	4
229	2.174	0.037	0.072	54	9	0
230	2.562	0.024	0.108	81	9	0
231	1.907	0.033	0.040	52	8	3
232	1.947	0.023	0.021	66	4	4
233	2.404	0.057	0.158	76	8	0
234	2.174	0.016	0.045	32	8	8
235	2.174	0.045	0.026	32	4	11
236	2.219	0.048	0.027	54	3	7
237	2.493	0.052	0.069	79	4	5
238	2.601	0.259	0.077	89	5	44
239	2.441	0.051	0.052	79	4	5
240	2.377	0.021	0.064	83	9	0
241	2.538	0.027	0.063	88	5	0
242	2.488	0.098	0.050	40	2	13
243	1.966	0.038	0.027	61	0	4
244	1.799	0.075	0.055	70	0	9
245	2.347	0.096	0.017	71	0	9
246	2.787	0.067	0.115	72	15	4
247	2.654	0.054	0.080	84	9	5
248	2.790	0.348	0.104	91	5	53
249	2.391	0.060	0.102	5	2	5
250	2.390	0.097	0.185	100	21	12
251	2.493	0.089	0.145	79	16	5
252	2.089	0.006	0.050	64	7	0
253	2.538	0.059	0.116	83	9	5
254	2.733	0.342	0.081	91	5	53
255	2.265	0.046	0.001	38	4	7
257	1.886	0.037	0.013	68	0	4
258	2.326	0.061	0.030	78	0	5

**Table B.1.** Masses ( $M$ ) and fractional ages on the main sequence ( $\tau$ ) for the 903 sample stars fulfilling our accuracy criteria. Values have been calculated assuming solar metallicity  $[Z] = 0.020$ . The columns denote: (1) Internal identification number. (2)  $M (M_{\odot})$ . (3)  $\sigma(M)-$ . (4)  $\sigma(M)+$ . (5)  $\tau (\%)$ . (6)  $\sigma(\tau)-$ . (7)  $\sigma(\tau)+$ .

(1) No.	(2) $M (M_{\odot})$	(3) $\sigma(M)-$	(4) $\sigma(M)+$	(5) $\tau (\%)$	(6) $\sigma(\tau)-$	(7) $\sigma(\tau)+$
259	1.550	0.050	0.031	3	0	7
260	1.874	0.025	0.025	67	4	0
261	2.814	0.058	0.059	99	6	6
262	2.074	0.036	0.055	75	4	4
263	2.462	0.021	0.110	54	18	3
264	3.210	0.100	0.138	54	18	7
265	2.615	0.015	0.055	81	5	5
266	2.251	0.033	0.047	71	4	4
267	4.123	0.254	0.189	98	11	19
268	2.158	0.046	0.016	53	0	10
269	2.427	0.071	0.084	83	5	5
271	3.508	0.075	0.121	86	9	5
272	2.356	0.078	0.034	76	0	9
273	2.202	0.073	0.100	53	18	3
274	2.635	0.121	0.099	58	9	15
275	3.810	0.181	0.086	71	4	18
276	2.129	0.013	0.038	76	4	0
277	2.322	0.207	0.019	92	0	38
278	2.792	0.112	0.058	55	14	10
279	2.668	0.073	0.052	48	19	9
280	2.269	0.046	0.047	82	5	5
282	3.266	0.072	0.181	75	15	9
283	3.383	0.140	0.073	49	3	16
284	2.293	0.074	0.009	56	6	7
285	2.584	0.066	0.109	74	8	4
286	2.083	0.045	0.046	54	6	7
287	2.356	0.074	0.021	29	13	12
288	2.083	0.019	0.054	48	12	6
291	2.792	0.072	0.159	55	18	7
292	2.390	0.064	0.051	79	4	5
293	2.246	0.131	0.208	100	25	19
294	2.479	0.052	0.059	83	5	5
295	3.296	0.212	0.151	61	10	16
296	2.173	0.093	0.059	72	0	9
297	2.129	0.046	0.090	54	16	3
298	2.174	0.091	0.077	68	4	4
299	2.219	0.048	0.046	61	3	7
300	3.090	0.077	0.176	57	14	7
301	2.391	0.050	0.255	100	29	6
302	2.201	0.086	0.202	100	25	12
303	2.356	0.027	0.085	48	10	9
304	1.914	0.065	0.079	42	14	8
305	2.334	0.069	0.022	9	6	16
306	2.167	0.051	0.065	76	4	4
307	2.538	0.000	0.112	47	16	6
308	1.928	0.029	0.065	61	7	0
309	2.734	0.196	0.168	61	10	12
310	3.629	0.298	0.183	79	9	20
311	2.176	0.053	0.089	65	7	4
313	2.720	0.085	0.014	54	3	14
314	4.358	0.181	0.364	11	4	1
315	2.414	0.058	0.104	73	12	0
316	2.538	0.033	0.098	23	17	14
317	2.298	0.047	0.058	71	8	4
318	3.865	0.178	0.337	79	20	15
319	3.266	0.182	0.182	25	21	15
320	2.792	0.192	0.140	86	9	36
321	2.459	0.082	0.027	86	0	5



**Table B.1.** Masses ( $M$ ) and fractional ages on the main sequence ( $\tau$ ) for the 903 sample stars fulfilling our accuracy criteria. Values have been calculated assuming solar metallicity  $[Z] = 0.020$ . The columns denote: (1) Internal identification number. (2)  $M (M_{\odot})$ . (3)  $\sigma(M)-$ . (4)  $\sigma(M)+$ . (5)  $\tau (\%)$ . (6)  $\sigma(\tau)-$ . (7)  $\sigma(\tau)+$ .

(1) No.	(2) $M (M_{\odot})$	(3) $\sigma(M)-$	(4) $\sigma(M)+$	(5) $\tau (\%)$	(6) $\sigma(\tau)-$	(7) $\sigma(\tau)+$
322	2.368	0.017	0.120	43	14	3
323	3.629	0.130	0.189	30	19	15
324	2.202	0.035	0.030	79	4	0
325	2.708	0.109	0.247	100	25	12
326	2.720	0.125	0.182	54	25	7
327	2.178	0.052	0.087	69	7	4
328	2.087	0.049	0.050	68	7	0
329	2.880	0.172	0.163	100	16	19
330	1.749	0.025	0.025	22	10	7
331	2.493	0.137	0.048	5	0	16
332	1.968	0.033	0.025	46	5	3
333	2.325	0.060	0.031	18	16	6
334	2.599	0.052	0.249	100	29	6
335	2.038	0.071	0.091	76	8	0
336	2.902	0.024	0.182	32	24	6
337	1.993	0.076	0.090	75	4	4
338	1.993	0.069	0.045	3	0	9
339	2.670	0.070	0.050	81	5	10
340	3.252	0.068	0.195	31	14	10
341	2.083	0.036	0.090	72	8	0
342	2.218	0.088	0.060	72	4	9
343	3.084	0.133	0.084	36	13	15
344	1.500	0.000	0.018	24	10	8
346	2.821	0.274	0.081	89	5	44
348	2.047	0.042	0.082	68	7	0
350	2.377	0.061	0.050	83	5	5
352	2.071	0.042	0.058	53	8	6
353	1.874	0.050	0.073	63	7	4
354	2.846	0.126	0.111	72	11	9
355	3.053	0.151	0.031	25	12	17
356	2.293	0.047	0.299	100	33	6
357	2.720	0.143	0.014	51	10	13
358	2.005	0.039	0.033	61	3	4
359	2.615	0.107	0.152	81	13	5
360	3.812	0.042	0.132	23	11	8
361	2.416	0.060	0.108	69	11	4
362	2.083	0.078	0.046	60	0	7
363	2.252	0.033	0.099	64	10	0
364	2.902	0.102	0.088	24	15	14
365	2.797	0.099	0.105	65	10	12
366	2.352	0.100	0.064	68	4	8
367	2.038	0.114	0.095	42	20	14
368	2.411	0.055	0.052	54	9	7
369	2.158	0.000	0.249	100	33	0
370	2.562	0.069	0.108	81	9	5
371	2.265	0.046	0.037	58	3	7
372	2.782	0.103	0.147	76	8	9
373	2.219	0.090	0.082	86	5	5
374	2.265	0.047	0.091	61	10	4
375	2.905	0.185	0.124	2	0	18
376	2.562	0.069	0.108	81	9	5
377	2.129	0.076	0.051	54	6	7
378	2.391	0.145	0.218	100	25	19
379	1.913	0.039	0.037	89	5	0
380	2.316	0.103	0.092	82	5	5
381	2.219	0.090	0.065	3	0	4
382	2.130	0.043	0.048	72	8	0
383	2.873	0.327	0.082	94	5	46
384	2.792	0.083	0.110	86	9	5

**Table B.1.** Masses ( $M$ ) and fractional ages on the main sequence ( $\tau$ ) for the 903 sample stars fulfilling our accuracy criteria. Values have been calculated assuming solar metallicity  $[Z] = 0.020$ . The columns denote: (1) Internal identification number. (2)  $M (M_{\odot})$ . (3)  $\sigma(M)-$ . (4)  $\sigma(M)+$ . (5)  $\tau (\%)$ . (6)  $\sigma(\tau)-$ . (7)  $\sigma(\tau)+$ .

(1)	(2)	(3)	(4)	(5)	(6)	(7)
No.	$M (M_{\odot})$	$\sigma(M)-$	$\sigma(M)+$	$\tau (\%)$	$\sigma(\tau)-$	$\sigma(\tau)+$
385	2.414	0.049	0.104	73	8	0
386	2.720	0.120	0.130	85	9	10
387	1.869	0.020	0.032	59	6	3
388	2.083	0.009	0.046	76	4	0
389	2.219	0.061	0.046	58	0	11
390	2.326	0.072	0.057	87	5	5
391	2.048	0.082	0.082	64	4	8
392	2.299	0.080	0.057	64	4	8
393	3.728	0.160	0.345	71	15	9
394	2.158	0.046	0.022	53	0	10
395	2.101	0.046	0.048	37	14	7
396	2.825	0.155	0.088	80	4	15
398	2.219	0.048	0.012	10	7	13
399	2.041	0.012	0.042	57	6	0
400	2.520	0.053	0.065	69	7	4
401	2.341	0.048	0.305	100	33	6
402	2.038	0.045	0.046	60	7	4
403	2.404	0.060	0.059	51	8	10
404	2.787	0.093	0.115	72	8	9
405	2.538	0.196	0.117	88	10	36
406	2.585	0.067	0.108	70	8	8
407	2.764	0.217	0.086	89	10	37
408	2.427	0.050	0.052	83	5	5
409	2.825	0.105	0.077	80	9	10
410	3.699	0.252	0.113	79	4	20
411	2.202	0.028	0.044	53	6	6
412	2.408	0.031	0.078	86	5	0
413	2.942	0.233	0.333	100	29	26
414	2.080	0.040	0.042	71	4	4
415	2.680	0.103	0.040	52	8	13
416	2.518	0.114	0.053	73	0	14
417	2.902	0.052	0.120	57	9	11
418	2.902	0.182	0.120	48	14	20
419	2.219	0.049	0.046	19	11	17
420	2.538	0.120	0.005	39	8	13
421	3.629	0.127	0.373	67	25	8
422	2.589	0.148	0.257	66	24	4
423	1.774	0.025	0.025	48	8	3
424	3.143	0.125	0.193	71	11	9
425	2.047	0.042	0.075	68	7	0
426	1.808	0.034	0.016	45	7	3
427	2.097	0.059	0.032	82	0	5
428	3.089	0.129	0.066	86	5	10
430	1.774	0.025	0.040	60	7	4
431	2.532	0.105	0.098	83	5	10
433	2.493	0.103	0.039	79	0	10
434	2.902	0.166	0.101	17	14	17
435	2.720	0.076	0.088	34	14	14
436	1.907	0.009	0.040	52	8	3
437	2.055	0.062	0.032	29	14	12
438	2.383	0.181	0.024	88	0	36
439	2.787	0.089	0.170	72	15	4
440	1.824	0.050	0.032	3	1	2
442	2.265	0.034	0.097	58	14	3
443	3.084	0.133	0.143	57	12	11
444	2.518	0.052	0.066	73	4	4
445	3.336	0.137	0.443	100	33	12
446	2.466	0.050	0.072	73	8	4

**Table B.1.** Masses ( $M$ ) and fractional ages on the main sequence ( $\tau$ ) for the 903 sample stars fulfilling our accuracy criteria. Values have been calculated assuming solar metallicity  $[Z] = 0.020$ . The columns denote: (1) Internal identification number. (2)  $M (M_{\odot})$ . (3)  $\sigma(M)-$ . (4)  $\sigma(M)+$ . (5)  $\tau$  (%). (6)  $\sigma(\tau)-$ . (7)  $\sigma(\tau)+$ .

(1)	(2)	(3)	(4)	(5)	(6)	(7)
No.	$M (M_{\odot})$	$\sigma(M)-$	$\sigma(M)+$	$\tau$ (%)	$\sigma(\tau)-$	$\sigma(\tau)+$
447	2.219	0.048	0.084	65	10	0
448	2.169	0.000	0.050	40	13	2
449	3.081	0.063	0.185	72	15	4
450	3.005	0.105	0.261	75	15	9
451	2.462	0.058	0.076	54	6	7
452	3.231	0.408	0.305	97	20	48
453	2.441	0.085	0.066	47	10	12
454	2.654	0.054	0.430	100	37	6
455	1.881	0.032	0.044	45	9	5
456	2.538	0.020	0.100	74	8	0
457	2.301	0.082	0.133	85	9	5
458	2.902	0.092	0.127	7	5	11
459	3.057	0.348	0.096	88	5	52
460	2.507	0.089	0.070	51	13	6
461	2.351	0.058	0.068	60	10	4
462	2.709	0.109	0.407	100	37	12
463	2.471	0.115	0.067	62	0	12
464	1.849	0.025	0.050	72	4	4
465	2.600	0.068	0.109	84	9	5
466	2.256	0.037	0.047	68	4	4
467	2.709	0.162	0.141	84	9	16
468	2.538	0.030	0.078	33	13	11
469	2.265	0.046	0.037	54	6	7
470	3.266	0.116	0.046	53	6	18
471	2.246	0.088	0.239	100	29	12
472	2.562	0.158	0.172	81	9	10
473	2.538	0.122	0.187	74	12	4
474	3.189	0.307	0.274	88	14	44
475	3.776	0.206	0.138	62	13	21
478	3.348	0.141	0.209	71	8	13
479	2.902	0.204	0.055	64	4	21
480	2.420	0.073	0.000	65	0	8
481	1.993	0.046	0.015	56	0	7
482	2.265	0.057	0.000	7	5	12
483	1.924	0.025	0.023	21	6	9
484	2.472	0.179	0.152	65	7	12
485	2.347	0.049	0.069	71	8	4
486	2.653	0.159	0.302	100	29	19
487	3.407	0.076	0.222	75	15	9
488	2.122	0.039	0.051	71	4	4
489	2.441	0.051	0.091	79	4	5
490	2.902	0.036	0.208	48	21	6
491	2.520	0.164	0.118	69	4	8
492	1.674	0.052	0.025	3	0	9
493	2.968	0.066	0.146	7	5	6
494	1.829	0.030	0.045	33	11	4
496	3.084	0.016	0.182	76	16	0
497	2.265	0.046	0.091	18	15	11
498	3.056	0.456	0.191	93	10	63
499	2.038	0.036	0.006	57	6	3
500	2.420	0.064	0.052	65	4	8
501	2.720	0.182	0.130	43	22	18
502	2.437	0.106	0.104	9	6	10
503	3.199	0.067	0.430	100	37	6
504	2.083	0.121	0.149	68	4	4
505	2.063	0.025	0.066	25	13	10
506	1.947	0.048	0.060	50	8	6
507	2.325	0.048	0.036	52	11	3
510	2.370	0.019	0.050	65	7	4

**Table B.1.** Masses ( $M$ ) and fractional ages on the main sequence ( $\tau$ ) for the 903 sample stars fulfilling our accuracy criteria. Values have been calculated assuming solar metallicity  $[Z] = 0.020$ . The columns denote: (1) Internal identification number. (2)  $M (M_{\odot})$ . (3)  $\sigma(M)-$ . (4)  $\sigma(M)+$ . (5)  $\tau$  (%). (6)  $\sigma(\tau)-$ . (7)  $\sigma(\tau)+$ .

(1)	(2)	(3)	(4)	(5)	(6)	(7)
No.	$M (M_{\odot})$	$\sigma(M)-$	$\sigma(M)+$	$\tau$ (%)	$\sigma(\tau)-$	$\sigma(\tau)+$
511	2.630	0.053	0.090	55	14	7
512	2.471	0.060	0.067	62	10	8
513	3.689	0.130	0.127	16	12	11
514	2.302	0.050	0.054	60	3	7
515	2.334	0.069	0.022	9	6	11
516	1.824	0.025	0.030	65	7	0
517	2.562	0.107	0.108	81	9	5
518	2.151	0.118	0.103	88	10	29
519	2.479	0.089	0.068	83	5	5
520	1.749	0.149	0.100	3	0	23
522	3.022	0.257	0.133	86	9	42
523	2.122	0.082	0.045	71	0	9
524	4.905	0.221	0.183	34	15	17
525	2.038	0.045	0.049	67	4	0
526	2.507	0.089	0.128	51	21	13
527	2.479	0.102	0.032	83	0	10
529	2.219	0.045	0.047	31	10	10
530	2.202	0.035	0.063	79	4	5
531	2.584	0.118	0.136	74	8	9
532	1.874	0.005	0.027	63	7	0
534	3.005	0.105	0.079	75	8	9
535	2.601	0.259	0.077	89	5	44
536	2.514	0.102	0.067	54	11	14
538	3.026	0.132	0.058	46	3	19
539	2.823	0.114	0.426	100	37	12
540	2.219	0.052	0.059	77	4	5
541	2.562	0.158	0.172	81	9	10
542	1.833	0.034	0.033	52	6	3
543	2.246	0.131	0.208	100	25	19
544	3.150	0.131	0.116	64	10	12
545	3.084	0.152	0.182	54	16	10
546	1.874	0.025	0.050	47	10	6
547	2.338	0.049	0.076	75	8	4
548	1.981	0.073	0.057	78	4	5
549	2.303	0.084	0.111	68	4	8
550	2.943	0.097	0.141	75	12	4
551	2.791	0.071	0.111	58	19	7
552	2.083	0.095	0.119	36	31	15
553	3.312	0.108	0.176	49	18	9
554	2.356	0.091	0.116	64	16	4
555	2.571	0.215	0.240	77	12	9
556	3.180	0.096	0.094	7	3	14
557	2.835	0.289	0.084	96	5	39
558	2.792	0.107	0.110	61	7	16
559	4.358	0.361	0.364	34	27	23
560	3.447	0.230	0.143	55	11	23
561	2.197	0.066	0.035	89	5	5
562	2.879	0.087	0.089	47	10	12
563	2.325	0.060	0.044	52	8	6
564	2.299	0.044	0.057	64	7	4
565	2.763	0.064	0.231	47	26	6
566	2.167	0.045	0.065	76	4	4
567	2.936	0.115	0.107	99	11	12
569	2.048	0.055	0.082	64	7	4
570	1.824	0.035	0.055	69	7	0
571	2.584	0.194	0.159	98	16	25
572	2.538	0.097	0.107	59	20	7
574	2.866	0.146	0.102	33	15	19

**Table B.1.** Masses ( $M$ ) and fractional ages on the main sequence ( $\tau$ ) for the 903 sample stars fulfilling our accuracy criteria. Values have been calculated assuming solar metallicity  $[Z] = 0.020$ . The columns denote: (1) Internal identification number. (2)  $M (M_{\odot})$ . (3)  $\sigma(M)-$ . (4)  $\sigma(M)+$ . (5)  $\tau (\%)$ . (6)  $\sigma(\tau)-$ . (7)  $\sigma(\tau)+$ .

(1) No.	(2) $M (M_{\odot})$	(3) $\sigma(M)-$	(4) $\sigma(M)+$	(5) $\tau (\%)$	(6) $\sigma(\tau)-$	(7) $\sigma(\tau)+$
575	1.924	0.125	0.165	48	31	9
576	2.219	0.045	0.079	68	7	4
578	2.038	0.070	0.046	53	6	10
581	2.219	0.136	0.145	61	10	7
582	2.584	0.066	0.054	74	4	4
583	3.024	0.189	0.242	61	12	16
584	2.547	0.000	0.470	100	40	0
585	2.408	0.115	0.102	86	5	29
586	2.129	0.091	0.090	38	14	13
587	2.720	0.071	0.112	45	9	6
588	2.419	0.068	0.053	61	3	12
589	2.377	0.158	0.171	83	9	21
590	2.104	0.048	0.032	25	14	10
591	2.352	0.194	0.186	68	7	8
592	1.799	0.040	0.050	37	16	7
593	2.562	0.158	0.230	81	13	10
595	2.390	0.101	0.142	79	9	5
596	2.411	0.055	0.060	54	3	10
597	4.370	0.273	0.535	76	19	5
599	2.510	0.217	0.060	91	5	37
600	2.087	0.049	0.043	68	4	4
601	2.572	0.079	0.058	51	8	6
602	2.038	0.039	0.045	76	8	0
603	2.943	0.059	0.141	75	12	9
604	2.884	0.102	0.153	80	13	5
606	2.749	0.102	0.116	98	11	12
607	2.174	0.136	0.129	51	22	10
608	2.881	0.281	0.435	100	33	33
609	2.639	0.119	0.099	70	8	9
610	2.538	0.021	0.058	39	13	7
611	3.031	0.080	0.137	41	16	8
612	2.356	0.061	0.055	48	10	9
614	2.219	0.045	0.046	65	7	4
617	3.465	0.199	0.186	7	3	4
618	2.303	0.038	0.067	68	11	4
619	2.943	0.103	0.141	75	12	9
621	2.255	0.036	0.101	40	12	8
622	2.547	0.053	0.301	100	33	6
623	2.096	0.083	0.123	29	25	14
625	2.404	0.066	0.051	76	4	5
626	1.724	0.124	0.100	3	1	23
627	2.084	0.003	0.005	60	3	4
628	2.419	0.068	0.095	61	13	12
629	1.810	0.030	0.039	67	4	0
631	2.508	0.053	0.076	76	8	5
632	2.589	0.126	0.054	66	7	12
633	2.211	0.082	0.082	45	9	12
634	2.792	0.192	0.140	86	9	36
635	2.356	0.091	0.182	61	22	4
636	2.518	0.063	0.066	73	4	9
637	2.178	0.049	0.041	69	0	8
638	2.213	0.039	0.052	76	8	0
639	2.562	0.030	0.053	81	5	5
640	3.465	0.199	0.164	7	3	13
641	2.902	0.077	0.135	81	13	5
642	2.960	0.281	0.306	86	14	42
643	1.724	0.124	0.142	55	20	7
644	1.899	0.058	0.069	55	9	3
645	2.710	0.216	0.138	89	10	37

**Table B.1.** Masses ( $M$ ) and fractional ages on the main sequence ( $\tau$ ) for the 903 sample stars fulfilling our accuracy criteria. Values have been calculated assuming solar metallicity  $[Z] = 0.020$ . The columns denote: (1) Internal identification number. (2)  $M (M_{\odot})$ . (3)  $\sigma(M)-$ . (4)  $\sigma(M)+$ . (5)  $\tau (\%)$ . (6)  $\sigma(\tau)-$ . (7)  $\sigma(\tau)+$ .

(1)	(2)	(3)	(4)	(5)	(6)	(7)
No.	$M (M_{\odot})$	$\sigma(M)-$	$\sigma(M)+$	$\tau (\%)$	$\sigma(\tau)-$	$\sigma(\tau)+$
646	2.129	0.013	0.045	76	4	0
647	3.570	0.152	0.240	71	11	9
648	2.598	0.305	0.327	100	29	41
650	2.419	0.068	0.053	61	10	8
651	2.084	0.077	0.055	60	3	7
652	2.902	0.222	0.364	68	23	13
653	3.018	0.168	0.248	72	15	9
654	2.038	0.096	0.101	60	12	4
655	2.624	0.169	0.096	77	4	15
656	2.316	0.038	0.061	82	5	0
657	2.356	0.000	0.099	57	12	0
658	2.835	0.115	0.187	51	19	13
659	2.455	0.099	0.116	76	8	5
660	2.252	0.034	0.051	64	7	4
661	2.494	0.103	0.320	100	33	12
662	3.439	0.154	0.151	61	10	12
663	2.720	0.082	0.120	76	12	4
664	4.284	0.306	0.263	77	8	20
665	1.993	0.094	0.075	71	0	9
666	3.266	0.190	0.076	38	9	22
668	2.416	0.060	0.056	69	7	4
669	3.776	0.111	0.249	62	16	8
671	1.924	0.050	0.036	5	3	8
672	2.782	0.144	0.120	76	8	9
673	2.293	0.074	0.069	56	6	7
674	2.414	0.067	0.104	73	8	4
675	2.942	0.119	0.264	100	25	12
679	2.516	0.054	0.075	58	9	7
680	2.129	0.055	0.062	81	5	0
681	2.596	0.116	0.124	40	8	20
682	2.390	0.101	0.148	79	9	5
683	1.874	0.033	0.039	50	5	3
684	2.538	0.066	0.101	70	8	4
685	2.963	0.082	0.121	30	18	15
686	2.173	0.090	0.105	72	8	4
687	2.412	0.061	0.050	58	6	11
688	2.463	0.101	0.075	58	6	7
690	2.151	0.157	0.046	88	5	36
691	2.652	0.114	0.068	9	7	12
692	2.265	0.003	0.091	34	15	0
693	2.494	0.152	0.283	100	29	19
694	2.750	0.106	0.116	33	14	14
695	1.993	0.069	0.055	50	8	9
697	2.368	0.065	0.022	43	9	11
698	2.455	0.117	0.038	76	0	9
699	2.055	0.062	0.074	29	18	14
700	2.083	0.045	0.046	54	9	7
701	2.493	0.155	0.107	79	4	10
702	2.094	0.058	0.086	49	18	6
703	2.219	0.045	0.080	58	9	3
704	2.572	0.065	0.058	51	6	6
705	2.584	0.066	0.054	74	4	4
706	1.808	0.034	0.016	45	7	5
707	2.919	0.267	0.195	98	16	33
708	2.265	0.091	0.105	58	19	3
710	2.472	0.116	0.113	65	10	4
711	2.174	0.052	0.091	77	8	5
712	2.219	0.029	0.046	48	10	3
713	1.924	0.050	0.044	38	13	7

**Table B.1.** Masses ( $M$ ) and fractional ages on the main sequence ( $\tau$ ) for the 903 sample stars fulfilling our accuracy criteria. Values have been calculated assuming solar metallicity  $[Z] = 0.020$ . The columns denote: (1) Internal identification number. (2)  $M (M_{\odot})$ . (3)  $\sigma(M)-$ . (4)  $\sigma(M)+$ . (5)  $\tau (\%)$ . (6)  $\sigma(\tau)-$ . (7)  $\sigma(\tau)+$ .

(1)	(2)	(3)	(4)	(5)	(6)	(7)
No.	$M (M_{\odot})$	$\sigma(M)-$	$\sigma(M)+$	$\tau (\%)$	$\sigma(\tau)-$	$\sigma(\tau)+$
714	2.174	0.058	0.091	81	9	0
715	1.899	0.025	0.020	41	2	8
716	2.538	0.075	0.000	59	3	11
717	2.720	0.041	0.126	76	12	4
719	2.455	0.190	0.145	76	4	14
720	2.427	0.050	0.032	83	0	5
721	2.356	0.053	0.000	34	5	9
722	2.811	0.240	0.183	83	9	34
723	2.763	0.217	0.280	100	25	26
724	2.101	0.018	0.035	37	11	0
725	3.197	0.374	0.495	100	33	41
726	1.967	0.020	0.040	57	6	3
727	2.420	0.001	0.052	65	13	0
728	1.774	0.025	0.025	67	4	0
730	2.404	0.057	0.062	76	8	5
731	2.902	0.182	0.092	48	10	20
732	2.211	0.042	0.066	45	11	6
733	1.899	0.025	0.048	35	11	4
734	2.630	0.239	0.080	87	5	43
735	2.538	0.083	0.086	79	9	5
736	2.265	0.046	0.001	32	2	11
737	1.919	0.020	0.023	45	5	5
738	2.913	0.102	0.047	82	0	10
739	2.160	0.129	0.105	80	4	10
740	3.084	0.133	0.159	54	11	10
741	2.295	0.076	0.049	47	5	12
742	2.589	0.075	0.151	66	19	4
743	2.698	0.113	0.042	66	4	12
744	2.577	0.136	0.113	55	14	14
745	2.293	0.047	0.009	56	6	7
747	2.623	0.282	0.134	91	10	45
748	2.719	0.328	0.146	95	10	47
749	3.375	0.140	0.148	35	15	17
750	2.356	0.057	0.060	64	4	8
751	1.947	0.073	0.082	83	5	5
752	1.835	0.036	0.039	56	6	3
753	2.720	0.022	0.182	68	17	4
754	2.710	0.163	0.138	89	10	30
755	2.538	0.085	0.019	19	12	13
756	2.083	0.077	0.084	72	4	4
758	1.849	0.050	0.052	54	9	3
759	2.464	0.108	0.074	31	13	15
760	2.668	0.136	0.124	48	19	12
761	1.999	0.100	0.130	71	8	0
763	2.850	0.152	0.052	61	3	20
764	2.615	0.077	0.055	81	5	5
765	2.326	0.048	0.030	78	4	5
766	2.601	0.259	0.077	89	5	44
767	1.849	0.026	0.050	51	8	3
768	3.997	0.185	0.026	24	11	19
769	2.083	0.090	0.095	36	22	15
770	1.749	0.050	0.025	3	0	7
771	1.924	0.025	0.034	25	9	5
772	2.902	0.248	0.154	91	10	37
773	1.937	0.071	0.056	77	4	5
774	2.782	0.112	0.058	76	4	14
775	1.874	0.075	0.073	67	4	4
776	2.219	0.107	0.128	68	7	4
777	2.511	0.169	0.090	86	5	35

**Table B.1.** Masses ( $M$ ) and fractional ages on the main sequence ( $\tau$ ) for the 903 sample stars fulfilling our accuracy criteria. Values have been calculated assuming solar metallicity  $[Z] = 0.020$ . The columns denote: (1) Internal identification number. (2)  $M (M_{\odot})$ . (3)  $\sigma(M)-$ . (4)  $\sigma(M)+$ . (5)  $\tau$  (%). (6)  $\sigma(\tau)-$ . (7)  $\sigma(\tau)+$ .

(1)	(2)	(3)	(4)	(5)	(6)	(7)
No.	$M (M_{\odot})$	$\sigma(M)-$	$\sigma(M)+$	$\tau$ (%)	$\sigma(\tau)-$	$\sigma(\tau)+$
778	2.846	0.064	0.110	72	8	9
779	1.742	0.018	0.013	34	5	6
781	2.720	0.143	0.072	54	9	14
782	1.799	0.075	0.030	7	4	21
785	2.420	0.078	0.052	65	4	8
786	2.467	0.168	0.148	69	0	13
787	2.520	0.101	0.118	69	14	4
788	2.523	0.111	0.066	61	7	12
789	2.064	0.071	0.065	44	13	8
790	2.441	0.085	0.091	79	4	5
791	2.246	0.072	0.116	56	16	7
792	2.538	0.101	0.073	7	5	11
793	2.902	0.182	0.055	61	3	20
794	2.884	0.175	0.200	80	20	21
795	2.265	0.091	0.091	72	8	4
796	2.081	0.074	0.008	57	0	11
797	3.755	0.419	0.378	97	20	40
798	3.326	0.444	0.212	88	10	60
799	2.639	0.119	0.099	70	8	9
800	2.600	0.062	0.120	84	9	0
802	2.825	0.155	0.135	80	4	15
803	3.057	0.155	0.186	50	18	9
804	2.122	0.039	0.051	71	4	4
806	2.347	0.048	0.023	63	7	4
807	2.738	0.044	0.057	69	7	8
808	2.391	0.145	0.218	100	25	19
809	2.577	0.070	0.143	55	16	3
810	1.947	0.123	0.136	56	18	7
811	2.219	0.045	0.058	48	8	6
812	2.356	0.063	0.013	57	6	7
813	2.538	0.101	0.073	7	5	15
814	1.799	0.075	0.050	62	0	8
815	3.266	0.182	0.070	75	4	14
817	2.148	0.065	0.071	83	5	5
818	3.019	0.062	0.141	64	16	4
819	2.356	0.018	0.099	76	8	0
820	2.089	0.051	0.050	64	7	4
821	3.084	0.182	0.182	27	19	21
822	2.902	0.048	0.117	68	11	4
823	2.083	0.045	0.011	43	5	5
824	2.902	0.135	0.187	86	14	5
825	1.993	0.046	0.009	47	5	6
826	2.219	0.045	0.046	48	3	9
827	2.414	0.000	0.053	73	8	0
828	1.874	0.025	0.025	63	4	0
829	2.599	0.052	0.249	100	29	6
830	2.821	0.113	0.134	100	16	12
831	2.223	0.094	0.103	82	5	5
833	2.340	0.139	0.191	100	21	19
834	2.493	0.137	0.118	5	2	5
835	2.720	0.071	0.054	43	12	14
838	2.547	0.000	0.301	100	33	0
839	2.511	0.169	0.090	86	5	35
840	2.112	0.074	0.068	53	6	6
841	3.143	0.187	0.123	71	11	13
842	2.792	0.122	0.140	86	9	5
843	2.693	0.155	0.074	74	0	14
844	2.083	0.046	0.046	34	8	11
845	2.941	0.232	0.334	100	29	26



**Table B.1.** Masses ( $M$ ) and fractional ages on the main sequence ( $\tau$ ) for the 903 sample stars fulfilling our accuracy criteria. Values have been calculated assuming solar metallicity  $[Z] = 0.020$ . The columns denote: (1) Internal identification number. (2)  $M (M_{\odot})$ . (3)  $\sigma(M)-$ . (4)  $\sigma(M)+$ . (5)  $\tau (\%)$ . (6)  $\sigma(\tau)-$ . (7)  $\sigma(\tau)+$ .

(1) No.	(2) $M (M_{\odot})$	(3) $\sigma(M)-$	(4) $\sigma(M)+$	(5) $\tau (\%)$	(6) $\sigma(\tau)-$	(7) $\sigma(\tau)+$
846	3.447	0.479	0.369	4	1	13
847	2.408	0.139	0.078	86	5	10
848	1.724	0.025	0.025	25	8	10
849	3.629	0.363	0.274	22	18	25
850	1.947	0.040	0.046	59	6	3
851	2.404	0.000	0.062	76	8	0
852	1.874	0.000	0.025	30	12	4
853	2.377	0.108	0.057	83	0	10
854	2.129	0.091	0.062	76	0	9
855	2.232	0.019	0.046	78	4	0
856	2.466	0.062	0.042	73	0	9
859	2.356	0.241	0.200	91	14	45
860	1.799	0.028	0.025	50	3	6
861	1.929	0.030	0.018	81	0	5
862	2.792	0.102	0.110	61	7	16
863	2.038	0.045	0.045	13	9	11
864	1.967	0.093	0.116	57	9	7
866	1.993	0.119	0.090	3	0	16
867	2.081	0.043	0.003	57	3	7
870	1.976	0.055	0.062	41	12	11
871	2.208	0.125	0.057	5	2	11
872	1.874	0.025	0.033	47	5	3
873	2.996	0.276	0.188	16	13	26
874	2.626	0.119	0.108	52	11	10
875	1.824	0.050	0.050	58	3	3
876	3.319	0.417	0.497	7	3	3
877	2.356	0.031	0.048	54	9	3
878	1.947	0.048	0.034	74	0	4
879	2.130	0.047	0.089	72	4	4
880	2.173	0.090	0.105	86	9	5
881	3.997	0.368	0.273	45	34	23
882	1.947	0.048	0.046	12	9	13
883	1.993	0.003	0.045	53	8	3
884	2.630	0.083	0.134	87	9	5
885	1.899	0.025	0.025	8	5	5
886	2.471	0.009	0.067	62	10	4
887	1.993	0.000	0.045	22	10	4
888	3.160	0.141	0.106	61	7	16
889	1.862	0.063	0.045	44	11	8
890	2.289	0.024	0.075	75	8	0
891	2.038	0.045	0.045	60	3	7
892	2.219	0.045	0.047	34	15	9
893	2.479	0.052	0.068	83	5	5
894	2.219	0.045	0.046	29	11	7
895	4.173	0.233	0.366	40	34	20
896	2.342	0.000	0.281	100	33	0
897	2.734	0.187	0.087	86	5	36
898	1.947	0.023	0.020	53	6	3
899	2.251	0.033	0.047	71	4	4
900	2.038	0.045	0.045	38	11	7
901	1.966	0.038	0.027	61	0	4
902	1.993	0.046	0.003	33	2	9
903	1.983	0.036	0.010	22	6	9
904	2.356	0.014	0.014	61	3	4
905	2.356	0.227	0.214	81	9	27
906	3.405	0.338	0.369	100	25	33
907	2.720	0.094	0.014	51	6	13
908	3.290	0.286	0.181	86	9	43
909	1.899	0.025	0.025	46	3	6

**Table B.1.** Masses ( $M$ ) and fractional ages on the main sequence ( $\tau$ ) for the 903 sample stars fulfilling our accuracy criteria. Values have been calculated assuming solar metallicity  $[Z] = 0.020$ . The columns denote: (1) Internal identification number. (2)  $M (M_{\odot})$ . (3)  $\sigma(M)-$ . (4)  $\sigma(M)+$ . (5)  $\tau$  (%). (6)  $\sigma(\tau)-$ . (7)  $\sigma(\tau)+$ .

(1) No.	(2) $M (M_{\odot})$	(3) $\sigma(M)-$	(4) $\sigma(M)+$	(5) $\tau$ (%)	(6) $\sigma(\tau)-$	(7) $\sigma(\tau)+$
910	2.523	0.112	0.122	61	23	4
911	2.538	0.071	0.100	74	8	0
912	2.523	0.111	0.068	61	7	8
913	1.649	0.024	0.009	43	9	5
914	2.463	0.051	0.075	58	12	3
915	2.507	0.095	0.031	51	3	13
916	2.538	0.021	0.000	31	8	8
917	3.155	0.071	0.111	86	9	5
918	2.902	0.217	0.181	61	15	11
919	1.849	0.025	0.044	72	0	4
920	3.084	0.094	0.110	81	9	5
922	1.874	0.025	0.025	79	4	0
923	3.344	0.078	0.121	10	6	6
924	2.441	0.051	0.091	79	4	5
925	2.219	0.017	0.046	58	9	0
926	3.812	0.067	0.185	54	11	7
927	1.799	0.025	0.024	47	5	6
928	2.581	0.065	0.054	58	6	11
929	3.082	0.063	0.145	64	10	4
930	2.902	0.051	0.040	14	10	10
931	2.390	0.046	0.051	47	5	9
932	1.699	0.000	0.025	33	8	2
933	2.846	0.000	0.111	72	11	0
934	2.356	0.018	0.048	76	4	0
935	2.511	0.052	0.065	86	5	5
936	3.849	0.037	0.156	35	15	7
937	2.902	0.077	0.054	76	8	9
938	2.792	0.168	0.234	86	14	29
941	3.290	0.046	0.157	86	14	0
944	2.538	0.020	0.047	74	8	0
945	3.150	0.000	0.162	64	21	0
946	6.682	0.291	0.508	44	22	22
947	2.664	0.054	0.056	25	13	5
948	2.720	0.035	0.130	57	9	3
949	2.303	0.005	0.062	68	7	4
950	2.356	0.009	0.110	76	12	0
951	2.823	0.169	0.359	100	33	19
952	2.734	0.089	0.006	61	7	7
953	1.799	0.025	0.025	12	9	12
954	2.823	0.114	0.293	100	29	12
955	3.084	0.127	0.182	68	14	8
957	3.391	0.125	0.074	7	2	9
958	3.629	0.317	0.183	53	13	22
960	2.356	0.031	0.007	26	9	9
961	2.902	0.302	0.154	91	10	45
962	2.902	0.148	0.127	2	0	4
963	2.129	0.046	0.000	22	4	9
965	2.720	0.090	0.014	51	6	13
966	2.097	0.077	0.078	82	5	5
967	3.088	0.265	0.168	91	14	37
968	2.763	0.078	0.072	47	7	12
969	2.412	0.056	0.102	58	9	7
970	3.463	0.331	0.152	93	10	38
971	1.783	0.009	0.016	26	11	7
972	2.289	0.115	0.152	75	8	4
973	1.874	0.033	0.025	70	0	4
974	2.994	0.229	0.161	88	14	36
975	2.174	0.016	0.045	57	6	3

**Table B.1.** Masses ( $M$ ) and fractional ages on the main sequence ( $\tau$ ) for the 903 sample stars fulfilling our accuracy criteria. Values have been calculated assuming solar metallicity  $[Z] = 0.020$ . The columns denote: (1) Internal identification number. (2)  $M (M_{\odot})$ . (3)  $\sigma(M)-$ . (4)  $\sigma(M)+$ . (5)  $\tau (\%)$ . (6)  $\sigma(\tau)-$ . (7)  $\sigma(\tau)+$ .

(1)	(2)	(3)	(4)	(5)	(6)	(7)
No.	$M (M_{\odot})$	$\sigma(M)-$	$\sigma(M)+$	$\tau (\%)$	$\sigma(\tau)-$	$\sigma(\tau)+$
976	4.344	0.547	0.306	89	14	52
977	2.626	0.088	0.108	52	15	6
978	2.219	0.045	0.046	68	4	4
979	2.356	0.031	0.048	51	8	6
980	3.022	0.090	0.067	86	5	10
981	2.870	0.161	0.032	83	0	16
982	3.266	0.056	0.190	56	14	11
983	2.352	0.054	0.012	68	0	8
984	2.391	0.049	0.287	100	33	6
985	1.981	0.034	0.012	78	0	5
986	2.219	0.107	0.084	61	3	7
987	2.055	0.018	0.028	29	5	5
988	2.740	0.101	0.000	65	0	12
989	2.420	0.064	0.052	65	4	8
990	2.112	0.029	0.046	53	8	3
991	2.902	0.052	0.049	54	6	7
992	2.639	0.101	0.004	70	4	9
993	2.083	0.000	0.046	34	8	4
994	2.083	0.045	0.029	48	3	9
995	2.693	0.055	0.056	98	6	6
996	2.825	0.058	0.104	80	9	5
997	2.547	0.000	0.301	100	33	0
999	2.418	0.050	0.120	43	22	3
1001	2.854	0.057	0.103	69	11	4

**Table C.1.** Standard stars of the *liblamost* library. The columns denote: (1) Original LAMOST spectrum FITS file name. (2) Identification number from the *Kepler* input catalogue (Kepler Mission Team 2009). (3) 2MASS identifier (Skrutskie et al. 2006). (4) Spectral type, as derived by Gray et al. (2016). (5) Sloan g band S/N ratio of the spectrum according to Gray et al. (2016). (6) Quality flag according to Gray et al. (2016). (7) Suitability estimate as an MKK standard star (1 = suitable to a lesser extent; 2 = suitable; 3 = fully suitable).

(1) ID_Spec	(2) ID_KIC	(3) ID_2MASS	(4) SpT	(5) S/N	(6) quality flag	(7) suitability
spec-56914-KP193637N444141V01_sp15-029	KIC09472174	19383260+4603591	B3 IV	224	vgood	1
spec-56561-KP195920N454621V01_sp01-071	KIC08324482	19570365+4413556	B3 V	314	vgood	2-3 <sup>a</sup>
spec-56561-KP195920N454621V02_sp12-045	KIC10501393	20064002+4736539	B5 III	311	vgood	1-2
spec-56591-KP195920N454621V3_sp13-174	KIC09860322	20063327+4637279	B5 V	265	vgood	1 <sup>b</sup>
spec-56562-KP192102N424113V02_sp06-083	KIC06780397	19305469+4215203	B7 III-IV	413	vgood	2
spec-56096-kepler08B56096_2_sp13-250	KIC05380341	19454878+4033190	B7 V	182	vgood	2.5
spec-56561-KP195920N454621V02_sp06-117	KIC08530971	20111938+4435273	B8 III-IV	242	vgood	2 <sup>a</sup>
spec-56562-KP192102N424113V02_sp08-216	KIC06121547	19243929+4124248	B8 V	382	vgood	2 <sup>c</sup>
spec-56561-KP195920N454621V02_sp02-182	KIC08577307	19502070+4436477	B9 III	167	vgood	2
spec-56561-KP195920N454621V01_sp02-063	KIC08189641	19553255+4400228	B9 V	547	vgood	2-3 <sup>d</sup>
spec-56561-KP195920N454621V01_sp05-032	KIC08583770	19565852+4440592	A0 III	609	vgood	2-3
spec-56811-KP190339N395439V02_sp16-205	KIC06265185	18550325+4140225	A0 V	278	excel	3
spec-56919-KP190651N485531V01_sp12-144	KIC12055345	19105861+4503022	A1 III	589	vgood	2
spec-56561-KP195920N454621V02_sp11-197	KIC10624050	19590430+4749002	A1 V	395	excel	3
spec-56096-kepler08B56096_2_sp03-235	KIC04564619	19301385+3940339	A2 III-IV	114	excel	2
spec-56914-KP193637N444141V01_sp15-170	KIC09529773	19325433+4609042	A2 V	247	excel	2-3
spec-56914-KP193637N444141V02_sp03-104	KIC08887625	19302112+4509101	A3 III	328	vgood	2
spec-56568-KP195920N454621M01_sp12-241	KIC10628271	20035323+4750419	A3 V	407	excel	3
spec-56562-KP192102N424113V02_sp05-044	KIC06199731	19203196+4135194	A5 III	410	vgood	1 <sup>e</sup>
spec-56561-KP195920N454621V02_sp08-150	KIC08916492	20050274+4506175	A5 V	440	excel	3
spec-56550-KP194045N483045V02_sp04-175	KIC11090405	19391238+4836241	A7 III	605	vgood	2
spec-56550-KP194045N483045V02_sp04-202	KIC11252382	19422768+4854228	A7 V	275	excel	3
spec-56094-kepler05B56094_2_sp10-065	KIC03535046	19143404+3836017	F0 III	265	vgood	1 <sup>e</sup>
spec-56562-KP192102N424113V02_sp15-119	KIC07748238	19203821+4329037	F0 V	478	excel	3
spec-56798-KP192314N471144V01_sp04-125	KIC10073601	19244870+4702411	F2 III	296	vgood	2
spec-56919-KP190651N485531V01_sp11-032	KIC12058428	19180566+5033358	F2 V	216	excel	3
spec-56918-KP192323N501616V_sp07-062	KIC11139951	19322218+4845539	F3 III Fe-0.6	100	vgood	1
spec-56780-KP185111N464417V01_sp15-194	KIC10320849	18495615+4726035	F3 V	242	excel	3
spec-56798-KP192314N471144V01_sp03-117	KIC10398258	19161952+4735107	F5 III-IV	254	vgood	2
spec-56561-KP195920N454621V01_sp08-245	KIC08985402	20043155+4517541	F5 V	377	excel	3
spec-56807-KP185111N464417V03_sp09-173	KIC10256595	18531919+4723443	F6 III	243	vgood	2
spec-56918-KP192323N501616V_sp11-087	KIC12785394	19221083+5203294	F6 V	287	excel	3
spec-56918-KP192323N501616V_sp01-135	KIC11028682	19253344+4830538	F8 III	306	vgood	2
spec-56550-KP194045N483045V02_sp10-121	KIC10732086	19284619+4802316	F8 V	286	excel	3
spec-56811-KP190339N395439V01_sp16-061	KIC06346065	18585279+4144275	F9 III	190	vgood	1
spec-56919-KP190651N485531V01_sp01-020	KIC09821151	19072635+4637318	F9 V	177	excel	3
spec-56550-KP194045N483045V02_sp08-014	KIC10482869	19454882+4739317	G0 III-IV	294	vgood	2
spec-56562-KP192102N424113V02_sp05-154	KIC06600155	19195410+4204013	G0 V	330	excel	3

Notes:

<sup>a</sup> Interstellar contribution to the Ca II K line. DIB at 4130 Å.

<sup>b</sup> Slightly broadened lines – rapid rotator? Glitch at 4315 Å.

<sup>c</sup> He lines slightly strong. Glitch at 4307 Å.

<sup>d</sup> Slightly metal-weak?

<sup>e</sup> Characteristica of luminosity class III only weakly expressed.